Atmospheric electric charge transfer in precipitation and associated synoptic conditions

W. P. Aspinall

ATMOSPHERIC ELECTRIC CHARGE TRANSFER IN PRECIPITATION AND ASSOCIATED SYNOPTIC CONDITIONS

by

W. P. Aspinall, B.Sc.

A Thesis presented in Candidature for the Degree of Doctor of Philosophy in the University of Durham.

December, 1969

ABSTRACT

Measurements of Atmospheric Electricity have been made in the unpolluted air of Weardale during conditions of precipitation and in fair weather.

An automatic recording system has been built to digitize instrument outputs on paper-tape for subsequent computer analysis. The system was installed and run at Lanehead Field Centre and was also used to process magnetic tape recordings from the LandRover mobile station. The system was expanded to include an 1-hour smoothing and sampling action for recording averaged values of fair weather Atmospheric Electricity.

At times of electrically quiet precipitation, measurements have been made of potential gradient, precipitation current density, space charge density and both polar conductivities. A new method of compensation for displacement currents has been used. Conductivity measurements have revealed a charge separation process close to the ground in rain, but not in snow.

Techniques of variance spectrum analysis have been adopted for the precipitation work. Coherency spectra of potential gradient with precipitation current have indicated electrical 'cells' in nimbostratus and their relevance to weather forecasting is discussed. The phase spectra for these two parameters have been examined to measure the height of electrical activity and this is found to coincide with the melting level, and an estimate is made of the conductivity of the charging region of the cloud. Digital filtering of records has disclosed a mechanical-transfer current of space charges, to an exposed rain receiver, opposite to the precipitation current.

The diurnal variation of potential gradient at Lanehead has been refined with a further year's continuous observations in fair weather and seasonal differences in the diurnal variations of potential gradient, air-

earth current density and space charge density have been explained by increased convection in summer. The conduction current has been estimated by the indirect method and the difference between this and the total air-earth current to an exposed plate is attributed to a mechanical-transfer current of space charges. Measurements in light winds have evinced the influence of the electrode effect.

CONTENTS

CHAPTER 1

THE ROLE OF ATMOSPHERIC ELECTRICITY IN MAN'S ENVIRONMENT

Electrical activity, in the region of the atmosphere surrounding the earth, initially made its existence felt in the awareness of man by the manifestation of lightning. The circumstances of the detection of activity in conditions other than those of thunderstorm are a matter of historical fact, and the details are well documented elsewhere (SCHONLAND, 1964; CHALMERS, 1967). Of more immediate pertinence to this work is the sum of knowledge accumulated over the years, which represents our current understanding of the subject of Atmospheric Electricity.

1.1 The spherical condenser hypothesis

The measurement of certain parameters linked together by the classical picture of the 'spherical condenser hypothesis' has been, and will remain for the purpose of this work, the basis on which the behaviour of these parameters is determined. This hypothesis considers the earth to be the inner conducting electrode of a giant spherical condenser, with the outer electrode being formed by the highly ionized region, referred to as the electrosphere, which marks the lower reaches of the ionosphere. The height of this region is about 50 km above the surface of the earth, and it is formed physically by the ionization of the upper atmosphere with cosmic ray particles. These electrodes are maintained, by a means specified later (Sect. 1.3) at a potential difference, V, of about 2.9×10^5 V (Fig. 1.1).

CHALMERS (1953) showed that, if the electrosphere is a conducting spherical surface, it must be impervious to lines of force, and the sum of all charges inside it and on its inner surface must be zero. These

charges are those in the atmosphere, in clouds, on the inner surface of the electrosphere and on the surface of the inside electrode, the earth.

1.2 Processes which tend to discharge the spherical condenser

1.2.1 The fair weather conduction current

The potential of the electrosphere gives rise to a conduction current, effectively a 'leakage', in the air layer between the two electrodes. This current is most easily detected and studied in conditions of fair weather, which are taken to be any conditions where precipitation is not falling and vigorous electrical activity is not occurring. The relationship between the current and the potential difference is governed by the ionic conductivity of the air, and the three are assumed to obey OHM's Law in the form:-

$$I = - F\lambda$$

where I is the current density, λ is the conductivity and F is the potential gradient, assumed vertical and defined by:

$$F = \frac{dV}{dx} .$$

The total conductivity is produced by the movements of positive and negative ions under the influence of the electric field.

1.2.2 The columnar resistance

The columnar resistance is defined as the resistance of a column of air of unit cross-section (1 m^2 in S.I. units) from the surface of the earth up to the electrosphere.

A value for this quantity can be obtained up to different altitudes from a knowledge of the conductivity of the air, and GISH and SHERMAN (1936), using the results from the balloon Explorer II, concluded that

the columnar resistance to a height of 18 km is of the order of $10^{17}\Omega$. If the conductivity from this height to the base of the ionosphere is estimated from cosmic ray data, then the total resistance from the ground to the electrosphere is about 110 per cent of this value, and if this is valid for the whole of the earth's surface, then the total resistance of the atmosphere amounts to about 200Ω.

It is possible to relate this resistance, R_c, to the potential V of the electrosphere by OHM's Law:

$$I = \frac{V}{R_c}$$

where I appears to be a current and not a current density as encountered in Section 1.1 :

$$I = - F\lambda$$

However, this apparent anomaly may be resolved if we consider R_c to be the resistance of a column of unit cross-section, and it will follow that the two I's are dimensionally the same, that is, current densities.

The potential gradient may be written as:

$$F = - \frac{I}{\lambda} = - \frac{V}{\lambda R_c}$$

If R_c remains constant then I is proportional to V, whereas F is proportional to V/λ. Now λ, the conductivity, depends closely on local influences, notably pollution, and this will affect F more than will V, and it would be expected that I, independent of λ except in that λ affects R_c, would be more responsive to changes in V. This deduction is important in the comparison of the world-wide thunderstorm activity with the atmospheric electric elements.

Indirect measurements of the conduction current density using the relationship

$$I = - F\lambda$$

give an average value for I of 2.4 pA m^{-2} for different land stations (CHALMERS, 1967). This is equivalent to a rate of arrival of charge at the earth's surface of + 75 C km^{-2} yr^{-1}.

1.2.3 Precipitation currents

The charge brought to earth on precipitation particles has been investigated by several workers, and, for measurements in this country, SCRASE (1938) obtained values for two successive years of + 7 C km^{-2} yr^{-1} and + 22 C km^{-2} yr^{-1}, and from 10 months observations, CHALMERS and LITTLE (1947) estimated + 40 C km^{-1} yr^{-1}. Insufficiency of data, particularly for tropical regions, makes this component of the total charge transfer equation a very uncertain quantity to assess.

1.3 Discussion of the mechanisms which maintain the potential of the spherical condenser

Given the conducting nature of air, a simple calculation by SCRASE (1933) shows that it would take about 50 minutes to discharge the spherical condenser, and a means must be sought whereby charge is supplied in such a manner and amount that it will compensate for the leakage of the fair weather conduction current.

1.3.1 The conduction current above thunderclouds

A considerable controversy existed in the 1920's over the polarity of a typical thundercloud; WILSON (1925) and SIMPSON (1927) were the main protagonists, the former believing that thunderclouds were of positive polarity, and the latter taking the opposite view. The measurement of the potential gradient in thunderclouds by the alti-electrograph (SIMPSON and SCRASE, 1937; SIMPSON and ROBINSON, 1940) resolved the debate in

favour of a positive upper charge and negative lower charge distribution. If the charge separation processes in the thundercloud are sufficiently powerful, the situation might arise where the top parts of the cloud become more positive than the electrosphere; in which case, the direction of conduction current flow above the cloud will be reversed and some compensation for the fair weather leakage is effected.

Measurements above active thunderclouds (GISH and WAIT, 1950; STERGIS, REIN and KANGAS, 1957) have indicated a positive conduction current upwards, of average value 0.5A, which, taken together with an estimate for the number of thunderstorms at one time, is a major contribution to the compensation mentioned.

The various theories of charge separation in clouds are not included here, but may be found in the literature.

1.3.2 The conduction current above nimbostratus cloud

The studies of CHALMERS (1956) indicated that the total vertical current downwards to the ground from a nimbostratus cloud giving snow is negative. Making the assumption that the horizontal extent of the cloud was such that conditions were 'quasi-static', that is the distribution of charges remains the same and continuity of current can be expected (CHALMERS, 1967), Chalmers suggested that the current downwards must be negative at all levels, so that the conduction current above the cloud brings down negative charge. This requires the potential at the upper boundary of the cloud to be above that of the electrosphere, and this pattern of behaviour is identical in form with that of the thundercloud. By considering that rain from nimbostratus started life as frozen particles of ice or snow, a not unreasonable premise in these latitudes, CHALMERS (1967) was also able to show that this structure of charges

might also be expected in the rain cloud, just as in the snow cloud. The magnitudes of the effects in continuous precipitation are very much smaller than those encountered in thunderstorms and, for this reason, they have been relatively neglected by research workers.

1.3.3 Point discharge

The production of charged ions, at times of high potential gradient, from elevated points, both natural and artificial, gives a resultant negative charge to the earth. WORMELL (1930), after a period of four years of measurement, made an estimate of - 100 C $km^{-2}yr^{-1}$ and later (WORMELL, 1953) increased this figure to - 170 C $km^{-2}yr^{-1}$. The work of STROMBERG (1968), in a plantation of trees, produced the value of - 270 ± 180 C $km^{-2}yr^{-1}$. This result, which is currently the best estimate available for natural point discharge, emphasises not only the uncertainty in this quantity, but also its potential importance as a mechanism of charge transfer.

1.3.4 Lightning discharge currents

On balance, lightning discharges to ground bring negative charge to earth. ISRAEL (1953) used the estimate of 1800 active storms at one time (BROOKS, 1925) to calculate the total charge brought to 1 km^2 of the earth's surface in a year, and obtained a mean value for the current density due to lightning charges of - 20 C $km^{-2}yr^{-1}$ for the earth as a whole.

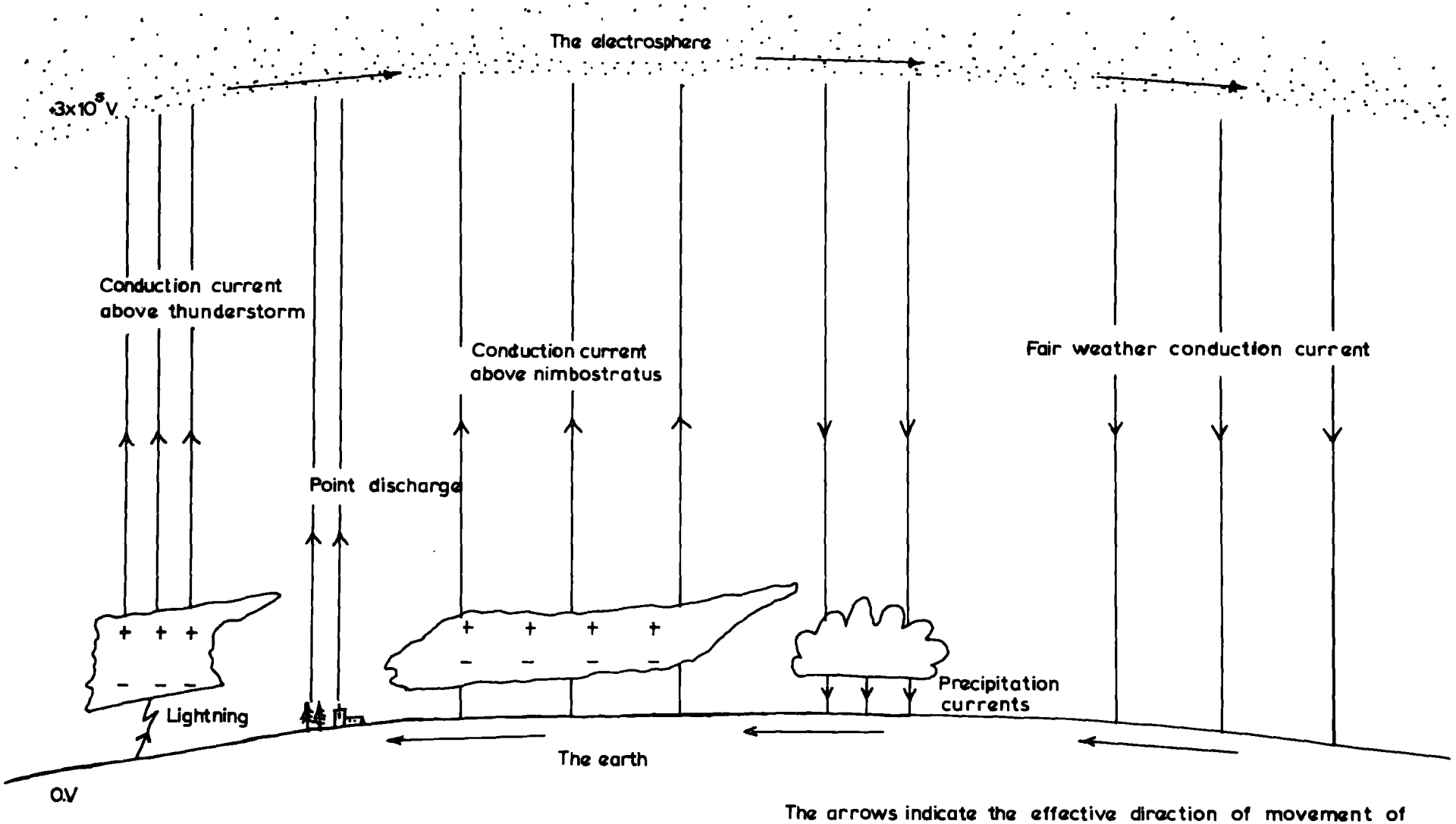

Fig. 1.1. The electrosphere – earth currents.

1.4 The total transfer of charge

Using the results for the different processes, it is possible to estimate the total transfer of charge at those places where the measurements were made. Several workers (WORMELL, 1930 and 1953; CHALMERS, 1949 and 1957; CHALMERS and LITTLE, 1947; WAIT, 1950; ISRAEL, 1953) have assessed the possible contribution by each process to the total. Their conclusions, however, differ widely and all suffer from the drawback of being based on measurements, made almost wholly in this country, which are unlikely to be typical of the whole globe.

The various processes are illustrated pictorially by Fig. 1.1. The arrows indicate the effective direction of movement of positive charge, but not the exclusive mode of behaviour; for example, point discharge brings both positive and negative charge to earth, but its net effect over a period is the one shown.

1.5 A theory of the origin of atmospheric electricity

It is thought to be worthwhile to mention a theory of the origin of atmospheric electricity founded on concepts which, until this time, have played little part in the general deliberations of physicists concerned with the lower atmosphere. The outline of this theory, in a paper read to the Fourth International Conference on The Universal Aspects of Atmospheric Electricity in Tokyo in 1968 by WEBB (1968), is presented without contention.

1.5.1 WEBB's theory

In October 1959 there was started a network of meteorological rocket studies of altitudes up to 80 km, the previous limit being 30 km (WEBB et al., 1966). This increased volume of information has yielded

three important large diurnal variations which are temperature (BEYERS and MIERS, 1965), wind (MIERS, 1965) and ozone density (RANDHAWA, 1967) in the stratopause region. Solar ultra-violet heating of the ozonosphere is indicated, by the data, to be encountered in the region 45 km to 50 km, but with a diurnal movement up and down from the stratopause level. This leads to the conclusion that, above the 40 km mark, circulation systems exist that exert a profound influence on the structure of the upper atmosphere, which will mix and transport the constituents of this region. The important result of these synoptic meteorological studies is the discovery of vertical motions of great magnitude in certain localities which involve the transport of charged particles through regions where differing mobilities of positively and negatively charged carriers produce e.m.f's. and hence modify the 'normal' fields and currents. Omitting the details of the interactions between the various fields, electric and magnetic, and the charged particles, the outcome of Webb's work is the postulate that these solar induced variations in the vicinity of the lower ionosphere are responsible for the large dynamo currents there, whose existence is well founded (BAKER and MARTYN,1952 and 1953). Webb suggests that the 1800 A of the fair weather conduction current represents a small alternative return path through the partially conducting atmosphere to the surface of the earth, thence as telluric currents (CHAPMAN and BARTELS, 1940) to the centres of thunderstorm activity where lightning strokes reduce the resistance back to the ionosphere (Fig. 1.2). The major return paths are taken to be horizontal global-scale currents around the regions where the dynamo current is generated.

1.5.2 Discussion of the atmospheric electricity aspects of Webb's theory

This theory has at least two important implications for the atmospheric physicist.

Fig. 1.2. Two views of the ionosphere-earth electrical network.

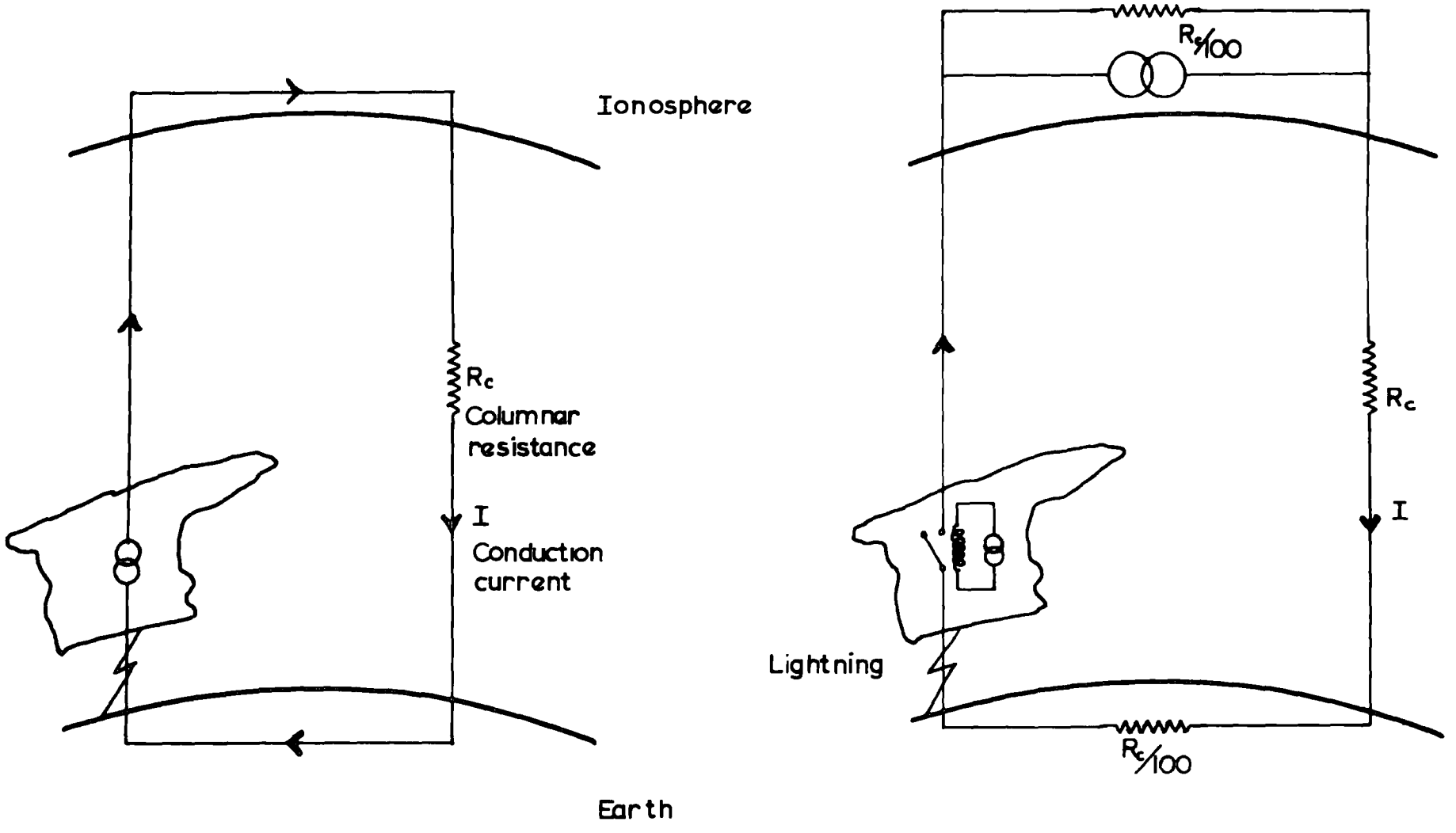

The spherical condenser hypothesis

Webb's theory

Firstly, the air-earth conduction current, under the 'noise' of localised effects, should be governed by the diurnal variation of the dynamo current. Secondly, the thunderstorm will conduct, through the medium of lightning, that current which is available from the above theory, rather than the current that it might generate internally. This notion is illustrated in Fig. 1.2 where the thunderstorm is represented as a self-powered relay switching the 'contacts' (lightning) which short out the relatively high resistance of the lower regions of the atmosphere.

Consideration of the two pictures (Fig. 1.2) of the ionosphere - earth electrical system, one due to WEBB (1968) and the other being the spherical condenser hypothesis, may be made from two standpoints; the ionospheric physicist will regard the current loop through the air-earth path as a negligible leak (about 1 per cent of his dynamo current) and the finer points of the characteristics of currents in the atmosphere will matter little to him. On the other hand, the atmospheric physicist, traditionally a student of effects of the magnitude of the air-earth current, will assume that the earth and the ionosphere, whose resistivities are factors of hundreds of times smaller than that of the atmosphere, may be considered as perfect conductors. It can be seen that Webb's picture will reduce to the classical concept if resistances of the order of 1 per cent, or less, of the columnar resistance are ignored, except for the essential difference in the rôle of the thunderstorm as an agency of charge transfer. This will, however, still allow the same relationships which have been experienced between thunder and the other atmospheric electric elements under the classical hypothesis, but for different reasons, and an explanation will still be required for the charge separation that occurs within the cloud.

It is possible that the true mode of behaviour lies in a combination

of these two outlooks.

1.6 The influence of Atmospheric Electricity on Man

The electrical activity in the environment of man intrudes, to varying degrees, into several distinct but interrelated phenomena. There is the electrical link between the ionosphere, which shields man from radiation and assists some of his communications, and meteorology, which has a powerful influence over his comfort. This link is carried further to the behaviour of the particulate and ionic matter in the air he breathes and the pollution he produces, and an association of physiological phenomena with electrical, as well as meteorological factors has also been conjectured (SCHILLING and CARSON, 1953; SCHILLING and HOLZER, 1954).

Our knowledge of the degree to which electrical effects are fundamental to the various processes of our environment is imprecise; this work is concerned with some of the processes of fair weather and rain, and the scope and guiding principles are set out in Chapter 2.

Fig. 2.1. A typical warm sector depression.

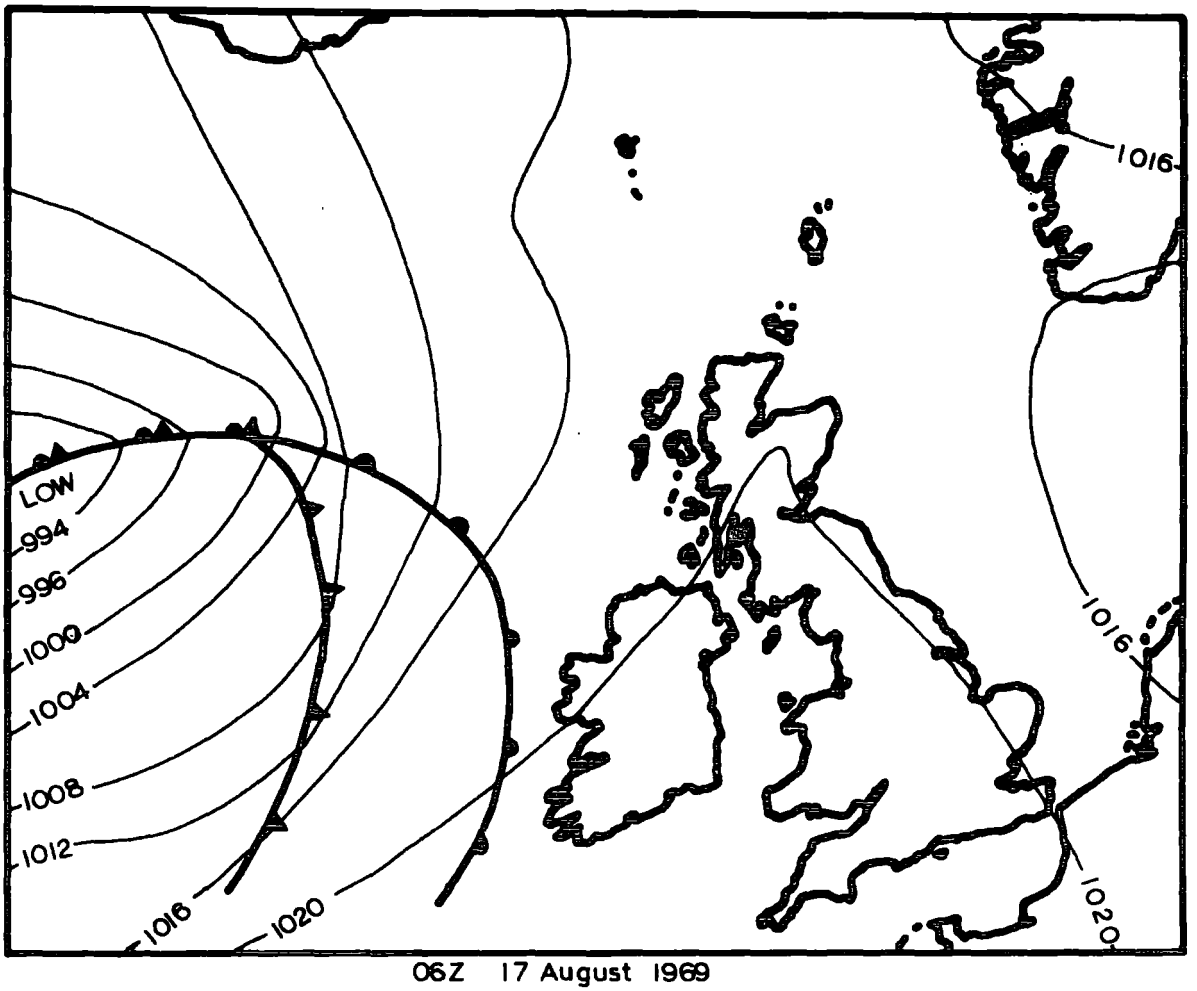

Vertical section:

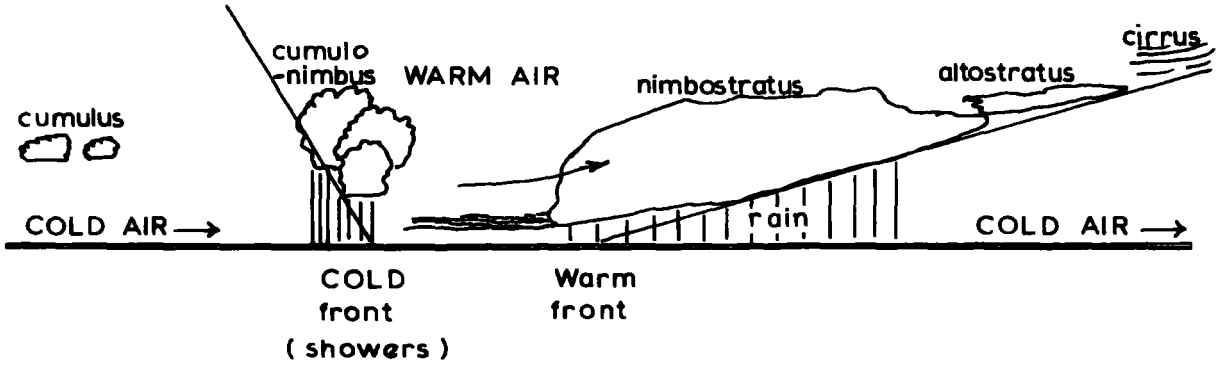

CHAPTER 2

THE PROPOSED INVESTIGATION OF THE TRANSFER OF ELECTRIC CHARGE IN NIMBOSTRATUS

The outline was given, in Chapter 1, of several processes of electric charge transfer between the atmosphere and the earth, and the meteorological conditions in which they are generally encountered. This thesis is devoted mainly to an investigation of the electrification of nimbostratus.

2.1 The governing factor of climate

The climate of the British Isles is dominated by the interaction of the continental-type climate of Europe with the oceanic climate of the North Atlantic. This produces weather of a changeable nature, characterised by the rapid development of frontal systems and depressions over the Atlantic which sweep across the country. A typical depression, with its warm and cold fronts, is shown in the weather map of Fig. 2.1, together with an idealized profile of the physical structure of the frontal system.

It will have been noted in Chapter 1 that nimbostratus, a feature of the warm front and a possible vehicle for a charge transfer process maintaining the potential of the electrosphere, has been relatively neglected by workers in the past. This is mainly because of the lesser intensity of its electrical effects and its rarity in most parts of the world. It is, however, common in Britain and should be more predictable as a subject for research than should, for example, the thunderstorm. In research of a mensural nature, accuracy and confidence are greatly increased if it is possible to make a large number of repeated measurements and it is felt that, with the development of the Automatic Data Recording System (Chapter 3), the occurrence of these warm fronts makes a study of the electrification of nimbostratus a worthwhile prospect.

2.2 Electrical measurements in rain

The origin of the electric charges on water drops and ice particles, falling as precipitation, excites interest because of the possibility that precipitation plays a fundamental part in the separation of electric charge in, or below, clouds.

Most measurements of precipitation currents in non-stormy conditions have been made with an insulated collector connected to an electrometer, and often the collector is shielded from the earth's electric field in order to avoid effects associated with changes in bound charge. The shielded collector, in its usual form, comprises an open-ended metallic cylinder, mounted vertically, with the collector fitted onto insulators inside. This arrangement is effective in eliminating, from the collector, the displacement currents arising from changes in the electric field, but considerable doubt surrounds the faithfulness with which it will collect rain in gusty conditions. SCRASE (1938) found that his apparatus collected only half the amount of rain caught by a standard rain gauge.

The purpose of the totally exposed collector is to isolate some portion of the earth's surface and to determine the charge reaching it on the rain, in conditions which are as close to the natural ones as possible. This collector will catch all the rain falling on it, but it is also exposed to electric field changes, and compensation is needed for displacement currents.

Early workers employed the measuring technique of allowing their collector to charge up for a period of time, taking the reading by eye, and then earthing the collector and starting again. ELSTER and GEITEL (1888), using this method, adopted periods of 5 s to 2 minutes depending on the rate of charging of their collector, but later workers, M'CLELLAND and NOLAN (1912) and SCRASE (1938), preferred to measure the amount of charge

associated with a definite quantity of rainfall. Scrase, for example, used a tipping-bucket device as an integral part of his collector. Early attempts at continuous recording were made by SIMPSON (1909) and SCHINDELHAUER (1913), but effective direct measurement had to await the development of modern electronic electrometers and suitable insulating materials before it became a realistic proposition. The Vibrating Reed Electrometer (hereafter referred to as V.R.E.) has been extensively used at Durham for this purpose, and the work of RAMSAY and CHALMERS (1960) may be cited as an example.

2.2.1 The work of Sir George Simpson

Since 1934 it has been the practice of the Kew Observatory to make continuous recordings of several parameters of Atmospheric Electricity (SCRASE, 1938) and these include potential gradient and the charge carried down to earth by rain. Observations made in the period October 1942 to May 1946 were considered by SIMPSON (1949) and, among other topics, he sought a relationship between potential gradient and the charge on rain. The whole body of his data did not yield an acceptable linear association between the two, but Simpson showed that different linear relationships existed for two distinct categories of the data. One grouping corresponded to potential gradients in excess of 2000 Vm^{-1}, and the other to potential gradients of less than 1000 Vm^{-1}.

In the former, a remarkable effect, the 'mirror-image effect', in which the two parameters show corresponding increases in magnitude but with opposite sign, was explained by the interdependence of rain current, point discharge current and rate of rainfall. In the latter, the observations were concerned with steady rain with no point discharge, and these gave rise to a less well-marked mirror-image effect. A theoretical

account of this effect, and the conditions in which it will and will not hold, is given by MAGONO and ORIKASA (1961). Simpson arrived at the following empirical relationship:

$$q = - 4.8 \times 10^{-8} (P - 400)$$

where q is the rain charge per unit volume of water, in Cm^{-3}, and P is the potential gradient in Vm^{-1}. He made the interesting suggestion that the constant term, 400 Vm^{-1}, might represent the normal fair weather potential gradient at Kew and that, as a consequence, the value of q was proportional to the measured displacement from this normal value. He also concluded from his measurements that, in general, the potential gradient is negative for steady rain and that the rain carries positive charge out of the cloud. A lack of information from steady snowfall prevented him from considering fully the joint rôles of snow and rain, but this has been developed by CHALMERS (1956) and is mentioned shortly (Sect. 2.2.2).

It is worth recording here some of the relationships between potential gradient and rain charge, or current, which have been obtained by other workers.

SIVARAMAKRISHNAN (1960) found results similar to those of SIMPSON (1949), but with q proportional to (P - 100).

CHALMERS (1956) measured the total current density, conduction and precipitation, to earth and obtained a relationship of the form:

$$K = - 1.18 \times 10^{-14} (P - 150)$$

where K is in Am^{-2} and P is in Vm^{-1}.

REITER (1965) also found the current to depend on (P - C) and in his case C was 40 Vm^{-1}, which agreed well with the local fair weather potential gradient. This work is discussed on Sect. 2.2.3.

2.2.2 The work of Chalmers

The extension of measurements from quiet rain to the comparable conditions for continuous snow was made by CHALMERS (1956). He imposed the restriction that the potential gradient should be in the range $\pm 800\ Vm^{-1}$ for both types of precipitation. A relationship of the form encountered with the rain results was computed and found to be:

$$K = -0.92 \times 10^{-14} (P + 425)$$

where K is the total current density in Am^{-2} and P is in Vm^{-1}. In contrast to rain, the downward snow current was usually negative while the potential gradient was positive or negative, but more frequently positive.

Bearing these general results in mind, CHALMERS (1956) discusses their relevance to the origin of the charges on rain and snow. He assumes that most, if not all, of the precipitation involved in his measurements must have been in a frozen state during some part of its time in the cloud. If a process of charge separation exists which is, in some way, connected with solid precipitation particles, then it will operate in all cases, whether the precipitation reaches the ground as rain or snow. Such a process must cause the particles to bring negative charge down - wards in order to meet the conditions, observed experimentally, for snow. In the case of rain, a second process must apply which will convert the negative snow into positive rain.

This indicates that the direction of charge separation in nimbo-stratus is the same as that in the cumulonimbus cloud and CHALMERS (1956) suggests that, if the separation is sufficiently large, it will lead to a reversal of the conduction current above the cloud, thus replenishing the charge of the electrosphere.

A further consequence of this work is that, in the region where the

snow melts and turns to rain, there seems to be a process of charge reversal on the precipitation, and this constitutes an area of interest as compelling as that of the origin of the charge on the particles in the first place. OWOLABI and CHALMERS (1965), in a single period of measurement, detected a time lag of 40 s between maxima of potential gradient at the ground and the precipitation current to their shielded collector. They suggested that this lag was a consequence of the time that it took for the precipitation to fall from the height of the melting level on that day. By itself, this result is not conclusive; OWOLABI and CHALMERS (1965) took no account of the wind profile at the time, and this could alter their estimate, of the height from which the drops had fallen in 40 s, by a factor of 2 or more. But it is clear that a careful investigation should be conducted to verify the existence of such time lag effects, as the work of REITER (1965) has shown that the melting level is indeed a region of electrical activity.

2.2.3 The work of Reiter

It is significant that the continuous collection of data over long periods, in the manner which enabled SIMPSON (1949) to do his pioneer studies of precipitation electricity, is also the method which REITER (1965) adopted for his interesting work. The establishment, in 1954, of a network of seven stations in the Wetterstein Mountains of West Germany, between the heights 675 m and 3000 m above sea level, allowed a continuous examination to be made, within and below cloud, of the temporal development of atmospheric electric processes in disturbed weather. In addition, the vertical disposition of the stations meant that the variation of these processes with altitude could be investigated in terms of the different levels represented by each

station. Over a number of years, the results from the observations in the Garmisch-Partenkirchen area have been published (REITER, 1956; 1958; 1960; 1965 and 1968), and a summary of the sections which relate to steady precipitation is pertinent to the present work.

During several periods of precipitation, the melting zone, where the average atmospheric temperature is in the range $0^{o}C$ to $+2^{o}C$, was at a height such that some stations were above its level and some were below. This led to the discovery that, in the zone of solid precipitation, the potential gradient has the same sign as the fair weather potential gradient and the precipitation particles carry negative charges, although there is a balance of positive space charge. Between the zones of liquid and solid precipitation the charge signs are reversed. This result is valid inside the cloud as well as below it and is irrespective of the height of the cloud base. A physical explanation of this effect is not offered (REITER, 1965). The records of precipitation current density and potential gradient exhibited the mirror-image effect, and REITER (1965) has derived an expression relating the two in the form given by SIMPSON (1949). It is:

$$J = - 0.74 \times 10^{-14} (P - 40)$$

for steady rain, and

$$J = - 0.93 \times 10^{-14} (P - 40)$$

for continuous snowfall, where J is in Am^{-2} and P is in Vm^{-1}. The constant term, 40 Vm^{-1}, is in good agreement with the normal fair weather potential gradient at Garmisch.

The observations for the period 1954 to 1968 have been extensively analysed and the results were published in a paper (REITER, 1968) presented at The Fourth International Conference on The Universal Aspects of Atmospheric Electricity in Tokyo. This paper constitutes a

comprehensive assessment of the characteristics of behaviour of atmospheric electric parameters in relation to differing meteorological synoptic conditions, and verifies the results mentioned above. A further development is the observed presence of negative charge in the base of nimbostratus cloud; this negative charge is evident for rain-, snow- and non-precipitating clouds alike and produces a small diminution from the fair weather positive potential gradient at the ground beneath the non-precipitating cloud. For this reason REITER (1968) believes that the variations from this smaller positive value during precipitation are caused by electrical effects associated with the falling particles, rather than any activity within the cloud. It is worth mentioning that SHARPLESS (1968) detected a high correlation of space charge density and potential gradient at the ground in quiet rain, which was taken to indicate the existence of a layer of space charge a few tens of metres deep. It seems, in view of these results, that the existence of more than one basic separation of charge, as preferred in Sect. 2.2.2, will have to be considered.

Confirmation of the variations of the parameters with height, which had been interpolated between the levels of the stations, has recently been achieved by the instrumentation of a cable car which climbs from the Garmisch Valley (730 m above sea level) to the Wank Summit (1780 m above sea level), and this was also reported to the Fourth International Conference (REITER, 1968). In far-ranging manner, REITER (1968) also discusses the rôle of atmospheric instability, in the cloud region, as an influential factor in electrical phenomena, and he has no hesitation in emphasizing that this is a subject which must feature in any consideration of precipitation electricity.

2.3 The measurements for the proposed investigation

These are to be made, using the Automatic Recording System, for the potential gradient F, the total current I to an exposed receiver, the space charge density ρ and both polar conductivities (λ_+ and λ_-) at ground level, during conditions of continuous, electrically quiet rain. The criteria for such conditions are set out in Sects. 2.3.1 and 2.3.2. The precipitation current density J is to be computed by subtracting the conduction current I_c at the ground, given by the product:

$$I_c = F(\lambda_+ + \lambda_-)$$

from the total current I. From the data collected, the relationship between F and J will be evaluated and the analysis methods, given in Chapter 5, are to be used to examine, in fine detail, the behaviour of these two parameters in both the time-domain and the frequency-domain. Meteorological observations of interest, for example, cloud base height and speed, will be made in connection with this search.

Restrictions are laid down, in the next two sections, to ensure that each different period of measurement will be a valid example of quiet, continuous precipitation from nimbostratus.

2.3.1 A meteorological definition

The physical structure of a warm front is illustrated in Fig. 2.1; the region of warm air, trapped behind the more dense cold air at the front, is gently forced up and over it by the following mass of faster-moving cold air. As the warm air rises it cools and condensation occurs until a time is reached when the water drops, or ice particles, begin to fall out of the cloud. The inclination of the 'wedge' of cold air, over which this takes place, is very shallow, probably about

1 in 100, and the precipitating cloud which forms over it, nimbostratus, has very great horizontal extent. The cloud will exist for many hours until the two fronts join to form an occluded front.

The time that it will take for the cloud to pass over a given region will depend on the speed of the whole frontal system and on the size of the cloud, which itself is a function of the size of the system. Typically, such rain will last from 2 to 10 hours.

It was decided to restrict measurements to those periods of quiet rain associated with warm fronts, when the duration of the rain was in excess of 1 hour. This is in line with the practice of other workers, and should preclude the possibility of short-lived non-stratiform disturbances dominating the record.

The same mechanism, the upward movement of moist, warm air, which causes the formation of the cloud, may also occur when a flow of air is forced to rise to clear an obstacle, such as a mountain or a hill. This effect is known as orographic lifting and its magnitude is of the same order as that encountered in the vertical motion of a warm front. The cloud, forming on the up-wind slope and with the down-wind edge evaporating continuously, often appears to remain stationary over the obstacle although the wind may be blowing through it with considerable force. A classic example of this, the Helm Wind of Crossfell, in Cumberland, is fully described by MANLEY (1945).

The cloud itself may be stationary but the air flowing through it will be varying in moisture content and temperature, and as a result the cloud structure will not be unchanging. To an observer below, capable of detecting the changes in form of the cloud, there will appear to be no difference between this type of cloud and the true warm front sort, and it would be very surprising if the two involved different electrical properties.

A combination of the two processes will occur when a warm front passes over a hilly region, and it must be borne in mind that on the upslope side of a hill, the orographic lifting will increase the vertical motion of the air; while on the downslope side, the motion will be diminished. These may be considered as being equivalent to a more vertical and a more horizontal profile of the warm front, but should in no other way alter the physical concept of the system.

2.3.2 Restrictions on the electrical activity

In order that the conditions in which the electrification of nimbostratus is studied be as straightforward as possible, measurements will only be made at times of low and slowly changing potential gradient. This is to rule out point discharge currents which complicate the general pattern of charge transfer and, for this purpose, limits of $\pm$ 1000 Vm^{-1} are imposed.

2.4 The instruments

An atmospheric electric observatory has been established at the Geography Department Field Centre at Lanehead in Weardale, by SHARPLESS (1968). This station is equipped with tried and tested instruments (Chapter 4), in an area where air pollution is as low as any in the country, and constitutes an admirable site at which to conduct this experiment.

The desire to utilise the instruments fully at all times is the moving influence behind the fair weather work which will be the second investigation into electric charge transfer to be undertaken by the author (Chapters 7 and 8).

CHAPTER 3

THE AUTOMATIC DATA RECORDING SYSTEM

3.1 General Background

It has been well appreciated that the application of computer techniques to the handling of data gathered in Atmospheric Electricity would allow a considerable saving in time and effort on the part of the investigator. The feasibility of constructing a relatively simple electronic system for converting analogue measurements to digital paper tape form for input to a computer has been successfully demonstrated by COLLIN (1969), and put to use by Collin himself, BENT (1964) and a number of other workers. This analogue - to - digital converter was installed in the Atmospheric Physics laboratory at the Durham University Observatory and used, in conjunction with a Honeywell-Brown 16-point potentiometric recorder, to monitor various of the atmospheric electric parameters on a site adjoining the Observatory. At that time, GROOM (1966), a contemporary of Collin's, was making observations with an instrumented LandRover, and found that the taking down of readings by hand for any length of time imposed a strain on the individual and a constraint on his ability to deal with unexpected occurrences. It was felt that an automatic recording system, of a transportable nature, would alleviate many of the difficulties encountered with a mobile station, and to this end, Collin and Groom combined to explore the possibilities of recording data on a magnetic tape-recorder. Their laboratory tests, using a mains-powered recorder, showed that, with suitable changes to Collin's analogue-to-digital converter, the idea of recording a train of 'packets' of pulses, the number of pulses in each 'packet' being related to the value of the parameter being recorded, was a practical proposition, within the limitations imposed by the frequency response of the tape-recorder. The two

main actions of the method, the recording and the playback of a data signal, were shown to work, but the system was not developed or applied beyond this stage.

3.2 The guiding principles and design criteria for the system

3.2.1 Considerations of accuracy

The accuracy of a recording system must be such that the parameters being measured are in no way limited by the system and that their values can be recorded as accurately with the system as they can without it. The fundamental unit of the proposed system, for which good performance is of paramount importance, is the voltage-to-frequency converting circuit. COLLIN (1969) used the circuit given by DE'SA and MOLYNEUX (1962) for this purpose, and it was shown to be accurate to better than ± 1 per cent, which is adequate for the purposes of Atmospheric Electricity (Sect. 3.6). For this reason it was felt that this circuit could again be satisfactorily used, and that no real benefit could be gained from the investigation of alternative possibilities.

3.2.2 The two modes of operation of the system

One of the proposed topics of research in the Group was the simultaneous recording of precipitation currents at two sites in the line of the wind. It was envisaged that one site, the fixed one, would be the Field Centre at Lanehead School, Weardale, and that the other sites would be reached by means of the LandRover. It was necessary, therefore, to make two identical recording systems for the sake of consistency, and this was achieved by splitting the system into two separate units. The second unit, the playback processor, was designed to accept the data signal from whichever source was being employed, and to punch the

information on paper-tape. The first part of the system, the recording unit, was designed so that it could either transcribe the data onto the magnetic tape for playback into the processor at a later date, or it could be coupled directly to the processor to give an instantaneous output of paper-tape. By this means, simultaneous records could be taken, one directly at the Field Centre, the other, on a battery portable tape-recorder, in the LandRover.

This arrangement could be extended, if desired, to use any number of recording units, each with its own tape-recorder.

3.2.3 The Tape-recorder

The working range of the voltage-to-frequency converter of De'Sa and Molyneux gives a nearly linear output of 0 to 10 k Hz for an input of 0 to - 10V. This characteristic governs, in part, the choice of a suitable tape-recorder; GROOM (1966) had experienced difficulty with playback from a poor quality recorder, so that a prime requirement for the instrument would be a good frequency response up to not less than 15 k Hz. The further requirement that the recorder be powered by rechargeable batteries limited the possible choice to a few instruments, and the make and model finally selected was the E.M.I. L 4B Battery Portable Tape-Recorder, which has been extensively used by the British Broadcasting Corporation, and for this reason would seem to be of reasonable quality (Fig. 3.15).

3.2.4 The Tape-punch

The second-hand tape-punch employed by Collin at the Observatory became unreliable and an order was placed for a Teletype Larp 28 Tape-punch, (Fig. 3.14), which was duly in the possession of the Group when

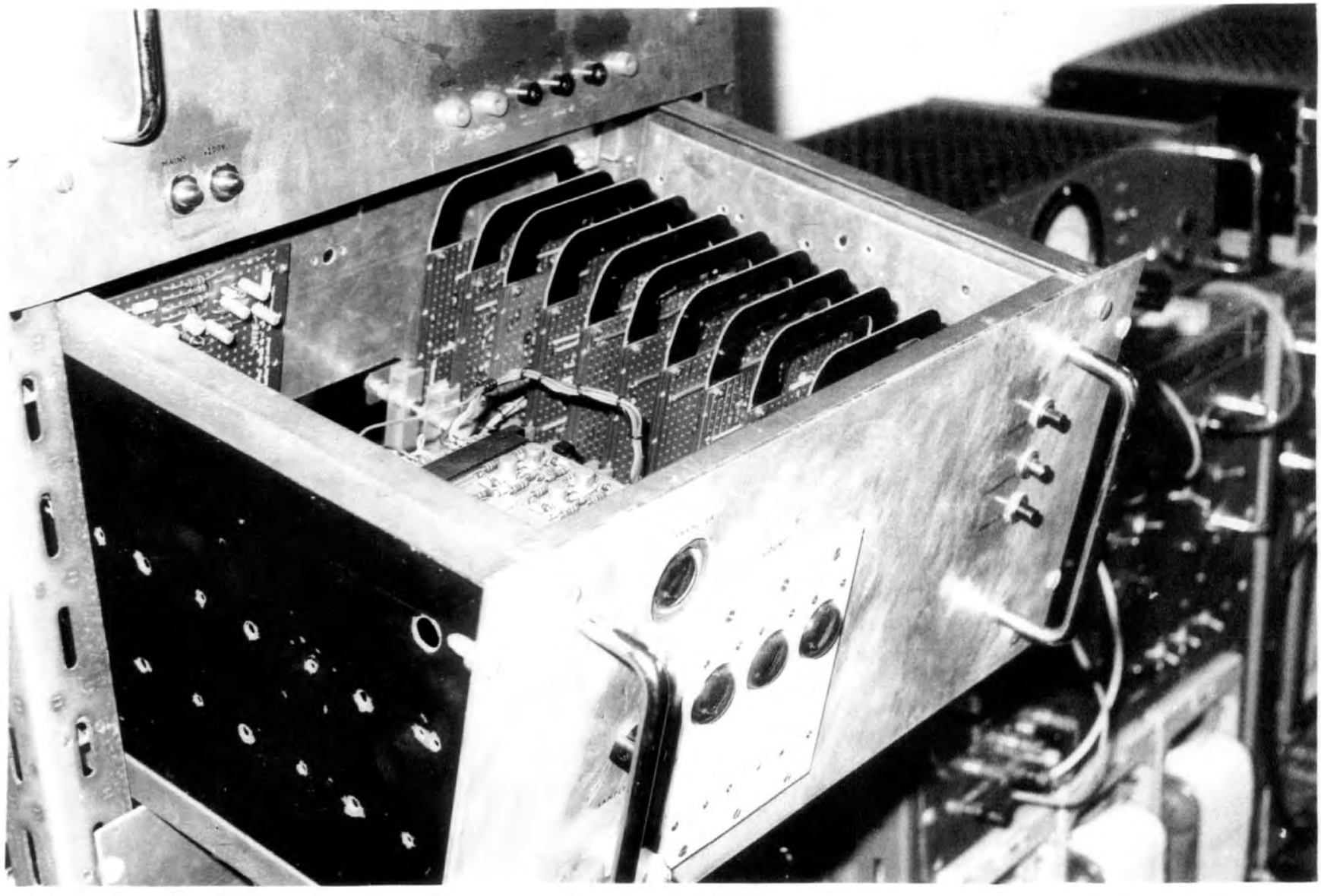

Fig. 3.1 The playback processor

the author joined. The input requirements of this machine were further factors in the consideration of the design of the system.

3.2.5 Some design aspects of the system

The electronics of Collin's system had been built on to 'tag-boards', which were permanently mounted onto a chassis. This prevented easy access to individual parts of the circuit for the purposes of repair or testing, and the choice was made to use 'Veroboard' printed circuit boards, (Fig. 3.1) which can be plugged into the unit, to allow a more versatile approach to the new system. A further improvement, recommended by GROOM (1966), was the use of reed relay switches, which can be controlled by a single switching transistor, in place of the less reliable, and in terms of current consumption, more demanding, conventional relays. These devices are designed to fit the 0.1" x 0.1" matrix of holes in a standard printed-circuit board, and were, therefore, suitable for use with "Veroboard".

A further improvement in the system was made possible by the timely advent of a decade counter module (Type DCM 503) manufactured by Quarndon Electronics Limited, capable of counting rates of up to 1 MHz. The counters are triggered by low voltage (+ 4V) pulses and give both a binary logic output and a decimal digit readout on a built-in numerical indicator tube. Three such modules, used in series, are capable of a count of 999, and have suitable output facilities for decoding to the tape-punch; they obviate the necessity of switching large D.C. voltages, characteristic of the 'Dekatron' counting tubes used by Collin, and have the further advantage of a digital readout, as opposed to the small dot of light which circulates round the ten positions of the 'Dekatron'.

By these means a complete break was made from thermionic valve circuitry, and its power supply problems, and semiconductor transistors were used throughout the whole system.

3.2.6 A recommendation

The increasing cheapness, availability and versatility of standard 'integrated circuits' makes the use of these components a reasonable basis for a data-handling system of this nature, and the saving in space, together with the increase in efficiency make these circuits a more attractive proposition than the use of discrete components, as undertaken by the author.

3.3 An outline of some of the circuit elements and their applications in the recording system

It is not the purpose of this thesis to be a comprehensive textbook of electronics, and the assumption is made that the reader is acquainted with the principles and applications of semiconductor transistors. However a brief outline of some of the basic circuit functions may be helpful to a consideration of the complete system. The three members of the multivibrator 'family' are described, together with some circuits, specifically designed, which do individual tasks in the recording system.

3.3.1 The astable (or free-running) multivibrator

For the astable multivibrator there are two active circuit elements, the two transistors in Fig. 3.2, connected with positive feedback; in practice, the circuit is not stable if both transistors are conducting, but oscillates between two temporarily stable extremes, first, with one conducting and the other cut off, and then with the

states reversed. The transition between these two states gives rise to square pulses at the collectors of the transistors, with the time lapse in each state, before transition, being governed by the coupling networks R_1C_1 and R_2C_2. This circuit is 'free-running', and is used in the playback part of the system to control the actions of the tape-punch (Sect. 3.5.3).

3.3.2 The monostable multivibrator

This circuit produces an output pulse on receipt of a trigger pulse, the duration of the pulse being determined by the designer with the value of the product R_3C_3. The form of the output pulse (C) from such a circuit is not sufficiently well defined for accurate timing purposes, so the output is treated by a three-transistor 'pulse shaper' (Fig. 3.2), which gives the desired square pulse, albeit inverted. This, however, is not a drawback as the designer can take the output either from B or, in its inverted form, from C, to give the 'positive-going' or 'negative-going' pulse at D.

This circuit is employed in the recording system to control the opening and closing of 'gating' circuits, for example, to allow a 100 ms train of pulses to be recorded on the magnetic tape, to time the various steps in the playback process and to provide a short trigger pulse, recorded on the tape, to initiate the playback action.

3.3.3 Gating circuits

The basic requirement of a gating circuit is that it shall have two states, in one of which (gate open) input signals are faithfully transmitted to the output, and in the other (gate shut) there is no output. The gate is controlled by the application of an auxiliary

pulse, often derived from an external device.

A simple transistor-transistor logic (TTL) gate (Fig. 3.3(a)) is used to regulate the transmission of pulses to the tape-recorder, with a switching pulse derived from a monostable (or 'one-shot') multivibrator (Sect. 3.3.1). The input pulses and resulting output pulse form are shown in Fig. 3.3(a).

An alternative form of gating circuit, extensively used in the recording system, comprises a diode AND network switching a diode-transistor logic output (DTL), as in Fig. 3.3(b). The transistor will enter the 'on' state if, and only if, all inputs have the correct voltage level applied to them (in this case, negative voltages, - 6V, are required at the three diodes). A positive voltage applied to one, or more, of the diodes will bias it into the conducting state, causing the potential at the base of the transistor to become positive, thus switching the transistor off. This corresponds to 'no signal'. The other logic functions (OR, NOR, NAND, NOT, etc.) are similarly formed in DTL for the purposes of the recording system, and the reader is referred to any text-book of electronic logic element design for fuller details (for example,'Electronic Counting Techniques', published by Mullard Limited, 1967).

3.3.4 The bistable multivibrator

The circuit and logic symbol of a bistable multivibrator are shown in Fig. 3.4. This circuit is a stable two-state device which, with some alterations to its configuration, can be used in two different modes. Firstly in the case of Fig. 3.4, the bistable will change state (that is, exchange the output voltage levels at A and $\bar{A}$) with the arrival of a valid pulse at input I_1 and will remain in this state,

Fig.3.2. The Multivibrator Family

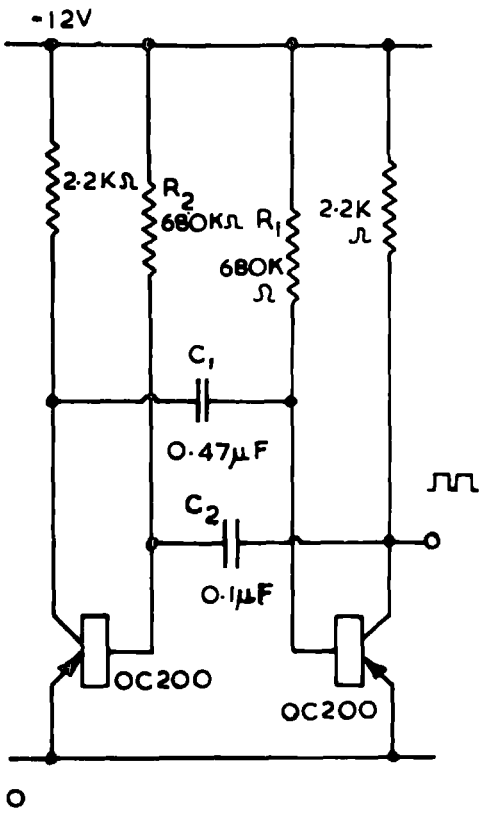

Astable Multivibrator

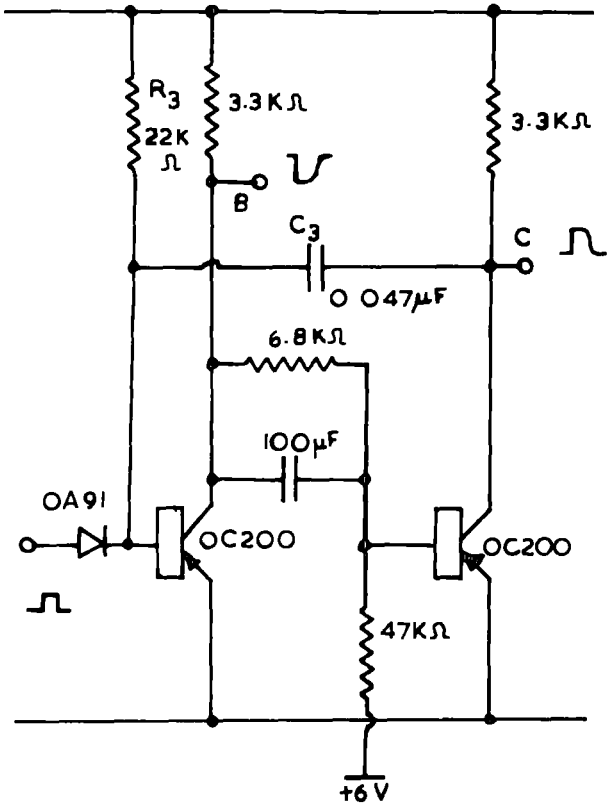

Monostable Multivibrator

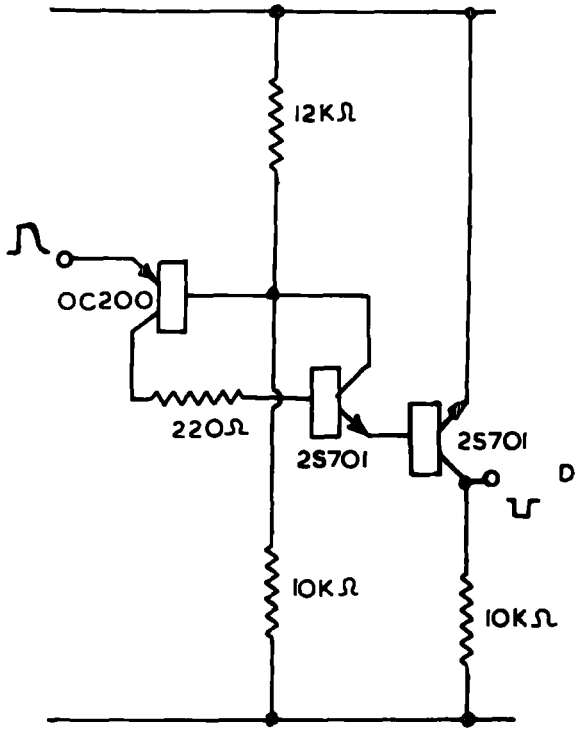

Pulse Shaper

Fig. 3.3. Gating Circuits.

(a) Transistor — Transistor Logic

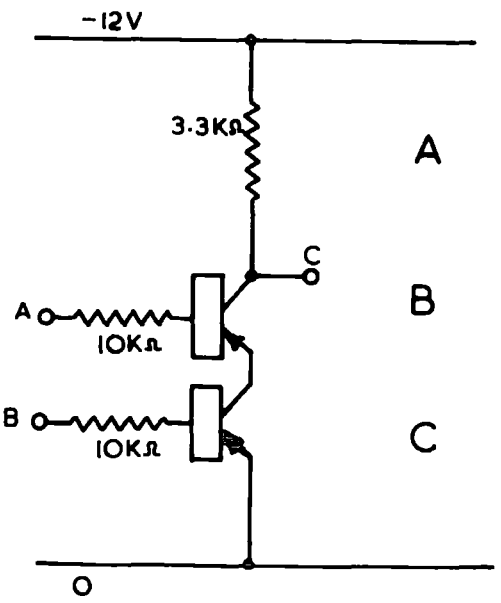

Input and Output form for TTL:

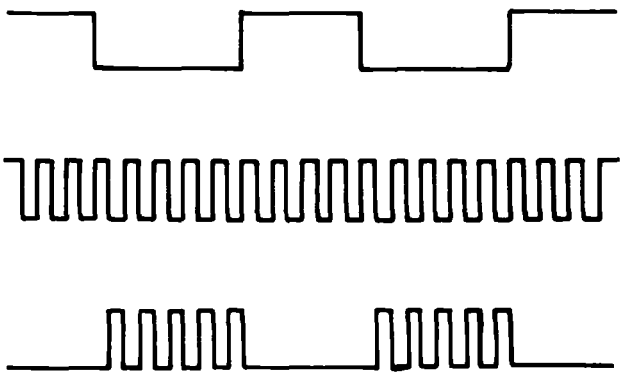

(b) Diode — Transistor Logic

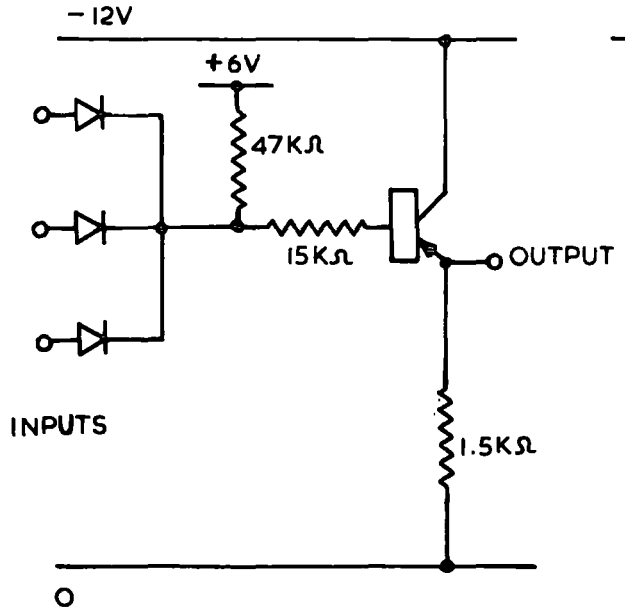

Truth Table for Both Gates:

INPUTS				OUTPUT
A	B	-	-	C
0	0	-	-	0
1	0	-	-	0
0	1	-	-	0
1	1	-	-	1

o Indicates absence of signal.

Fig.3.4. The Bistable Multivibrator as a Switch.

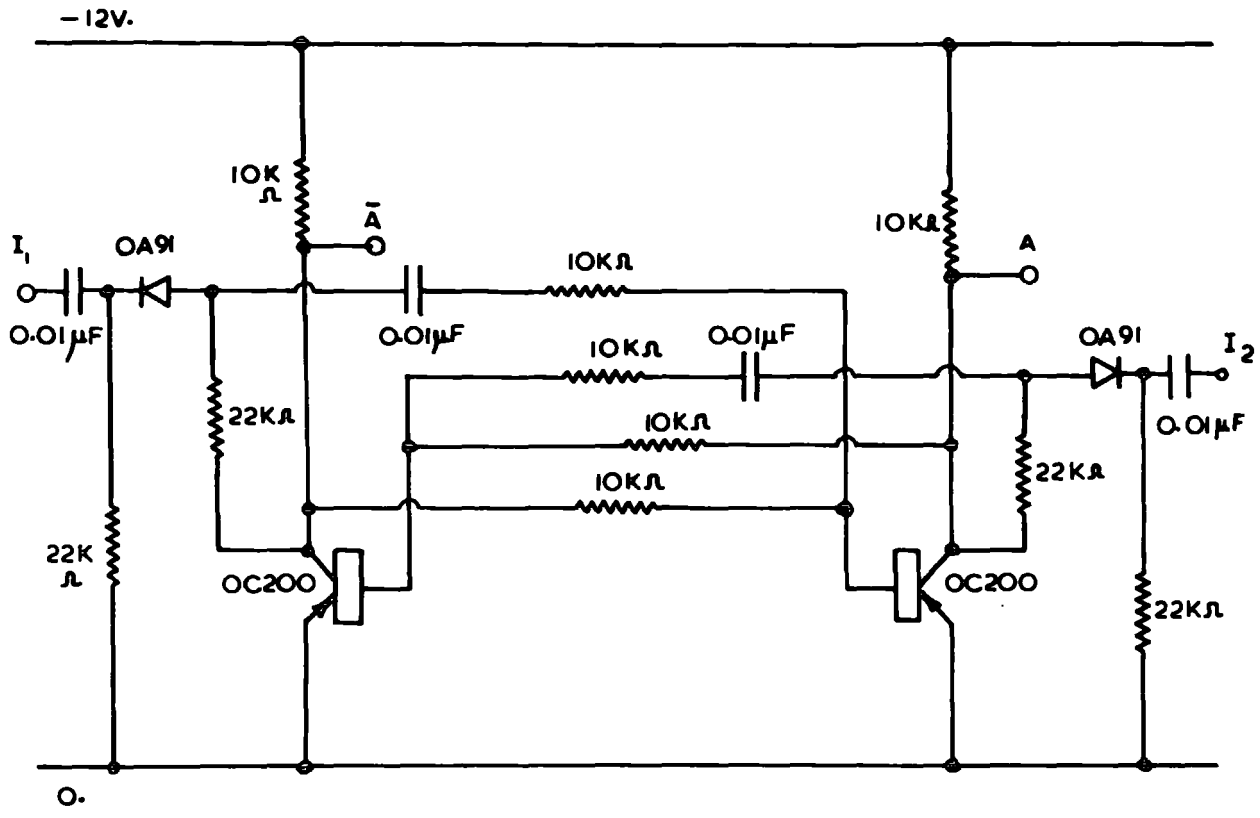

Logic Symbol for a Bistable Switch:

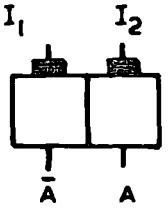

This circuit will change states as pulses are applied alternately to the two inputs.

Fig. 3.5. The Bistable Multivibrator as a Binary Counter.

Circuit diagram:

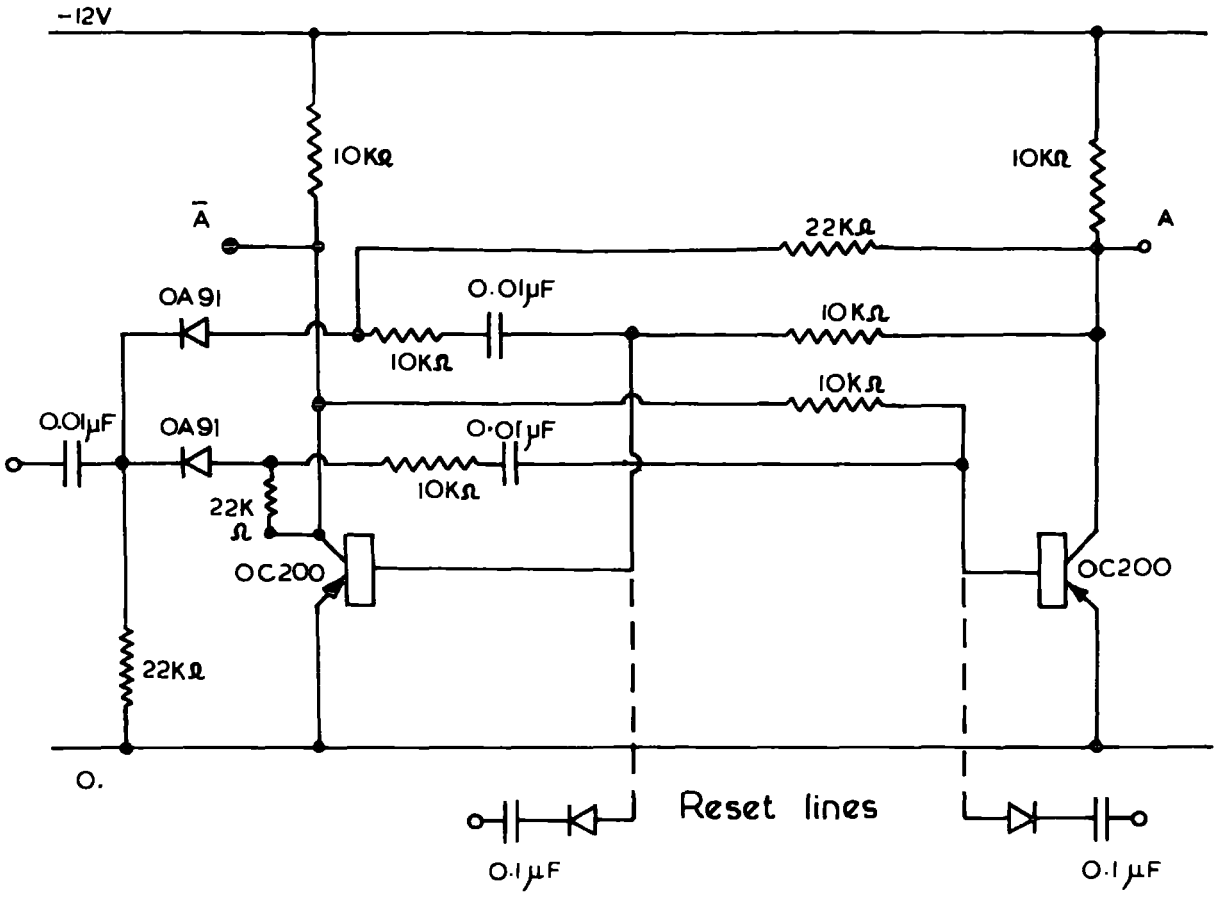

Logic Symbol for a Bistable Binary Counter:

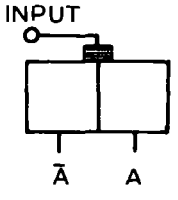

The Configuration for a Self Resetting Decade Counter:

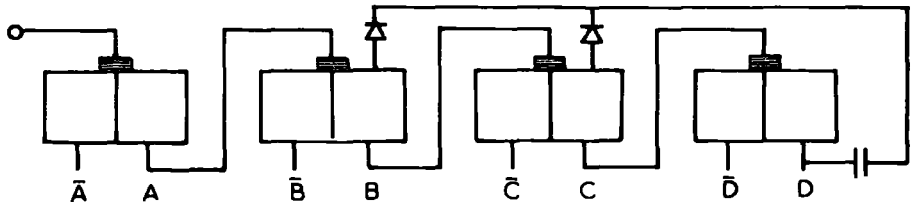

A scale of 3 :

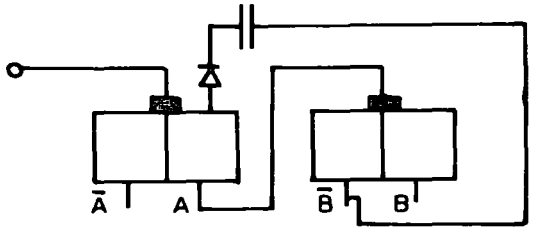

Fig. 3.6. Regulated Power Supply for -12V & -6V.

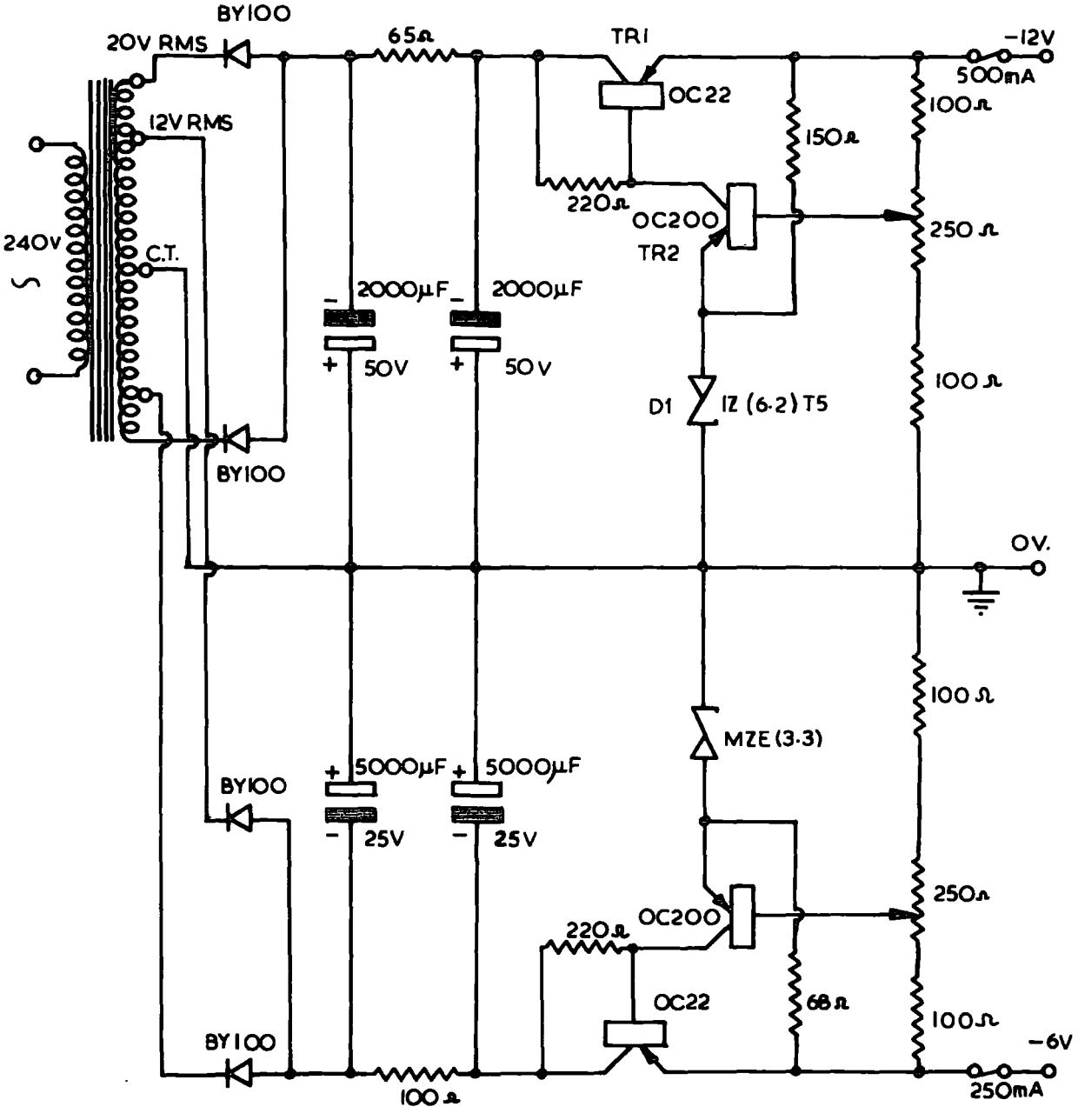

irrespective of the arrival of further pulses at I_1, until a pulse (probably a reset) is applied to input I_2, when the device is then returned to its original state. In this manner, the bistable can be used as a controllable switch, with the advantage that it will respond only to the first pulse received, and for this reason it is used in the recording system to eliminate the spurious pulses caused by 'chatter' and 'bounce' on mechanical switches.

In the alternative configuration, Fig. 3.5, with the two inputs connected together, the bistable will respond to each and every pulse, and is, therefore, acting as a binary scaler. Four such scalers, connected as in Fig. 3.5, will form a binary counter with a counting capacity of 10, and the outputs can be decoded by a diode matrix to obtain a decimal value of the count. Resetting to a particular state can be achieved by means of a pulse applied to the reset line, which is shown as a dashed line in Fig. 3.5.

This type of counter is used in the playback device (Sect. 3.4.3) as a 'programmer' for the necessary steps in the punching control logic, and in the recording system as a 'programmer' for the channel selector.

A combination of two bistables (Fig. 3.5), as a'scale of three', will give one output pulse for every three input pulses. This type of divider is used in the clock of the recording system (Sect. 3.4.2).

3.3.5 The power supplies

The demands for electrical power in this system can be separated into three distinct groups: the high current loadings made by electro-mechanical devices, the stabilised supplies required to provide fixed reference voltages for logic intelligence levels, and a power source for the general electronic circuitry.

A standard regulated power supply circuit was adopted and this was adapted to provide each of the different nominal voltages for the above groups. A dual purpose example (for -12V and -6V) is shown in Fig. 3.6. In this circuit, the Zener diode D1 provides a reference voltage in the emitter circuit of TR2. Transistor TR2 compares a fraction of the output voltage with the reference voltage of D1; it amplifies the difference and feeds a signal to TR1 in order to maintain a constant difference between the two voltages.

All supplies were stable for the loads imposed upon them, and the ripple on the outputs were typically less than 1 mV. For a full discussion of the problems of power supply design the reader is referred to 'Voltage Regulator (Zener) Diodes', published by Mullard Limited.

3.4 The basic actions of the system: recording

This consideration of the overall system is divided into two parts: firstly, the data conversion and recording process (as outlined in Fig. 3.7), and secondly, the playback of the record and the production of the paper-tape (Sect. 3.5).

3.4.1 The sampling rate of the recording system

The decision to set the sampling interval of the system to 3s was arrived at after consideration of several factors. The speed of the tape-punch and the number of different steps to be made by the electronics will set an upper limit to the sampling rate. This upper limit, however, is well above the rate which, according to the work of COLLIN, GROOM and HIGAZI (1966), will give a detailed and meaningful record of the sort of changes encountered in Atmospheric Electricity.

Fig.3.7. BLOCK DIAGRAM OF THE RECORDING OF THE SYSTEM.

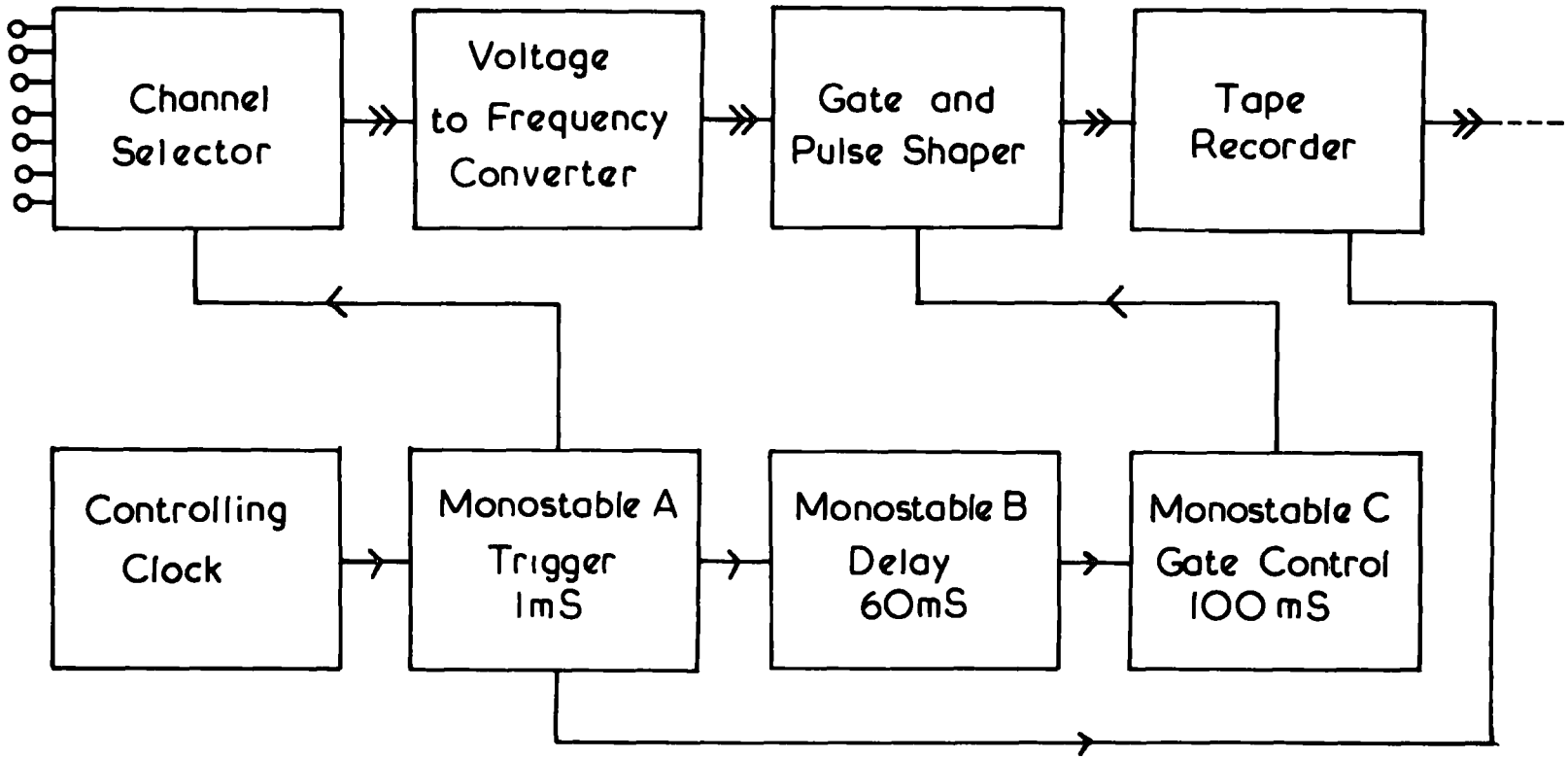

Using calculations of the autocorrelation coefficient for measurements of total conductivity these workers estimated a time interval within which there exists correlation between the members of the time series; this interval was found to be of the order of 5 minutes, and the difference between this and the 'relaxation time' of the atmosphere, given by ϵ_0/λ = 15 minutes (CHALMERS, 1967), was attributed to the influence of the wind. Repeated measurements taken more frequently than every few minutes are not, therefore, truly independent and could give rise to errors in the use of standard statistical tests. When the recording system is being employed to its full capacity of 10 different channels, a particular parameter would be sampled twice per minute, which ensures that no loss of detail should occur if the above considerations are valid.

Finally, a period of 3s allows the researcher to keep a written record of the data, and will also permit him to keep an eye on the behaviour of his instruments.

3.4.2 The clock and the channel selector

The operation of this part of the system is governed initially by the clock which produces an electric pulse every three seconds, derived in the case of the LandRover equipment from a Swiss-made precision clockwork movement opening a set of contacts once every second, and, in the case of the Lanehead apparatus, derived from a cam-operated micro-switch, driven by a synchronous mains motor, and also having a period of one second in the first instance. In both cases, the mechanically produced pulses are divided by a factor of 3 electronically (Sect. 3.3.4) and the resulting pulse is used to trigger the 1 ms monostable (A in Fig. 3.7). This causes the channel

selector to move on to the next channel, while, at the same moment, a pulse is inserted onto the recording. The channel selector is controlled by using four bistable circuits (Sect. 3.3.4) as a decade counter with their outputs decoded to switch the desired reed relay connecting the output of the measuring instrument to the voltage-to-frequency converter (Sect. 3.4.3). A facility is incorporated in the design of the channel selector whereby the programming decade counter will reset to the first channel after a predetermined number of channels have been sampled. Thus by changing the setting of a switch the system can be made to record cyclically any number, from 1 to 10, of different parameters.

3.4.3 The voltage-to-frequency converter

The channel selector connects the different parameters to the voltage-to-frequency converter of DE'SA and MOLYNEUX (1962), the circuit of which is given in Fig. 3.8, with a conversion characteristic, in Fig. 3.9. This circuit converts a given voltage level into a train of pulses, the frequency with which the pulses are repeated being proportional to the applied voltage (Fig. 3.10). Full details of the theory of this part of the system are given by DE'SA and MOLYNEUX (1962), but it is relevant to explain the necessity of the 'pulse-degrader' circuit which has been added after the 'gate'. One of the difficulties encountered by GROOM (1966), in his exploratory tests (Sect. 3.1), arose when he tried to record square pulses of the sort derived from the voltage-to-frequency converter on a magnetic tape-recorder of poor response, with the result that the recorder attempted a Fourier analysis of the pulses, giving, on playback, not only the basic frequency but also harmonics of this frequency. This was unsatisfactory. In order to avoid this in the present system, the form of the pulses is rounded off by means of

Fig. 3.8. The Voltage to Frequency Converter.

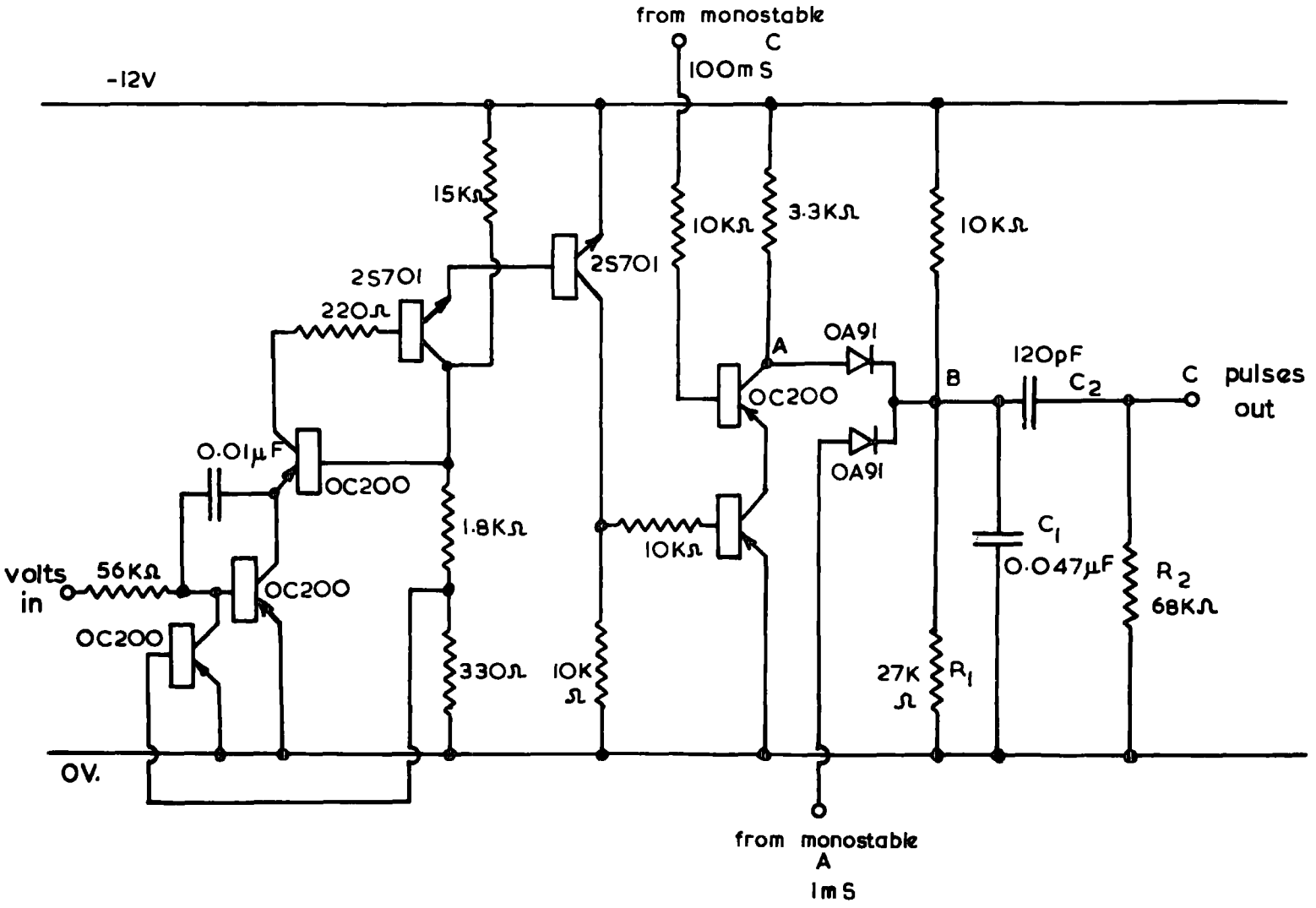

Fig. 3.9. Voltage-to-Frequency Conversion Characteristic

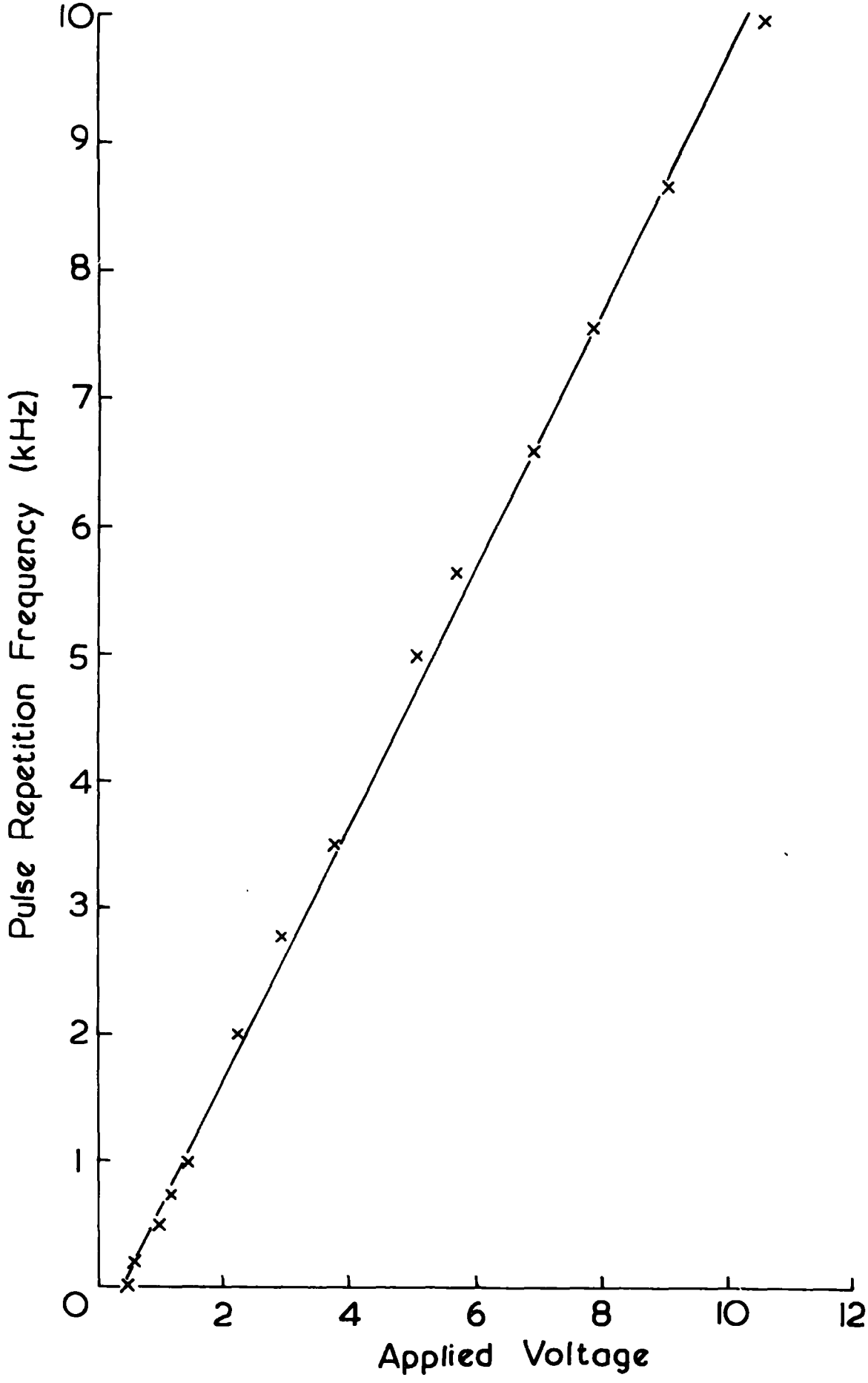

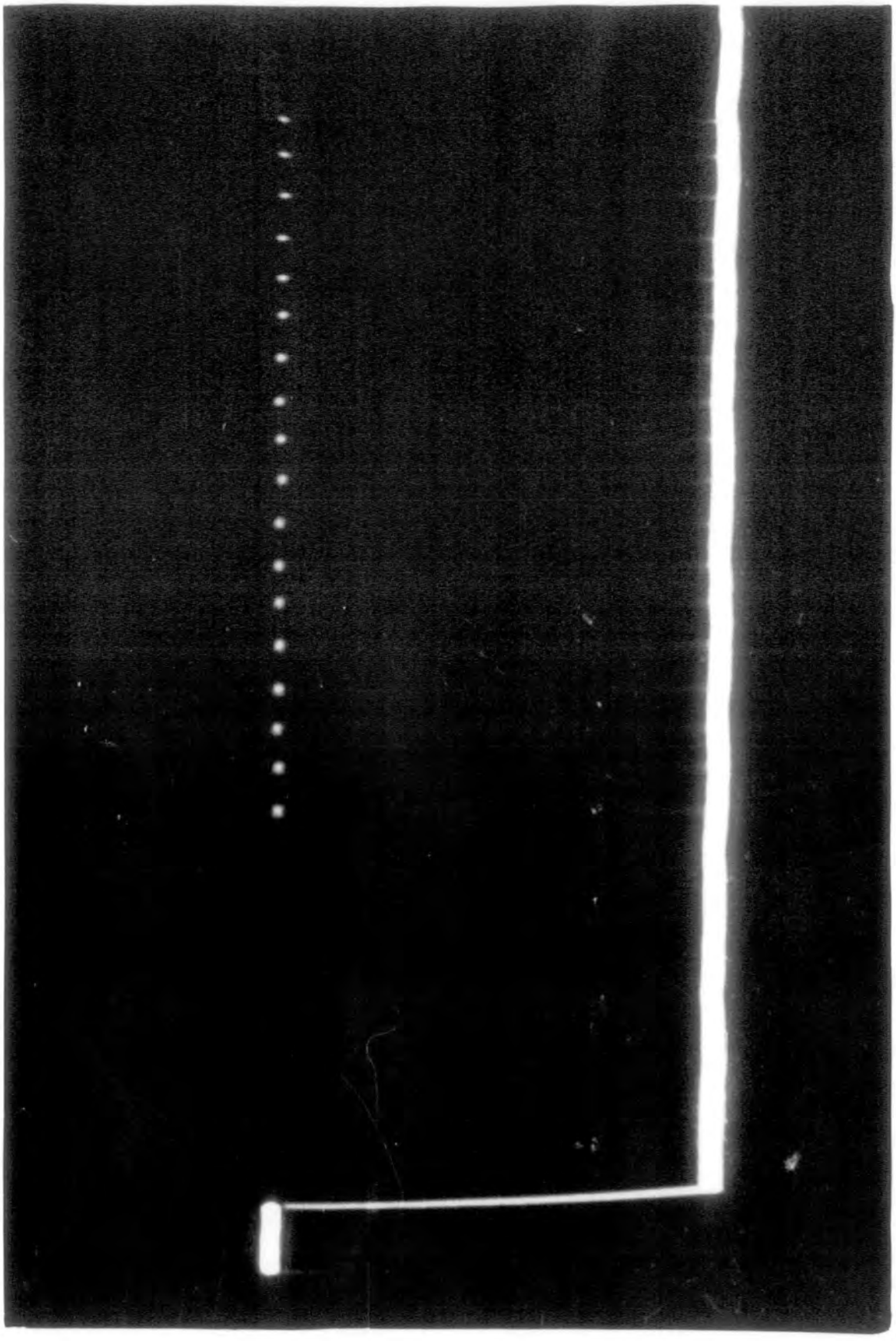

Fig. 3.10 Frequency-dependent pulses

R_1C_1 (Fig. 3.8) until they approximate to a sinusoidal shape, which, together with the better frequency response of the E.M.I. tape-recorder (Sect. 3.2.3) completely eliminates this problem.

However, another difficulty had to be resolved before the recording action could be deemed satisfactory. The output pulses from the converter are, by sign, positive only, with the consequence that when they are recorded a time-averaged voltage level is superimposed on the record; reasonably, the higher the repetition frequency of the pulses, the higher the level attained by the averaged voltage and this creates difficulties when the tape is replayed into the pulse analyser (Sect. 3.5.1). To alleviate this the pulses are passed through an RC filter (R_2C_2) which holds the average voltage level of the waveform at zero, irrespective of the repetition frequency. With these modifications incorporated into the system, satisfactory recording and playback were achieved on both speed ranges of the tape-recorder ($3\frac{3}{4}$ or $7\frac{1}{2}$ i.p.s.).

3.4.4 The 'time division multiplexing' of the data

In order that each parameter sampled should occupy a distinct and unique position on the magnetic tape (time division multiplexing, or TDM), careful timing of the recording process is required. A delay (monostable B in Fig. 3.7) of 60 ms is introduced between the recording of the trigger pulse from monostable A and the start of the period of 100 ms during which pulses are transmitted to the tape-recorder (Fig. 3.10). This delay is to allow the several reed relay switches involved to settle, for they have a finite period of 'bounce', both in the recording unit and in the playback processor. At the end of the 60 ms delay monostable C 'opens' the gate in the voltage-to-frequency circuit, thus allowing a certain number of pulses, dependent on the repetition frequency and

therefore also on the applied voltage, to pass as a 'packet' to the recording heads of the tape deck. It will readily be seen that with a maximum repetition frequency of 10 kHz (Fig. 3.9) and a gating period of 100 ms that the maximum number of pulses in any 'packet' can be taken as 999 and that a counter of this capacity is required to indicate the number of pulses per packet.

Thus far, the total time taken to record one parameter has been 161 ms, in a sampling period of 3s; this would clearly permit a much faster sampling frequency, but the limiting factor is the speed of the paper-tape punch which may have to punch up to 10 different characters for one parameter, at a rate of 5 per second. This does not, therefore, allow much room for increasing the sampling rate.

3.4.5 A summary

The stage has been reached where different output levels from measuring instruments are sampled cyclically, and are converted into a train of 'packets' of frequency-dependent pulses in a form suitable for magnetic tape recording or for direct introduction into the playback system (Sect. 3.2.2).

3.5 The basic actions of the system: playback

This section describes the operation of the playback processor which is represented in schematic form in Fig. 3.11.

At the start of the work on this system the University was using an Elliott 803 Computer, so that Elliott 5-hole code was the choice for the characters to be punched onto the paper-tape. Fortunately, when the University acquired an I.B.M. 360/67 Computer in 1968, it had facilities to read Elliott 5-hole code, and did not require major amendments to be

Fig. 3.11. BLOCK DIAGRAM OF THE PLAYBACK UNIT.

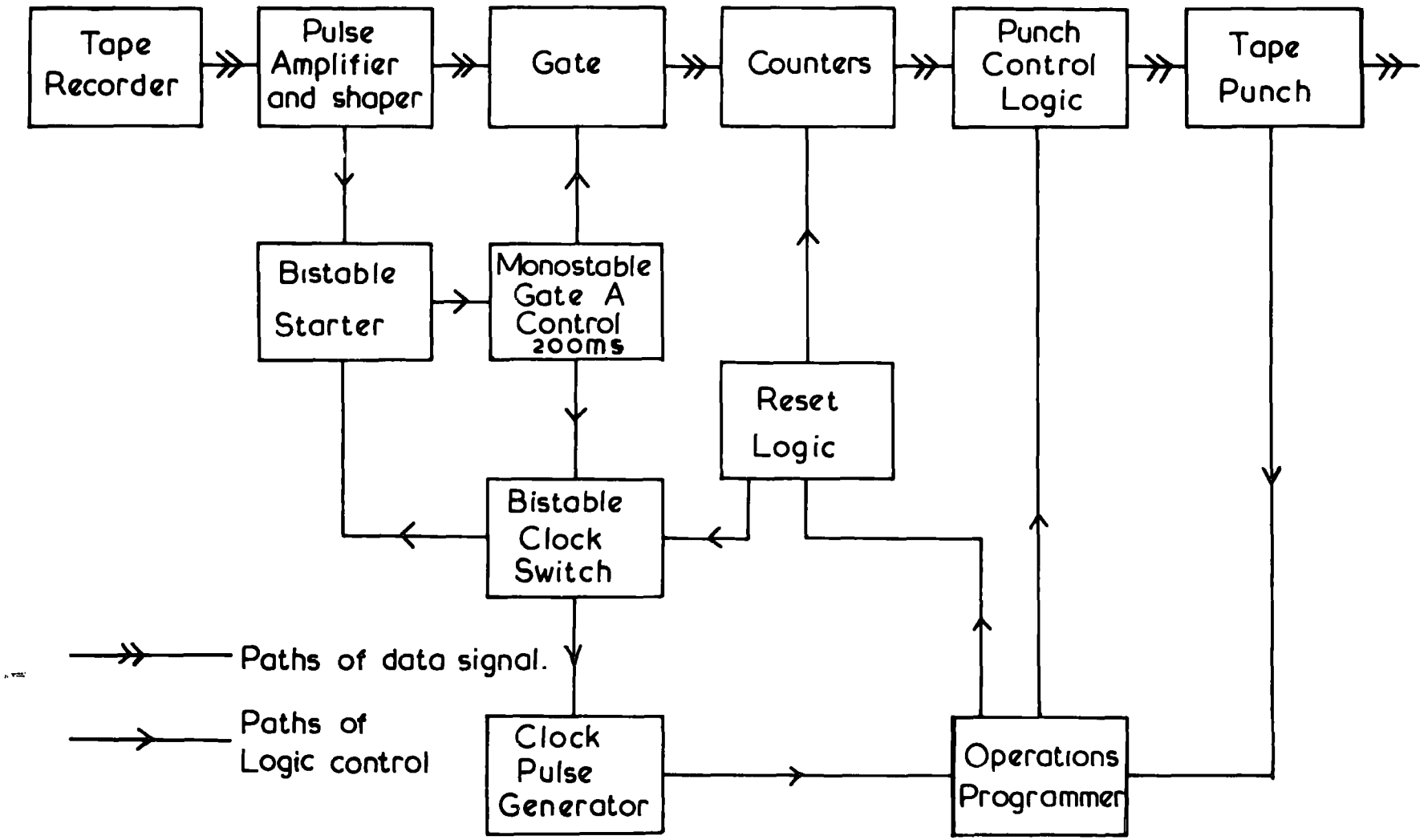

made to the recording system.

3.5.1 The pulse analyser and amplifier

The characteristic of peak-to-peak voltage against pulse frequency for the output of the tape-recorder is given in Fig. 3.12, and shows for the lower recording speed ($3\frac{3}{4}$ i.p.s.) that at the upper end of the frequency range the voltage is reduced by a factor of 10. It is necessary to treat this output in order to submit it to the counters as identical pulses, irrespective of their repetition frequency. This is achieved by amplifying the signal with a two-stage transistor audio-frequency amplifier (Fig. 3.13) to a level such that the smallest peak-to-peak input voltage encountered will overdrive the following stage. The constant size pulses produced in this way are fed into a pulse-shaper (Sect. 3.3.2) to invert them and to give them a rise time (less than 200 ms) fast enough to trigger the Quarndon counters (Sect. 3.2.5). The trigger pulse, duly recorded before each data 'packet', undergoes the same treatment; it is used to switch the bistable unit which initiates the succeeding operations in the system, and is also registered by the parameter counter decade.

3.5.2 The starting circuit

The bistable 'starter' circuit which is switched by the trigger pulse in turn triggers the monostable A (Fig. 3.11); the leading edge of the 200 ms opens the gate to allow the 'packet' of frequency pulses to pass to the counters. The trailing edge of the pulse closes the gate before the arrival of the next parameter, and also operates the bistable clock switch.

3.5.3 The clock pulse generator

The leading edge of the clock pulse, derived from an astable multivibrator (Sect. 3.3.1), having been passed by the clock switch gate, triggers a bistable 'memory unit', and passes a pulse to the programmer. No further pulses can pass this way until a 'message complete' signal arrives from the punch, to reset the 'memory unit'.

The trailing edge of the pulse causes the solenoid-controlled clutch of the tape-punch to engage, and one punching operation is undertaken and completed with the closing of the micro-switch which signals 'message complete' to the 'memory unit'. The next clock pulse to arrive will be able to drive the programmer on one step only on completion of the current task, and the system is safeguarded against missing or duplicating a punching operation.

3.5.4 The programmer

This circuit dictates the sequence in which the various tasks allotted to the tape-punch are carried out. It comprises a decade counter unit (Sect. 3.3.4), taking the allowed clock pulse as its signal to pass to the next position, and uses a conventional diode matrix network to decode its binary output to control the punch-pin selector logic. There are normally 5 different operations to be performed in the punching of a number but on reading the last parameter of a cycle 9 operations are engaged. The tasks can be tabulated thus:

Fig. 3.12. Peak to Peak Output Voltage Against Pulse Repetition Frequency for the E.M.I. Tape-Recorder.

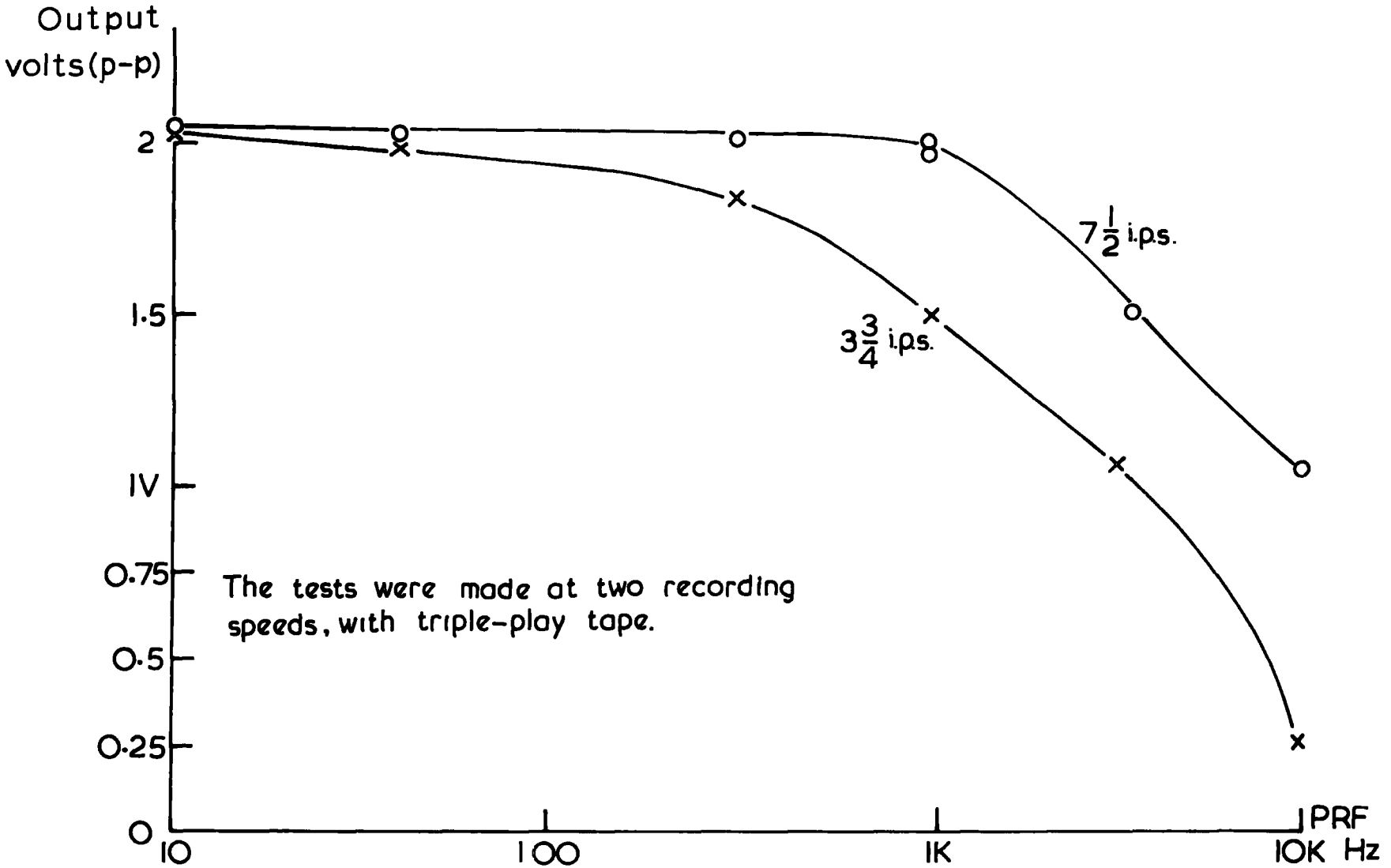

Fig. 3.13. Pulse Amplifier and reshaper.

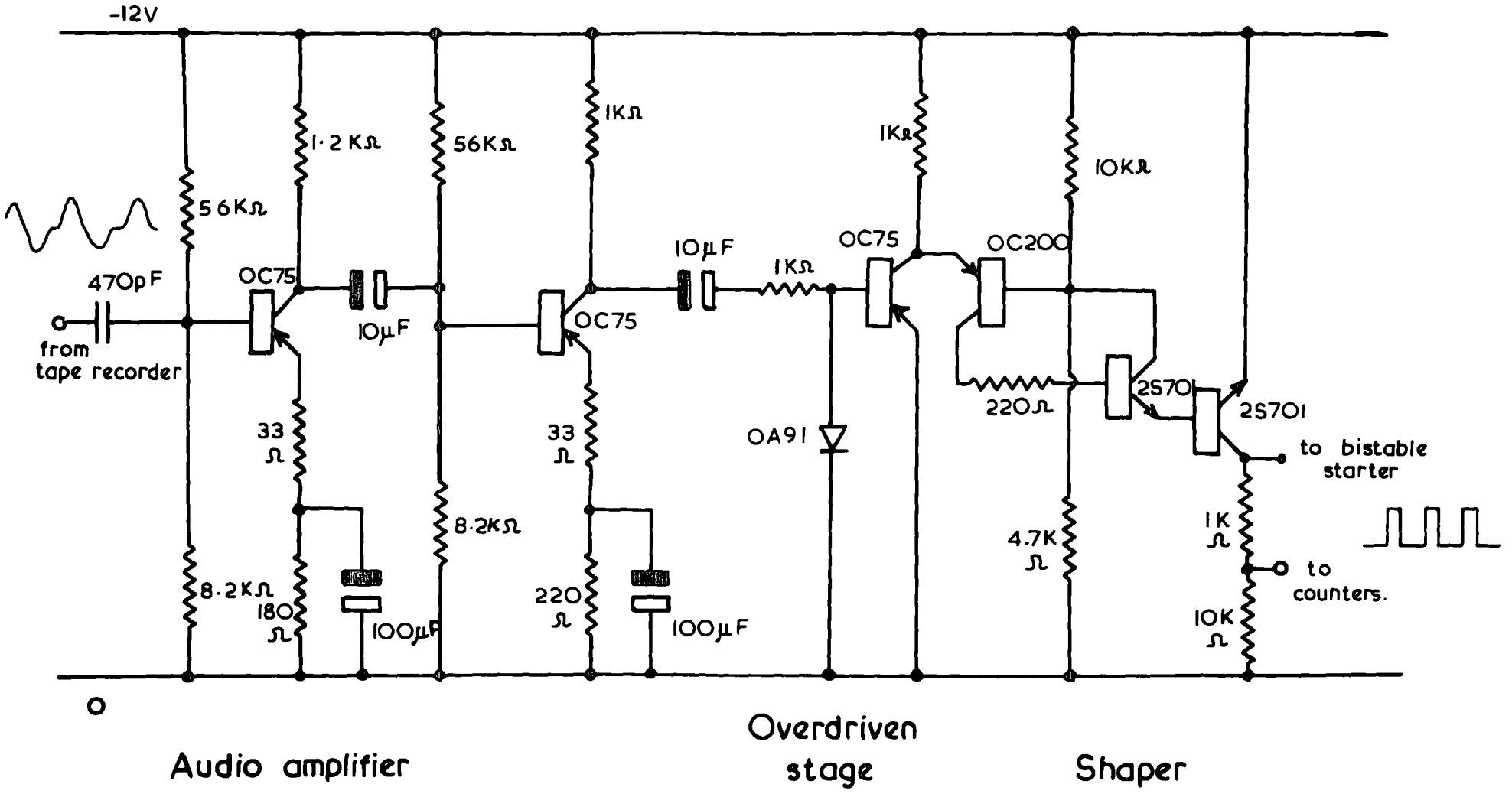

Order of execution	Appointed task
0	wait for pulse
1	punch the space character
2	punch the hundreds digit character
3	punch the tens digit character
4	punch the units digit character
5	reset to 0 normally, or go to 6
6	punch carriage-return character
7	punch line-feed character
8	reset to 0.

Steps 6 and 7 command the punching of the carriage-return and line-feed characters necessary to give a tabulated form if a printed list of the data is required.

3.5.5 The reset procedure

If step 5 of the programmer is valid, reset pulses are applied to the Quarndon counters, the programmer and the bistable starter circuits. The system is then prepared for the arrival of the next trigger pulse, heralding another parameter.

If, however, the parameter currently being processed is the final one of the cycle, as indicated by the parameter counter, step 5 is by-passed and the programmer executes 6, 7 and 8. Step 8 resets the system in the same manner as step 5, with an added reset pulse being applied to the parameter counter, indicating that the next trigger pulse to arrive is the first of the cycle.

3.5.6 The parameter counter

This is a further application of the binary decade scaler (Sect. 3.3.4) and it is employed to count the number of trigger pulses which arrive at the processor. The system operator is able to select the number of channels (from 1 to 10) appropriate to the number of parameters he wishes to record, and on arrival at this number, the parameter counter circuit causes step 5 (the normal reset) to be overridden, and the carriage-return and line-feed characters are duly punched.

3.6 The performance and accuracy of the recording system

The short- and long-term consistencies of measurement of the system were tested by applying known reference voltages to the inputs, and then examining the resulting count values. These were found to remain accurate to better than $\pm \frac{1}{4}$ per cent of full-scale in the case of short (one day) runs, and over a longer period (one month) the output values showed a maximum variation of $\pm \frac{1}{2}$ per cent of full-scale. These values are worth comparing with the $\pm$ 2 per cent accuracy quoted by SHARPLESS (1968) for his paper-chart measurements with the same instruments which were employed in this research, and this tolerance is deemed to be entirely satisfactory in view of the accuracy with which measurements are normally possible in Atmospheric Electricity. The operation in the field by Mr. Stringfellow, a colleague of the author's, of the magnetic-tape recording facility of the system revealed no loss of accuracy.

During the early testing of the system, random character punching errors were encountered, which were at first attributed to possible faults in the electronic circuitry. It was eventually discovered that the errors were due to insufficient tensioning in the return springs of the punch pins, on what should have been a new and perfect machine. Once this had

Fig. 3.14 The automatic recording system

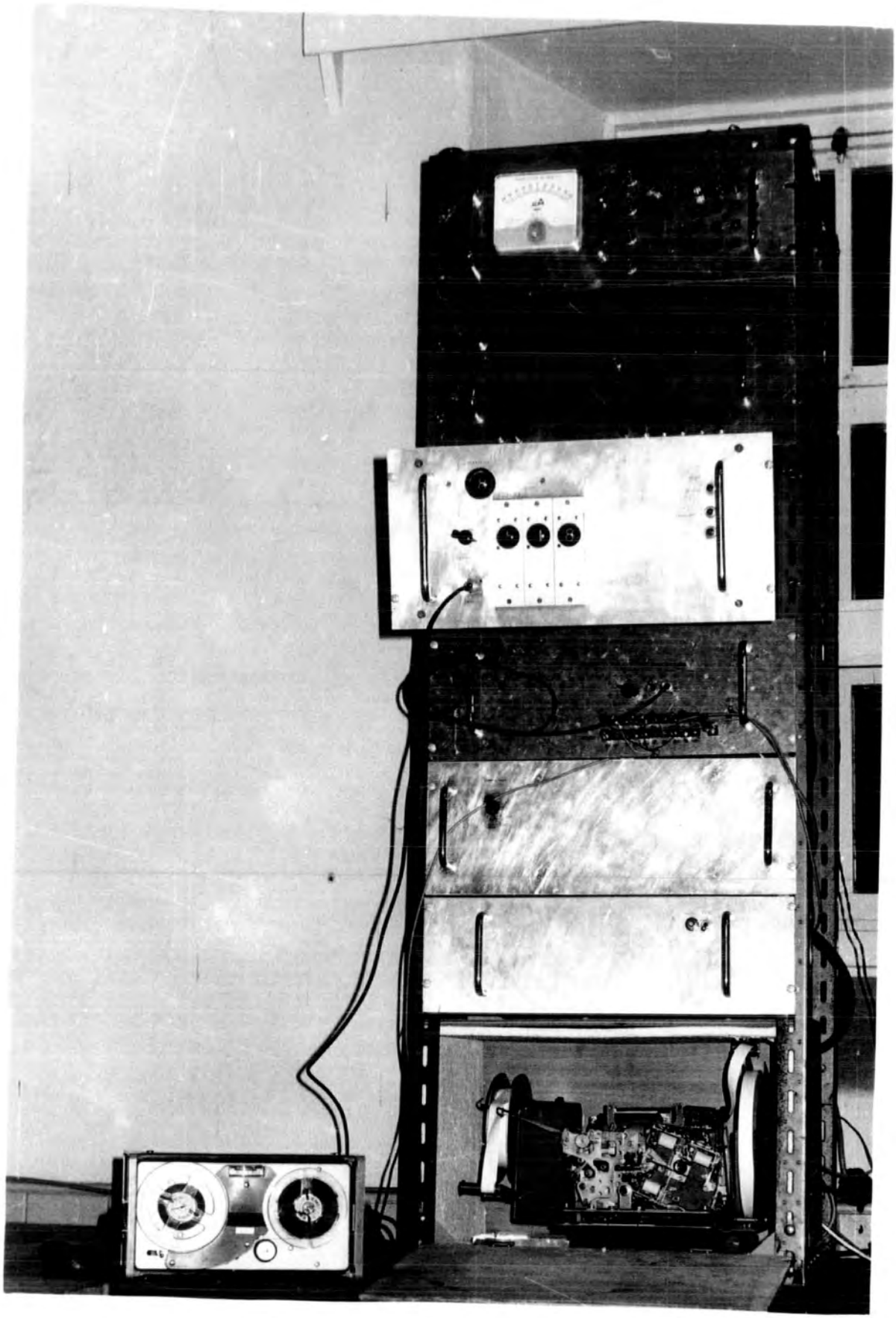

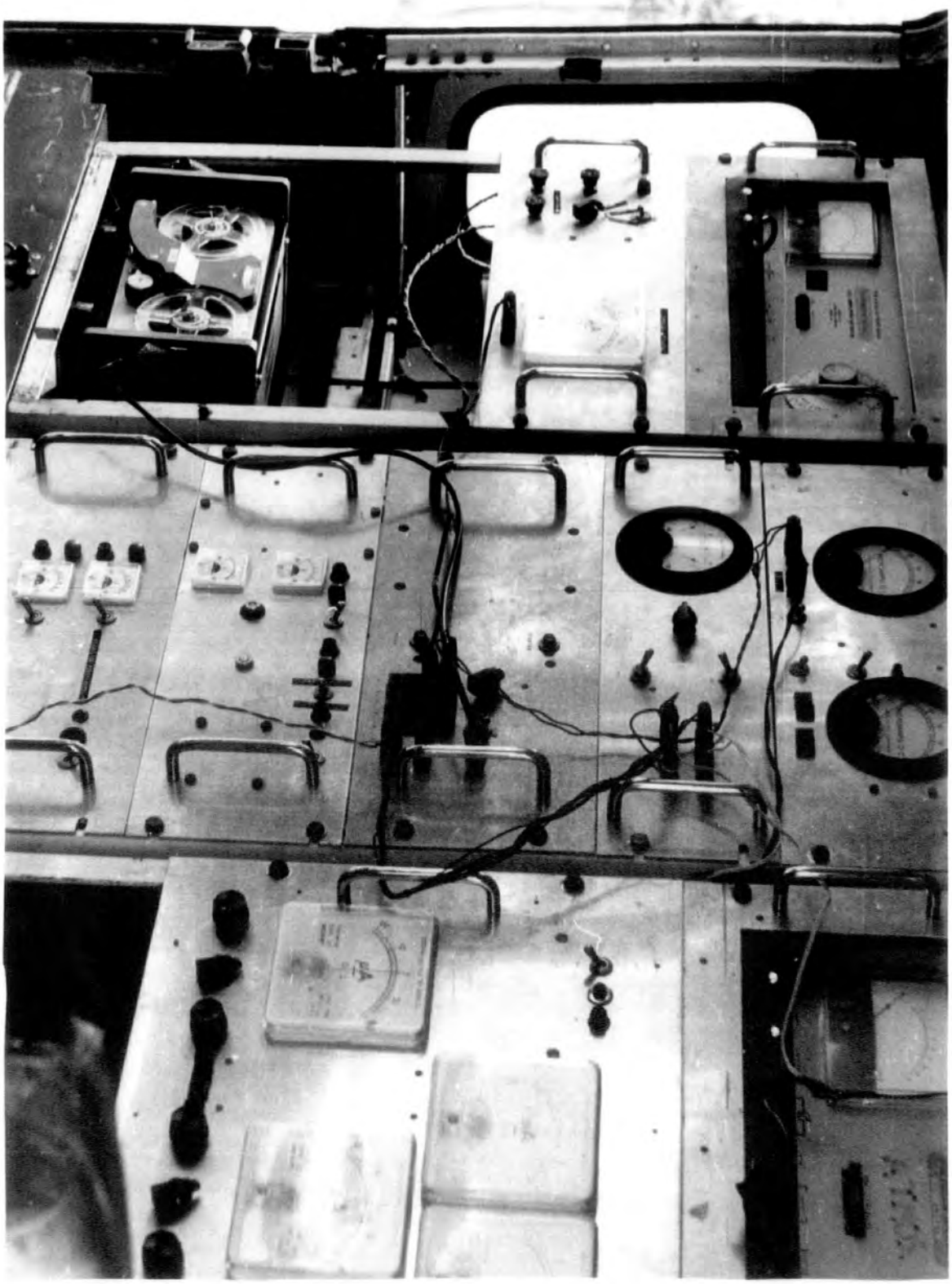

Fig. 3.15 The recording unit in the LandRover

been corrected the recording system functioned as reliably and well as any of the commercially produced devices of a similar nature which the author has had occasion to use. The panel rack housing the system, together with the 1-hour recording circuitry (Chapter 7) is illustrated in Fig. 3.14.

CHAPTER 4

THE INSTRUMENTATION AT LANEHEAD SCHOOL

4.1 The situation of the school

Lanehead is a small settlement in Upper Weardale, situated at a height of 440 m above sea level, and on the eastern facing slopes of the North Pennines. The building, which used to house the village school, has been the property of the Durham University Department of Geography for a number of years and serves as an accommodation centre for field trips. The surrounding countryside undulates quite gently, being of an agricultural nature on the lower levels, whilst heath and moorland cover the tops of the hills. The geographical position of Lanehead is latitude $54^{\circ}39'$ north and longitude $2^{\circ}15'$ west from the Greenwich meridian; the Ordnance Survey Map reference is 843417.

A class B road gives access to the school from Durham and this road continues over the Pennines to Alston and the Lake District. The density of traffic is very low, with the exception of a few weekends in the summer months, and, as a consequence, the pollution effects of vehicle exhausts are small and transient.

The Weardale Cement Works are reasonably remote at 11 km away to the east and with the prevailing wind from the west, this source of particulate pollution has no discernible influence on electric measurements made at Lanehead (SHARPLESS, 1968).

A survey conducted by members of the Geography Department, failed to detect any solid airborne matter at the school, except on the rare occasions when the wind was from the direction of the iron and steel works at Consett. It is probable that the region of Upper Weardale is as free from pollution as any in the country maintaining the necessary services

Fig. 4.1 The Atmospheric Physics plot at Lanehead

and facilities.

Lanehead was chosen as the site for a study of atmospheric electric elements in conditions of low air pollution and an experimental station was established at the Field Centre by SHARPLESS (1968). The school building faces south over the valley, its frontage comprising a tarmacadam playground with margins of grass. An area of grass in the north-eastern corner has been fenced in to form an enclosure free from invasion by stray sheep and calves. The plot (Fig. 4.1) is provided with surface drainage and has a cable duct linking it to the laboratory in the school. Concrete pits were constructed to house the instruments at ground level . This preliminary work was undertaken by SHARPLESS (1968) before starting his investigation and the fact that it has been possible to take over and run for a further year, with a minimum of trouble, the instruments installed at Lanehead is testimony to the ability and foresight with which the station was prepared by Dr. Sharpless.

Part I The permanent instrumentation

4.2 The field mill

4.2.1 Special features

Potential gradient can be measured by a number of different techniques and the reader is invited to study CHALMERS (1967) for a full discussion of the subject.

A standard pattern of field mill (Fig. 4.2) was adopted for the work at Lanehead which employed an artificial bias to displace the zero reading, thereby giving a form of sign discrimination. The output signal was amplified by a two-stage amplifier, using n-p-n silicon planar transistors (type BC 109), which was designed by STROMBERG (1968). An input impedance

of 30 MΩ was obtained and this proved adequate for the purposes of the field mill. The two amplifier stages, each employing negative feedback to control the gain, had an overall gain of 100 and a facility was included in the design of the circuit such that a relay, switched from inside the laboratory, could alter this overall gain thereby achieving a change of range of measurement. The two ranges of the instrument finally decided upon were ± 9000 Vm^{-1} and ± 900 Vm^{-1}, but for the purpose of this work only the lower range was employed.

The field mill, which was operated in an inverted position to protect it from the weather, was calibrated by SHARPLESS (1968) by placing it, in an upright position, under a calibration plate. The same treatment was afforded to a spare mill of identical design. A comparison was then made, at Lanehead, between the output of the inverted mill, with its stator 1m above the ground, and the output of the spare mill, which was set in the surface of the ground. This was done continuously for several hours during fair weather so that different conditions of space charge could be averaged out. The exposure factor of the inverted mill represents the ratio of the potential gradient at the mill to that over perfectly level ground, and this factor is dependent on the density of space charge between the mill and the ground. It is for this reason that it is necessary to average out the space charge fluctuations. Having been calibrated, the mill remained unaltered save only for the regular check which was made on the zero field setting by covering the exposed part of the mill with a suitable aluminium box.

4.2.2 The installation and maintenance of the field mill

The components of the field mill were housed in an aluminium box which was bolted to a Handy-angle framework stand set in the ground.

Fig.4.2. The Field Mill.

(a) Principal of Operation

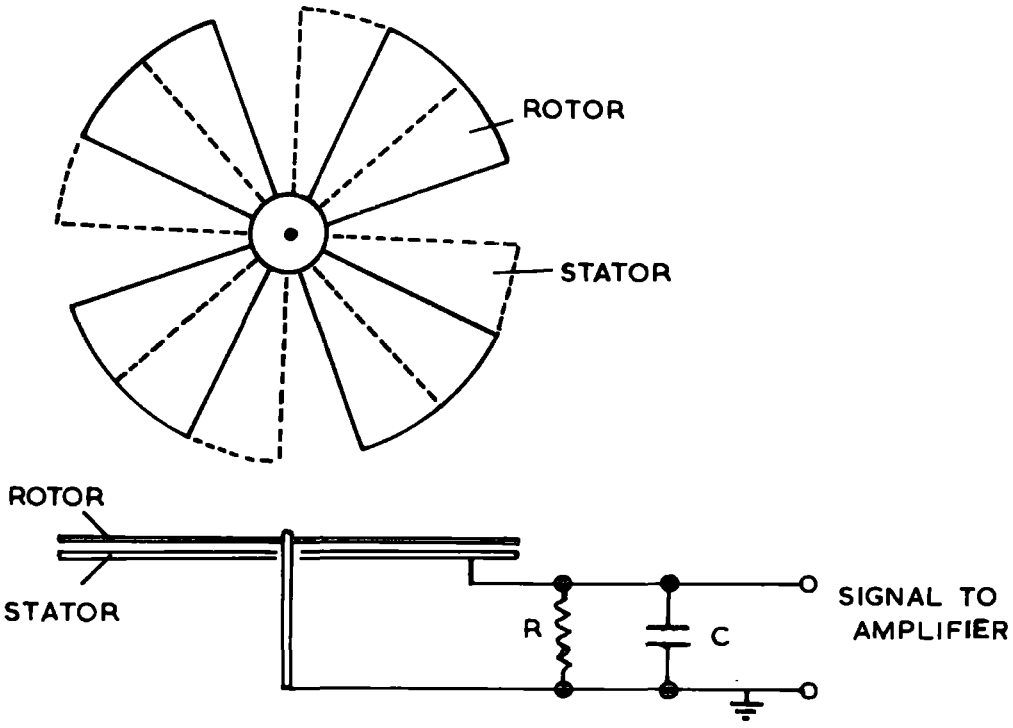

(b) Construction

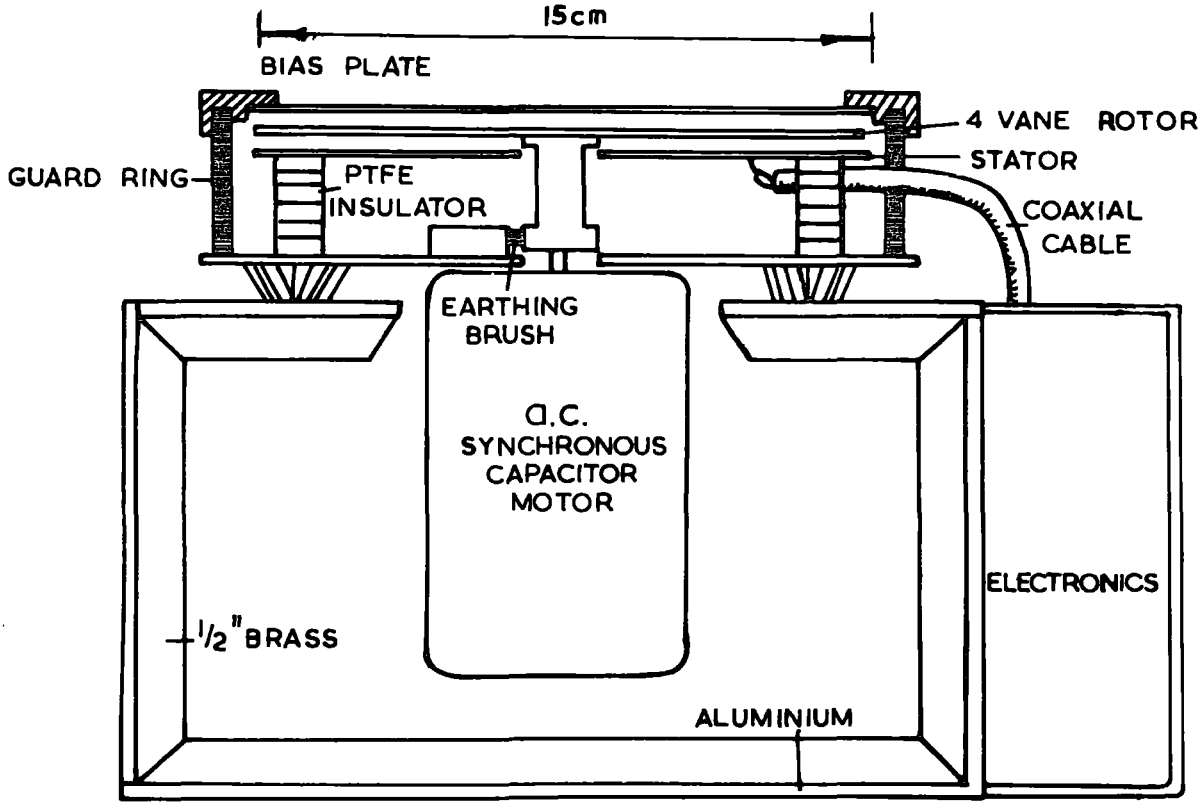

Protection from the weather was afforded by a piece of aluminium, in the form of a truncated pyramid, which fitted over the top of the stand (Fig. 4.1).

The rotor, stator and bias plate assembly was attached to the housing by means of flexible rubber mounts (Fig. 4.2). These have a tendency to perish and collapse, but regular inspection ensured that it was possible to replace these parts with new ones before any damage could occur. It was also felt advisable to clean, at the same time, the polytetrafluoroethylene (P.T.F.E.) insulations which isolate the stator plate from the rest of the mill. Trichlorethylene was used for this purpose. In these respects the field mill was trouble-free, but the brushless a.c. synchronous capacitor motor was damaged by a mains power failure, in the hard weather of March 1969, which allowed the moving parts to become frozen solid. When the supply was restored some windings of the commutator were burnt out, but the author had the good fortune to find a suitable substitute motor in an old field mill relinquished by a former member of the Research Group.

4.2.3 Accuracy

The displaced zero method of sign discrimination required high standards of stability of both amplifier gain and bias voltage. The latter could be maintained to within 1 per cent, but the stability of the amplifier depended on the variation of the supply voltage. With a stabilised power supply, the long term variations were mostly no more than 3 to 4 per cent of full-scale positive or negative, so that with frequent zero checks the error could be taken as about 2 per cent. For the range $\pm$ 900 Vm^{-1}, the error was about 18 Vm^{-1} which is equivalent to about 10 per cent of the normal fair weather potential gradient. SHARPLESS (1968)

was satisfied that the variation of the exposure factor of the inverted field mill, dependent on the density of space charge near the ground, was small in fair weather.

4.3 The total air-earth current collector

4.3.1 The measurement of the fair weather air-earth current density

The charge arriving at a point on the earth's surface in fair weather may be divided into two components, one of which is the conduction current representing the net movement of charged ions under the influence of the electric field. The other component is derived from the transport of charged particles to the surface by non-electrical mechanisms such as local air movements. For the whole globe the sum of the charges brought to earth by these mechanical means is presumably zero, but for a small portion of the earth's surface, such as we are considering, this component is not zero and, at any given time, will make a major contribution to the current density measured at that point. Two methods have been employed by experimentalists to study the air-earth current density. The 'direct method' measures the actual current to an electrically isolated portion of the earth's surface and the 'indirect method' measures the conduction current density in the air above the earth's surface at the place of measurement. NOLAN and NOLAN (1937) showed that, for their measurements, the difference between the two methods was less than 10 per cent, but LAW (1963), with field measurements at Cambridge, and DAYARATNA (1969), with some wind-tunnel experiments, have shown that we must consider there to be advective transport of charge of the same magnitude as the conduction current. For the purposes of this work, the term 'mechanical-transfer current' is preferred to indicate all mechanical transfer of charge, whether by convective motion, eddy diffusion or general wind forces, and

the value of this current will be calculated from the difference between measurements by the direct and the indirect methods.

4.3.2 Compensation for displacement currents

The total air-earth current in fair weather comprises both conduction and mechanical-transfer currents and may be measured by the direct method by observing the rate at which an isolated section of the earth's surface accumulates charge. As a result of the potential gradient, the surface of a collector will contain a bound charge and this bound charge will change as the potential gradient changes. This gives rise to the displacement current (CHALMERS, 1967) the magnitude of which can be illustrated by an example.

The bound change Q associated with a potential gradient F is given by:

$$Q = - A \epsilon_o F$$

where A is the area of the surface and ϵ_o is the permittivity of free space. The current density due to a change dF in time dt is:

$$\frac{dQ}{dt} = - A \epsilon_o \frac{dF}{dt}$$

If $A = 1\ m^2$ and $\frac{dF}{dt}$ is $1\ V\ m^{-1}s^{-1}$ then the value of $\frac{dQ}{dt}$ is $8.85\ pA\ m^{-2}$, and this must be compared with a typical fair weather air current density of $2\ pA\ m^{-2}$.

CHALMERS (1967) describes various techniques for the compensation of displacement currents and gives full details of the well-known method of KASEMIR (1955) which sets the time constant of the measuring instrument equal to the relaxation time of the surrounding air. A form of compensation similar to Kasemir's was used in this work.

4.3.3 Precipitation current measurements

In rain, the exposed collector will also receive a current-contribution due to the charge on the precipitation particles, and if the conduction current is estimated by the indirect method, it is possible to obtain a value for the precipitation current. The collector at Lanehead was used for both purposes: precipitation current and fair weather air-earth current measurements. For the precipitation work, a normal KASEMIR (1955) compensation network, with RC equal to about 15 minutes, would prevent the instrument from responding to short-term changes in the precipitation component of the total current, and as the work was aimed at accurate time correlations between precipitation current and potential gradient, this would not be satisfactory. The fact that the recording method involved digital data meant that it was possible to use the computer to calculate and compensate for displacement currents, but it was still necessary to take steps to prevent such currents from causing the output of the V.R.E. from being continually 'off-scale'. It was found, by trial and error, that the shortest time constant, which achieved a desirable attenuation of the displacement current, was with RC equal to 20 s. It was felt that this time constant would not seriously inhibit the recording of fine detail as, once again, the computer could be used to estimate true currents from the values integrated over a short period (Chapter 5).

4.3.4 Fair weather air-earth current measurement

A new approach to the continuous recording of fair weather measurements (Chapter 7) has been made by using integrating circuits with long time constants (RC = 15 minutes), the outputs of which are sampled, digitized and punched on to paper-tape every hour. We must consider how

Fig. 4.3 The air-earth current collector

partial KASEMIR compensation (RC = 20 s) fits into this scheme as the V.R.E. will still measure a large fraction of any displacement current occurring. These relatively fast changes in current will be smoothed out by the integrating circuits, which respond to variations taking at least 60 to 75 minutes, and it follows that the only contribution to the measured current made by a change in bound charge will be that due to the net difference between the bound charge at the beginning and the end of each hourly period. If the net change in potential gradient in the hour is 20 Vm^{-1} then the net change in bound charge will be 177 pC m^{-2}, and the average displacement current will be 0.05 pA m^{-2} or about 2 per cent of the normal air-earth current.

4.3.5 The construction of the collector

The collector was a circular aluminium dish shape of effective area 0.4 m^2, which was filled with soil in order to approach, as nearly as possible, natural conditions. A concrete pit contained a Handy-angle frame supporting the collector so that its soil surface was flush with the surrounding ground (Fig. 4.3). A gap of 2 cm separated the collector from an aluminium guard ring set into the ground, and the insulation from earth was effected by standing the collector on four pairs of P.T.F.E. mounts, which were shielded and fitted with heating coils to prevent condensation. The V.R.E. head unit was attached to the Handy-angle frame and the input was taken to the unit by a rigid copper-clad coaxial cable from a brass pin on the underside of the collector.

4.3.6 The accuracy and reliability of the collector

The long term stability of the air-earth current zero was always well within 2 per cent of full-scale of the 1 mA pen recorder, which was used for checking purposes. These checks were made at the times when the

field mill was being tested, and were done by placing a large earthed aluminium plate over and close to the collector. The V.R.E. generally needed no adjustment.

It was also necessary to make very frequent examinations of the P.T.F.E. insulators as the warmth from the heating coils was attractive to insects. This difficulty was alleviated to some extent by putting a regular charge of strong disinfectant into the concrete pit. The other major causes of insulation breakdown were seasonal: in the summer months grass and clover would grow across the gap between the collector and the guard ring, and, in the winter, snow would cause the same failing. The only tactic to combat this problem was to inspect the gap as frequently as possible.

The V.R.E. for this instrument, in common with two of the three others, was put out of action for three days in March 1969 when a number of mains powers failures caused valves to be alternately heated and cooled, and in a laboratory temperature of about - 10°C it was not surprising that some of the valves cracked.

4.4 The conductivity chambers

The practice of using totally exposed air-earth current collectors for a study of the characteristics ofprecipitation currents (for example, CHALMERS, 1956) has relied on the assumption that the conduction current, although its presence was acknowledged, was small compared to the precipitation current. For this work, in conditions of electrically quiet rain, a conduction current of 4 pA m^{-2} might represent more than 20 per cent of the total current to ground. This would produce a serious uncertainty in the value, and even the sign, of the computed precipitation current. It was felt desirable to allow for

Fig.4.4. The Conductivity Chamber

(a) Principal of operation:

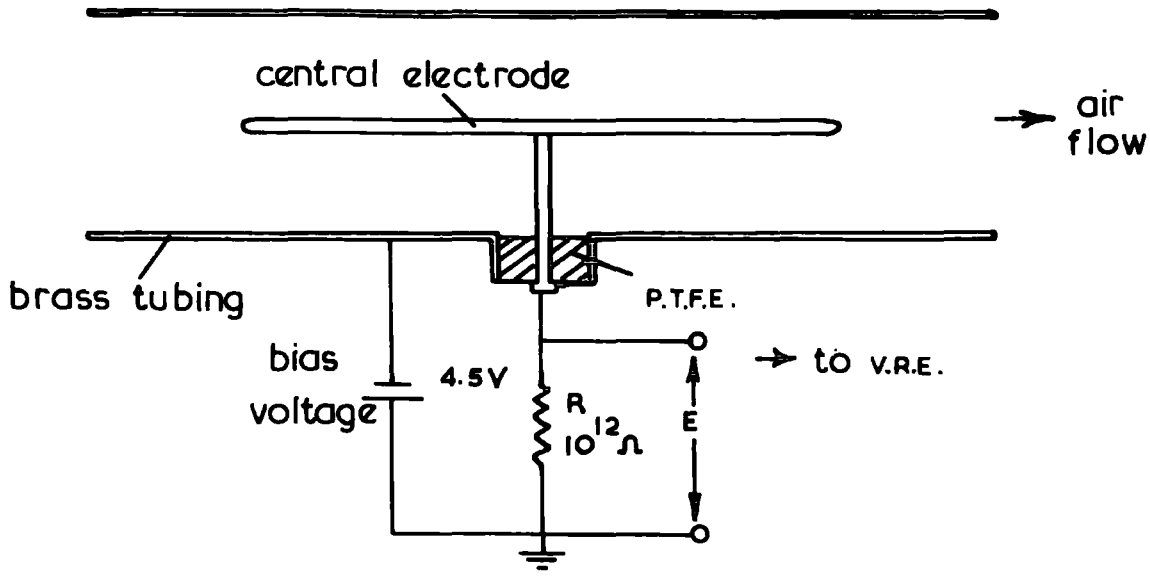

(b) Ionic current – Bias voltage characteristic:

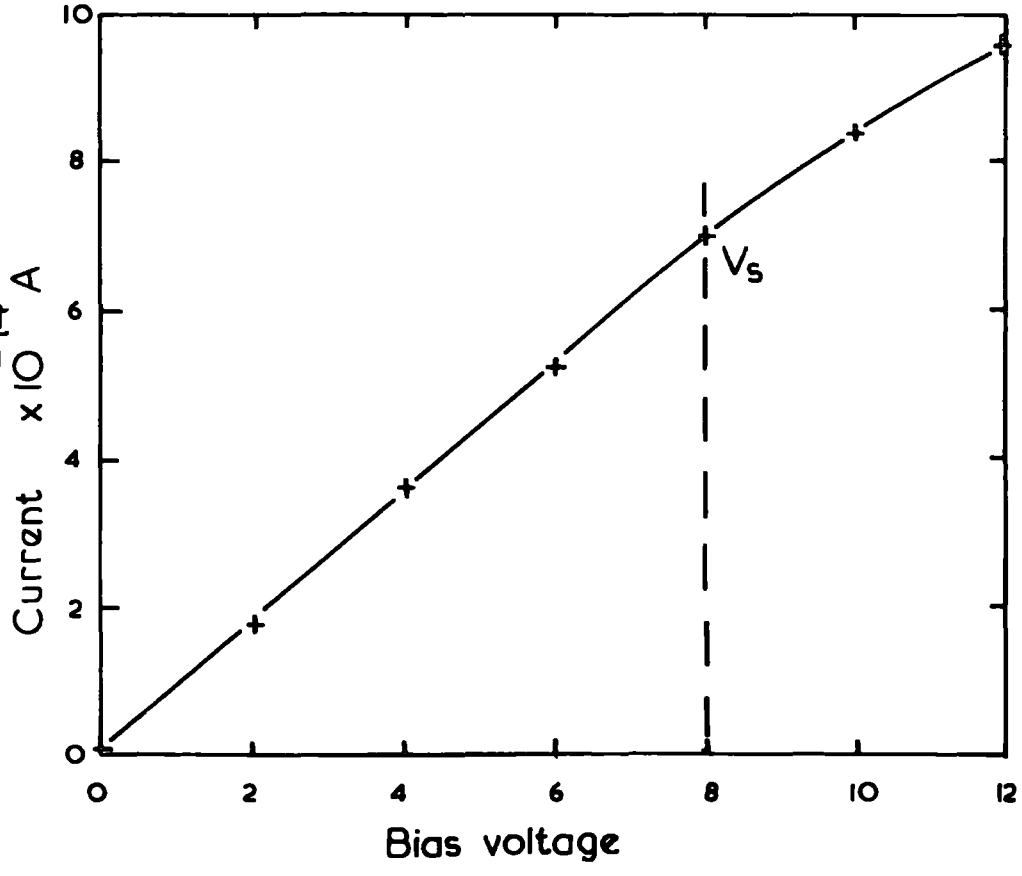

this possible discrepancy by estimating the conduction current by the indirect method. This entailed measuring the potential gradient F and both positive (λ_+) and negative (λ_-) conductivities at ground level. By the theory of the electrode effect, defined by BENT and HUTCHINSON (1966), under normal calm fair-weather conditions the conduction current close to the ground can be carried only by positive ions. But if any sort of convection or diffusion currents are acting both polar conductivities will be involved and the conduction current will be given by the product $F(\lambda_+ + \lambda_-)$.

The Field Station at Lanehead had already been equipped by SHARPLESS (1968), with a Gerdien chamber for measuring positive conductivity and a second, identical chamber was manufactured and installed to give simultaneous measurement of both polar conductivities.

4.4.1 Gerdien's conductivity chamber

The principle of operation of GERDIEN'S (1905) cylindrical condenser, described by CHALMERS (1967), is depicted in Fig. 4.4.

The conductivity, λ, of the air flowing through the condenser, of capacitance C, is related to the voltage E measured by the V.R.E. by:

$$E = \frac{RCV\lambda}{\epsilon_o}$$

where R is the high resistor in series with the central electrode, V is the bias voltage and ϵ_o is the permittivity of free space. For a given mobility of ions, the relationship between V and λ is linear up to a certain bias, the saturation voltage Vs, shown in the characteristic of Fig. 4.4. At this voltage the current i to the central rod can be equated to the total flow of ions through the condenser, Wne, where W is the volume rate of flow of air, n is the number of ions per unit

volume and e is the electronic charge. It is assumed that each ion carries a single electronic charge. From the equation above we may write:

$$\frac{E}{R} = \frac{CV\lambda}{\epsilon_o} = i$$

Therefore, at saturation:

$$\lambda = \frac{\epsilon_o}{CVs} \cdot Wne$$

But:

$$\lambda = nek$$

where k is the mobility of the ions in ms^{-1} per Vm^{-1}, and thus:

$$Vs = \frac{\epsilon_o W}{Ck}$$

This equation expresses the relationship between the bias voltage, the rate of flow of air and the consequent limiting mobility of the ions collected. An accurate value for C is required for its evaluation and HIGAZI (1966) obtained a capacitance of 8.51 pF for the type of chamber used at Lanehead. With a flow rate of $10^{-3} m^3 s^{-1}$ and a bias of 4.5 V, saturation will occur for ions of mobility equal to, or greater than $2.2 \times 10^{-4} ms^{-1}$ per Vm^{-1}. The class of 'small' ions is taken to be those ions with mobilities between 1×10^{-4} and 2×10^{-4} ms^{-1} per Vm^{-1}, so these values of bias and flow rate are acceptable for the measurement of the conductivity of air, due to small ions, using a Gerdien chamber.

At Lanehead, air was drawn through each chamber by a common fan unit (Sect. 4.4.3) and the bias voltage applied to each was 4.5 V, positive for the instrument measuring positive conductivity and negative for the other.

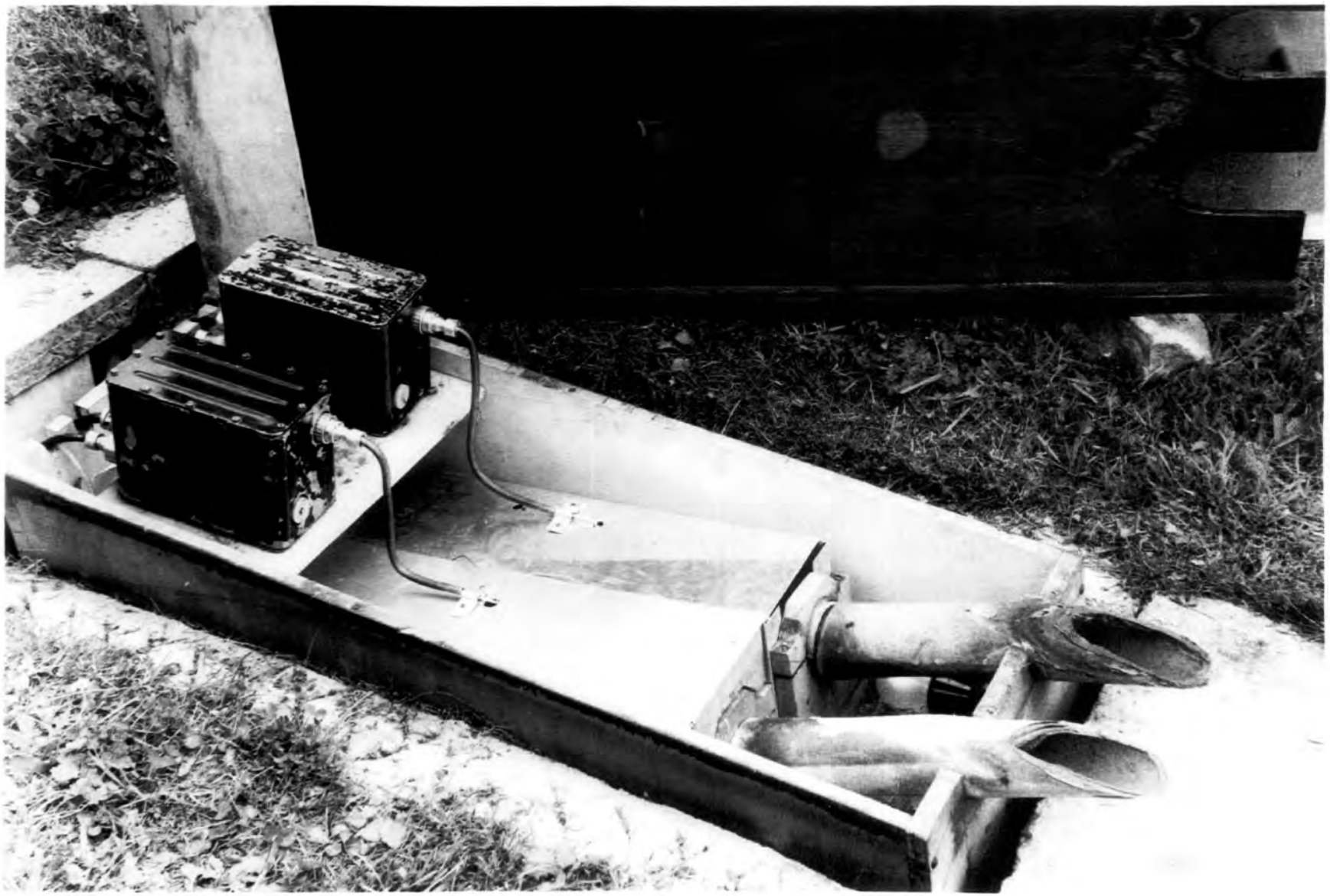

Fig. 4.5 The Gerdien chambers

4.4.2 Maintenance of the conductivity instruments

The two chambers were installed in a timber box set into a concrete pit at ground level (Fig. 4.5). The box was heated by electric lamps to maintain the insulation of the P.T.F.E. supporting the central rod of each chamber. Electrical screening from external effects, particularly displacement currents, was afforded by mounting the chambers in individual earthed aluminium boxes, and the coaxial leads to the V.R.E. head units were passed through clamped copper tubes to eradicate piezo-electric currents.

Air was drawn into the chambers through cardboard tubes, 6 cm in diameter, which were angled up to ground level (Fig. 4.5). The ends of these tubes were chamfered to be level with the surrounding surface. A small, earthed aluminium plate was mounted a few centimetres above the openings to prevent the direct entry of rain into the chambers, and tests were made on several occasions, by removing and replacing this plate, to determine whether it had any effect on the efficiency of the instrument. None was detected.

Throughout the period from October 1968 to July 1969, both chambers functioned satisfactorily in fair weather and without any insulation breakdown. On a few occasions breakdown did occur during prolonged rain, usually in the negative conductivity chamber, but this did not persist for very long after the cessation of the rain. The V.R.E. units used with these instruments were less stable than those of the air-earth collector and the space charge collector, and the zero of the negative conductivity varied by up to 10 per cent of the normal mean value in a week. No preferred direction of drift from true zero was noticed and it was felt that these variations would probably cancel out over the period of a month. This V.R.E. was replaced in July 1969.

4.4.3 The fan unit

The box housing the fan unit (Fig. 4.1) was placed some distance away from the instruments so that the air exhausted by the fan should not interfere with their measurements. The electric motor fan unit from a domestic vacuum cleaner was used to suck air through the conductivity chambers and the space charge collector, and the rate of flow in each leg was monitored by a household type gas meter. Each meter had a micro-switch fitted to its rotating arm which, on closing, caused a small panel lamp to light in the laboratory; 10 flashes of the lamp corresponded to the passage of 0.1 m^3 of air, so that, with the aid of the second-hand of a watch, the flow rate could be accurately checked. Adjustment of this rate was achieved by altering the supply voltage to the fan motor; this was usually about 120 V a.c.

SHARPLESS (1968) experienced several failures with fan units from vacuum cleaners, which were not designed for continuous working at the high suction pressure required by the space charge collector. But a new unit, installed in May 1968, ran for a further 14 months on a single change of brushes. However, when this unit deteriorated its demise was rapid and, in line with the policy of improving the instrumentation at Lanehead, a more robust suction fan, designed for this sort of work, was installed in August 1969.

4.5 The space charge collector

By the term space charge is meant the free, unbalanced charge in a volume of air, taking no account of the charges of both sign which balance one another. Space charges may be carried on small ions, large ions, dust, cloud or fog droplets, or precipitation particles, and the net charge density is expressed in Cm^{-3}.

Two methods of measurement of space charge are generally employed. Firstly, the charges may be drawn into an earthed Faraday cage where the potential at a point inside can be measured. Alternatively, the space charge may be collected by filtering and the net charge on the filter measured. POISSON'S Law may also be invoked to deduce the amount of space charge from the change of potential gradient with height. If we assume that the space charge is uniformly distributed through the region under consideration, for a potential gradient F and space charge density ρ, POISSON's equation reduces to:

$$\frac{dF}{dz} = -\rho/\epsilon_o$$

where z is in the vertical direction, and ϵ_o is the permittivity of free space.

The space charge collector at Lanehead was of the filtration type; a full description of its design and efficiency is given by BENT (1964).

4.5.1 Operation of the collector

Air was drawn, by means of the fan unit (Sect. 4.4.3), through a special filter mounted on P.T.F.E. insulators, which was contained in a tapered, cylindrical Faraday cage (Fig. 4.6). The filter comprised a fibrous glass-asbestos substance, described by its manufacturers as 'absolute filter material', which was encased in an aluminium frame. It was claimed to have an efficiency of 99.97 per cent, or better, for the collection of particles of diameter 0.3 μm. BENT (1964) tested its efficiency by measuring the number of artificially produced negative small ions that would pass through the filter with an air flow of $10^{-3}m^3s^{-1}$, and he stated that the filter retained 99.8 per cent of these ions.

In the nose of the collector the filter was protected by two prefilters

which trapped large particles and insects. The aluminium frame of the 'absolute' filter was connected, via a Plessey plug and a rigid coaxial cable, to the head unit of a V.R.E. employing a $10^{12}\Omega$ resistor. This required the insulation between the filter and the outer earthed casing to be better than 10 times this value, so that heating, by electric lamps, was provided to prevent condensation.

The collector was mounted, nose-down and enclosed in the box, on top of a Handy-angle framework, with the level of the inlet hole at about 0.8 m above the ground. This arrangement proved efficacious in preventing the insulation breakdown in rain which was encountered by GROOM (1966).

4.5.2 Reliability and accuracy

Left in the position established by SHARPLESS (1968), the space charge collector behaved well apart from occasional insulation breakdown in heavy rain and once in fair weather when an insect got inside. In this case the collector was dismantled and the insulators were cleaned, but otherwise an overhaul was unnecessary.

The accuracy of the space charge measurements depended on the constancy of the rate of flow of air through the apparatus, and SHARPLESS (1968) estimated this to be better than 5 per cent for the system at Lanehead. Regular zero checks, made as a matter of course on all the instruments, supported his assessment that the V.R.E. output was stable to better than 2 per cent of full-scale. The overall accuracy of measurement by this instrument was better than 10 per cent of the normal fair weather space charge density.

Fig. 4.6. The Space Charge Collector. (from BENT, 1964)

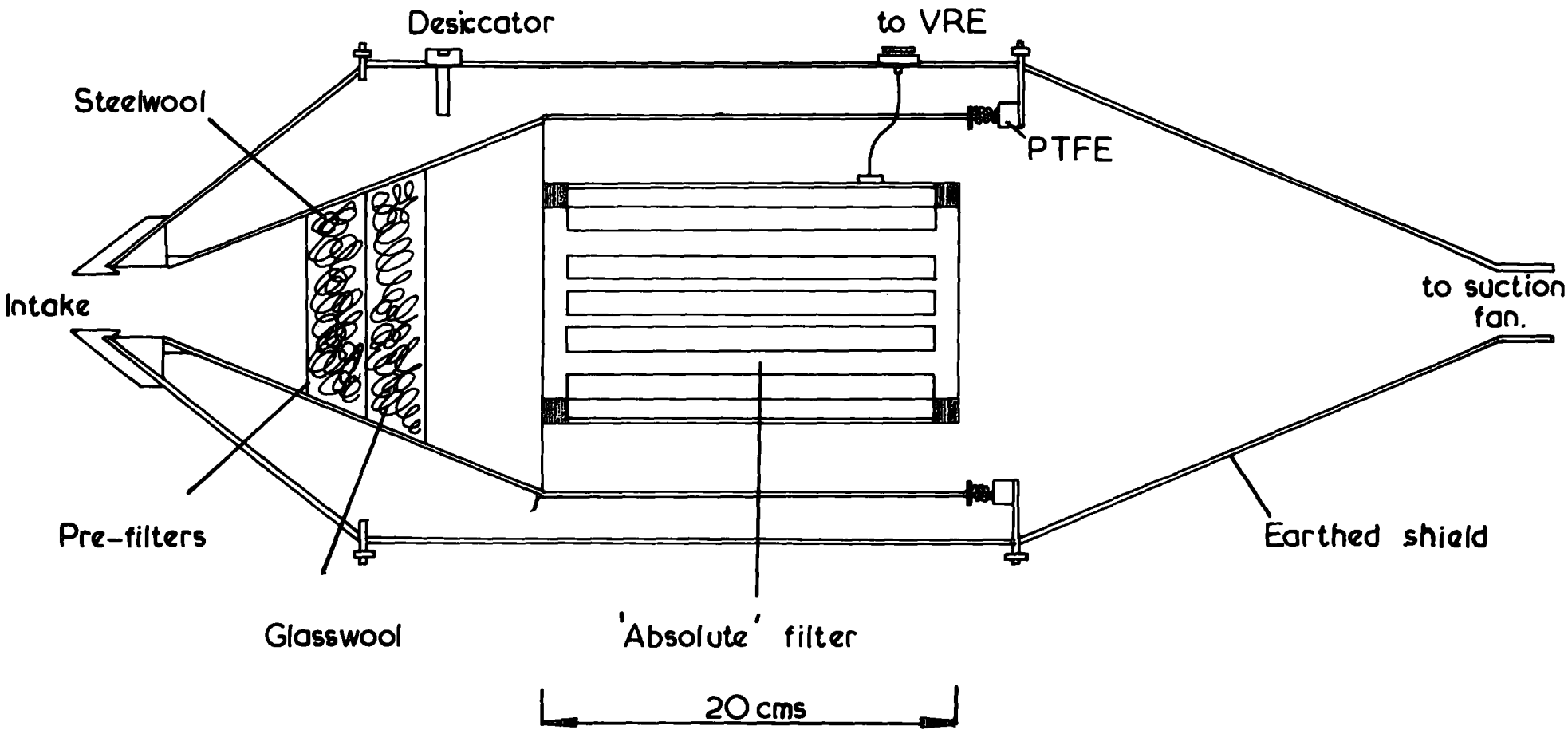

4.6 The electronic interface between the instruments and the automatic recording system

The five instruments, described in the preceding sections, constituted the permanent Atmospheric Electricity apparatus at Lanehead (Fig. 4.12), and were run for 24 hours a day from early in 1967. The practice of SHARPLESS (1968) was to record the outputs on paper charts with 1 mA pen recorders, but for this work it was wished to employ the automatic data recording system developed and built by the author (Chapter 3). However, the chart recorders served the very useful purpose of supplying an immediate past history of the behaviour of the instruments and it was felt desirable to retain this facility, so an electronic interface unit was required to convert the outputs of the V.R.E.'s and the field mill into a form suitable for the voltage-to-frequency converter of the recording system. It was decided to design a d.c. amplifier, with high input impedance, to sample the voltages developed across the pen recorders by the output currents.

4.6.1 The d.c. amplifier

Two separate applications needed consideration. Each channel of the four-channel pen recorder had an impedance 500Ω but the single channel recorders were 1 kΩ impedance. The amplifier, therefore, needed the minimum capability of amplifying, linearly, the full scale range of the low impedance recorders, effectively - 0.25 V to + 0.25 V, to the range of the voltage-to-frequency converter, 0 to - 10V.

Further requirements of the amplifier were that its input impedance should be sufficiently large that it did not shunt the pen recorders, and that its output impedance should be low enough to provide sufficient current for the voltage-to-frequency converter. In the device, good

stability and a minimal temperature dependence were characteristics of paramount consequence as the amplifier was required to function for many months in varying ambient temperatures.

The developed circuit and its characteristic are shown in Fig. 4.7. The input stage was a simple differential type, sometimes referred to as a long-tailed pair, with feedback from the output to stabilise the gain. In the output stage a constant current source was used to give a shunt-compensated emitter-follower. Because this type of stage cannot be driven directly from a long-tailed pair, a single-ended amplifier was interposed. The gain of the amplifier was adjusted by the 3.3 MΩ skeleton preset, and the set-zero by the 1 kΩ preset.

4.6.2 The performance of the amplifier

The open loop gain of this design was of the order of 100 and in use the overall voltage gain required was only 20, so the circuit exhibited a high degree of stability. No change was observed in its characteristic over a period of 9 months.

The effectiveness of the differential input stage as temperature compensation was tested by heating the components of the amplifier with a domestic hair drier. Over a temperature range of about 30°C, the zero drift was of the order of 50 $\mu V^{o}C^{-1}$, and this value was judged to be satisfactory for present purposes.

The five amplifiers, one for the output of each instrument, completely fulfilled the requirements made of them.

Fig. 4.7. The D.C. Amplifier

(a) Circuit diagram:

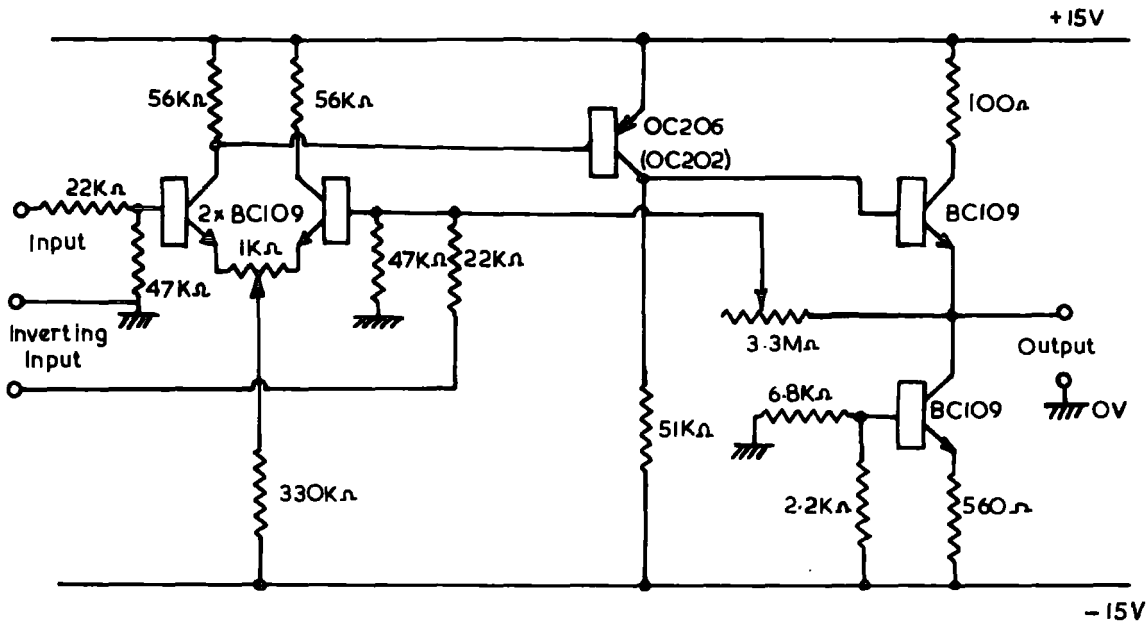

(b) Transfer characteristic:

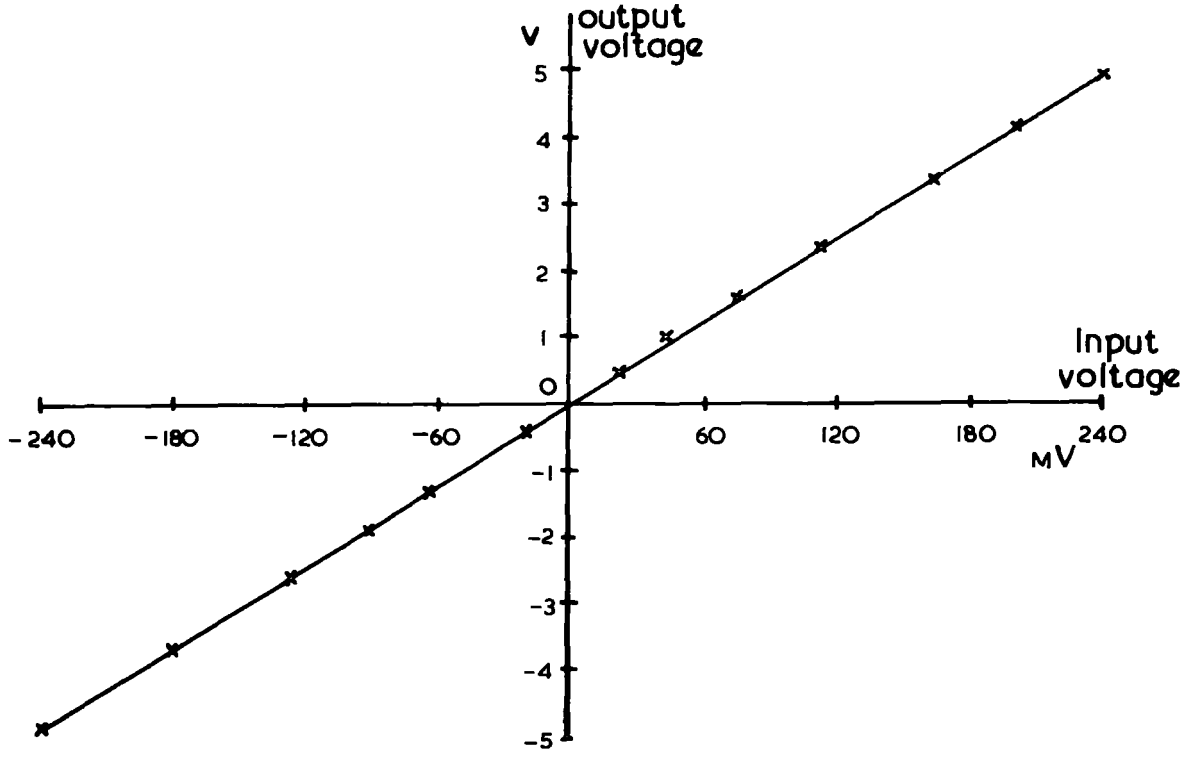

Fig. 4.8. The Anemometer.

(a) Diode pump circuit:

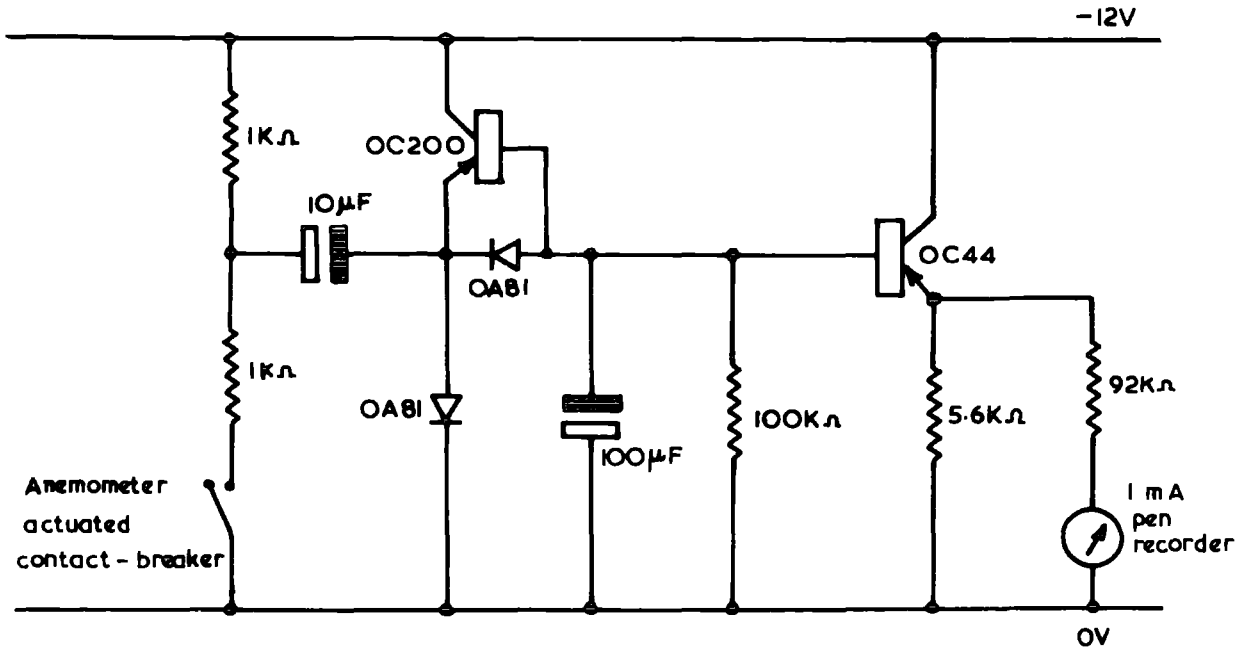

(b) Calibration curve:

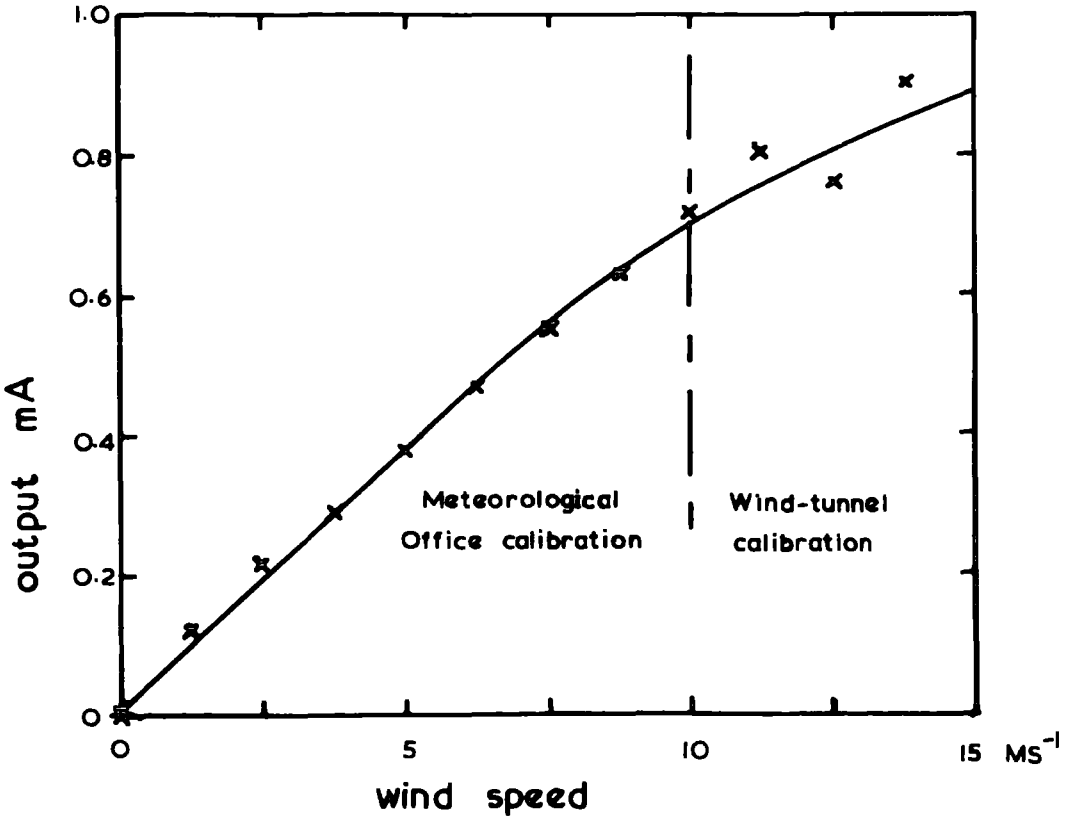

Fig. 4.9 The sky photometers

Part II Ancillary Instruments

The following instruments were assembled and used only during those periods when precipitation records were being taken. They served to give some indication of the meteorological conditions prevailing at the time.

4.7 The anemometer

Wind speed was measured at a height of 2 m by a sensitive three-cup anemometer, hired from the Meteorological Office. The anemometer would start turning for wind speeds in excess of 0.25 ms^{-1} and operated a contact breaker which closed twice every three revolutions of the cups. A calibration was supplied by the Meteorological Office for wind speeds up to 10 ms^{-1} and with the assistance of a colleague, Mr. Dayaratna, a calibration was obtained, in the wind-tunnel of the Department of Engineering Science, for speeds in the range 10 to 15 ms^{-1}. Voltage pulses were produced by the contact breaker and these were counted by a diode pump circuit. The current output of the pump was recorded on a spare 0 - 1 mA pen recorder (Fig. 4.10), and the calibration of wind speed against current is given in Fig. 4.8, together with a circuit diagram.

4.8 The sky photometers

4.8.1 A method for estimating cloud height and speed

The sky photometer, as used at Durham University Observatory by WHITLOCK (1955), comprises a photo-resistor (type ORP 16) placed at the bottom of a brass sighting tube of length 33 cm and diameter 2 cm. The resistance of an ORP 16 alters with the intensity of the light falling on it and this variation can be used to control the current through a

pen recorder. OGDEN (1967) utilised a combination of two such photometers to measure the horizontal speed of fair weather cumuliform clouds, and he proposed a method, using four photometers, which would determine both cloud speed and height. The time lag between corresponding changes in output, caused by one cloud, from two vertical photometers will give the cloud speed if the separation of the tubes, in the line of movement of the cloud, is known. A time lag of a similar nature between the responses of two photometers, each mounted at a known angle to the vertical on the same spot (Fig. 4.9), will give the angular velocity of the cloud about that point, provided these tubes are also lined up with the direction of movement of the cloud. The trigonometrical ratio, relating the cloud speed V with time lag t between the angled photometers and giving the cloud height H, is:

$$\tan \alpha = \frac{Vt}{2H}$$

where 2α is the angle between the two photometers.

4.8.2 Use of the photometers in rain

It was felt that, with suitable adaptation, four sky photometers could be used to give the speed and height of nimbostratus during rain. The sighting tubes of the photometers were closed with transparent perspex discs and the bases, containing the photoresistors, were made weather-proof with a sealing compound. It proved necessary, later, to insert some crystals of silica gel into the tubes to prevent excessive condensation from damaging the photoresistors; a glass sealed photoresistor (type ORP 50) would have been better suited to the conditions. During periods of prolonged rain, which were often very dull, it was found that the changes in resistance of the ORP 16's were too small to register on the chart recorder and amplifiers were used to increase the

Fig. 4.10 A sky photometer and wind speed record

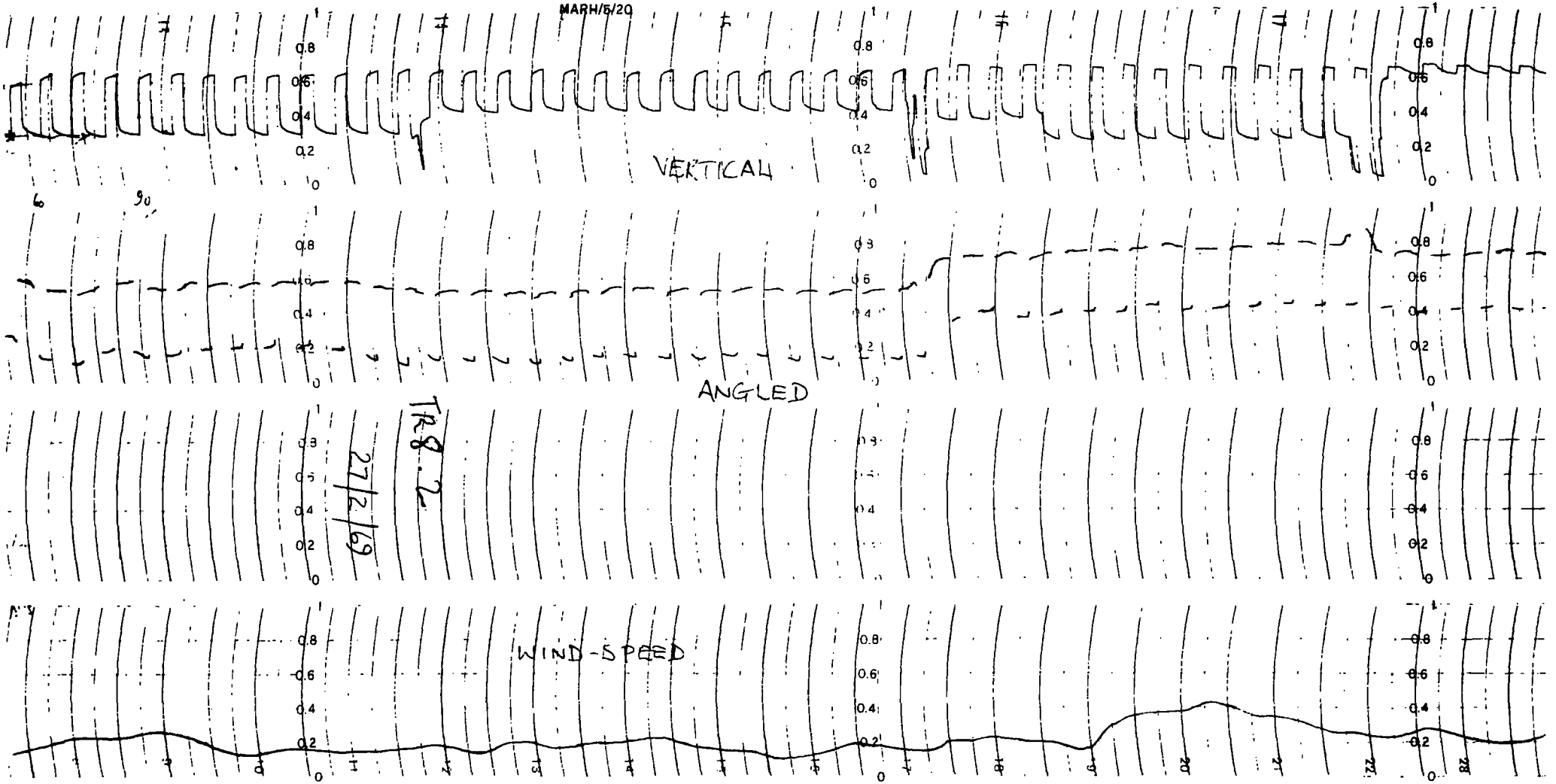
MARH/5/20
VERTICAL
ANGLED
TR8.2
27/2/69
WIND-SPEED

magnitude of the variations. This arrangement, with four photometers, entailed the occupation of four channels of a pen recorder and to overcome this extravagance, the outputs were grouped in pairs, the two vertical and the two angled ones together. A circuit was built which switched alternately from one member of a pair to the other; this produced two records of a castellated appearance (Fig. 4.10) and, with diligence, it was possible to fill in the missing parts of the record without loss of detail. From the chart speed $1/10^{th}$ inch per second, a time lag between corresponding maxima and minima was evaluated.

The accuracy of the results obtained with the photometers depended mainly on the precision with which the direction of cloud movement could be assessed by eye. A check was made with a nephoscope which indicated that, surprisingly, the chosen line was always within 2^{o} of arc of the true direction. This implied an accuracy of better than 5 per cent in the cloud speed and better than 10 per cent for the cloud height. The absence of any Meteorological Office weather station, close enough to give more accurate readings, indicates the value of these measurements.

4.8.3 Wind speed profile

By combining the measurements of the photometers with the wind speed at 2 m, a rough, but useful profile of wind speed can be derived. This profile depends on the assumption that the observed cloud is moving with the speed of the wind at that height. This is not always the case. However, it has been stated that for orographic clouds, a change in structure will occur in the cloud as air of a varying nature blows through it (Sect. 2.3.1) and it is held that this structure may be detected by the photoresistors, if not by the human eye. It is, therefore, reasonable to assume that the variations indicated by the photometers are

dependent on the wind speed at the height of the cloud structure.

4.9 The rate of rainfall meter

The design was contemplated of a circuit which would continuously monitor rate of rainfall, suitable for use in conjunction with the recording system.

Previous workers in conditions of light rain have used, among others, the tipping-bucket method (SIVARAMAKRISHNAN, 1952) and the 'rainfall condenser' (RAMSAY, 1959), none of which gave a continuous reading. SHARPLESS (1968) used an acoustic method though the calibration was not entirely satisfactory.

It was decided to allow the rain, collected by a large funnel, to flow through the channel formed by two parallel aluminium plates set, 3 mm apart, in a perspex mould (Fig. 4.11). These plates, 5 cm x 30 cm comprised the condenser part of the inductive-capacitive 'tank' circuit of an oscillator, and the variation of the volume of water within the plates caused the capacitance, and hence the frequency, of the oscillator to change. This frequency was 'mixed' with the output from a constant frequency oscillator and the resulting 'beat' frequency was measured with a direct reading frequency meter (Fig. 4.11). The 'beat' frequency was calibrated against the rate of flow of water, in $m^3 s^{-1}$, and a knowledge of the effective collecting area of the funnel gave the rate of rainfall.

The device worked very satisfactorily while under brief test in the laboratory, but the simple design of the oscillators meant that the circuit was very unstable and difficult to zero.

This trial execution of the idea, although proving unsatisfactory for the field, showed real promise and it is hoped that the principle will be developed to produce a worthwhile instrument.

Fig. 4.11. The rate of rainfall meter..

(a) The condenser:

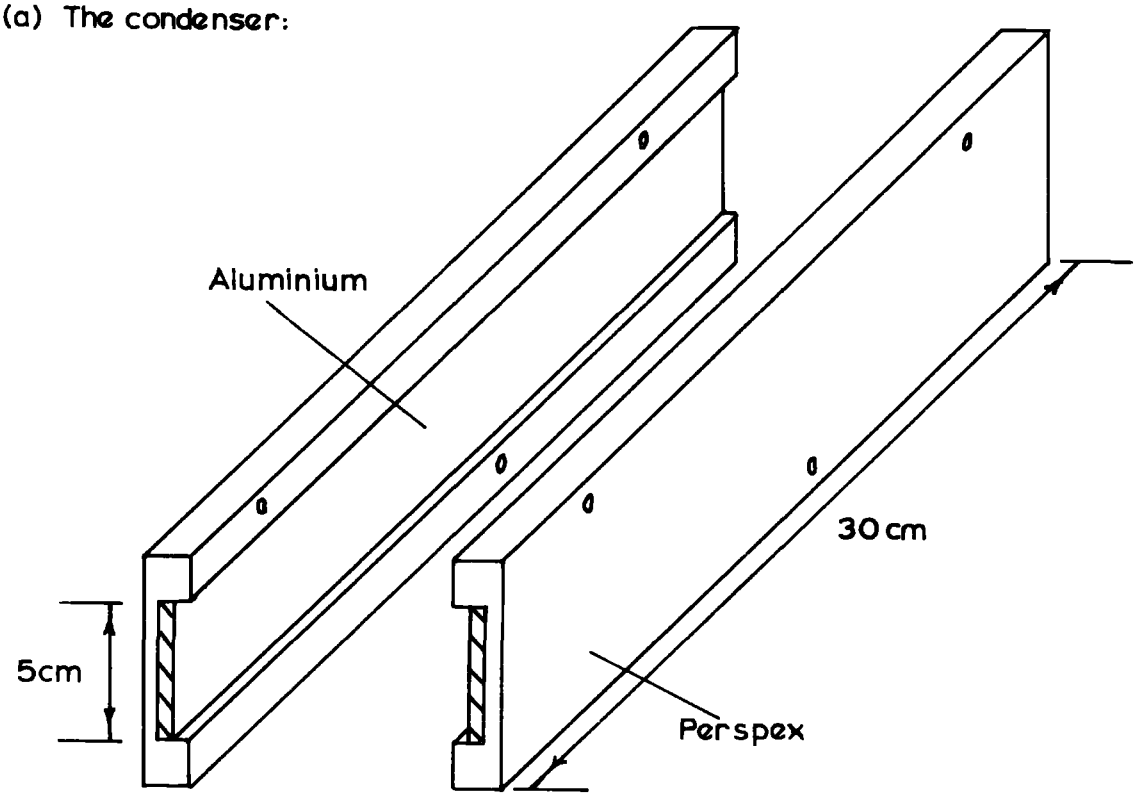

(b) Block diagram:

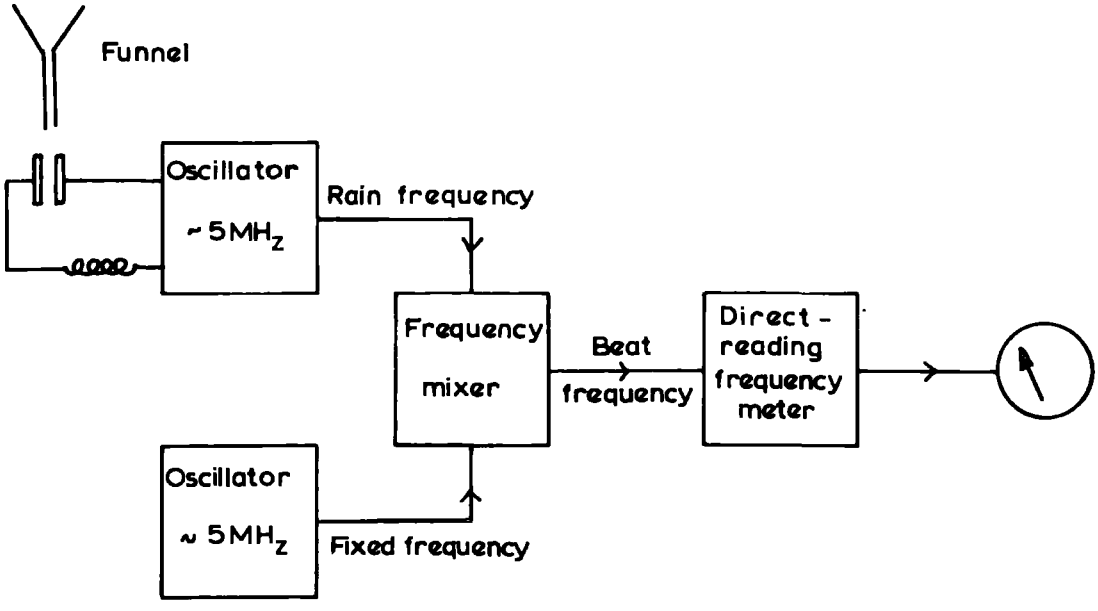

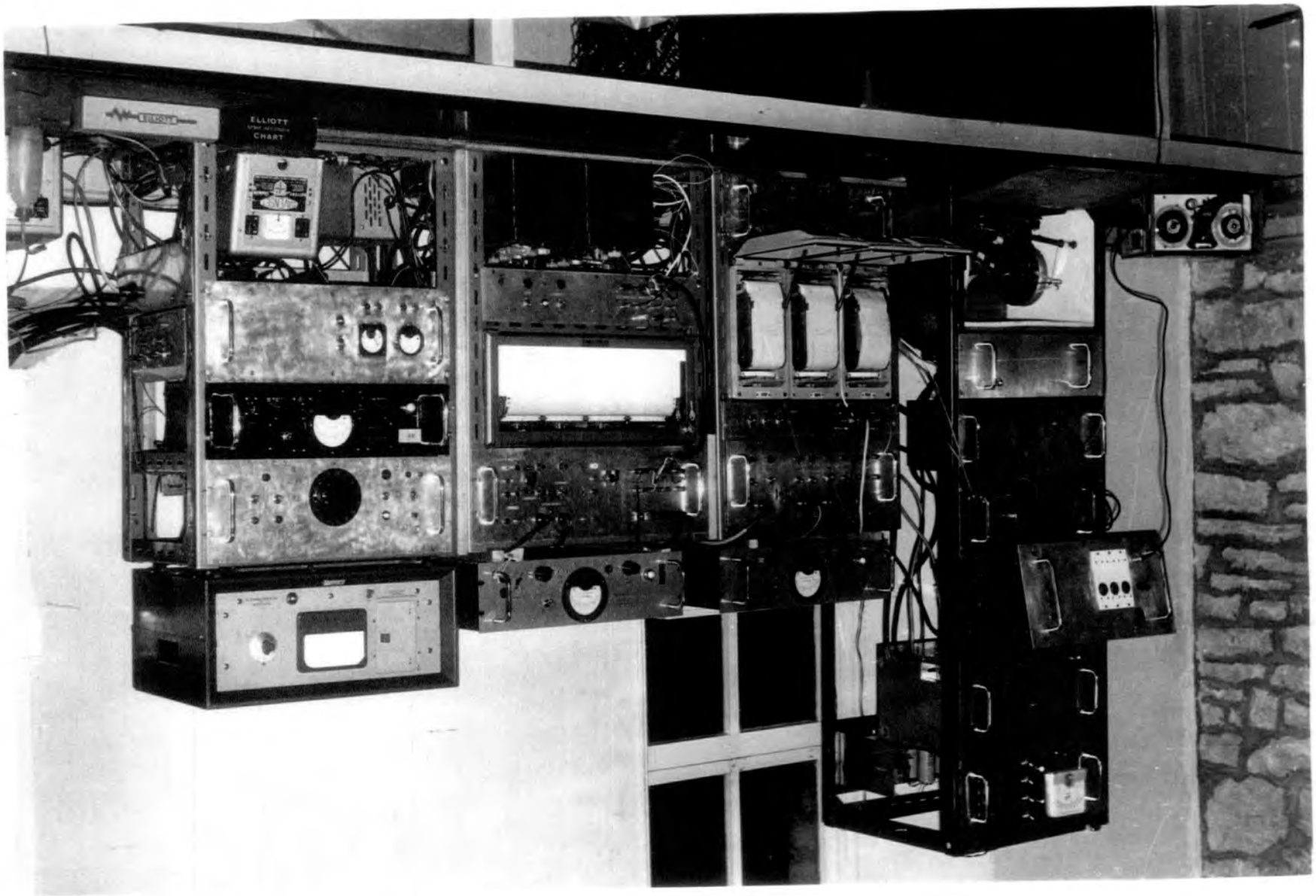
ELLIOTT
CHART

Fig. 4.12 The instrumentation in the School

CHAPTER 5

THE ANALYSIS OF THE MEASUREMENTS OF PRECIPITATION ELECTRICITY

5.1 Data processing

The numerical analysis of the raw data was undertaken on the Northumbrian Universities Multiple Access Computer (NUMAC), an I.B.M. 360/67. For this purpose the author wrote his own programs in Programming Language One (PL 1), with the exception of those for the Graph Plotter unit which required the Fortran IV Language. The author is indebted to the staff of the Durham University Computer Unit, without whose advice and assistance this work would have been impossible.

5.1.1 Conversion of the raw data

Measurements were made, using the automatic recording system, during 32 periods of quiet rain. The majority of these periods involved the recording of four parameters: potential gradient, total air-earth current, space charge density and the rain current to a shielded collector. The last constituted a part of an experiment which was being conducted by a colleague of the author's. On ten of the occasions both polar conductivities were also measured, and on five occasions only two variables, potential gradient and total air-earth current, made up the record.

The calibration of the digitising system was achieved by comparing the punched 3-digit count number with the meter reading of the vibrating reed electrometer (V.R.E.) for a known voltage applied to the resistor in the V.R.E. head unit. The voltage was derived from a specially designed zener-regulated power supply with temperature compensation. In this way the resistor (nominally $10^{10}\Omega$ or $10^{12}\Omega$) was indirectly calibrated. Corresponding values of voltage and count, from full-scale negative to

full-scale positive, were noted and the line of best fit between the two was obtained by the method of least squares. This method is one of many scientific subroutines which are available, on call, with I.B.M. 360 Operating System.

For the potential gradient calibration, the output of the field mill was varied by changing the voltage to the bias plate (Sect. 4.3.1). The count obtained was compared with the amplifier output current, indicated on the chart recorder, which had been calibrated in terms of the potential gradient by SHARPLESS (1968). In 9 months there was no discernible change in any of the calibrations for the overall system.

The first job of the computer was to read the digitised data and to fit it to the calibration equations, giving its output in the more familiar forms of so many Vm^{-1}, $pA\ m^{-2}$ and so on. This completed, it was possible to proceed to the computation of conduction and displacement currents, and hence to the computation of the precipitation current.

5.1.2 The computation of conduction and displacement currents

Two different approaches were required to estimate the instantaneous conduction current. In the cases when six parameters were being recorded, this current was calculated from the product of corresponding values of potential gradient and total conductivity. Otherwise readings were taken from the conductivity chart recorders every 15 minutes, and the average value of their sum, for the recording period, was substituted into the product. This latter course was not felt to be unduly inaccurate as observation showed that both conductivities remained fairly constant during quiet rain and variations were less than $\frac{1}{4}$ of full-scale on either side of the average. This represented a value of about $\pm\ 2 \times 10^{-15}\ \Omega^{-1}m^{-1}$ which, for a potential gradient of 300 Vm^{-1}, gave a

discrepancy of less than 1 pA m^{-2}.

On the other hand, the accuracy of the computed displacement current was of major consequence. It was stated, in Sect. 4.4.2, that a form of partial KASEMIR (1955) compensation for displacement currents was employed and a careful study of the measurement technique is essential.

When the system was recording two parameters it sampled, alternately, potential gradient, PG, and the total air-earth current, AEC, with a time interval a, of 3s, between each. This is represented diagrammatically in Fig. 5.1(b) where the system is assumed to have reached the N^{th} samples, PG(N) and AEC(N). The total air-earth current comprises three component currents: conduction, displacement and precipitation. It is assumed that the precipitation and conduction currents remain unchanged in the period $a < t < 3a$, which corresponds to the interval between samples AEC(N -1) and AEC (N), and that step changes occur between intervals. These two currents will be considered together and denoted by J(N). However, by virtue of the fact that the potential gradient is sampled during the period $0 < t < 2a$, it is possible to split the displacement current into two parts. One part, DISPA, is derived from the average displacement during the period $0 < t < a$ and the other, DISPB, from the period $a < t < 2a$ (Fig. 5.1(b)). Displacement current density is given by:

$$\text{DISPA} = -\epsilon_o \frac{d}{dt} (\text{PG})$$

In this present terminology the average displacement current may be determined by:

$$\text{DISPA(N)} = -\epsilon_o (\text{PG(N)} - \text{PG(N-1)})/2a$$

This value, and the value for DISPB(N), were calculated by the computer.

The integrating effect of the resistance R and capacitance C in a parallel network (Fig. 5.1) coupling the total air-earth collector to

ground, may now be considered. If a steady current i, steady in that its changes are slow compared to the sampling interval, flows into such a collector then:

$$i = i' + \frac{CdV}{dt}$$

where i' is the current through R, V is the potential difference across R and t represents time. By elementary circuit theory, this may be rewritten as:

$$i' = i + \frac{A}{R} \exp\left\{ -t/RC \right\}$$

where A is a constant determined by boundary conditions.

Putting the steady current i equal to the sum DISPA(N) + J(N), the measured current i_A' through R is given by:

$$i_A' = \text{DISPA}(N) + J(N) + \frac{A'}{R} \exp\left\{-t/RC\right\} \qquad 0 \leq t < a$$

When t = 0 :

$$i_A' = \text{AEC}(N - 1)$$

This is the previous measured sample.

Substituting for i_A' and rewriting the equation:

$$A'/R = \text{AEC}(N - 1) - (\text{DISPA}(N) + J(N))$$

and substituting for A'/R back into the general equation:

$$i_A' = \text{DISPA}(N) + J(N) + \left(\text{AEC}(N-1)-\text{DISPA}(N)-J(N)\right) \exp\left\{-t/RC\right\} \qquad 0 < t < a$$

Now at t = a, the measured current is i_A'' where:

$$i_A'(t = a) = i_A'' = \text{DISPA}(N) + J(N) + \left(\text{AEC}(N-1)-\text{DISPA}(N)-J(N)\right) \exp\left\{-a/RC\right\}$$

For the period $a \leq t < 2a$, the current through R is given by

$$i_B' = \text{DISPB}(N) + J(N) + \frac{A''}{R} \exp\left\{-t/RC\right\}$$

Fig. 5.1. The current measurements.

(a) Collector circuit:

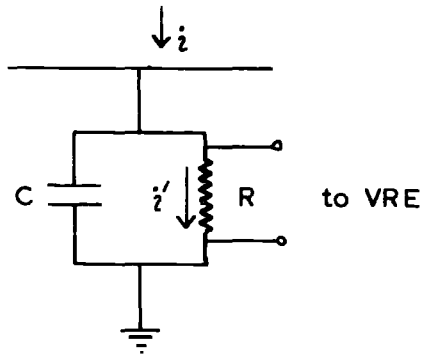

(b) Composition of the total air-earth current:

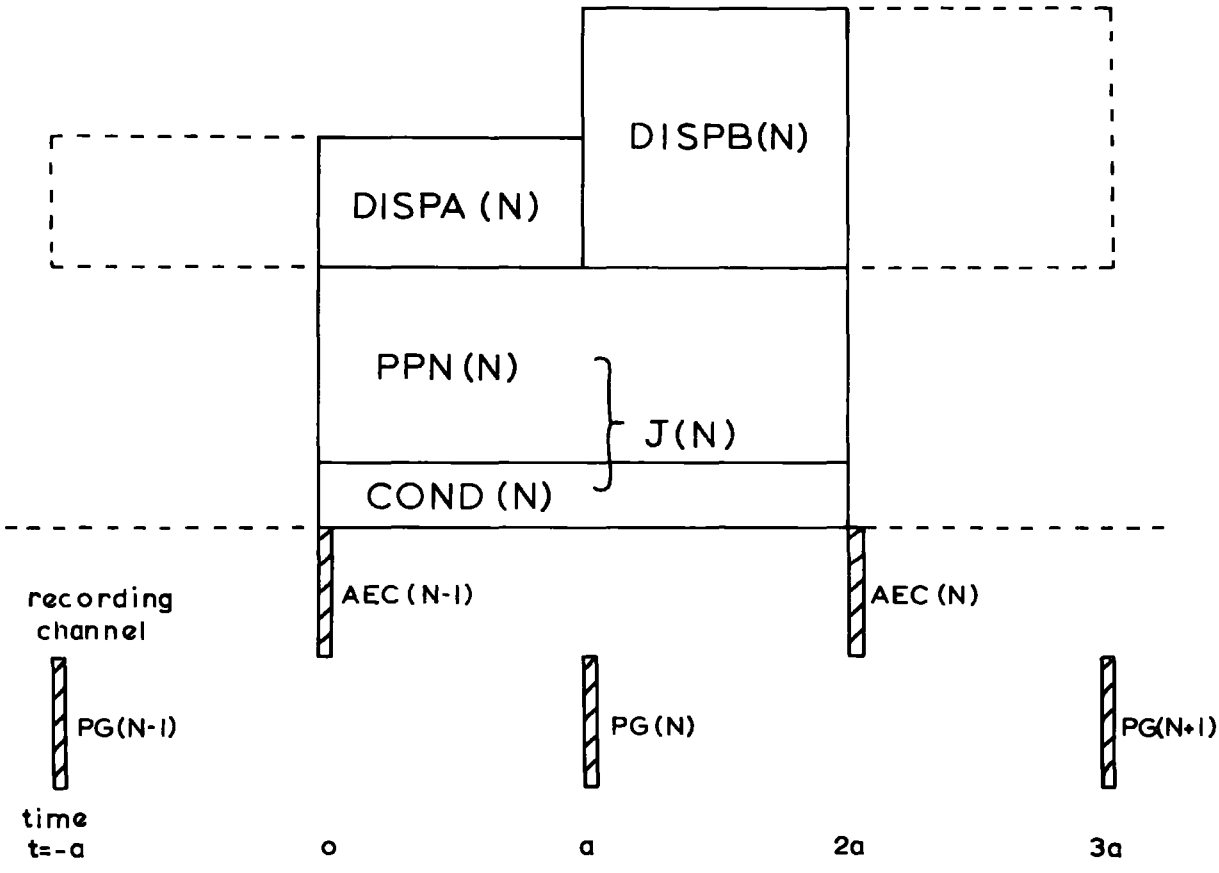

When $t = a$:

$$i_B' = i_A''$$

so that, substituting for i_B' :

$$\frac{A''}{R} = \left(i_A'' - DISPB(N) - J(N) \right) \exp\left\{ a/RC \right\}$$

and, in turn, for A"/R

$$i_B' = DISPB(N) + J(N) + \left(i_A'' - DISPB(N) - J(N) \right) \exp\left\{ (a-t)/RC \right\} \quad a < t < 2a$$

At $t = 2a$, substituting for i_A'' from above:

$$i_B' = DISPB(N)\left(1 - \exp\left\{-a/RC\right\}\right) + J(N)\left(1 - \exp\left\{\frac{-2a}{RC}\right\}\right) + DISPA(N)$$
$$\left(\exp\left\{-a/RC\right\} - \exp\left\{\frac{-2a}{RC}\right\}\right) + AEC(N-1)\exp\left\{-2a/RC\right\}$$

and $i_B' = AEC(N)$

This expression may be rewritten to give the steady current J(N), and hence the precipitation current PPN(N), in terms of the present and the previous samples of the current through R, that is AEC(N) and AEC(N-1), and the computed conduction COND(N), and displacement currents. For the RC network used, the product RC was equal to 20s and the sampling period a, was 3s. Substituting these values in the equation above yielded the expression used by the computer to give the N^{th} value of precipitation current, in pA m^{-2}, as:

$$PPN(N) = 3.85 \times AEC(N) - 2.85 \times AEC(N-1) - 0.46 \times DISPA(N) - 0.54 \times DISPB(N) - COND(N).$$

Similar equations were derived for the cases when four and six parameters were recorded.

The two series PG(N), PPN(N) (N = 1, 2, 3 .....), of potential gradient and precipitation current, were put on punched cards by the

computer for input to the graph plotter at a later date. This enabled the author to obtain a visual display of his record and an example is shown in Fig. 5.2. After a few recording periods had been plotted in this way it became obvious that the computed compensation for displacement currents was not always accurate and investigation showed this to be due to an effect known as 'aliasing'.

5.1.3 Aliasing

This problem is an unavoidable consequence of the nature of discretely spaced records, and does not occur for continuous records. It is illustrated by an example in Fig. 5.3 where it can be seen that equally spaced time samples from any cosine wave might have come from each of many other cosine waves. These are aliases of one another.

Consider the case when the change in potential gradient is a cosine wave (Fig. 5.3). It is not possible to determine, in theinterval a_3 to a_4, whether it is following the faster or the slower changing wave form. The average rate of change of potential gradient over the period is the same in both cases. The air-earth current is sampled at the mid-point of this period, but the displacement current, which contributes to this sample, depends on the rate of change of potential gradient at that instant, and, in this example, it could have two very different values. It is not, therefore, possible to compensate reliably for displacement currents unless certain precautions are taken to prevent aliasing.

In a discretely spaced record, of interval t, if the frequency of change F_n of a parameter is greater than $\frac{1}{2t}$ then aliasing will occur (see BLACKMAN and TUKEY, 1958). Here F_n is the folding, or Nyquist, frequency. It is necessary, to prevent aliasing, to ensure that no frequency exists in the record being sampled, which is greater than F_n

Fig. 5.2 Computer drawn record of potential gradient and precipitation current (x-x)

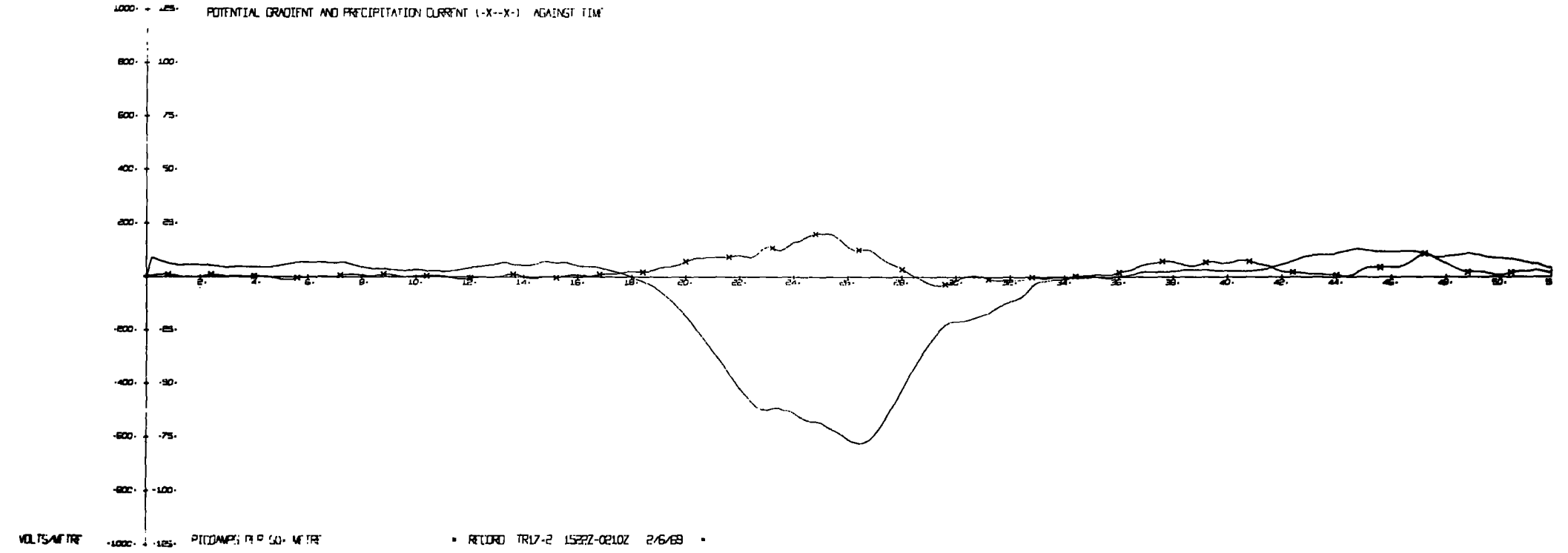
POTENTIAL GRADIENT AND PRECIPITATION CURRENT (-X--X-) AGAINST TIM
1000
800
600
400
200
-200
-400
-600
-800
-1000
100
75
50
25
-25
-50
-75
-100
-125
2
4
6
8
10
12
14
16
18
20
22
24
26
28
30
32
34
36
38
40
42
44
46
48
50
VOLTS/METRE
PICOAMPS PER SQ. METRE
RECORD TR17-2 1522Z-0210Z 2/6/68

Fig. 5.3. Discretely spaced record samples of two cosine waves.

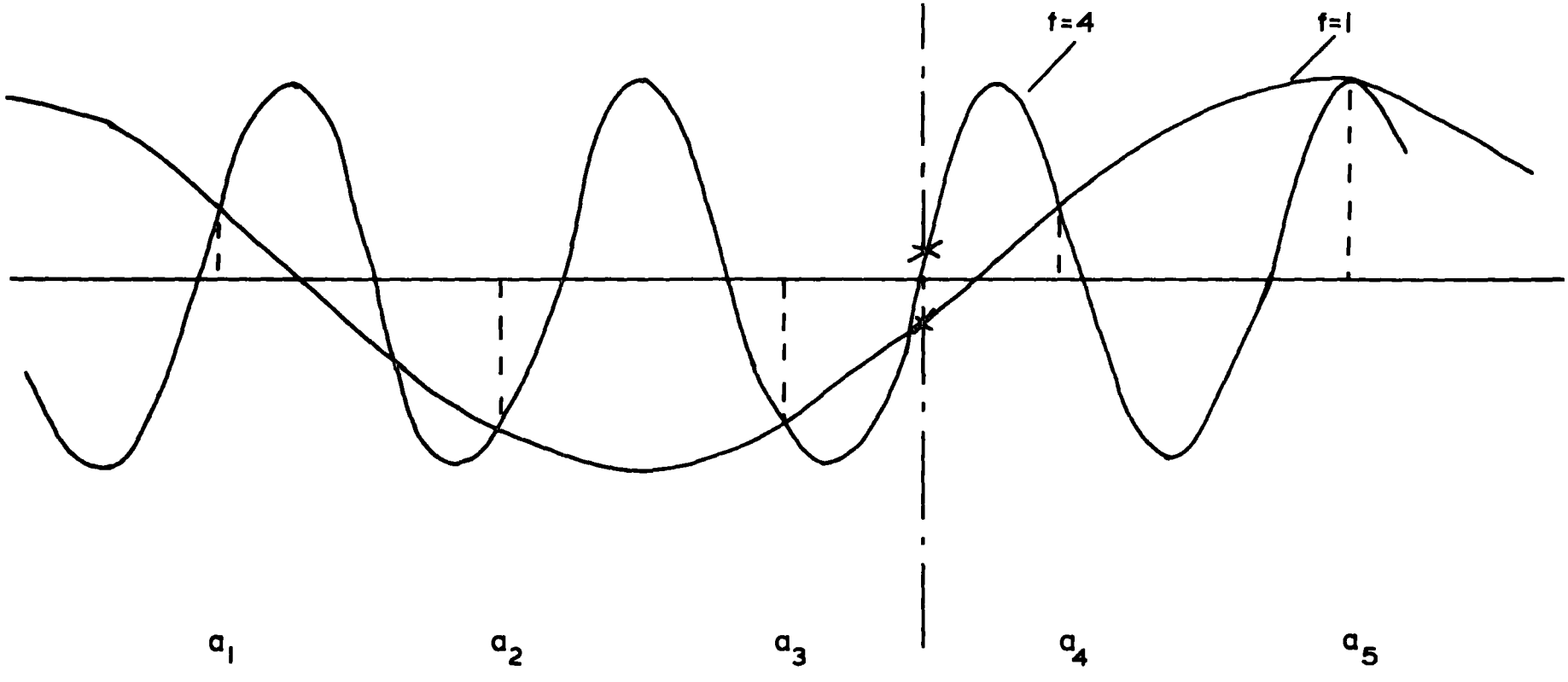

and the best way to achieve this is to make the cut-off frequency of the instrument equal to the folding frequency of the sampling period being employed.

This effect came to the author's notice only after nearly all his records were taken, and, as an alternative course of action, it was decided to apply a low-pass digital filter to the sampled data, before compensation for displacement currents was undertaken. The filter selected involved smoothing the records with weighted averages of the form:

$$PG(N) = 0.25 \times PG(N-1) + 0.5 \times PG(N) + 0.25 \times PG(N+1)$$

This technique is known as 'Hanning', and is named after the Austrian meteorologist, Julius von Hann. The filter proved effective in reducing the errors due to aliasing and, thereafter, no exaggerated displacement effects could be detected in the plots of precipitation current.

5.2 The statistical analysis of time-series in the time domain

This section outlines, and reappraises, some of the statistical methods which have been used to study phenomena of Atmospheric Electricity in the time domain. A basic understanding of the concepts of statistics is assumed and neither the mathematical derivations nor any justification for usage will be given. All the functions discussed are included, in general forms, in the Scientific Subroutine Package on I.B.M. 360 O.S. and may be applied to individual tasks by the substitution of the user's values into variable key parameters.

5.2.1 Correlation coefficients

The observations of pairs of variables, x_i and y_i may be written as a series (x_1,y_1), (x_2,y_2), $\ldots\ldots(x_N,y_N)$. In the analysis, the purpose is to discover whether or not there exists some functional

relationship between the two variables, that is, if $y = f(x)$. For a simple case this function might be linear, so that any deviation of the observed points, (x_i, y_i), from this straight line will be due to inaccuracies in measurement or similar errors. For a linear relation, the correlation coefficient for the whole population of N pairs of variables is given by:

$$r = \frac{1}{N\sigma_x\sigma_y} \sum_{i=1}^{N} (x_i - \bar{x})(y_i - \bar{y})$$

where $\bar{x}, \bar{y}$ are the means of x,y and σ_x, σ_y are the standard deviations of the two populations. This coefficient varies between -1, representing an absolute inverse relation, to +1, indicating an absolute direct relationship between the two variables. A coefficient $r = 0$ implies no association. The value of r^2 gives the proportion of the variability in y which can be accounted for by a change in x. For example, if $r = + 0.8$, then 0.64 of the variability of y is due to x, and the remaining 0.36 is due to other influences.

The statistical significance of r may be tested by the variance ratio test or by 'Student's' t-test (QUENOUILLE, 1950; BROOKS and CARRUTHERS, 1953).

5.2.2 Regression lines

If either x or y can be assumed free from error, it is a straightforward matter to calculate the line of best fit between the two by the method of least squares. For x free from error, the regression line for y on x is given by:

$$y - \bar{y} = r \frac{\sigma_y}{\sigma_x} (x - \bar{x})$$

and for x on y:

$$x - \bar{x} = r \frac{\sigma_x}{\sigma_y} (y - \bar{y})$$

These two lines intersect at $(\bar{x}, \bar{y})$, and the ratio of their slopes is equal to r^2.

In the case of pairs of measurements in Atmospheric Electricity, both variables are prone to error and we must resort to the method of MORGAN (1960) in order to obtain the line of best fit. Here, the absolute errors, α_x' and α_y', in the two variables must be estimated to give the relative errors:

$$\alpha_x = \frac{\alpha_x'}{\sigma_x} \qquad \text{and} \qquad \alpha_y = \frac{\alpha_y'}{\sigma_y}$$

K is a parameter defined by:

$$K = - \frac{\alpha_x}{\alpha_y} \qquad \text{for} \qquad 0 < \left| \frac{\alpha_x}{\alpha_y} \right| \leq 1$$

or

$$K = \frac{\alpha_y}{\alpha_x} - 2 \qquad \text{for} \qquad 0 < \left| \frac{\alpha_y}{\alpha_x} \right| \leq 1$$

The line of best fit is:

$$(y - \bar{y}) = c \frac{\sigma_y}{\sigma_x} (x - \bar{x})$$

where c lies between r and $\frac{1}{r}$ and is given by the equation:

$$(k + 2)\, c^2 - 2r\,(k + 1)c + k = 0$$

This method will be employed to obtain the regression lines of the records of potential gradient and precipitation current.

5.2.3 Cross-correlation coefficients with time lags

The pairs of observations, (x_i, y_i) mentioned in Sect.5.2.1, may both be time dependent, and it is also possible that the maximum association between them may occur for pairs of values (x_i, y_{i+s}), where s indicates some time lag of y behind x. In this work the maximum cross

correlation is of more consequence than the instantaneous correlation coefficient r(0). The cross-correlation coefficient is given by:

$$r(s) = \frac{1}{N\sigma_x\sigma_y} \sum_{i=1}^{N-s} (x_i - \bar{x})(y_{i+s} - \bar{y})$$

and s = 0, ± 1, ± 2, ... ± L, where L is the maximum lag number and is necessarily less than N, the effective length of the record.

If the maximum cross-correlation between two parameters does occur for s not zero (for example, Fig. 5.4(a)), it will be necessary to offer a physical explanation for the time lag or lead.

The validity of the cross-correlation function for records of finite length is discussed in Sects. 5.2.4 and 5.2.5.

5.2.4 The autocorrelation function

As a special case, the cross-correlation of a single time series with itself may be calculated for different lags. This is known as autocorrelation and the normalised coefficient is given by:

$$c_x(s) = \frac{1}{N\sigma_x^2} \sum_{i=1}^{N-s} (x_i - \bar{x})(x_{i+s} - \bar{x})$$

for s = 0, + 1, + 2, ...+ L.

This function gives us information about the persistence of the series by the degree to which subsequent values are dependent on their predecessors. The extent of the persistence will be indicated by the behaviour of $c_x(s)$ with s (Fig. 5.4(b)). For high persistence $c_x(s)$ will be larger for a particular value of s than for low persistence. The variation of $c_x(s)$ with s can also indicate the form of the process which generated the time series. For example, the autocorrelograms for linear processes and for second-order autoregressive schemes have basic differences in shape, but the details do not concern us here.

Fig. 5.4. (a) Cross-correlation r(s) for potential gradient with rain current.

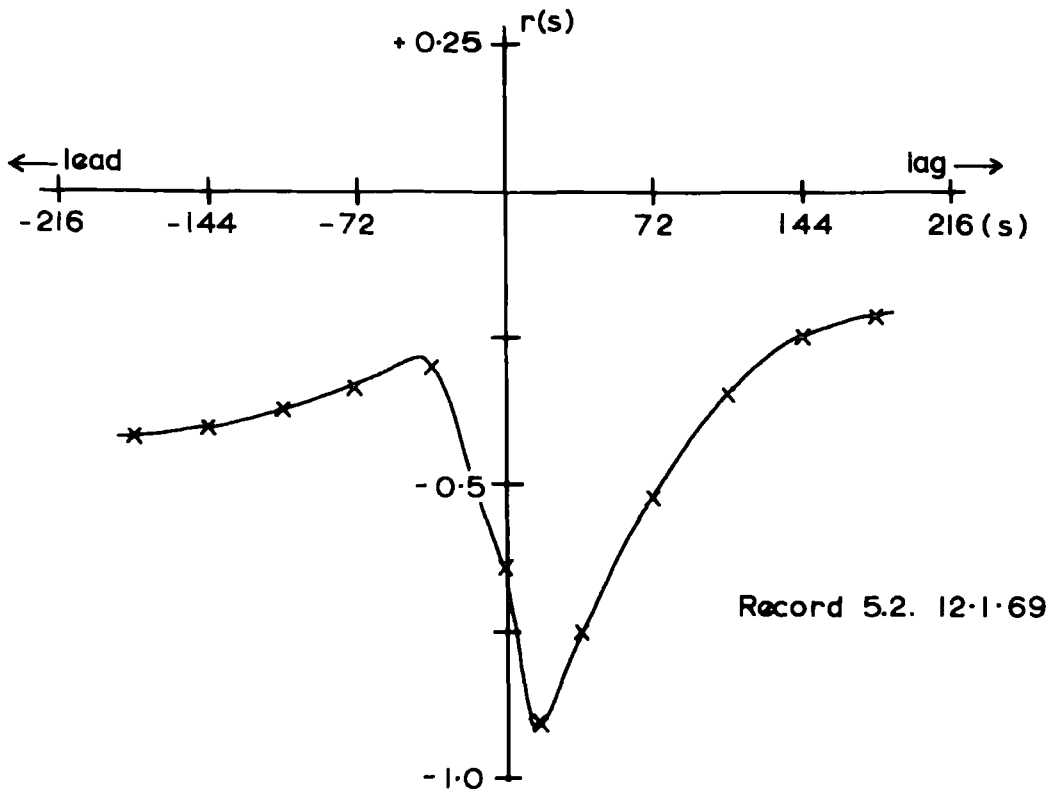

(b) Autocorrelation $C_x(s)$ for rain current.

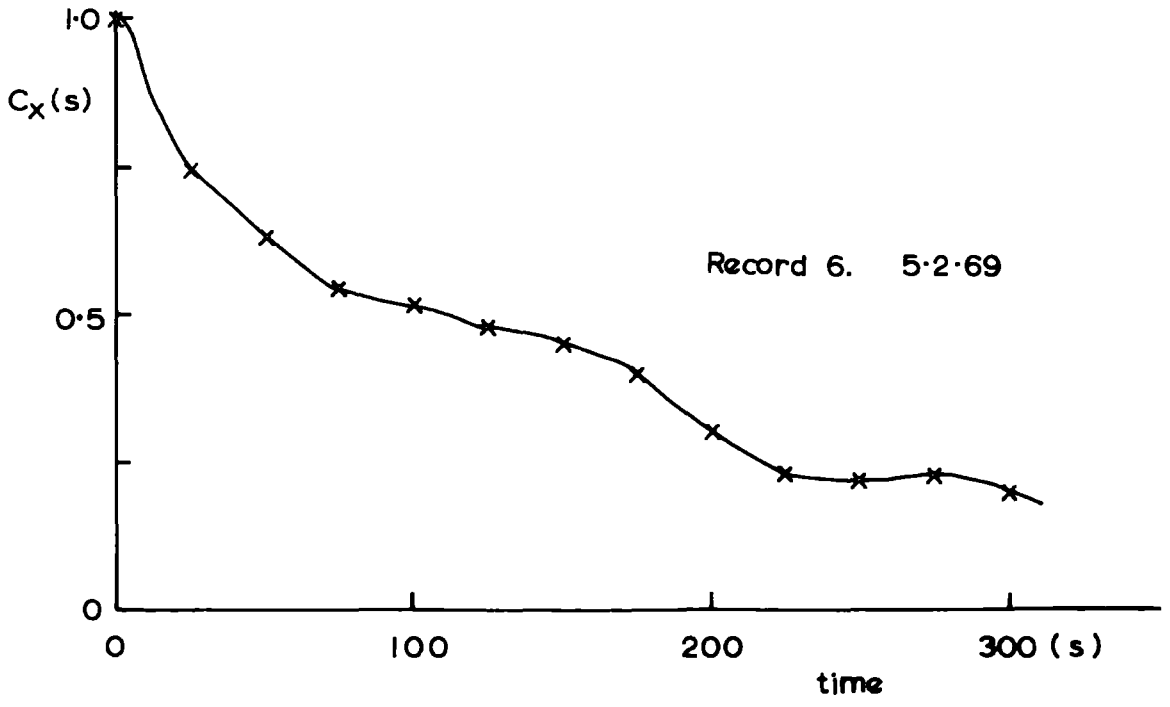

The concept of autocorrelation has been used by COLLIN, GROOM and HIGAZI (1966) to illustrate the electrical 'memory' or persistence of the atmosphere. Their work shows that observations of conductivity include some significant influence from the conditions extant up to 5 minutes previously, and, as a consequence, repeated measurements taken within this period are not truly independent. The theory of the statistical functions is usually based on the independence of the observations and it is evident that care must be exercised when making repeated measurements of a parameter with a long autocorrelation interval (AWE, 1964).

The autocorrelation function will be used extensively in the variance spectrum analysis methods discussed in Sect. 5.3 et seq.

5.2.5 The nature of physical data

Any observed data representing a physical phenomenon can be broadly classified as being either deterministic or random. Deterministic data are those that can be described by an explicit mathematical relationship and for which an accurate prediction of future behaviour may be made. For example, the potential across a condenser discharging through a resistor, or the temperature of a volume of water to which heat is being applied, are basically deterministic.

On the other hand, there is no way to predict an exact value at a future instant of time for random data. These data must be described in terms of probability statements and statistical averages, rather than by explicit equations. In general, observations in Atmospheric Electricity yield such random data. It is further necessary to divide random data into two distinct categories: stationary and non-stationary. Qualitatively, a stationary series is one which is in statistical equilibrium

in the sense that it contains no change in its mean value or variance with time, whereas the statistical properties of a non-stationary series are continuously changing. Realizations of three non-stationary processes, and one stationary process, are shown in Fig. 5.5.

These considerations are important in that, at the present state of the art, an adequate probability theory exists only for stationary random data analysis and the analysis of non-stationary data, such as we are dealing with, relies on the ability to reduce the data to weak stationarity in order to approximate to the desired stationary state. This can be achieved by removing trends in the running mean of the data series. The principles underlying the probability theory are outside the scope of this thesis and only those practical techniques are adopted which are generally accepted as valid for the type of analysis being undertaken here. A full discussion of this topic may be found in the literature (BENDAT and PIERSOL, 1966; JENKINS and WATTS, 1968; KORN, 1966).

5.2.6 The effects of non-stationarity on the statistical functions in the time domain

If two time series, of the type shown in Fig. 5.5(c), both with increasing trends in the mean, are submitted to a cross-correlation analysis, the fact that the corresponding values in each are increasing will enhance the coefficient obtained. If it is desired to gain information about the joint behaviour of these series on a time scale shorter than the record length, then the trends in the means will cause a serious overestimate of the cross-correlation coefficient and the trends should be removed before the analysis is started.

On the other hand, if the time scale of interest is of the same order as the record length it will be seen that considerations of the autocorrelation for each series will probably reduce the number of

Fig. 5.5. Random data series.

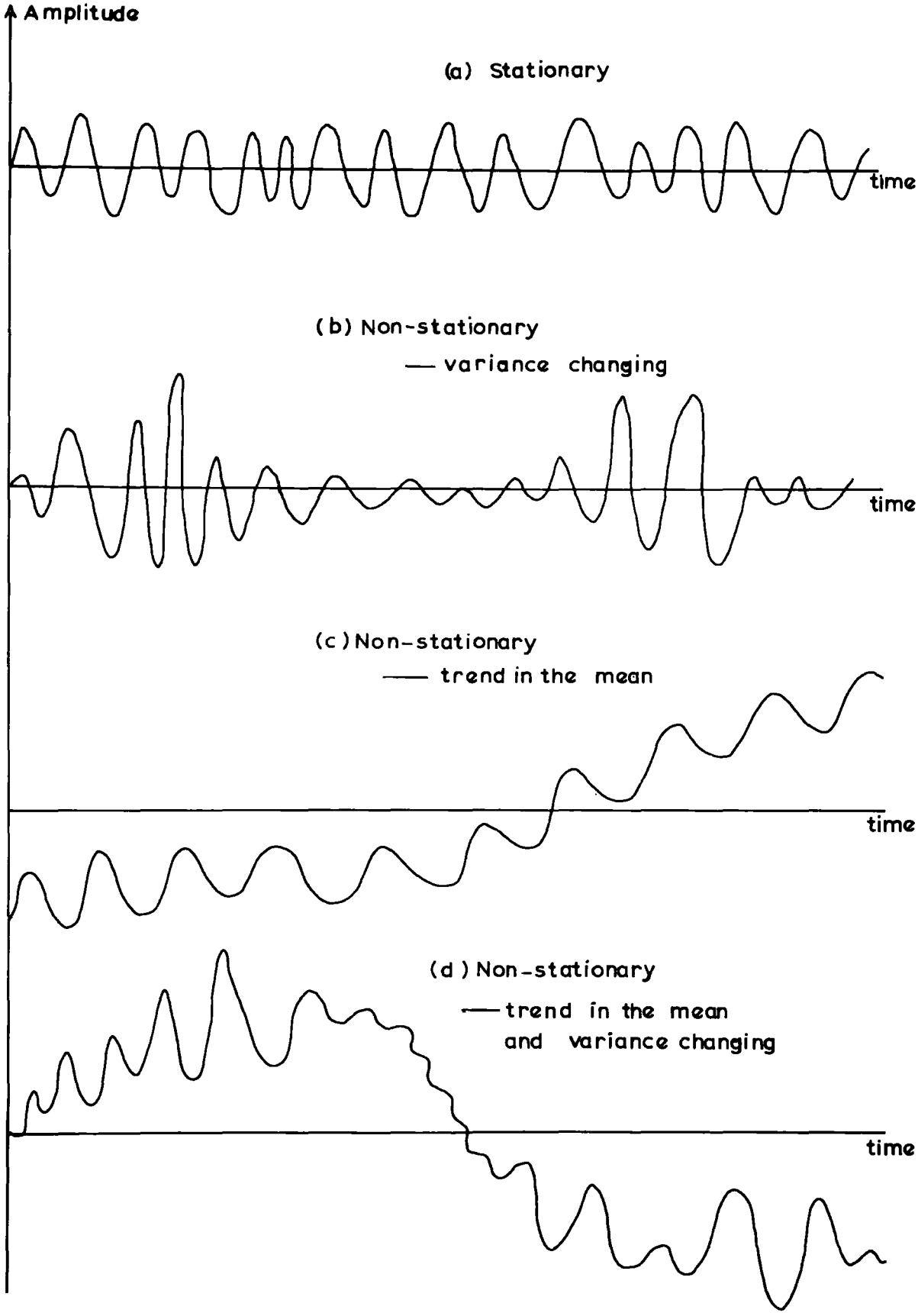

independent values to a level where a significant analysis cannot be completed. It would be necessary to increase the record length by a considerable amount to obtain sufficient data for this purpose. The definitive work on planning for a time series analysis is BLACKMAN and TUKEY (1958), and it is feared that some workers in Atmospheric Electricity have proceeded with such analyses without being aware of the existence of problems of the kind indicated above.

However, when due cognisance is taken of these arguments, the statistical functions are powerful tools for discovering the relationship between, for example, potential gradient and precipitation current in the time domain. A more complete picture will be derived if, in addition, the records are analysed in the frequency domain, and this constitutes the subject of the next sections.

5.3 The analysis of time series in the frequency domain

This part of the work is concerned with the application for the first time, to the author's knowledge, of variance spectrum analysis techniques to Atmospheric Electricity. The aim is to determine whether the fluctuations in the electric elements associated with quiet rain clouds are completely random or whether they are ordered in some manner which is not obvious from the records. Briefly, the analysis has been applied extensively to some geophysical problems in the last 15 years and its major spheres of influence have been the hydrodynamics of oceanography and the problems of boundary layer turbulence in micro-meteorology. Many examples may be found in the literature.

Precedence in geophysics is not, in itself, a sufficient reason for the adoption of an analysis technique, but the work of ACKERMAN (1966) on the water content of clouds, suggests that it might offer an objective

study of the sort of time series encountered in Atmospheric Electricity.

5.3.1 General principles of spectrum analysis

The power spectral density function for random data describes the general frequency composition of the data in terms of the spectral density of its mean square value. This is known variously as the variance, power, or energy spectrum. It involves the use of Fourier techniques which are assumed to be sufficiently commonplace not to warrant explanation here. (General reference: BARBER, 1966).

The determination of the spectrum is based on the fact that the power spectral density function is equal to the Fourier transform of the autocorrelation function (Sect. 5.2.4). Given $x(t)$, a continuous series with zero mean and of infinite length, the autocorrelation $C_x(s)$ is by definition:

$$C_x(s) = \underset{T \to \infty}{\text{Limit}} \frac{1}{T} \int_{-T/2}^{T/2} x(t)\, x\,(t + s)\, dt$$

where s is the lag in time. The spectral function is the Fourier transform of $C_x(s)$:

$$L(f) = 4 \int_0^{\infty} C_x(s) \cdot \cos(2\pi fs) \cdot ds$$

In practice, the series are not infinite and have generally been evaluated at discrete intervals of time. It is necessary, therefore, to adopt a numerical approximation to the integrals in order to make digital computation possible.

5.3.2 Numerical approximations

The first step is to replace the continuous series, $x(t)$, by x_i, where $i = 1, 2, \ldots\ldots N$, and the interval between i's is Δt. The numerical approximations to the integrals are fully discussed by BLACKMAN

and TUKEY (1958) and are of the form:

$$C_x(s) = \frac{1}{N-s} \sum_{i=1}^{N-s} (x_i)(x_{i+s}) \qquad s = 0,1,2,.....M$$

and

$$L(h) = \frac{1}{M} \sum_{s=0}^{M} \delta_s . C_x(s) . \cos \frac{\pi hs}{M} \qquad h = 0,1,2,.....M$$

where

$$\delta_s = 1 \text{ for } s = 0, M$$

and

$$\delta_s = 2 \text{ for } s \neq 0, M$$

and s and h are the lag and harmonic numbers respectively.

Simply, the average contributions to the variance, or power, L(h), are obtained for M + 1 frequency bands, each identified by the central frequency $\frac{h}{2M\Delta t}$. These bands are of width $df = \frac{1}{2M\Delta t}$, except for h = 0, m which have half the width.

5.3.3 Leakage

As a consequence of the finite length of the series it is not possible to identify frequencies exactly and, on occasion, a particular frequency may fall at the edge of one of the frequency bands with the result that the contribution to the variance in that band is inflated, whilst the variance in the adjacent bands is depleted. This is known as 'leakage' (BLACKMAN and TUKEY, 1958) and compensation is effected by smoothing the spectrum by the Hanning technique (Sect. 5.1.3), thus:

$$U(h) = 0.5\ L(h) + 0.25\ [L(h-1) + L(h+1)]$$

This technique is standard.

5.3.4 Aliasing

This problem, encountered in Sect. 3.15, recurs again in the variance spectrum when frequencies approach the folding frequency. Here, leakage from higher frequencies across the folding frequency result in spurious contributions to the variance and the easiest way to deal with this problem is to ignore the estimates of U(h) near to the folding frequency.

5.3.5 The design of a spectral analysis

It is possible to specify, in advance, how much data and what sampling interval are required to give good frequency resolution and a good spectral estimate in the frequency range of interest, and without leakage and aliasing becoming excessive problems. Such planning ahead is desirable but in the present work the length of record was dependent upon the duration of rain, and the sampling interval was fixed at that of the automatic recording system. So we must examine the converse approach and determine how far we can take the analysis without meeting discrepancies due to leakage and aliasing.

5.3.6 The upper frequency limit for the spectrum

Aliasing will occur for the frequency:

$$f \geq \frac{1}{2\Delta t}$$

where Δt is the sampling interval, and for this work was usually equal to 6s. Thus the upper frequency limit for the spectrum was about 0.1 Hz.

5.3.7 Frequency response

A critical parameter to be considered in the interpretation of the spectrum is the frequency resolution, given by:

$$df = \frac{1}{2M\Delta t}$$

where M is the maximum lag number. An oscillation which contributes significantly to the variance may go undetected if there is inadequate resolution in the spectrum. If the elementary bandwidth, df, is one half or more of the frequency separation between two oscillations, they cannot be resolved in the spectrum, and will appear as a single contributing region. As df decreases below this value the two oscillations will start to separate. The conclusions which may be drawn from a variance spectrum may be taken to indicate the presence of an oscillation at that frequency, but the absence of a peak is not sufficient evidence to conclude that that frequency does not contribute to the variance.

The frequency resolution, df, varied from record to record and the value of M, the maximum lag number, was arbitrarily set at $\frac{4N}{5}$, where N is the number of measurements in the record. This value, $\frac{4N}{5}$, has no theoretical justification but was employed to prevent the instabilities which arise in the spectrum as M approaches N. It will be seen that the longer the record the better is the frequency resolution.

5.3.8 The removal of low frequency trends

The measurement of atmospheric electric parameters nearly always involves trends in the means of these observations. This causes a large proportion of the power of the spectrum to be concentrated in the lower frequencies, with consequent loss of resolution at higher frequencies. In view of the fact that, at the outset of this work, it was not known which frequency range would be of greatest interest, it was decided to compute spectra both with the trends present and with them removed.

The example (Fig. 5.6) shows a rough plot of the original potential gradient record (No. 8.4 - 27/2/69) and the filtered series with the

trend removed. Compression of the time scale has reduced the fine detail which was on the record, but this is brought out in the filtered series spectral estimate, where the frequencies 0.9, 1.45 and 1.95 cycles per minute give significant contributions to the variance.

Several techniques are available for removing trends and the one chosen for this work was the application to the data of a high-pass digital filter of the form:

$$x_i' = x_i - x_{i-1}$$

This is sometimes referred to as 'prewhitening' (BLACKMAN and TUKEY, 1958) and derives its name from the desire to make the spectrum more like that of purely random 'white' noise, rather than the 'red' noise spectrum obtained from data with a degree of persistence (Fig. 5.6).

5.3.9 Testing the significance of peaks in the spectrum

A rough test of the significance of peaks in the low frequency spectrum can be made by computing the underlying autocorrelation, or 'red' noise spectrum, for the data. The assumption is made that the variance is distributed as Chi-square about this spectrum and, if the variance spectrum is plotted on a logarithmic scale, the ordinate lengths of the upper and lower confidence levels are constant over the whole frequency range (Fig. 5.7). The values of these levels are given by:

$$\frac{\chi^2(\alpha) \cdot U(h)}{DF} \quad ; \quad \frac{\chi^2(100-\alpha) \cdot U(h)}{DF}$$

Here χ^2, which is given in all statistical tables, is a function of DF, the number of degrees of freedom, which is approximately given by $\frac{2N}{M}$ (JENKINS, 1961). N is the number of observations and M is the maximum lag number.

Fig. 5.6. Removal of trends from time series.

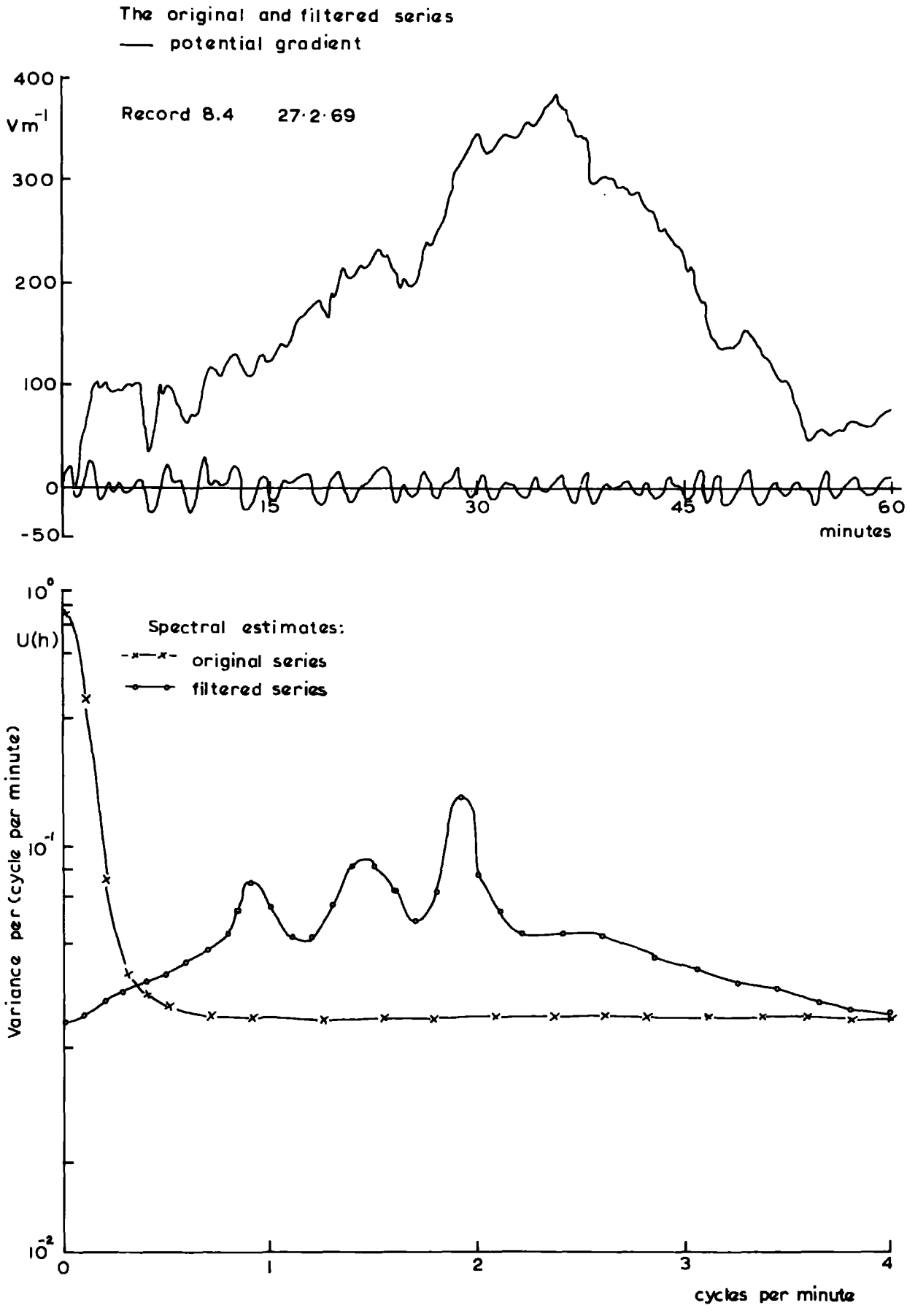

Fig. 5.7. Significance levels for peaks in the variance spectrum.

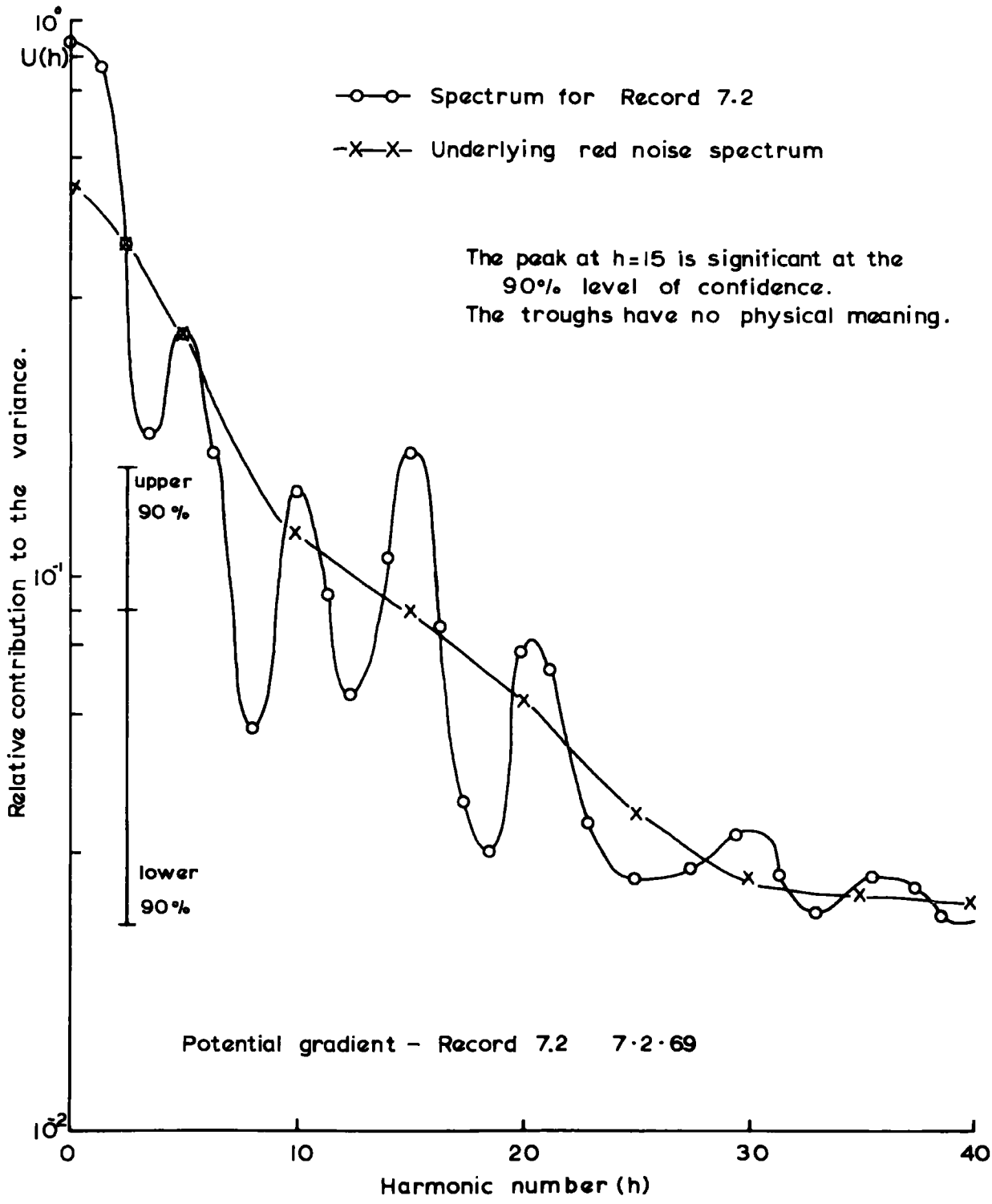

A similar test can be adopted for the filtered series spectrum.

5.3.10 Harmonics

The occurrence of multiple peaks in the spectrum raises the question as to whether some might not be harmonic oscillations of a longer wave component. They may be real, but this is very difficult to establish and if peaks do occur having a central frequency which is a higher multiple of some other frequency, then these peaks should be ignored.

One frequency component is nearly always present in the spectrum and this corresponds to the length of the record being analysed. It should also be ignored.

5.4 Cross-spectral analysis

The concept of a cross-spectral density function for two sets of random data evolves directly from the cross-correlation function. As the power spectral density function for a single time history record is the Fourier transform of the autocorrelation function, so the cross-spectral density function for a pair of time history records is the Fourier transform of the cross-correlation function.

These considerations allow us to analyse the cross-correlation between two series in the frequency domain. The cross-correlation coefficient in the time domain is made up from the net effect of the cross-correlations over the whole frequency spectrum, and it is possible that a significant proportion of this correlation is carried by one, or more, particular frequencies. This would be of great consequence in a study of the processes relating precipitation current to potential gradient.

The cross-spectrum can be presented as a phase spectrum, indicating the relative phase between corresponding frequencies in the two series, and as a coherency spectrum which indicates the correlation of the amplitudes of variance for corresponding frequency components.

5.5 A summary

The methods outlined have been adopted in an attempt to gain new knowledge of the processes governing the electrical effects of quiet rain. It must be stressed that many of the techniques of spectral analysis are still being developed and are the subjects of much controversy amongst specialists in this field. It is felt, however, that here is a powerful tool for the analysis of Atmospheric Electricity measurements and that workers in this discipline should keep in touch with developments. A modern 'fast' Fourier transform program, for instance, can cut the 30 minutes computing time taken by the author's programs to a mere 7 seconds.

CHAPTER 6

THE PRECIPITATION MEASUREMENTS AND THEIR RESULTS

This chapter is devoted to the results of an analysis of measurements made in electrically 'quiet' precipitation, the conditions for which have been outlined in Sects. 2.3.1 and 2.3.2. The investigation extended from January 1969 to June of the same year and included periods of rain and snow. In all, 32 individual records were taken, giving more than 57 hours of data.

6.1 The records

6.1.1 The procedure for recording

On many occasions a timely forecast of the development and arrival of a warm front over Lanehead was obtained from the Meteorological Office Weather Centre at Newcastle. The author is indebted to the staff of the Centre for their assistance and interest as well as for their consistent accuracy. It was often possible to arrive at Lanehead, from Durham, well before the onset of rain and when this was the case the instruments were switched from their fair weather ranges (Chapter 7) and the zeros were checked. If, however, the rain had started the zero checks were deferred until the end of recording. On no occasion was there found to be any significant zero error and this can be attributed to the fact that the instruments were permanently in operation and required no time to settle. When precipitation commenced, the automatic recording system was switched on and checked to ensure that it was sampling and cycling correctly. A visual check of the instrument outputs was also made.

On being satisfied that recording was proceeding satisfactorily, the next task was to set the sensitive cup-anemometer on a 2m stand on ground adjoining the Atmospheric Physics plot, and to deploy the sky photometers

along the line of the wind. The distance between the two vertical photometers, from which the horizontal cloud speed can be estimated, was determined by tape-measure, and was usually about 60-100 m. The four-channel pen recorder, used to monitor the anemometer and photometer outputs was then set in motion and the remainder of the recording period was taken up by keeping an eye on the behaviour of the instruments. This required no action on the part of the author except on rare occasions; for example, a wet leaf once fell across the top of a photometer, causing its output to fall to zero.

At the conclusion of the precipitation, or when the necessary conditions for 'quiet' rain were not fulfilled, the record was terminated and the 1-hour recording system was reinstated.

6.1.2 The atmospheric electricity results

The precipitation electricity results are summarised in Table 6.1, in line with general practice, by computing the means and standard deviations for each of the parameters, in this work for potential gradient, precipitation current density and space charge density. The cross-correlation coefficients of maximum association between potential gradient and precipitation current, and potential gradient and space charge, are also given and demonstrate that the results obtained are in accord with previous work. Most of the coefficients for potential gradient with precipitation current are negative, indicating a general inverse relationship (SIMPSON, 1949), and, more often than not, the maximum association occurs for appreciable time differences between the two parameters. This was also found by RAMSAY and CHALMERS (1960), who further suggested that the relationship between potential gradient and precipitation current was probably not linear. The frequency-domain analysis (Sect. 6.3) has

confirmed this view and the author has refrained from deriving a linear line of best fit on each record for this reason.

The cross-correlation coefficients for potential gradient with space charge, on the other hand, are all positive and corroborate the results of SHARPLESS (1968). In general, the coefficients are smaller than those of Sharpless, but this is because his measurements were made with pen recorders which, by virtue of the inertia of the pen, attenuate the faster variations. As a trial, one of the digital records from the automatic recording system, which had a cross-correlation coefficient of + 0.85, was filtered to remove higher frequencies and the coefficient was increased to + 0.90.

6.1.3 The meteorological observations

A summary of the meteorological conditions for each recording period is given in Table 6.2. The wind and cloud measurements were made at Lanehead by the methods outlined in Chapter 4, and the air temperatures were taken from a thermometer in the Stevenson Screen in the grounds of the school. The estimates of the height of the $0^{\circ}C$ isotherm were obtained by interpolation between the temperature and pressure observations issued by the Meteorological Office in their Daily Aerological Record.

6.1.4 A record of interest - 5-6 February, 1969

The record TR 6, drawn by the computer, is shown in the two photographs of Fig. 6.1 and covers the period 2255 Z (5.2.59) to 0520 Z (6.2.69). In this time a depression moved across northern England from the N.W. The first hour and a half of the record shows conditions of precipitation from altostratus and indicates little electrical activity. The second part of Fig. 6.1 contains that portion of the record when the

precipitation was from nimbostratus; it is a good example of the mirror-image effect (SIMPSON, 1949). This period of electrical activity was terminated with the passing of a weak warm front and there followed 3 hours of continuous rainfall which was orographic in origin. This period, the third part of Fig. 6.1, was interspersed with brief bursts of activity probably originating in cumuliform clouds which are a feature of the warm sector. The last part of the record shows a considerable increase in activity as the heavier precipitation associated with the cold front arrived. The rain turned to snow at this juncture and enhanced electrical effects were observed, which became too violent for the instrument ranges being used.

Most of the other records exhibited similar behaviour for similar weather conditions, but this record is the only one which might be regarded as typical of the electrical conditions for a complete frontal system.

6.2 Analysis of the data in the frequency domain

6.2.1 Peaks in the variance spectra

It was explained in Sect. 5.3.9 that a statistically significant peak in the variance spectrum can be taken to indicate an important contribution to the variance by a particular frequency band. The central frequency of such a band defines the frequency of the periodicity which gives rise to the peak. All the records were analysed by computing the variance spectra for potential gradient and precipitation current, and, in all cases, one or more significant peaks were obtained. The frequency histograms of the periodicities, in steps of 15 minutes, are shown in Fig. 6.2.

The periodicities are not isolated events in their own right, but

TABLE 6.1 Precipitation electricity measurements

Record No.	Date (1969)	Potential gradient (Vm^{-1}) Mean	Potential gradient (Vm^{-1}) Std. dev.	Precipitation current ($pA\ m^{-2}$) Mean	Precipitation current ($pA\ m^{-2}$) Std. dev.	Space charge density ($pC\ m^{-3}$) Mean	Space charge density ($pC\ m^{-3}$) Std. dev.	Cross-correlation coefficients r_{12}	Cross-correlation coefficients r_{13}
1	3/1	-241	272	3.8	5.7	-70	46	-0.48	0.91*
4	8/1	- 55	178	1.9	1.0	-31	20	-0.89*	0.97*
5.1	12/1	-580	306	45.2	26.1	0	40	-0.74*	0.65*
5.2	"	-112	381	35.4	26.7	27	27	-0.85*	0.72*
5.3	"	-245	380	30.7	20.4	89	162	-0.82*	0.59*
6	5/2	-155	187	21.3	25.0	-	-	-0.41	-
7.2	7/2	253	61	-10.6	10.9	-	-	-0.58*	-
8.1	27/2	243	13	- 2.0	1.4	-	-	-0.31	-
8.3	"	262	148	-14.6	6.2	-	-	-0.31	-
8.4	"	125	119	-25.2	14.1	-	-	0.38	-
9	24/3	140	49	- 9.8	3.5	-	-	-0.60*	-
10.1	29/3	-174	230	1.0	25.6	-	-	-0.26	-
10.2	"	-119	132	- 1.2	4.2	-	-	0.26	-
10.3	"	-218	124	2.0	4.4	153	24	-0.51	0.85*
10.4	"	-518	220	- 9.4	33.9	201	47	-0.66*	0.33
10.5	"	-314	207	- 1.2	1.7	-16	8	-0.46	0.59*
11	14/4	-431	285	7.1	25.5	-	-	-0.48	-
12	21/4	73	379	33.6	34.3	-	-	-	-
13	7/5	- 82	197	6.3	9.9	-	-	-0.35	-
14	8/5	-245	142	2.9	14.2	-15	22	0.09	0.79*
15.1	25/5	- 33	21	- 0.8	0.6	- 4	5	-0.61*	0.50
15.2	"	- 94	73	0	2.0	-30	25	-0.48	0.50
16.1	26/5	- 95	93	7.5	13.2	-	-	-0.66*	-
16.2	"	-106	90	12.2	23.8	-75	151	-0.65*	0.62*
17.1	2/6	-184	256	3.5	7.2	-43	33	-0.84*	0.90*
17.2	"	-171	244	4.5	20.0	-81	103	-0.29	0.50
18	20/6	- 98	157	7.0	8.1	4	19	-0.78*	0.86*

* denotes significance at 95% level of confidence

TABLE 6.2 The Meteorological Observations

Record No.	Date (1969)	Time (Z) Start	Time (Z) Finish	Wind Direction	Wind Speed at 2m (ms^{-1})	Cloud Speed (ms^{-1})	Cloud Height (m)	Air Temp. at ground level (^{o}C)	Height of $0^{o}C$ isotherm (m)
1	3/1	1915	2017	W	3	12	300	+3	360
4	8/1	1718	1830	SE	3	5	450	+2	300
5.1	12/1	1257	1425	E	8	-	0	+2	250
5.2	"	1545	1620	E	8	-	0	+2	250
5.3	"	1640	1710	E	8	-	0	+2	250
6	5/2	2255	0520	NW	5	18	90	+2	230
7.2	7/2	0945	1030	NW	1	2	150	-7	0
8.1	27/2	0945	1010	NE	1	15	750	-2	0
8.3	"	1025	1115	NE	2	9	360	-1	0
8.4	"	1145	1305	N	2	9	280	-1	0
9	24/3	1830	1945	N	1	8	580	0	150
10.1	29/3	1330	1410	W	7	20	140	+4	700
10.2	"	1725	1900	W	7	20	140	+4	700
10.3	"	1905	2000	W	7	20	140	+4	700
10.4	"	2040	2155	W	7	20	140	+4	700
10.5	"	2255	2320	W	7	20	140	+4	700
11	14/4	1220	1830	W	8	16	270	+7	1900
12	21/4	1640	1815	NE	7	19	270	+2	1200
13	7/5	1856	0032	SE	6	12	700	+8	1350
14	8/5	0955	1030	S	5	-	0	+7	1600
15.1	25/5	1918	2014	SE	1	7	150	+13	2200
15.2	"	2035	2145	SE	3	7	150	+11	2200
16.1	26/5	0823	1000	SE	4	-	0	+8	1750
16.2	"	1033	1153	W	7	-	0	+8	1750
17.1	2/6	1355	1455	SW	4	9	790	+10	2300
17.2	"	1522	0210	SW	3	4	200	+10	2400
18	20/6	0720	1131	ESE	4	12	200	+10	2600

Fig. 6.1 (opposite and over) Record 6 (5 Feb.1969) of potential gradient and precipitation current (x-x)

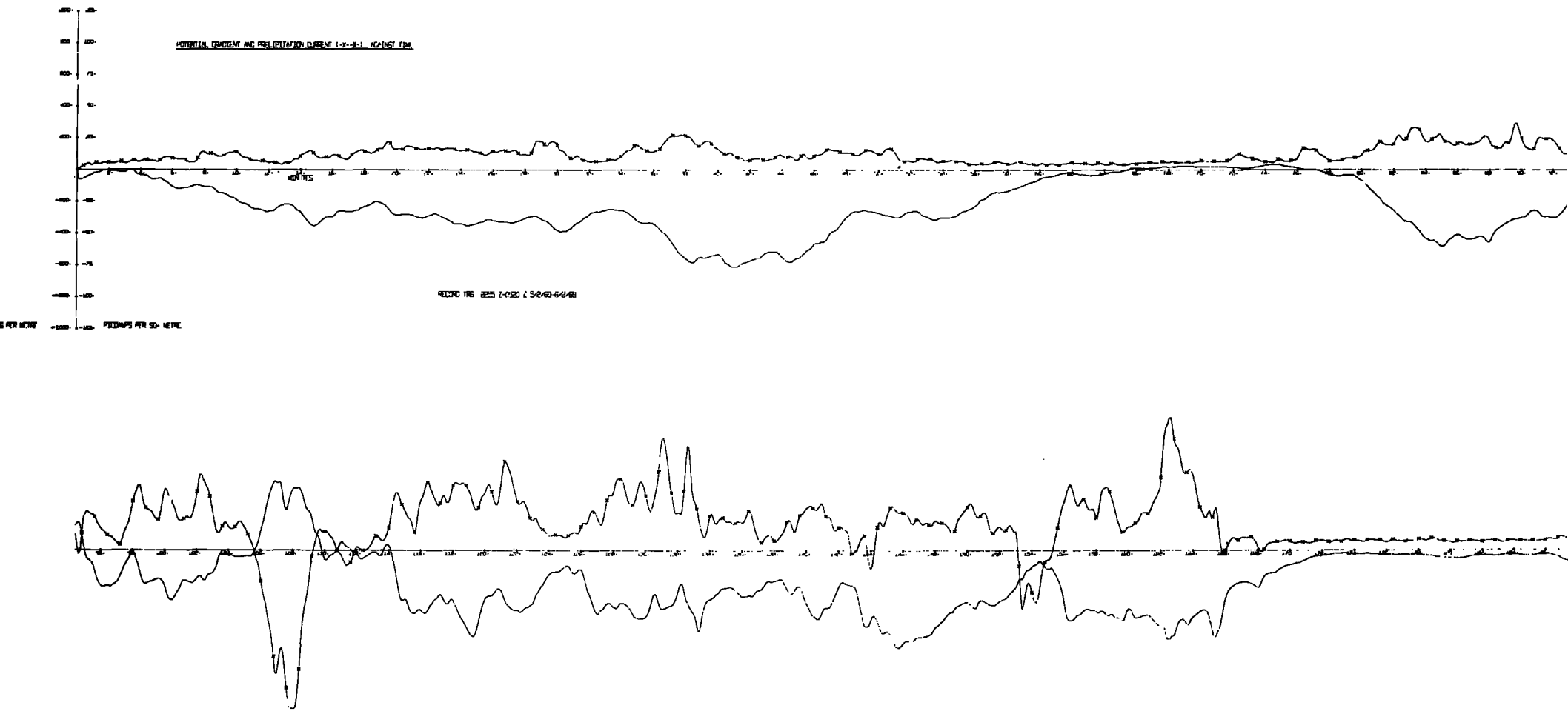
POTENTIAL GRADIENT AND PRECIPITATION CURRENT (-x--x-) AGAINST TIME
MONTHS
PICOAMPS PER SQ. METRE

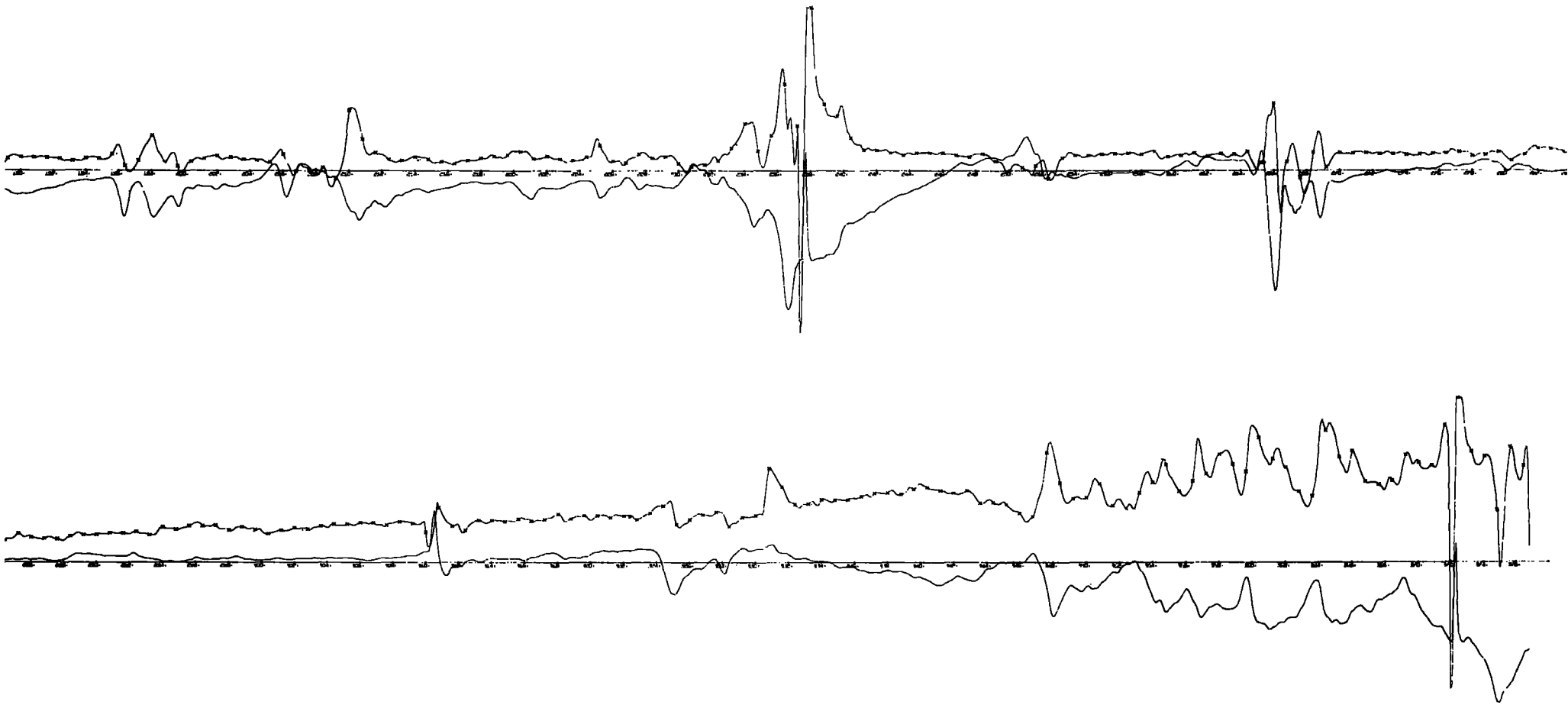

represent variations superimposed on small, long-term trends in the parameter records. SIMPSON (1949) describes wave patterns in his potential gradient records during rain which varied in period from a few minutes to over 1½ hours. No physical explanation was offered beyond the conjecture that some differential displacement of positive and negative charge was proceeding in the cloud. A varying charge separation process is a possible explanation but it is likely that the physical dynamics of precipitation, determining the manner of arrival of the particles at the ground, is a more powerful factor in the precipitation current periodicities. WHITLOCK and CHALMERS (1956), using two field mills, found that the potential gradient patterns could be produced either by horizontal motion of the charges over the observer or by vertical motion of the charges in the cloud. Meteorological studies of a warm front at Pershore, Worcestershire, by BROWNING and HARROLD (1969), have revealed complex but recurring variations of up-draughts and precipitation rates in the frontal cloud; electrical patterns on the same time-scale may well be associated with these variations.

The majority of periodicities, for both parameters, are of relatively short duration, but this is particularly true of the precipitation current periodicities. It is suggested that the potential gradient periodicities are longer because of the spreading effect of wind on the space charges which control the potential gradient and because the field mill will be influenced by the charges as they approach and recede with the wind.

The cases just mentioned are for periodicities in the individual parameters, and in order to learn something of their correlated behaviour we must examine the coherency spectra.

6.2.2 Peaks in the coherency spectra

The coherency spectrum expresses the cross-correlation between two time series in terms of a frequency-dependent coefficient. An example shown in Fig. 6.3, from record TR 15.2, typifies the spectra for all the records. Apart from the peaks at particular periodicities, it will be seen that the relationship between potential gradient and precipitation current is very complex and certainly not linear over the whole frequency spectrum. The form of the coherency spectrum indicates that the process which generates the observed effects is autoregressive, that is, it exhibits persistence (Sect. 5.2.4) and that it is a higher order scheme. A single order scheme, known as Markovian, has some contribution from its immediately previous value; a second order scheme has contributions from the two previous values and these contributions may be weighted by differing amounts. Such schemes produce recognizable coherency spectra, to which the example given is similar but not identical. It must be assumed that the process which we are seeking is of a higher order and extremely complex. The analysis required to uncover it is too protracted for the scope of this work.

However, we may gain some information from the spectra obtained. Fig. 6.4(a) is an histogram of the number of statistically significant peaks in the coherency spectra expressed as periodicities in steps of 15 minutes. It would be surprising if these peaks, derived effectively from coincident peaks in the potential gradient and the precipitation current variance spectra, were not representative of a process governing the joint effects observed in the two parameters. Their existence suggests that there is usually some regular 'cell'-like electrical activity occurring in nimbostratus and this calls into question the various theories which assume, a priori, an electrical quasi-static state. Evidence will

be presented in the next section to show that a charge separation process occurs within the cloud and so, here, the product of periodicity and cloud speed, for each record, is taken as a measure of the physical size of the electrical cell. An histogram of cell sizes is shown in Fig. 6.4(b); the mode is 10-20 km and more than 83 per cent of the cell sizes occur on the scale 0-30 km.

It was thought that the cell sizes might be a function of aerological turbulence, but no relationship could be discovered with a number of relevant meteorological parameters: wind speed, cloud speed and cloud base height. An index of turbulence was calculated from the rate of change of horizontal wind speed with height but this showed no correlation with cell size or with the power in the two electric parameters as expressed by their variances. REITER (1968) discusses the characteristics of precipitation electricity from stable and unstable stratiform clouds.

The interrelation of electrical and meteorological effects must also be considered on the sub-synoptic scale, that is, on a scale smaller than the overall frontal system but greater than the sub-cloud scale. The present electrical measurements fall in the range 0-70 km because of the difficulty of obtaining, in a limited period, records of the type TR 6 (Fig. 6.1) to give a meaningful picture on a scale of 100 km or greater. The analysis methods adopted here will apply if sufficient data are available.

The meteorological research into frontal rainfall is being intensified with the establishment of Project Scillonia (MASON, 1969). The main objectives of the investigation are to study vertical air motions and the constitution and development of the clouds and their precipitation on four scales: synoptic (> 300 km spacing), medium (100 km), small (10 km) and fine (0.1 to 1 km). This follows work by BUSHBY and TIMPSON (1967) who

developed a ten-level numerical model for predicting rainfall amounts on the synoptic scale, and BROWNING and HARROLD (1969) who found coarse rainfall regimes on the scale of 100 km in frontal conditions. The drawback to this type of work is the long delay inherent in collecting measurements from a network of rain gauges which means that predictions can only be made a posteriori. It is suggested that precipitation electricity measurements, which can be statistically treated in real-time by modern waveform analysers, may be an alternative method for studying cloud and frontal structure and could become a ready means for identifying, and hence forecasting, weather patterns. This view is supported, in principle, by REITER (1968).

6.2.3 The phase spectra

Fig. 6.5 is an example of the phase spectra which describe the phase relationship between potential gradient and precipitation current for all the data series analysed. This example is taken from record TR 16.2. For periodicities of 300 to 7000 s, the precipitation current has a phase lead over the potential gradient of 90°; there are exceptions which will be dealt with shortly. If the periodicities are shorter than 300 s or greater than 7000 s, the two parameters are in phase.

The general form of the spectrum fits the predictions of a model for nimbostratus electrification which has been developed by a colleague of the author's, Mr. M. F. Stringfellow.

Fig. 6.2. Frequency distribution of significant peaks in the variance spectra.

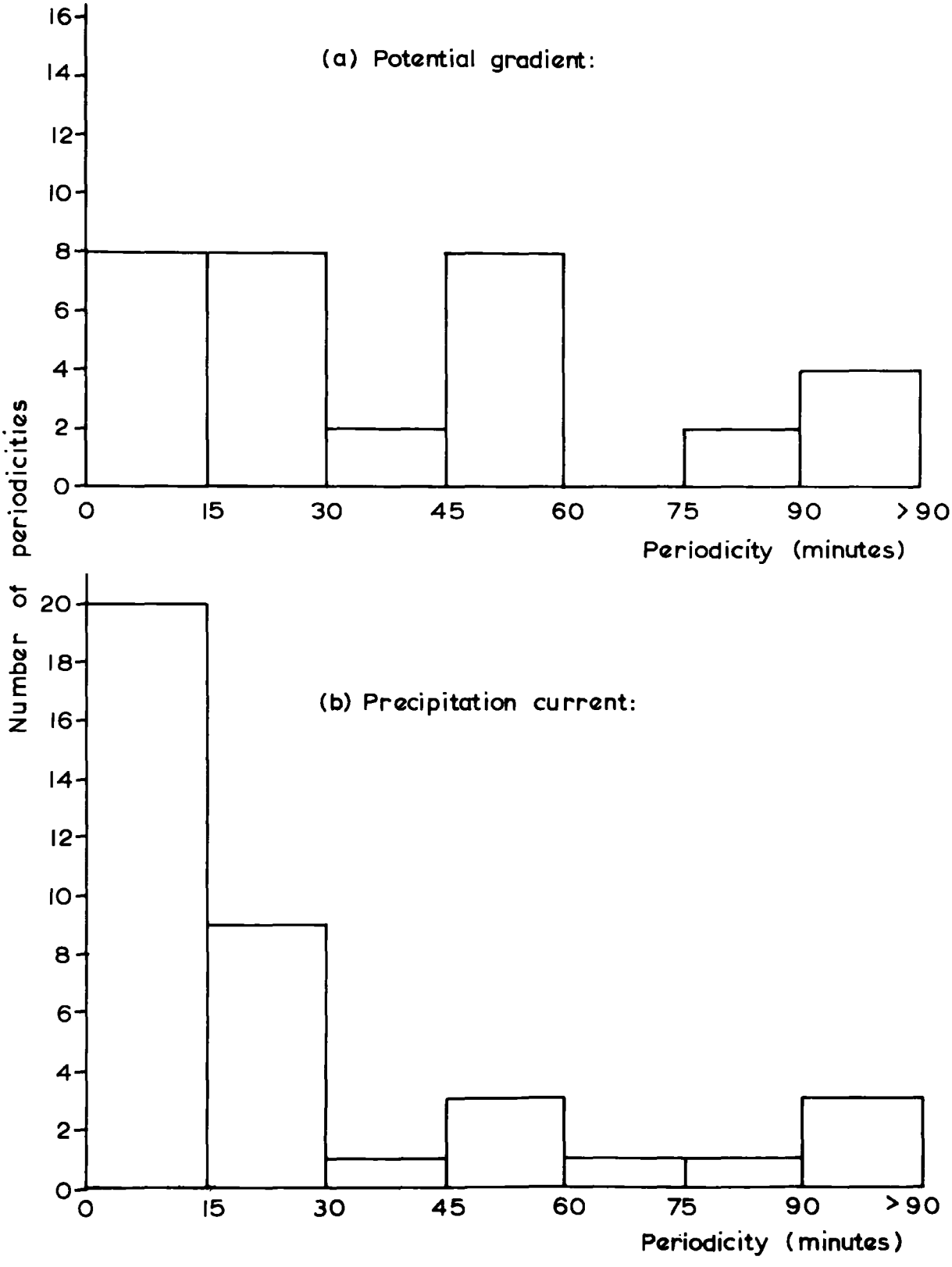

Fig. 6.3. The coherency spectrum of potential gradient with precipitation current.

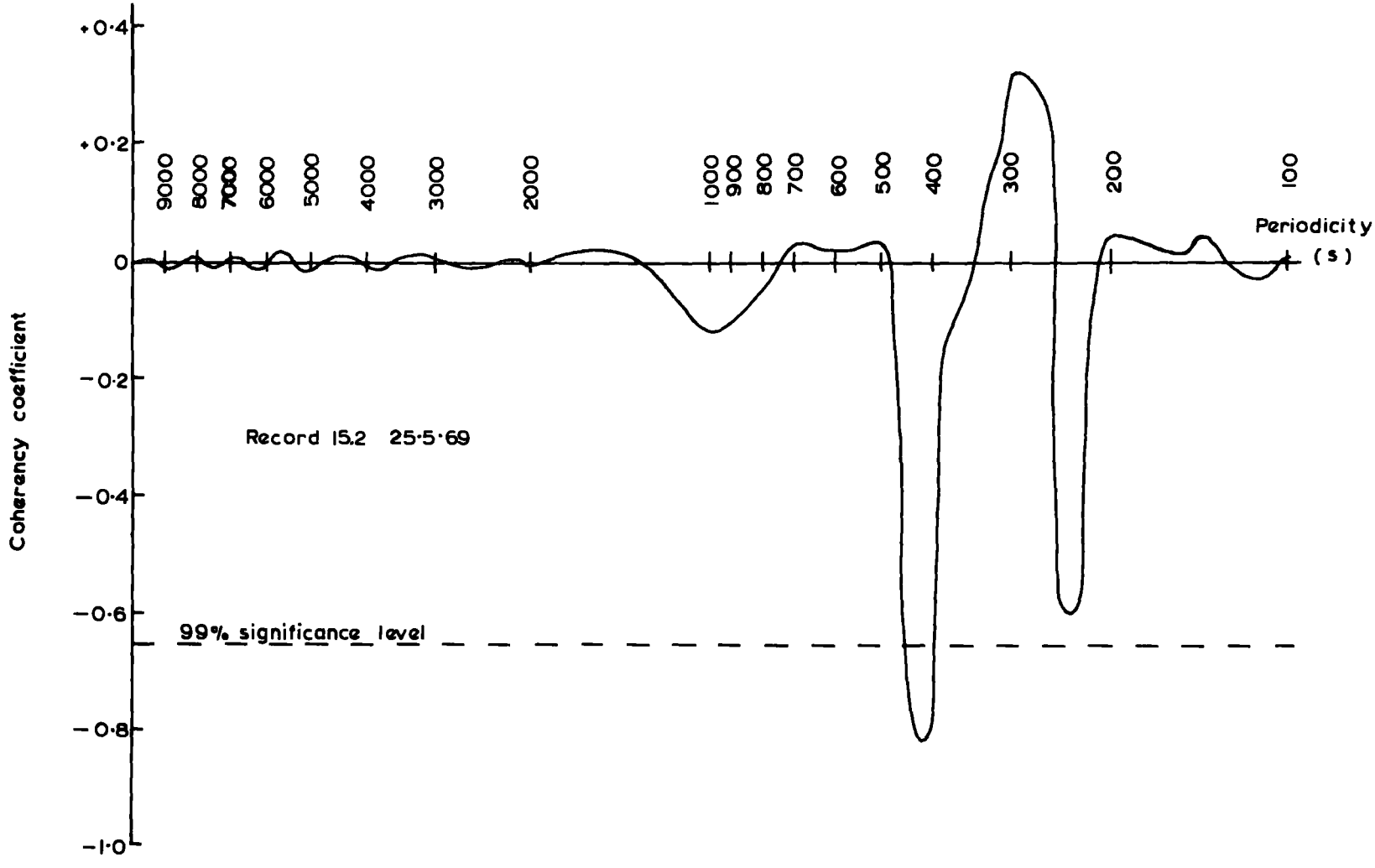

Fig. 6.4. Frequency distribution of significant peaks in the coherency spectra.

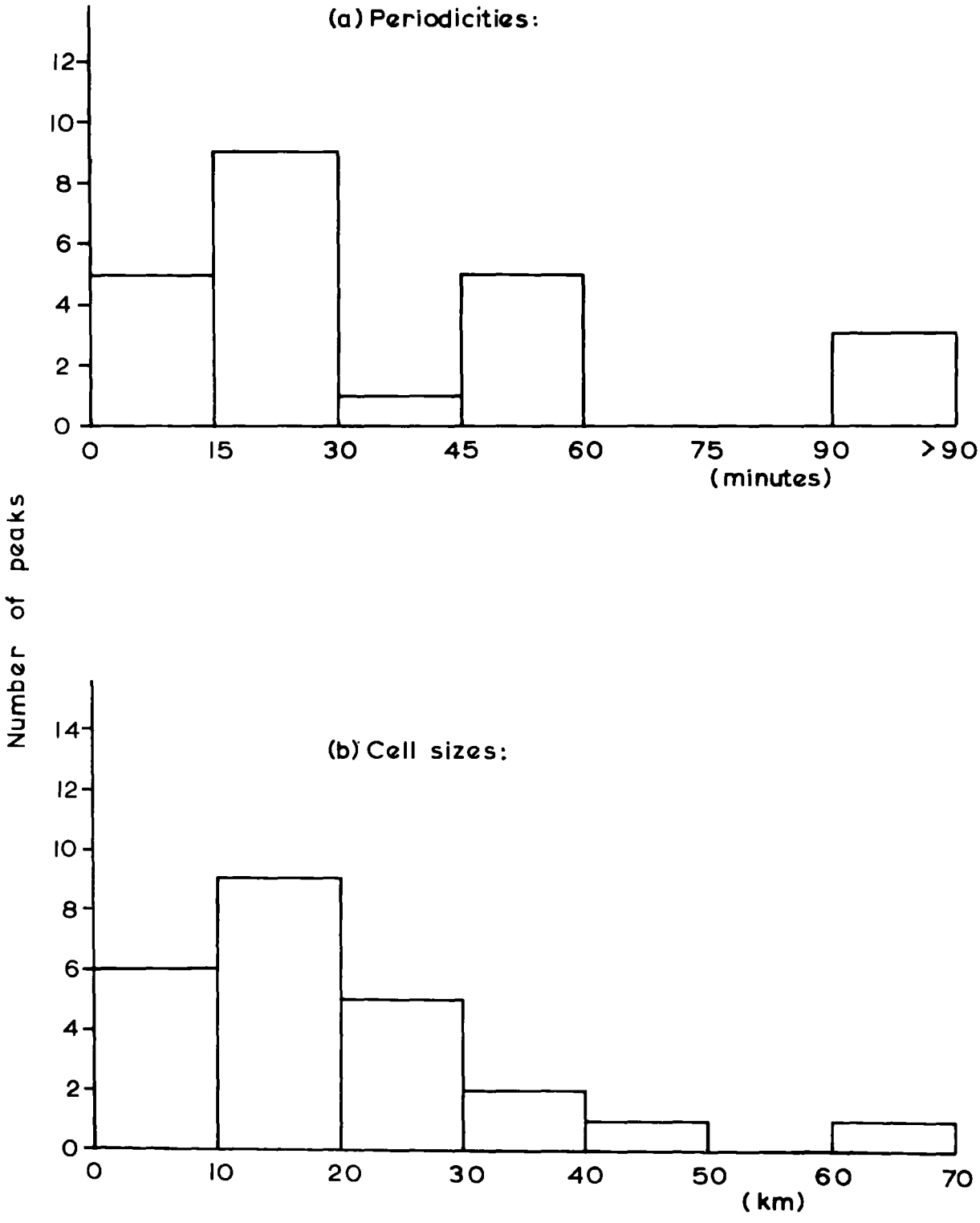

Fig.6.5. The phase spectrum of potential gradient with precipitation current.

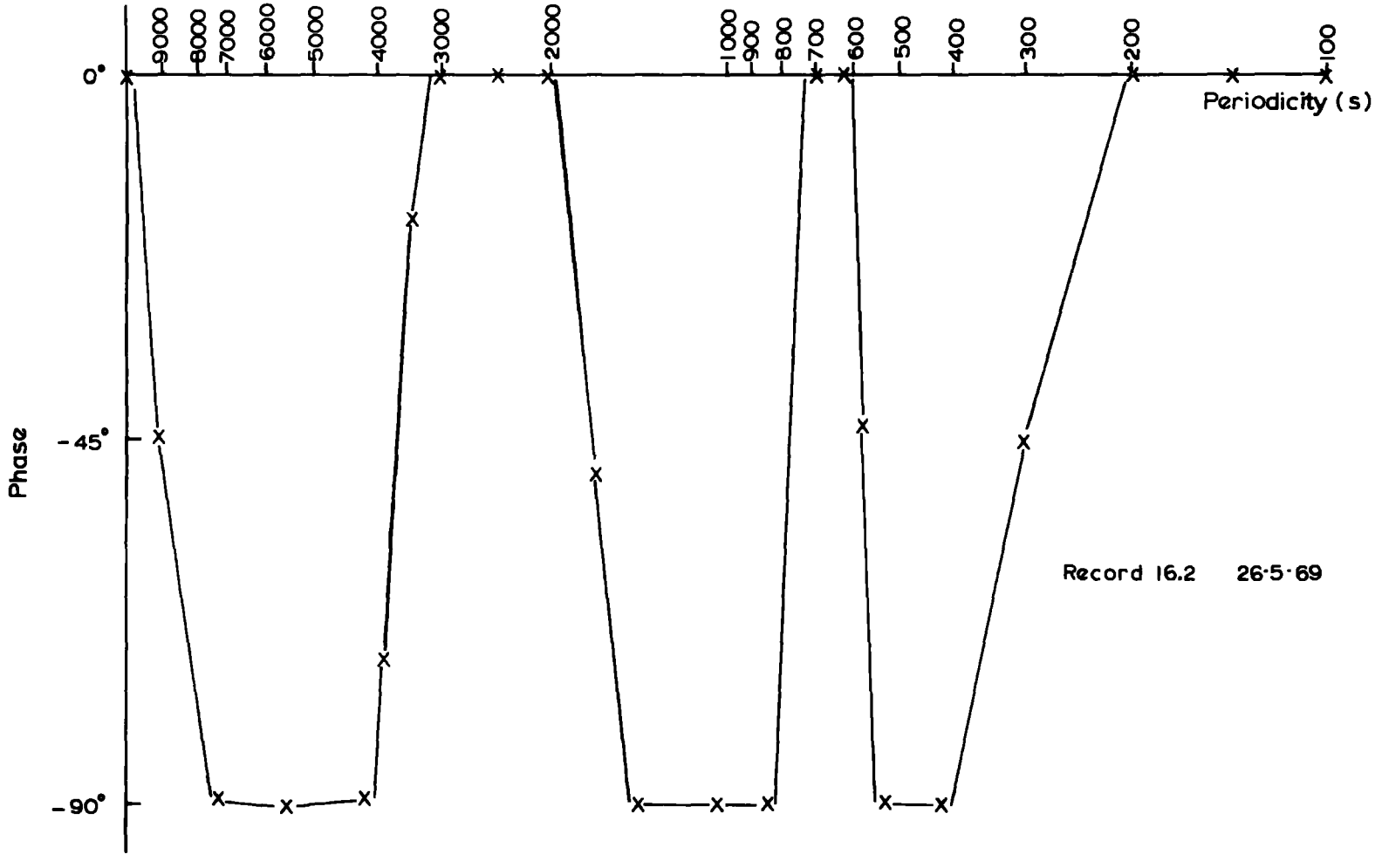

6.2.4 A model for nimbostratus electrification

In his model, STRINGFELLOW (private communication) makes the assumption that a charge separation occurs, within a given region of the cloud, which gives negative charge to the snow and yields positive charge into the charging region. The rate at which conduction will remove charge from this region is assessed and the effect that the various charges have on the potential gradient at the ground is estimated. He shows that the potential gradient F_ρ, due to the cloud charges, is given by

$$F_\rho = - \frac{I_c}{\lambda}$$

where λ is the total conductivity around the charging region and I_c is the precipitation current out of the region. The theory is extended to include the cases of the nimbostratus rain cloud and also the developing snow cloud. For the latter, assuming a sinusoidal charge separation variation with time, two solutions are reached. For the period of the sinusoidal variation T, very much ~~shorter~~ longer than the electrical relaxation time of the cloud τ, the cloud charge, and hence the potential gradient, varies as:

$$\rho = \frac{\tau}{H} \cdot I(t) \qquad (T \gg \tau)$$

where H is the depth of the charging region and τ is equal to $\frac{\epsilon_o}{\lambda}$ as usual.

If, however, T is much smaller than τ then:

$$\rho = \frac{I_o}{2\pi H} \cdot T \cos\left(\frac{2\pi t}{T}\right)$$

This will have a phase difference of between 0^o to 90^o for fast changes. It will be seen in Fig. 6.5 that, except for the very long and very short periodicities and for two particular periodicities, the two parameters have a phase difference of 90^o.

6.2.5 Anomalies in the phase spectra

The phase spectra give support to the predictions of STRINGFELLOW'S model, but for a group of periodicities in each record, the phase reverts from 90^{o} to 0^{o}. Each record exhibits a major anomaly of this kind and one, or more, secondary anomalies in the faster periodicities. A physical explanation for the major anomaly may be sought. Assume that precipitation leaves a region of varying charge separation, which has a characteristic period of, say, 2000s. The current of the precipitation will be leading the potential gradient, due to the charge remaining, by a quarter (90^{o}) of the period, in this case 500 s. If the precipitation takes 500 s to fall to the measuring collector at the ground, the lag due to this fall time will put the current and the potential gradient exactly in phase. It is suggested that if the anomaly covers the group of periodicities 2000 to 3000 s as in the case of TR 16.2, this corresponds to a mechanical lag of between 500 and 750 s. The range of times will be due to the different fall speeds of different sized drops. If the air, through which the precipitation falls, is calm, we can estimate the height of the charging process from the product of vertical terminal velocity and lag time. But if there is a profile of wind speed changing with height, we must allow for the horizontal separation of the precipitation particles from the cloud as well as for their vertical separation under gravity.

No explanation is offered here for the secondary anomalies, which may be caused by time lags from processes at different heights.

6.2.6 The effect of wind speed profile on the time lags

The problem is illustrated in Fig. 6.6. An increase of wind speed with height, assumed linear for simplicity, means that the cloud in which the precipitation originates will travel a greater horizontal

Fig. 6.6. The effect of a wind speed profile on the time lags.

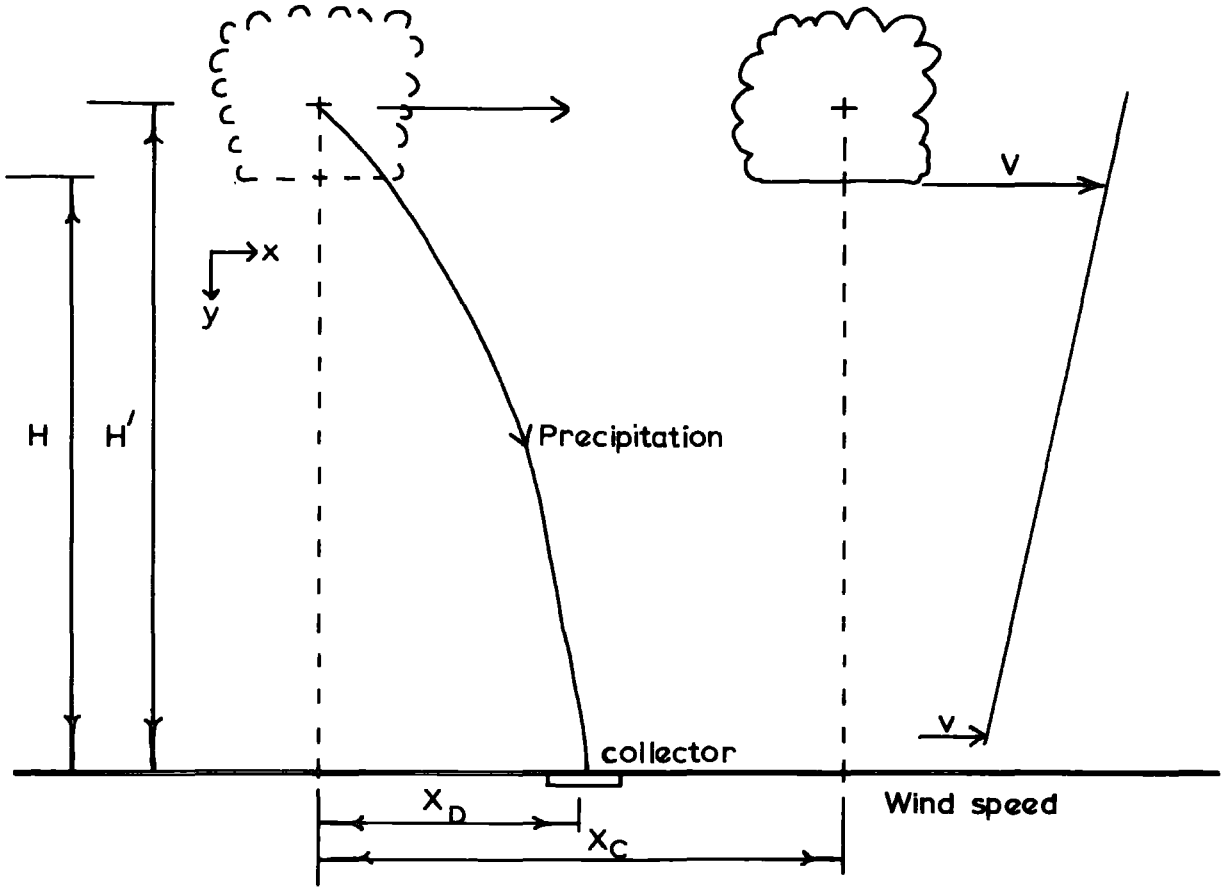

distance, X_c, than the precipitation particles. This will produce a time difference ΔT, between the maxima of potential gradient, when the cloud is overhead, and current, which will occur when the particles arrive at the ground. ΔT is given by:

$$\Delta T = \frac{X_c - X_d}{V}$$

where X_d is the horizontal range of the drops and V is cloud speed.

The variation of wind speed with height, y, may be written as:

$$V - \frac{(V - v)\, y}{H}$$

where v is the wind speed at 2m and H is cloud height. The origin of y is at H.

Let the mass of the particle be m, its vertical terminal velocity μ and its absolute horizontal velocity w. The horizontal drag force on a drop is proportional to the square of its velocity relative to the fluid through which it is passing (MASON, 1957). That is:

$$m \frac{dw}{dt} = \beta' \left(\left\{ V - \frac{(V-v)y}{H} \right\} - w \right)^2$$

where β' is a constant.

Substituting for the ~~time~~ distance, y, ~~t~~, elapsed from the origin, this may be written as:

$$\frac{dw}{dt} = \beta \left((V - \epsilon t) - w \right)^2$$

where β is another constant and ϵ is $\frac{(V-v)}{H} \cdot \mu$. This equation is solved twice (see Appendix 2) to give the height of electrical activity, H', as:

$$(V-v)H'^2 + \left(2(V+v)H + 2\mu\, (V-v)\, \Delta T \right) H' + \left((V-v)H^2 - 2\mu\, HV\Delta T \right) = 0$$

If the wind speed is constant with height, that is V = v, this equation reduces to:

$$H' = \tfrac{1}{2}\, \mu \Delta T$$

6.2.7 Estimates of the height of electrical activity

We can substitute the mechanical time lags for each record, derived from the anomalies in the phase spectra (Sect. 6.2.5), together with the meteorological conditions given in Table 6.2, into the above equation to obtain an estimate of the height of the main electrical activity. The results are given in Table 6.3 where they are compared with the height of the $0^{o}C$ isotherm. The agreement is good. The level of the $0^{o}C$ isotherm generally falls midway between the two extremes of the estimate, and, if allowance is made for the range of all speeds of different sized drops, then the estimate could be reduced to agree even more closely with the observed values. Reasonably, the estimates are less accurate for the later, warmer records when the melting zone is at a greater altitude.

These results make three contributions to Atmospheric Electricity. Firstly, confirmation is given to the idea, hinted at by OWOLABI and CHALMERS (1965) and investigated by REITER (1965), that themelting zone is a region of electrical activity. This latter worker made simultaneous measurements at stations at different heights above and below the $0^{o}C$ isotherm, whereas in the present work the effects were detected at a single station below this level. This leads to the second conclusion that it is possible to investigate, from the ground, some aspects of the electrical activity in the air above and that airborne instruments, on balloon or aeroplane, are not absolutely essential for this purpose. Finally, the methods of spectral analysis are presented as powerful tools for Atmospheric Electricity research and it is probable that more information exists in the various spectra than the author has been able to find.

TABLE 6.3 Estimated height of electrical activity

Record No.	Height of 0°C isotherm (m)	Estimated height (m)
1	360	330 - 390
4	300	-
5.1	250	230 - 250
5.2	250	230 - 250
5.3	250	220 - 250
6	0 - 90	40 - 50
7.2	0	-
8.1	0	-
8.3	0	-
8.4	0	-
9	150	120 - 150
10.1	700	-
10.2	700	670 - 760
10.3	700	500 - 900
10.4	700	620 - 720
10.5	700	550 - 900
11	1900	1700 - 2000
12	1200	1100 - 1300
13	1350	1300 - 1500
14	1600	1200 - 2400
15.1	2200	2000 - 2400
15.2	2200	1600 - 2200
16.1	1750	1600 - 1900
16.2	1750	1400 - 1800
17.1	2300	-
17.2	2400	2200 - 2600
18	2600	2300 - 2900

TABLE 6.4 Estimated total conductivity of the charging region of the cloud

Record Number	Estimated Conductivity
1	$4.0 \times 10^{-15} \Omega^{-1} m^{-1}$
4	-
5.1	-
5.2	2.7
5.3	2.2
6	-
7.2	1.8
8.1	1.8
8.3	0.5
8.4	5.7
9	1.5
10.1	2.4
10.2	2.9
10.3	-
10.4	2.4
10.5	2.7
11	1.0
12	2.0
13	0.9
14	-
15.1	1.8
15.2	1.8
16.1	0.9
16.2	2.6
17.1	2.6
17.2	2.9
18	2.7

Average estimate = $2.3 \times 10^{-15} \Omega^{-1} m^{-1}$

Average fair weather total conductivity = $8.2 \times 10^{-15} \Omega^{-1} m^{-1}$

6.2.8 An estimation of the conductivity of precipitating nimbostratus from the phase spectra

Two possible modes of behaviour of STRINGFELLOW's model were mentioned in Sect. 6.2.4. The first described the relationship of cloud charge, ρ, to precipitation current, I(t), when the charging process varied sinusoidally with period T such that $T \gg \tau$. It was:

$$\rho = \frac{\tau}{H} \cdot I(t)$$

where $\tau = \frac{\epsilon_o}{\lambda}$, the electrical relaxation time of the region and H was the depth of the charging region. This suggests that there will be no phase difference for very long periodicities and this is found to be the case in 25 of the coherency spectra from the 32 records.

In Fig. 6.5, periodicities of longer than 9000 s are in phase; if this is the lower limit, T_f, for which the condition $T \gg \tau$ holds, we can take T_f to be, arbitarily, about 2τ. Thus 2τ is about 9000 s. Now τ is equal to $\frac{\epsilon_o}{\lambda}$, and ϵ_o, the permittivity of free space is 8.85×10^{-12} Fm^{-1} which gives λ, the total conductivity of the charging region to be about 2×10^{-15} $\Omega^{-1}m^{-1}$. This calculation has been made for the 25 cases encountered and the results are given in Table 6.4.

It must be stressed that these are very rough estimates which depend on the arbitary choice of 2τ, but the salient fact brought out by the average value of 2.3×10^{-15} $\Omega^{-1}m^{-1}$ is that the conductivity is about one-third of the fair weather conductivity of air at Lanehead ($8.2 \times 10^{-15}\Omega^{-1}m^{-1}$). Indirect determinations for non-raining clouds have been made by LECOLAZET and PLUVINAGE (1948), and ISRAEL and KASEMIR (1952) which suggest in these cases that the conductivity is one-third of the conductivity near the earth's surface. Thus the result for the precipitating cloud, indicating the average conductivity of the region of the cloud to which the space charges are removed from the charging region by conduction, is similar to

the value expected for a non-precipitating cloud.

It is interesting to compare the conductivity of the cloud with measurements made at the ground, during precipitation, using the Gerdien chambers.

6.2.9 Conductivity measurements at the ground during precipitation

The purpose of using sheltered conductivity chambers during electrically quiet rain was to make an estimate of the conduction current in the air just above the surface of the air-earth current collector. On some occasions insulation breakdown occurred in the chambers and on others the readings were so erratic that it was decided to ignore them as unrealistic; this left 15 records, 5 in snow and 10 in rain for which the average conductivities were calculated.

The average fair weather values for the polar conductivities (Sect. 8.1) measured in the plane of the earth's surface at Lanehead, have been established as:

$$\lambda_+ = + 4.5 \times 10^{-15} \Omega^{-1} m^{-1}$$

and

$$\lambda_- = - 3.7 \times 10^{-15} \Omega^{-1} m^{-1}$$

This gives an excess of positive small ions equivalent to $+ 0.8 \times 10^{-15}$ $\Omega^{-1} m^{-1}$.

It was observed that, with increases in negative potential gradient in rain, the negative conductivity measurements showed corresponding increases. Accordingly, the displacements from the fair weather small ion conductivity excess have been plotted against average potential gradients for the 15 records (Fig. 6.7). Straight lines have been drawn, by eye, to fit both the rain and snow results.

It appears that there is an active relationship for rain, but not for

Fig. 6.7. Small ion conductivity excess and potential gradient in precipitation.

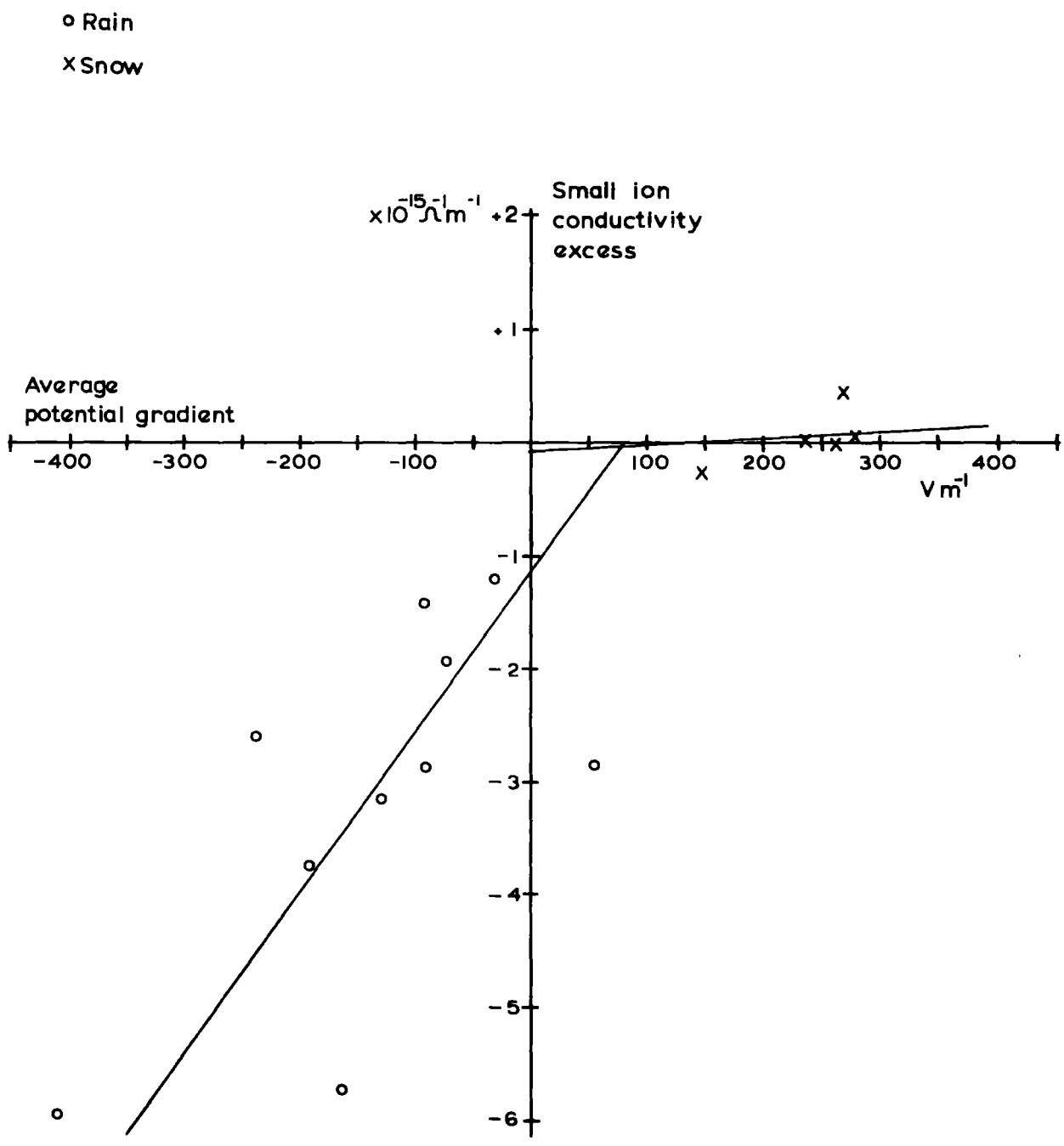

snow, which produces predominantly negative small ions for negative potential gradient close to the ground. It is difficult to say which, if either, of the two increasing parameters is the cause and which is the effect. Charge separation by 'splashing' under the influence of the electric field (SMITH, 1955) will give negative charge to the air, leaving an equal and opposite charge on rain drops; this could be acting here, as snowflakes do not give this effect and the results suggest that the 5 cases of snow are not active. Alternatively, the charge separation may be mechanical in origin, for example, wind induced drop shattering (MAGONO and KOENUMA, 1958; MATTHEWS and MASON, 1964), with the potential gradient resulting from the space charges produced.

In any event, the excess of negative small ions, near the ground, seems consistent with the negative space charge measured at 0.8 m (Sect. 6.1.2). The problems posed by these results await solution.

6.3 Analysis of the filtered data series

In Sect. 5.3 it was explained how it is possible, with digital filter techniques, to eliminate long-term trends from the records in order to enhance the analysis of faster frequencies. The next section describes one interesting result which arose from an analysis of the filtered records.

6.3.1 Peaks in the coherency spectra of the filtered records

Statistically significant peaks are found in 24 of the 32 filtered record coherency spectra, but, in contrast to the original records (Sect. 6.2.2), these peaks describe a positive correlation for potential gradient with the current to the exposed collector. It has already been seen in Table 6.1, that there is a high positive correlation between potential gradient at the ground and space charge density at 0.8 m (Sect.6.1.2)

and it is suggested that these positive coherencies indicate a current of space charges to the exposed receiver, opposite in sign to the precipitation current. This notion will be encountered again in the fair weather results of Sect. 8.4.

Fig. 6.8(a) depicts the frequency histogram of significant peaks in the filtered spectra, in steps of 30 s. The products of wind speeds at ground level and periodicities for each record are shown as 'cell' sizes in the histogram of Fig. 6.8(b).

It is probable that these relatively fast periodicities are associated with processes close to the instruments rather than at any great distance, and this is supported by the linear relationship discovered between cell size and the square of wind speed at the ground (Fig. 6.9). It is well known that the energy of the mechanical turbulence in the lower atmosphere increases in proportion to the square of wind speed (PASQUILL, 1962) and it is postulated that, during precipitation, some free space charges are transferred to the collector by turbulence influences. The cell sizes may be characteristic of the aerodynamical properties of the site at Lanehead which is, to a certain degree, sheltered (see Fig. 4.1), and may indicate a periodic replacement of the air in the plot.

In fair weather an average space charge density of + 20 pC m^{-3} produces about + 1 pA m^{-2} of 'mechanical-transfer' current (Sect. 8.4) so that, in precipitation when the space charge density can be - 200 pC m^{-3}, we may get up to - 10 pA m^{-2} of such current. This is large compared with the precipitation current density of 'quiet' rain and is worthy of consideration, in view of the fact that it could cause the cancellation of the mirror-image effect.

Fig. 6.8. Frequency distribution of significant peaks in the coherency spectra of the filtered records.

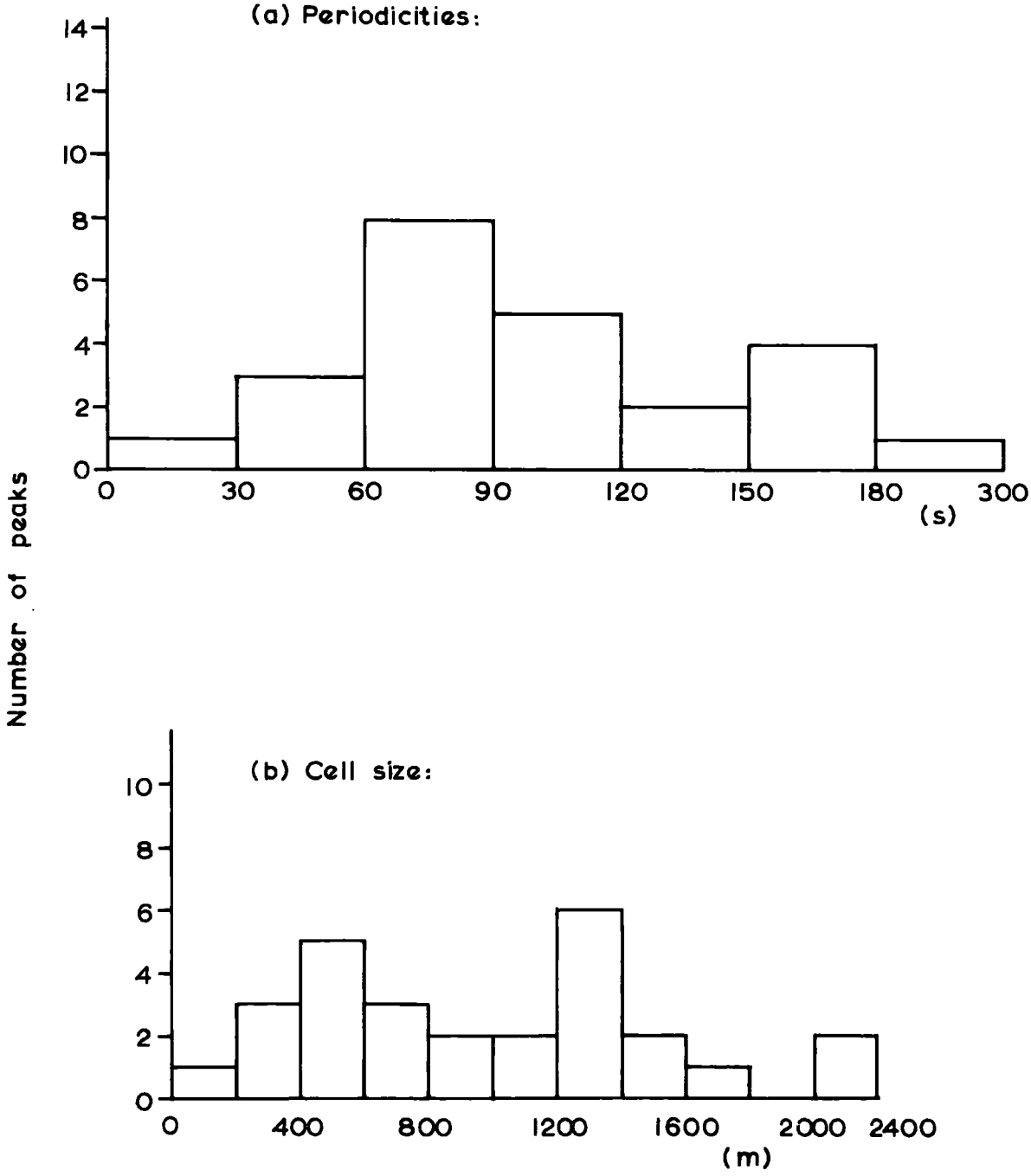

Fig. 6.9. Cell size against the square of wind speed for the filtered records.

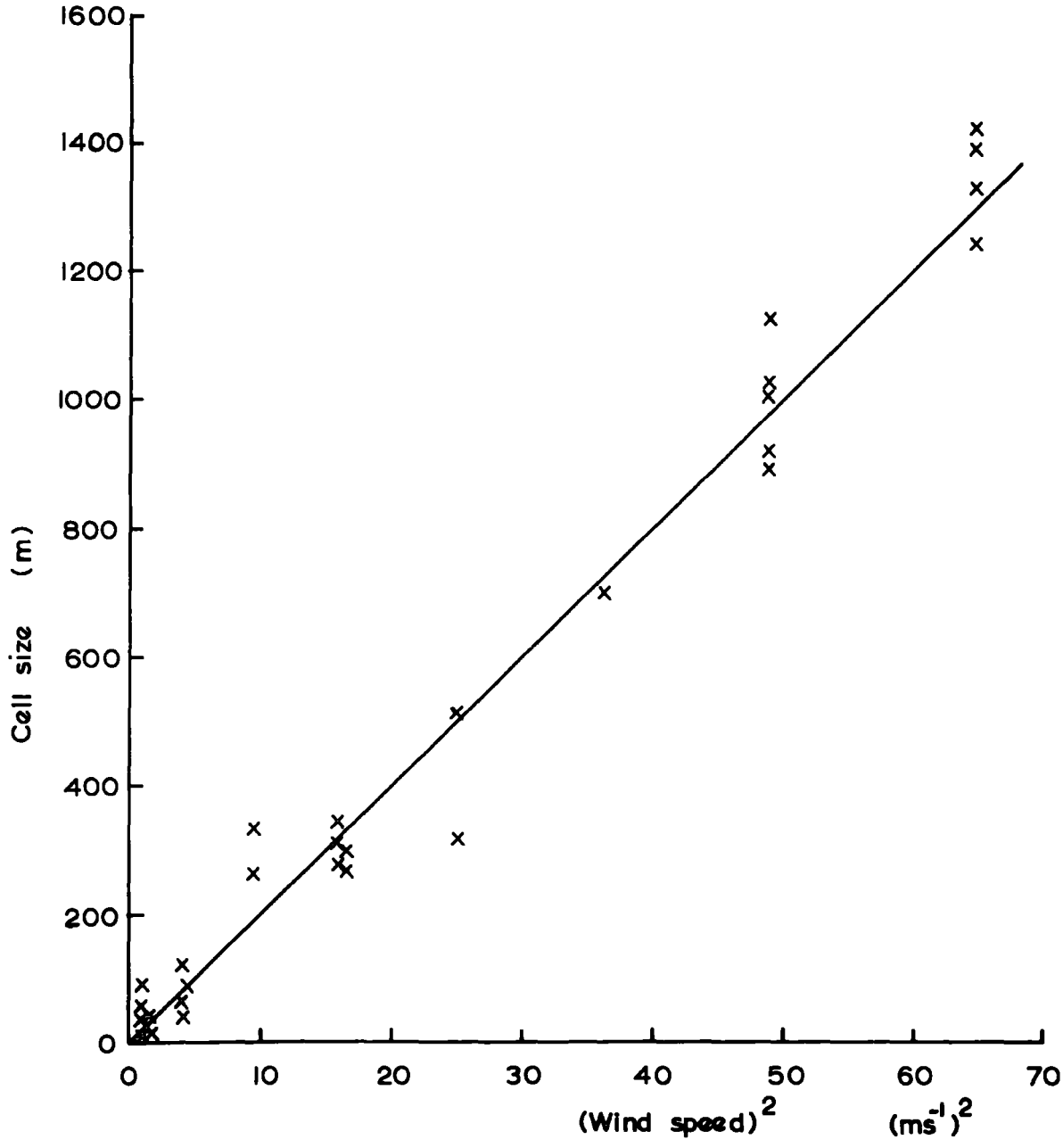

CHAPTER 7

CONTINUOUS MEASUREMENTS OF ATMOSPHERIC ELECTRICITY AT LANEHEAD

7.1 Fair weather Atmospheric Electricity

7.1.1 Global and local effects

The global atmospheric electric 'circuit' has been divided under the spherical condenser hypothesis (Sect. 1.1), into 'generators', which build up and maintain the electrical state of the atmosphere, and 'discharging' processes, which are a consequence of the existence of this electrical state. One of the major contributions to the latter category comes from the fair weather conduction current and investigation of this effect, together with the other inter-related parameters of Atmospheric Electricity, should help to explain the mechanisms of the global circuit in detail.

It has been the practice of many investigators to set up instruments, monitoring some of the parameters of interest, purely on a temporary basis and for use at such times as they are able or inclined to make observations. Many important additions to our knowledge of the behaviour of the atmospheric electric elements have come from such efforts, but all have failed to produce a consistent and coherent insight into the overall government of Atmospheric Electricity. The reason is straightforward. At any particular point on the earth's surface, measurements of air-earth current and potential gradient in fair weather, which should reflect the conditions prevailing in the electrosphere, are dominated by a welter of local effects such as pollution, wind and the electrode effect. The problem has been stated, and illustrated, by ISRAEL and de BRUIJN (1967), who attempted to correlate the simultaneous daily means of potential gradient for pairs of stations in North America separated by

large distances. They concluded, from the very low correlation coefficients obtained, that no world-wide effect was discernible. The prime reason for this is pollution of the air by particulate matter, which is produced in the urban and industrial regions of the world, and by radioactive fall-out from thermo-nuclear explosives. In order to escape from this influence it is necessary to venture to remote areas of the earth or to climb above the austausch region which effectively contains the pollution. For example, RUHNKE (1962) took his apparatus to the Greenland ice-cap in order to measure the electrical conductivity of free air, and COBB and PHILLIPS (1962) established an Atmospheric Electricity research station on top of Mauna Loa, Hawaii, well above the trade-wind inversion. Alternatively it is possible to conduct experiments over the oceans, where pollution is minimal, and the scientific cruises of the research vessel 'Carnegie' spring to mind. Because of the short-term nature of these cruises the various workers involved (MAUCHLY, 1923 ; TORRESON et al., 1946), have used every available hour to make observations and it seems likely that intensive continuous recording of this kind was the key to the success of these voyages. Here, then, is a guiding principle that one should attempt to accumulate data continuously and for as long as possible in fair weather. This course of action has been undertaken by a number of researchers who, in general, have expressed their results as daily, seasonal or yearly variations, which indicate the underlying, 'climatic-type' behaviour of the various parameters. These variations are established after sufficient data has been collected to average out the more random localised effects.

7.1.2 Diurnal variations of potential gradient and world-wide thunderstorm activity

The diurnal variation of potential gradient, measured on the 'Carnegie' by MAUCHLY (1923), led APPLETON (1925) to suggest that this variation might be similar to the variation of the number of thunderstorms active at the time, over the surface of the earth. WHIPPLE (1929) made use of the thunderstorm data of BROOKS (1925) to find this diurnal variation and WHIPPLE and SCRASE (1936), plotting the variation in detail, showed there to be good agreement with the variation of potential gradient. Very similar variations have been found, in the Pacific by TORRESON et al. (1946) and by SHARPLESS (1968) at Lanehead, a land station within the austausch. This latter result is contrary to the expectations of ISRAEL and de BRUIJN (1967) who state:

> " An isolation of the global effects from daily, monthly and annual means of the atmospheric electric elements at continental stations must be assumed impossible. "

The work of SHARPLESS (1968) demonstrates the need to make continuous measurements for at least a year in order to reduce satisfactorily the influence of local effects.

7.1.3 Some other fair weather diurnal variations

Whereas the diurnal variation of air-earth conduction current over the oceans is the same as that for potential gradient, at land stations within the austausch the current to an exposed plate shows no resemblance at all (SCRASE, 1933), and has a marked seasonal dependence. In contrast, COBB and PHILLIPS (1962), from a year's continuous measurements of total current density at Mauna Loa, produced a variation very similar to that obtained in 1929 on the 'Carnegie' (TORRESON et al., 1946). They also

measured the densities of small ions, and related their electrical measurements to meteorological observations. A novel approach to the determination of the diurnal variation of the air-earth conduction current density has been made by ANDERSON (1969). Measurements made every 15 minutes on a flight from Washington D.C. to Sydney produced a bimodal variation which is in substantial agreement with the accepted global curve, but here again, regional influences were also evident.

In Japan, HATAKEYAMA and KAWANO (1953) found that the total conductivity controls the potential gradient in large cities, but that its influence is considerably reduced in rural areas. Workers at many places agree that the conductivity shows a maximum in the early morning hours, with a drop soon after sunrise. This is probably due to the combined effects of meteorological changes and the increase in the output of pollution at that time.

On these various topics, the reader may care to refer to CHALMERS (1967) as a standard text on Atmospheric Electricity.

7.2 Atmospheric Electricity measurements at Lanehead

Over theperiod from July 1967 to June 1968 continuous measurements were made of the air-earth current density, potential gradient, space charge density and positive conductivity (SHARPLESS, 1968). These electric elements were recorded on paper charts by pen recorders, and the information thus acquired was processed by hand. The results are divided into two groups: fair weather and disturbed weather. Of the former, diurnal variations for the year were calculated and the potential gradient variation showed a marked similarity with that found 40 years previously by TORRESON et al. (1946), but the air-earth current was found to depend on the variation in columnar resistance, and its variation

is similar to that of the space charge density. SHARPLESS (1968) has assessed the rôle of pollution in controlling this variation at Lanehead. For disturbed weather, a high positive correlation was discovered between space charge density and potential gradient at the ground during steady participation. A full explanation of this phenomenon was not offered.

The atmospheric electric climate of the station at Lanehead has been established by SHARPLESS (1968) and the importance of continuous monitoring of parameters underlined.

7.3 The 1-hour recording system

7.3.1 Improvements in the collection and processing of data from continuous measurements

It was not felt possible to process by hand data from paper chart records in the manner of SHARPLESS (1968) while at the same time attempting a full-scale investigation into a separate topic. But the desire to maintain continuous recording at Lanehead motivated the author to seek alternative ways to conduct this function of the field station. Great saving in the time taken to compute the hourly means for the diurnal variations could be made if a computer were used for this task and as the automatic recording system (Chapter 3) was situated and working at Lanehead, here was a means to produce paper-tape records suitable for input to the I.B.M. 360/67. The development of interface circuitry between the outputs of the V.R.E's and the input of the recording system has been described (Sect. 4.6) and to complete the new system an electronic method of averaging the outputs over an hour was required, as well as some extra timing devices to govern the punching tasks.

Interest in the continuous measurements were centred on the diurnal variations of the parameters so an electronic circuit was needed which

would respond to long term variations, over a matter of a half-an-hour or so, while smoothing out the short term changes. This could have been easily achieved by increasing the input time constant of the V.R.E.'s, but as they were also being used for the precipitation work, it was impracticable to be continually altering the head units. The alternative was to smooth the outputs with a standard resistor-capacitor integrating circuit, with the product RC equal to about 15 minutes. This requires values of 1 μF for C and 10^9 Ω for R, and if it is desired to sample a voltage stored in this network, the input impedance to the measuring device must be greater than 10^{12} Ω to avoid attenuating the output voltage. Until recently this would have implied thermionic valve circuitry, but the timely development of the metal-oxide semiconductor field-effect transistor (hereafter referred to as a MOSFET) provided an attractive and simple way of overcoming this problem.

7.3.2 The MOSFET as an impedance converter

It was stressed earlier that this thesis would not give full details of electronic circuitry used but it is felt that there is some justification for outlining the basis characteristics of a new device which may find further applications in Atmospheric Electricity instrumentation.

A MOSFET consists of two very rich n^+ regions on a p-type silicon substrate as shown in Fig. 7.1. The n^+ regions known as the 'source' and 'drain', are close together. On the substrate between them, a thin layer of silicon dioxide acts as a dielectric between the substrate and an aluminium electrode called the 'gate'. When the gate is made positive with respect to the source, holes will be repelled from, and electrons attracted to, the surface of the substrate. Consequently, an n-type layer is formed in the substrate near the oxide dielectric. The greater the

applied potential, the thicker will be this inversion layer. The inversion layer forms a conducting path, therefore current will flow between the n^+ regions if a potential difference is applied between the drain and the source. Because it controls the thickness of the inversion layer, the gate voltage can either control the resistance between drain and source, or in an amplifying mode, it can control the current. The input impedance to the gate is better than $10^{12}\ \Omega$, and as a consequence, damage can occur to the gate oxide layer if an electrostatic charge, from a nylon shirt for example, builds up on the gate electrode. When handling MOSFETs it is usual to short the leads together with a special conducting clip.

The high input impedance enables the MOSFET to be used as an impedance converter, or source follower, of the type more generally known as a cathode or emitter follower. The gain of an impedance converter, normally about 0.92, may be increased to 0.95 by including a conventional bipolar transistor in the circuit as shown in Fig. 7.2, and this also serves to improve the output current availability of the circuit.

The circuit of Fig. 7.2 was used as a plug-in unit, one for each parameter, to give the desired averaging of the instrument outputs in forms suitable for the recording system. The fraction, 0.05, of the output which was lost in the source follower, was taken up by the calibration of the 1-hour system.

7.3.3 The operation of the 1-hour system

SHARPLESS (1968) derived his hourly values by considering the average values in the four 15-minute periods of each hour; it was felt that using the new system to sample the averaged values once every hour, on the hour, would provide equivalent data. The basic functions of the automatic

recording system were left unaltered, but a modification was made whereby the 3s system command pulses were diverted through a reed relay switch. This relay had a by-pass switch which could return the system to the 3s sampling mode for precipitation work, otherwise the relay was controlled by a bistable circuit. A sequence timer delivered a trigger pulse to the bistable at each hour and this caused the relay contacts to close and the system to start the execution of a sequence of parameter punching jobs. At the end of one cycle of parameters, a reset pulse to the bistable cut off the command pulses again. In this way the five parameters, potential gradient, air-earth current density, space charge density and both polar conductivities were recorded hourly.

Two other records were made on spare channels. The first was a rough indication of the time of day, derived by using a stepping-relay, also triggered by the sequence timer, to give an increasing output voltage at every hour. The sequence restarted at midnight (Z-time or GMT) each night. The second record was an indication of whether or not it had rained, or snowed, during the previous hour. This was achieved by using the electronic rain detector described by SHARPLESS (1968), to switch a self-holding relay which in its turn gave a voltage which changed the number, punched for the last channel of the sequence, from 001, for no rain, to 730. This relay was reset by the sequence timer after the completion of the punching cycle. It was then a simple matter to program the computer to ignore the data for any hour in which the 'rain number' was 730 (this was an arbitary figure).

The automatic recording system for the 1-hour mode of operation is shown in block diagram form in Fig. 7.3. This was left to run continuously day and night, and it was only interrupted for the purpose of taking precipitation measurements.

Fig. 7.1. The metal-oxide field-effect transistor.

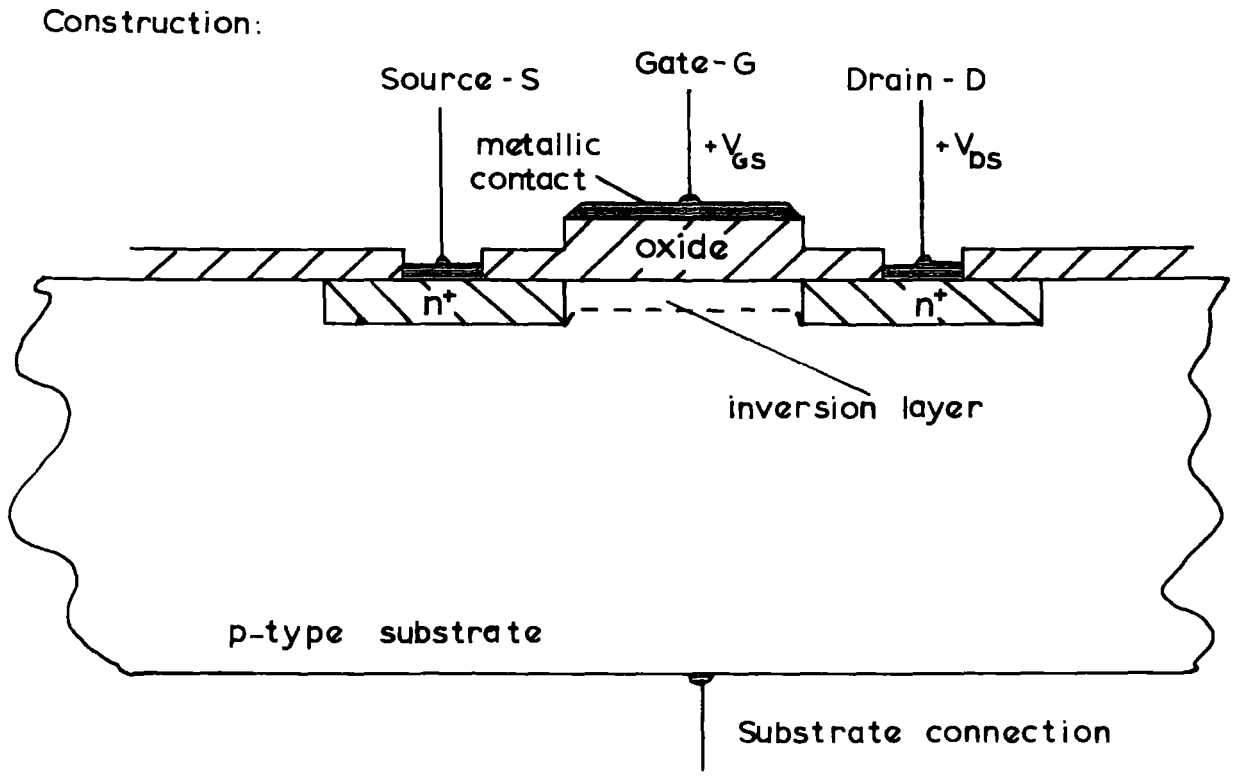

p-channel MOSFET (enhancement mode)

Circuit symbol:

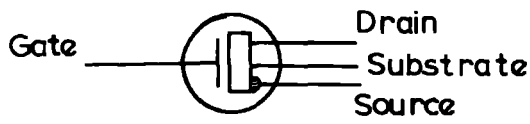

Output characteristic:

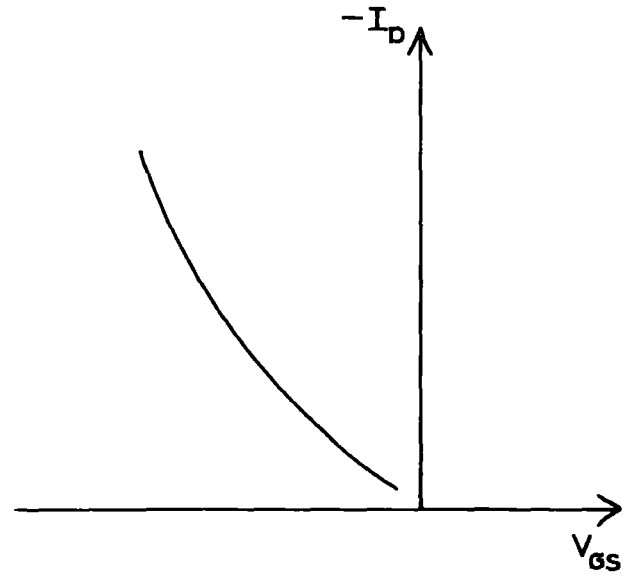

Fig. 7.2. The integrating circuit and MOSFET source-follower.

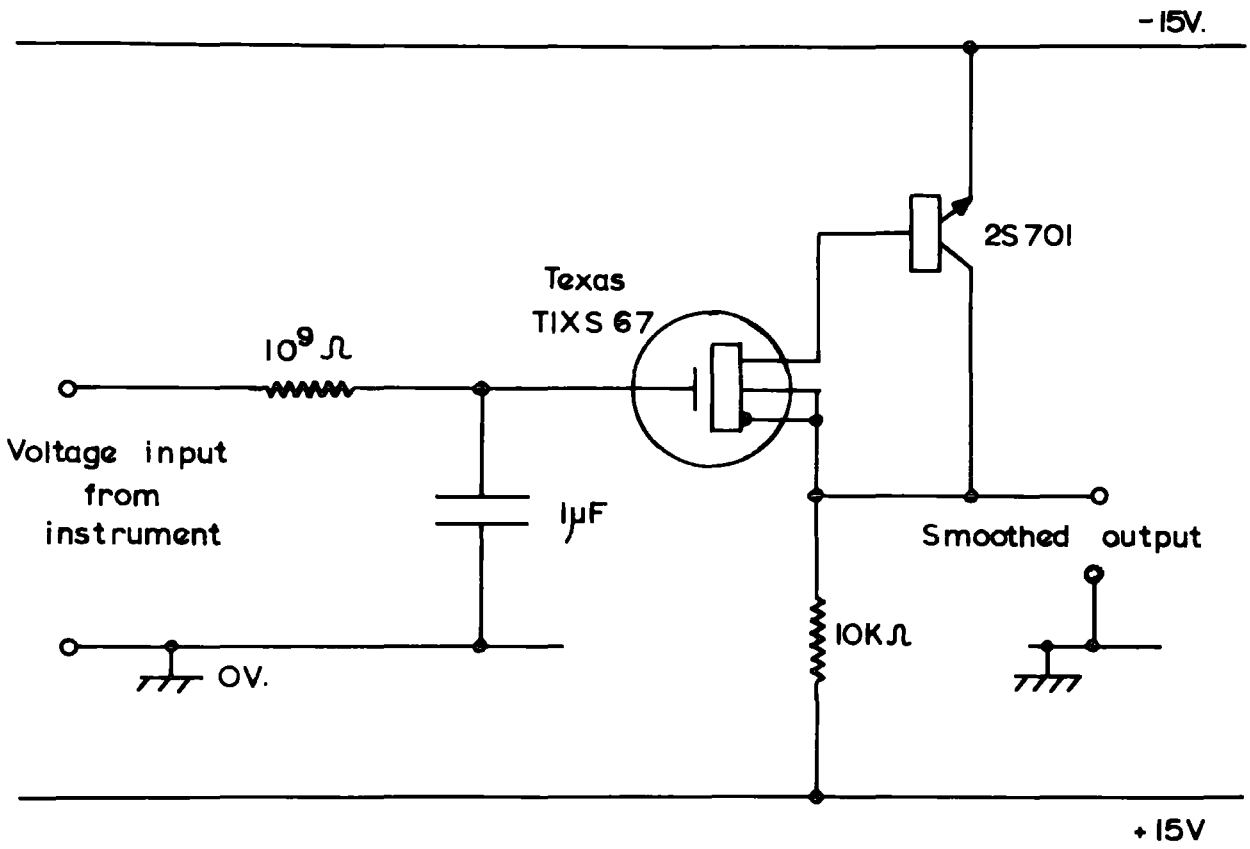

Fig. 7.3. Block diagram of the 1-hour recording system.

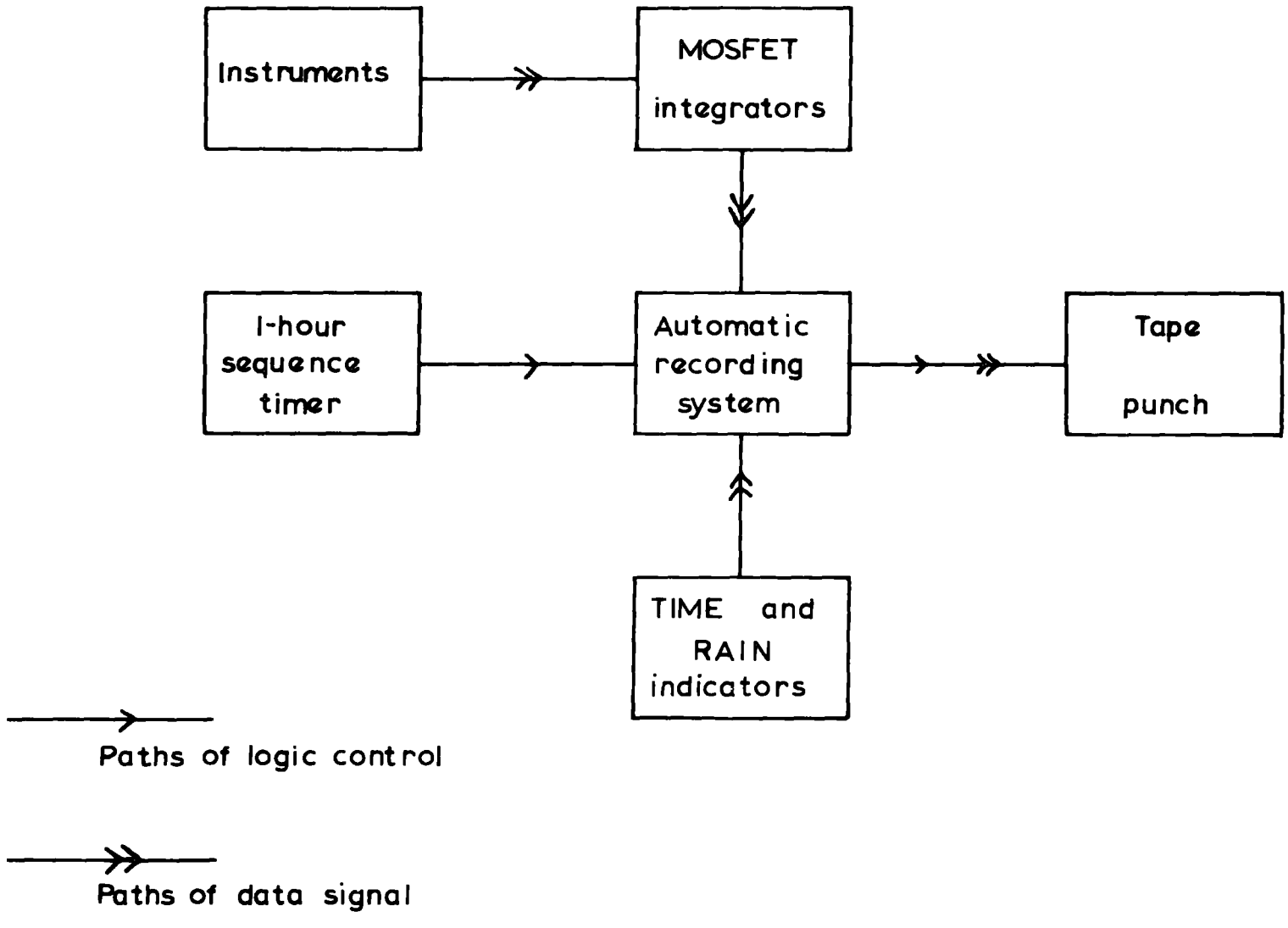

7.3.4 Calibration of the 1-hour system

Because of the very varying nature of the instrument outputs it was decided not to calibrate the integrating parts of the system in a single operation. Instead, the automatically recorded 1-hour counts for January 1969 were plotted against the corresponding values obtained by analysing the paper charts and the line of best fit was computed by the method of least squares. It was felt that this would probably give a more realistic calibration than one obtained by applying an artificial input to the system. The equations of the 1-hour calibration curves were only slightly different from those associated with the direct recording calibrations, and this was probably due to the fact that the gain of the MOSFET source followers was 0.95 and not 1.

7.3.5 The selection of fair weather values for the electric elements

A consequence of any automatic data handling system is that some loss of contact must occur between the analyst and the information contained in this data, and precautions must be taken to ensure that no invalid data are processed unwittingly.

At the outset of the work it was decided to define as valid any fair weather measurement which was a member of a population distributed normally about the mean value for that parameter, as established for Lanehead by SHARPLESS (1968). Then 99.9 per cent of such a population would be in the range

$$\bar{x} \pm 3\sigma_x$$

where $\bar{x}$ is the mean value and σ_x is the standard deviation calculated from the mean diurnal variation. This, however, takes no account of the variation of the monthly means and the range for fair weather values was

revised to be:

$$(\bar{x}_{MIN} - 3\sigma_{MIN}) \text{ to } (\bar{x}_{MAX} + 3\sigma_{MAX})$$

where $\bar{x}_{MIN}$ was the minimum monthly parameter mean encountered by SHARPLESS (1968), and $\bar{x}_{MAX}$ was the maximum monthly mean. For the potential gradient measurements in the period July 1967 to June 1968, the minimum mean was + 64 V m^{-1} for July 1967, with a standard deviation, from the diurnal variation for that month, of ± 12 V m^{-1}; the maximum was + 158 Vm^{-1} for February 1968, for which a standard deviation of ± 24 V m^{-1} was estimated. The fair weather values of potential gradient were thus defined by the range + 28 V m^{-1} to + 230 V m^{-1}. Similar ranges were calculated for the other parameters.

The method used to ignore those hourly records when precipitation was present was outlined in Sect. 7.3.3.

7.3.6 The performance of the 1-hour recording system

The electronics for this part of the system was housed in the lower two panels of the rack shown in Fig. 3.14, just above the tape-punch. On about half-a-dozen occasions in a month, spurious numbers were punched on the 1-hour record, but it was a simple matter to edit these from the paper-tape after locating them on a print-out of the data. Apart from this, and a sporadic tendency for the punch mechanism to jam, the 1-hour recording system worked satisfactorily from January 1969 to August 1969. Some modifications were made in September, 1969 by a colleague of the author's, but the system continued to function in basically the same manner.

The implementation of the automatic system for continuous recording was entirely justified by the considerable saving in time and effort it

Fig. 7.4 Computer output for April 1969

DIURNAL VARIATIONS FOR APRIL 1969

GMT	P.G. ($V\,m^{-1}$)		A.E.C. ($pA\,m^{-2}$)		S.C. ($pC\,m^{-3}$)		+COND. $\times 10^{-15}$ ($\Omega^{-1}\,m^{-1}$)		-COND. $\times 10^{-15}$ ($\Omega^{-1}\,m^{-1}$)	
0	142	(16)	2.7	(22)	25.5	(22)	5.0	(24)	3.4	(23)
1	117	(18)	2.5	(20)	24.0	(20)	5.5	(24)	3.8	(23)
2	116	(17)	2.6	(19)	22.4	(17)	5.8	(22)	4.0	(21)
3	121	(19)	2.7	(20)	26.0	(20)	6.0	(22)	4.0	(20)
4	116	(18)	3.1	(20)	23.6	(19)	5.8	(22)	3.6	(20)
5	109	(19)	2.9	(20)	23.6	(21)	5.8	(21)	3.7	(20)
6	117	(19)	3.0	(18)	26.1	(21)	5.7	(21)	3.4	(18)
7	133	(18)	3.4	(16)	21.3	(20)	5.7	(21)	3.4	(18)
8	152	(17)	3.1	(16)	30.5	(20)	6.0	(19)	3.8	(19)
9	150	(16)	3.1	(18)	25.5	(21)	6.2	(21)	3.7	(16)
10	130	(14)	2.8	(16)	20.9	(18)	6.3	(19)	4.2	(16)
11	151	(12)	2.2	(16)	17.1	(11)	6.3	(17)	4.3	(12)
12	147	(14)	1.8	(15)	17.7	(10)	6.3	(18)	5.3	(14)
13	146	(13)	1.4	(14)	10.0	(9)	6.1	(19)	4.8	(14)
14	154	(14)	1.8	(15)	15.2	(9)	6.6	(19)	3.9	(14)
15	167	(12)	1.3	(16)	14.8	(9)	5.6	(17)	3.6	(13)
16	156	(13)	0.9	(13)	3.5	(8)	5.5	(18)	4.1	(13)
17	148	(15)	1.1	(15)	1.7	(7)	5.4	(20)	4.1	(15)
18	131	(16)	1.8	(16)	12.1	(7)	5.2	(20)	3.6	(17)
19	152	(15)	0.7	(17)	6.1	(11)	5.2	(20)	3.7	(18)
20	140	(15)	1.8	(17)	8.0	(11)	4.9	(20)	3.8	(20)
21	150	(15)	1.4	(20)	10.4	(15)	4.9	(21)	3.9	(20)
22	162	(16)	1.7	(23)	16.2	(19)	4.9	(24)	3.7	(22)
23	149	(17)	2.5	(22)	25.0	(18)	4.7	(24)	3.4	(22)

THE DAILY MEAN VALUES

P.G.	A.E.C.	S.C.	+COND.	-COND
139.8	2.09	18.2	5.6	3.9

THE FIGURES IN BRACKETS INDICATE THE NUMBER OF DAYS FOR WHICH READINGS ARE VALID

NO. OF PUNCHING ERRORS= 0

afforded, and the results obtained, both since January 1969 and from the chart records for the period August 1968 to January 1969, are discussed in Chapter 8. An example of the computer output, for April 1969, is shown in Fig. 7.4.

CHAPTER 8

RESULTS OF THE CONTINUOUS MEASUREMENTS

This chapter is a summary of the results of measurements made at Lanehead in fair weather for the period August 1968 to July 1969. Where relevant, for instance, in the seasonal variations, the results have been combined with those of SHARPLESS (1968) to give a more meaningful contribution than would obtain with the separate measurements. The diurnal variations of the atmospheric electric elements for each month, August 1968 to July 1969, are given in Appendix 1.

8.1 The average diurnal variations, 1968-1969

The diurnal variations for potential gradient and total air-earth current density were obtained for the 12-month period from August 1968 to July 1969. Because of the failure of the suction fan in July 1969, the diurnal variation of space charge density relates to the 11-month period ending in June 1969. The two conductivity chambers were operational from October 1968 to June 1969, so the diurnal variations for these were derived from measurements made over 9 months. The average variations are shown in Fig. 8.1.

The forms of the variations for potential gradient, air-earth current density and space charge density are similar to those given by SHARPLESS (1968) and no new information can be gained from them as they stand.

The diurnal variations of the polar conductivities, the first for Lanehead, both exhibit the same basic shape but the extents of the variations, much less than 10 per cent on either side of the mean, are so small that these parameters can be taken to be constant. The complete absence of any suggestion of a 'sunrise effect' (CHALMERS, 1967) in these

Fig.8.1. The average diurnal variations —
August 1968-July 1969.

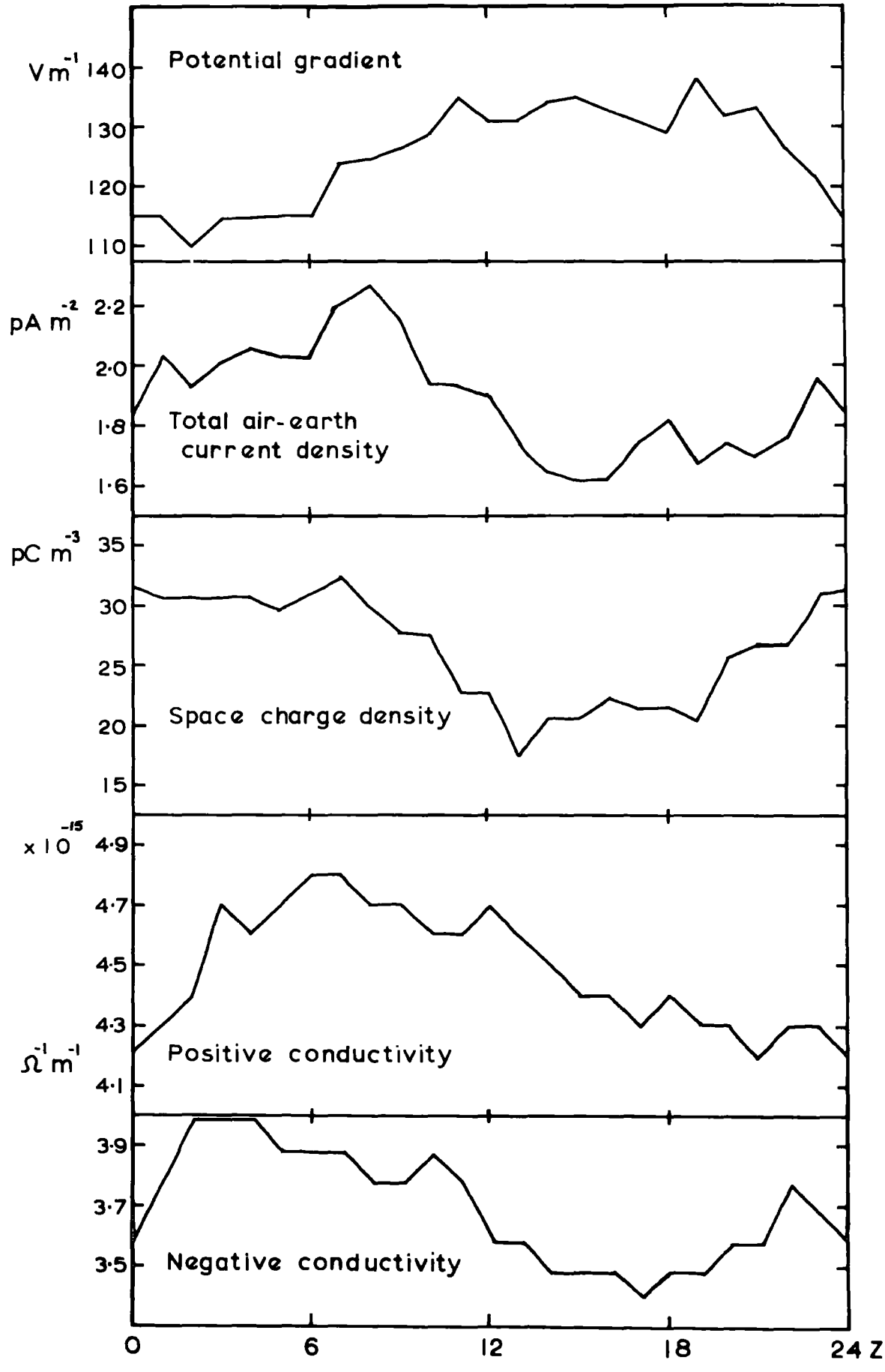

variations is taken to be evidence that the Lanehead region is free from the permanent pollution which gives rise to this effect. The constancy of the total conductivity, measured at ground level, also suggests that the ionization of the lower regions of the atmosphere is uniform and continuous. The ratio of the polar conductivities is 1.22.

Several measurements have been made of the ratio of negative to positive polar conductivities in the atmosphere; for pure air at high altitudes various workers, SAGALYN (1958), CURTIS and HYLAND (1958) and PALTRIDGE (1965), found the ratio to be around 1.06. At atmospheric pressure, this value of 1.06 would be closer to 1.28, but measurements at ground level, such as these at Lanehead, are complicated by the electrode effect. In polluted regions, the ratio of the polar conductivities at the surface is usually close to unity.

8.2 The diurnal variation of potential gradient

Potential gradient is the atmospheric electric parameter most frequently and most universally measured and the opportunity arises to make a direct comparison with results from different stations over a large number of years.

In Fig. 8.2 the diurnal variation of potential gradient at Lanehead, 1967 to 1969, is compared with the results obtained on the Pacific cruise of the Research Vessel 'Carnegie' in 1929 (TORRESON et al., 1946). The similarities are immediately obvious and bear witness, in view of the difference of 40 years in the measurements, to the existence of some universal process governing the variation of potential gradient. There are some discrepancies, notably at 11Z and at about 18Z.

The next step is to compare the potential gradient variation with the

variation in world-wide thunderstorm activity given by WHIPPLE and SCRASE (1936) following the suggestion of APPLETON (1925) that the two may be similar. This has been done in Fig. 8.3; the basic shapes are the same, both having a minimum in the early morning, rising to a maximum in the afternoon and falling again before midnight. The most noteworthy difference occurs between 12Z and 14Z; this corresponds to the contribution of the continents of Europe and Africa to the thunderstorm area. The fact that the 'Carnegie' results also undercut the thunder activity at these hours might indicate that this particular thunderstorm area has been overestimated.

The belief that there is no appreciable amount of locally produced pollution at Lanehead is supported by the single maximum of potential gradient at 19Z; this agrees well with the results of SHERMAN (1937) in Alaska, SIMPSON (1919) in the Antarctic and MAUCHLY (1923) who analysed results obtained on the 'Carnegie'. At most land stations the diurnal variation of potential gradient shows a dependence with local time (SCRASE, 1934) and often exhibits two maxima and two minima corresponding to local domestic and industrial behaviour patterns.

The annual variation of potential gradient at Lanehead is shown in Fig. 8.4. The low level of pollution is evident from the comparison with Kew (SCRASE, 1934) and the similarity to the measurements at Tortosa (RODES, 1933) is remarkable. Tortosa is on the south-east coast of the Iberian Peninsula, close to the Mediterranean, with mountains in the hinterland. The level of pollution there in the period 1910 to 1930 would, in all probability, be very similar to that of Lanehead at the present time.

Fig.8.2. The diurnal variation of potential gradient.

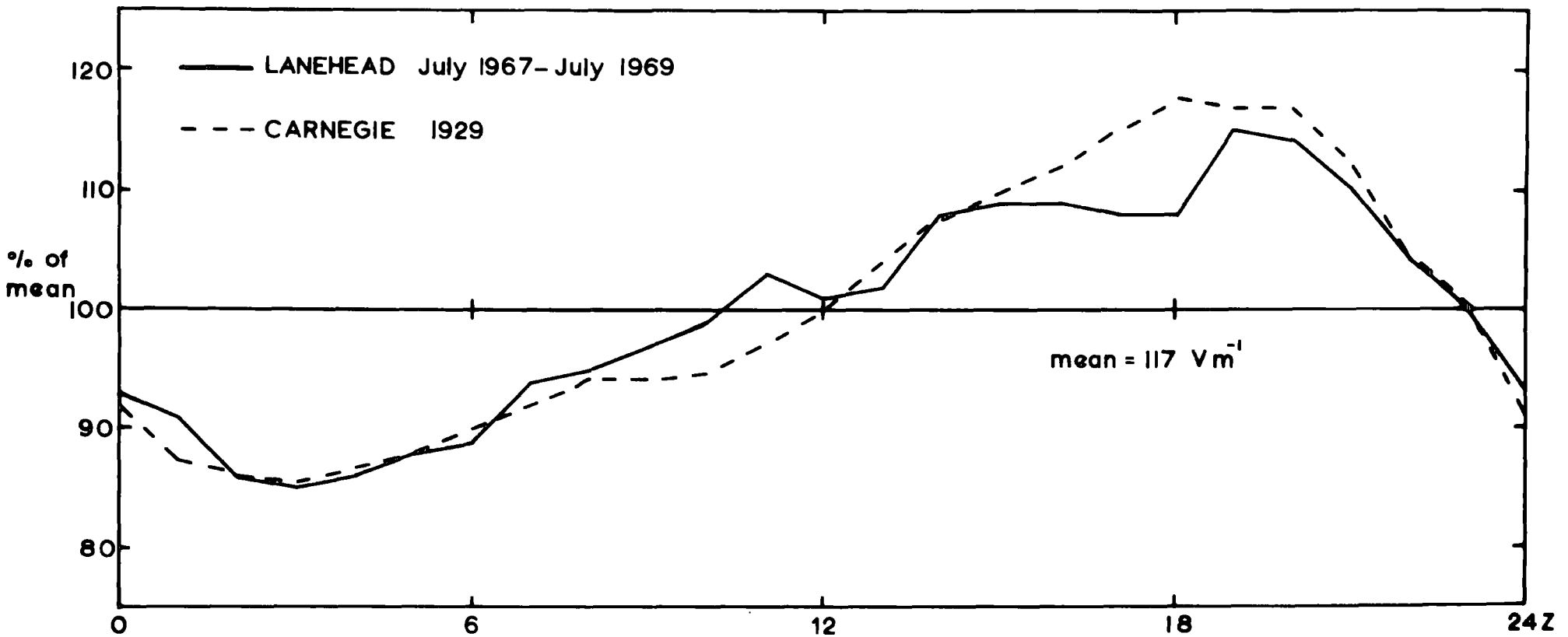

Fig. 8.3. Diurnal variations of potential gradient and World-wide thunderstorm activity.

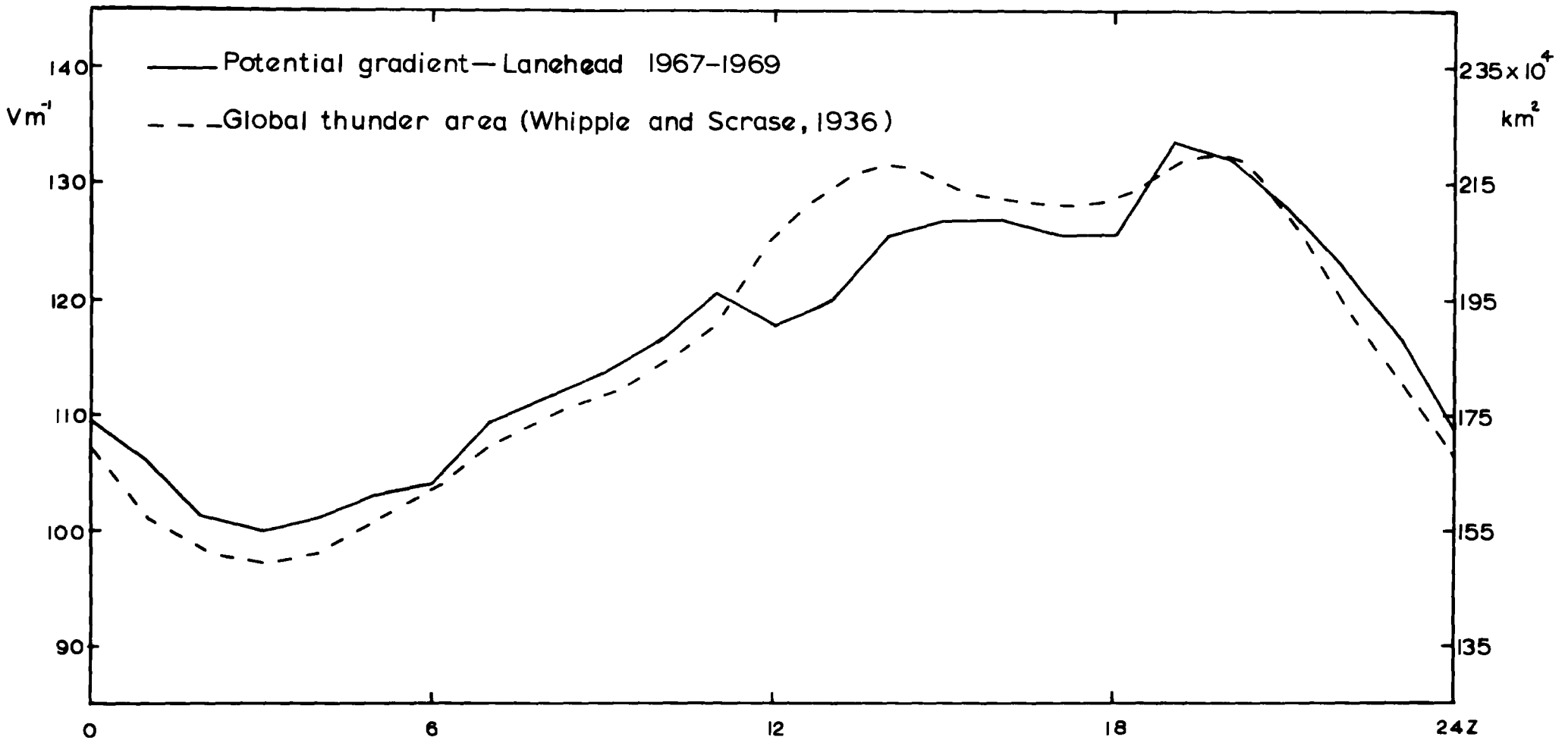

Fig. 8.4. Smoothed annual variations of potential gradient.

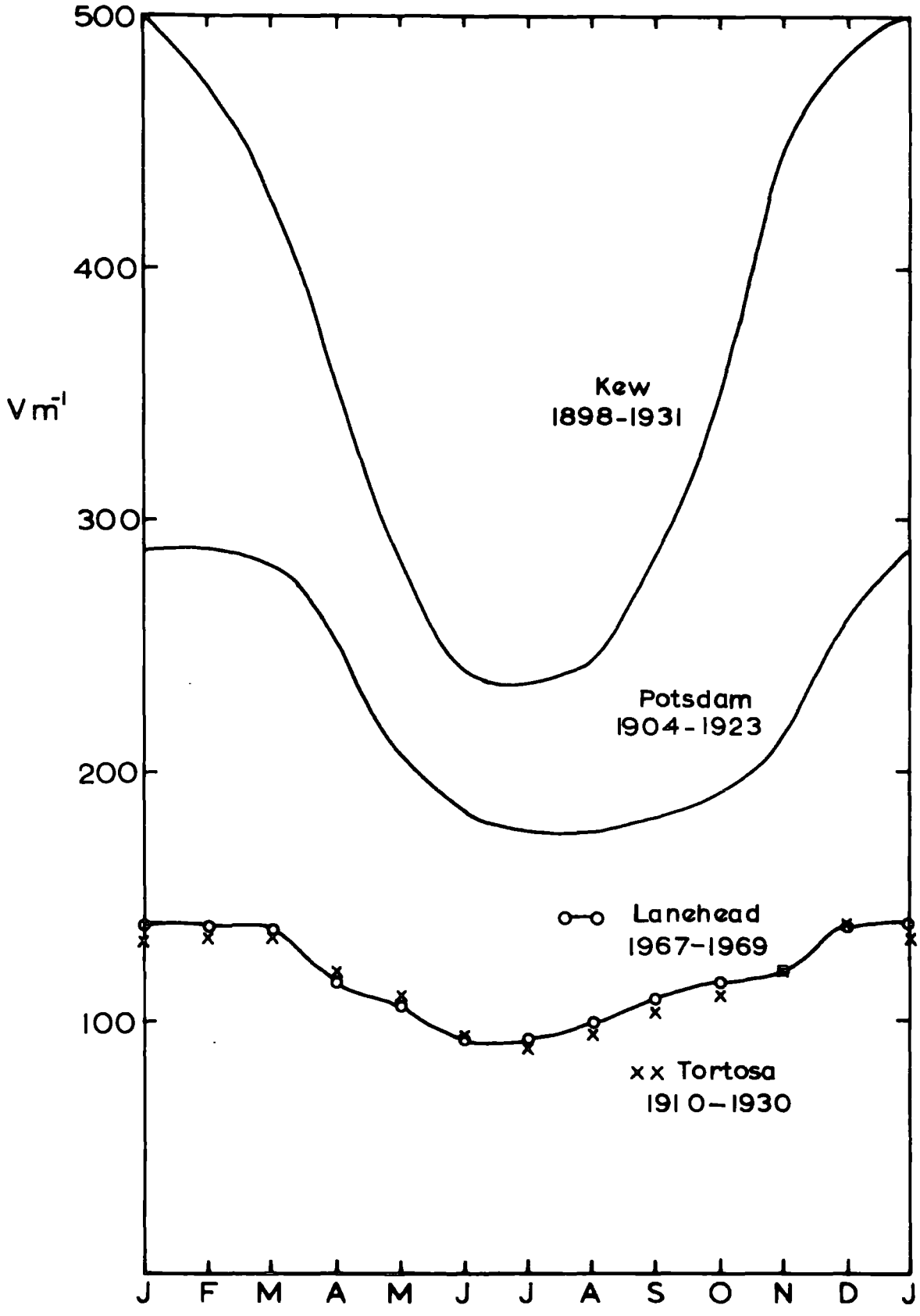

8.3 The seasonal variations

For the comparison of seasonal effects the measurements have been grouped so that Spring comprises February, March and April, Summer comprises May, June and July, and so on.

Figs. 8.5 to 8.7 show the seasonal variations of the three main parameters for the period 1967 to 1969 and these constitute a refinement of the variations given by SHARPLESS (1968).

The seasonal variation of total air-earth current density is very like the seasonal variation of space charge density; both exhibit marked variations in Spring, Summer and Autumn with no real variation in the winter months. As the average values of each are very similar for all four seasons it is probable that the increased convective activity in the atmosphere in the warmer months is responsible for the form of the variations. Convective air currents, in the hours after midday, will lift space charges up to higher levels within the austausch region thus causing a depletion at the level of the space charge collector. This will also reduce the 'mechanical-transfer' current (Sect. 8.4) to an exposed receiver. This convective influence is put forward as the predominant factor governing the seasonal variations of both space charge density and total air-earth current density.

In contrast, the more marked variation of potential gradient is in the winter months, with no real variation for summer measurements. The general diurnal variation of potential gradient shows a minimum in the morning and a maximum in the afternoon which is opposite in form to the general space charge variation. This raises the question, in view of the opposing seasonal modes of behaviour, whether or not there is some link between the two whereby one element controls the other.

The conductivity of the air is due almost entirely to small ions and

depends upon the number of small ions present. Their number is governed by the rate of combination with nuclei in the air so that when the number of nuclei is a maximum, the conductivity due to small ions is a minimum, giving a maximum of potential gradient under the relationship:

$$F \equiv \frac{V}{\lambda R_c}$$

This was discussed in Sect. 1.2.

The potential gradient will, therefore, exhibit an increase if the number of nuclei is increased. Such an increase would be expected during the winter months in a polluted area, but the seasonal constancy of the mean value of space charge density and the absence of pollution effects, for example the 'sunrise-effect' (CHALMERS, 1967), indicate that this is not the case at Lanehead.

The converse to this is when the number of nuclei present is diminished or when they are redistributed over a greater volume. This can be achieved by increased austausch which mixes the free nuclei more effectively to the top of the austausch region. If we assume that the total production of small ions is unchanged and that their destruction, by combination with nuclei, is also the same, then the total columnar resistance, R_c, is unchanged. Some of the combination, however, will be occurring higher up in the austausch region; the decreased number of potential ion-capturing nuclei close to the ground causes a rise in the conductivity which results in a decrease of potential gradient measured at ground level.

From these considerations, the seasonal behaviour of the parameters at Lanehead can be summarised. The small ion conductivity, which is based largely on winter measurements (Sect. 8.1), shows no diurnal variation and because this parameter is the major factor governing the

Fig. 8.5. Seasonal variation in potential gradient.

July 1967–July 1969

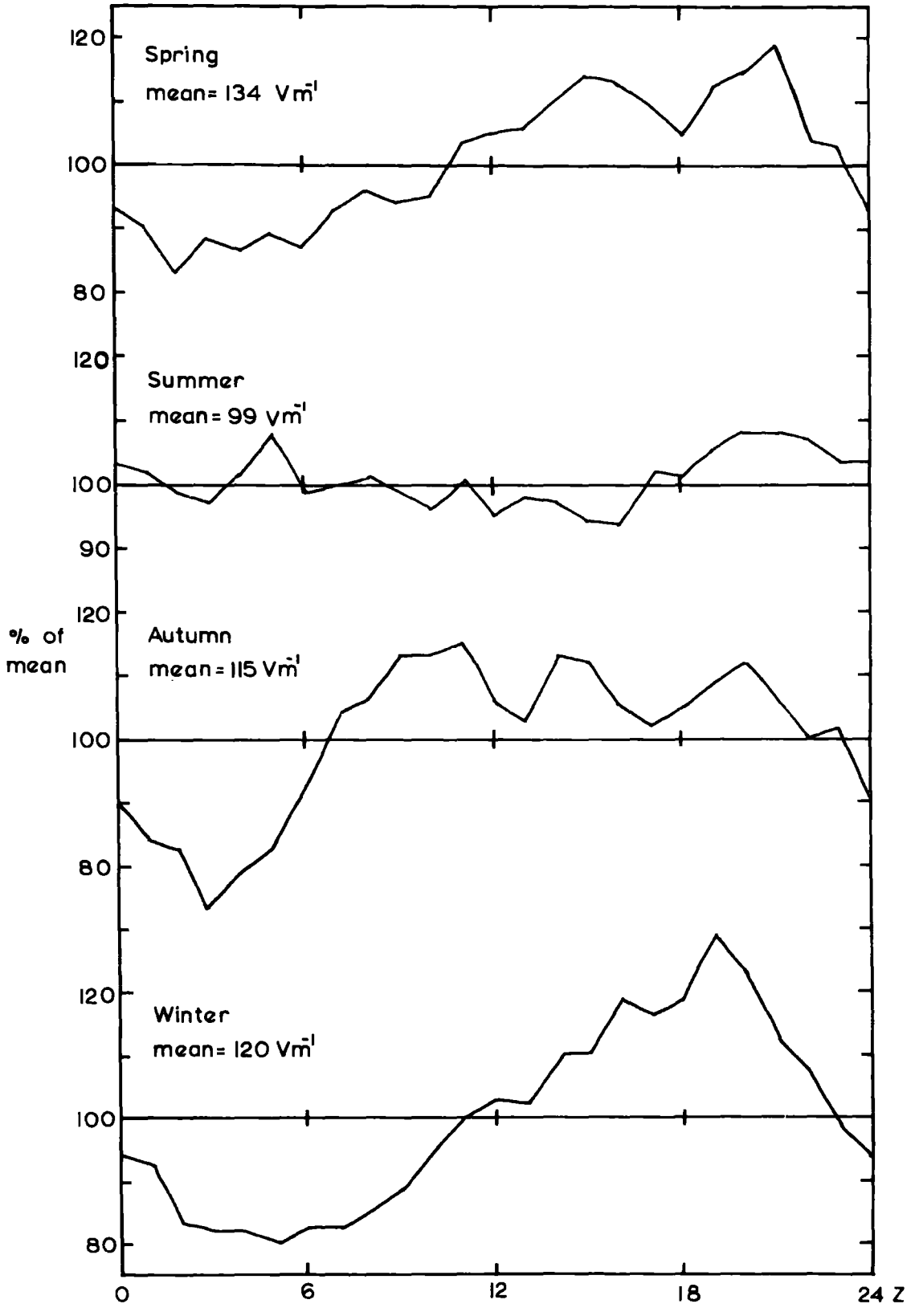

Fig. 8.6. Seasonal variation in total air earth current density. July 1967–July 1969

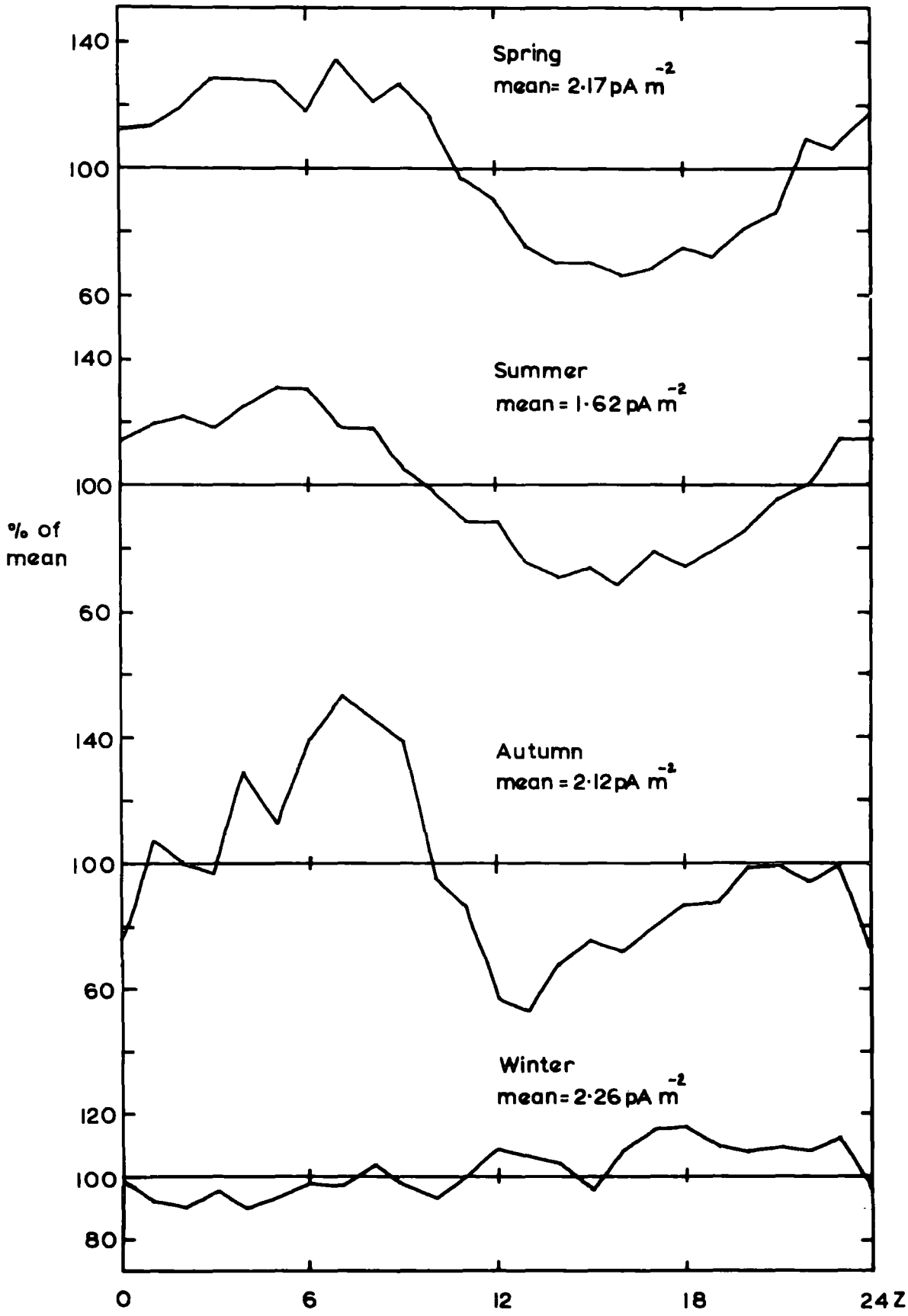

Fig. 8.7. Seasonal variation in space charge density. July 1967- July 1969

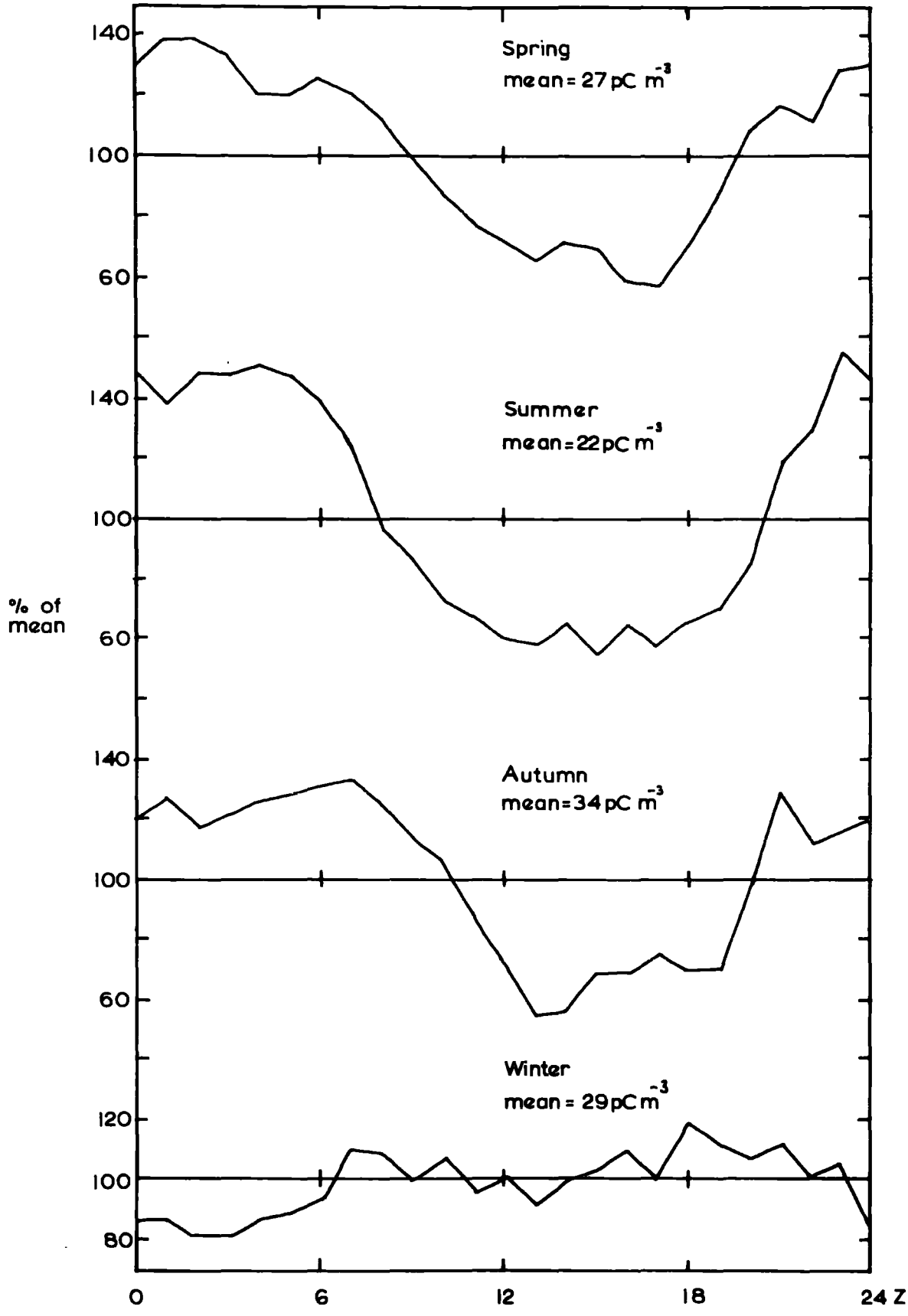

columnar resistance, R_c, it is assumed that R_c is also constant. Therefore the relationship:

$$F = \frac{V}{\lambda R_c}$$

implies that, in the winter months, F, the potential gradient, will vary as V, the potential of the electrosphere.

In summer, the more marked diurnal variation of insolation of the earth induces a diurnal variation in the convective energy of the lower atmosphere. This produces increased austausch with the consequence, explained above, of increased conductivity near the ground during the afternoon. Thus, under the relationship:

$$F = \frac{V}{\lambda R_c}$$

R_c is taken to be constant, and V and λ both have a maximum at roughly the same time of day. If the magnitudes of these two variations are similar their effects will cancel each other and this would explain the observation that there is no discernible diurnal variation of potential gradient in the summer time.

The conclusion is that it is possible to observe an average diurnal variation of the potential of the electrosphere by repeated measurements of potential gradient at the ground if the site chosen is one of low pollution and if the measurements are made in the winter months. Local influences will usually dominate measurements at any given time.

8.4 Diurnal variations of air-earth currents and space charge density

The measurement of both polar conductivities in the period October 1968 to June 1969 has made it possible to estimate the conduction current by

the indirect method. The diurnal variations of the total air-earth current and the conduction current for this period are shown in Fig. 8.8, together with the difference between the two. This is labelled the 'mechanical-transfer current' to denote its non-electrical nature. The conduction current remains virtually constant while most of the variation in the total current comes from the mechanical component. It will also be noticed that the mean values for the two are very nearly the same: 1.07 pA m^{-2} for the conduction current and 0.95 pA m^{-2} for the mechanical-transfer current. There is similarity in shape between the mechanical-transfer current variation and the corresponding variation for space charge density (Fig. 8.8), and this is borne out by the high correlation coefficient between the two of + 0.82, significant at the 99.5 per cent level of confidence. This indicates that more than 67 per cent of the variation in the mechanical current, and hence in the total current, is due to variation in the space charge density.

The line of best fit between mechanical-transfer current and space charge density was calculated and found to be:

$$i' = 0.1\rho - 1.0$$

where i' is the mechanical-transfer current density in pA m^{-2} and ρ is the space charge density in pC m^{-3}. The units of the slope, equal to 0.1, are ms^{-1} and the constant term is - 1.0 pA m^{-2}. Physically, the slope of the line suggests that the effective average vertical velocity of transfer of charged ions to the air-earth current collector is 0.1 ms^{-1}. The velocity of a large ion moving under the influence of an electric field of 100 Vm^{-1} is about 10^{-4} ms^{-1}, so that transfer of the charges to the plate must be due to the influences of air movements and not to the fair weather potential gradient.

Fig. 8.8. Diurnal variations of air-earth currents and space charge density.

October 1968–June 1969.

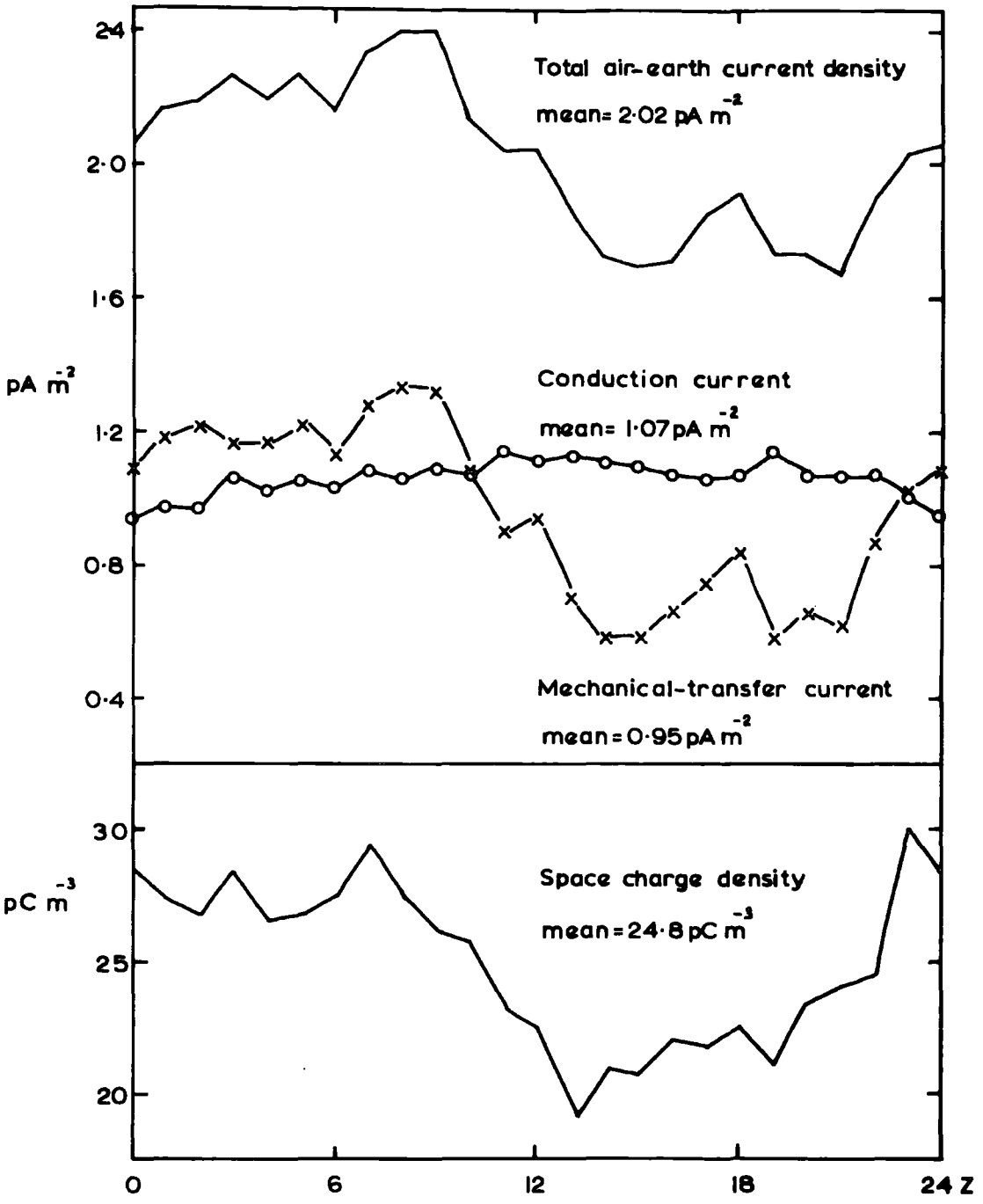

Total current measured by the DIRECT method.

Conduction current measured by the INDIRECT method.

Mechanical-transfer current given by the difference.

Space charge density measured by FILTRATION.

An explanation of the constant term may derive from the fact that the space charge measurements were made at a height of 0.8 m, and it is possible that the space charge density at ground level is different from this value. Rewriting the equation thus:

$$i = 0.1\ (\rho_{(0.8)} - 10)$$

suggests that there is a difference of - 10 pC m^{-3} from 0.8 m to the ground. Support for this argument comes from the work of DAYARATNA (1969) who found the space charge density to be negative at ground level but positive above 0.5 m at Durham University Observatory.

Because there is no correlation of space charge density with the difference in polar conductivities ($\lambda_+ - \lambda_-$) it is assumed that the space charge measurements are predominantly of large ion concentrations whilst the conductivity measurements indicate the behaviour of small ions. Therefore, it seems reasonable that, in conditions of fair weather, most of the mechanical-transfer current originates in the movement of large ions under non-electrical influences. The work of DAYARATNA (1969) again lends support to this. Using an exposed plate and an exposed wire to measure the air-earth current, Dayaratna found that the wire, which had a conduction cross-section six times that of the plate, collected a current several times smaller than the current to the plate. The difference was attributed to space charges advecting to the plate.

In respect of Sect. 8.6 it is mentioned here that there is no correlation of mechanical-transfer current with the total conductivity ($\lambda_+ + \lambda_-$).

8.5 The effect of light winds on the diurnal variations

A six months study of the effect of light winds on the electric parameters at Lanehead was made in the period November 1968 to April 1969. The output from an anemometer, erected on a mast on the end wall of the school, was recorded on a single channel pen recorder, but, because of the unsatisfactory inking of this instrument, the record was terminated in May 1969. Periods of light wind, with speeds less than 1 ms^{-1} at a height of 10 m, were chosen from those hours when the record indicated that the anemometer had not turned; this did not mean that there was no wind during the hour but that the breeze, if any, had been very light. The hourly atmospheric electric measurements for light winds were separated from the parent body of fair weather measurements and the resulting diurnal variations are shown in Fig. 8.9. Comparison can be made with the diurnal variations for all fair weather in the period November 1968 to April 1969.

Tests for the difference between the means for each parameter, for light winds and for all fair weather, showed that the variations of potential gradient and total air-earth current density in light winds were not significantly different, statistically, from the parent population. On the other hand, the space charge density and both polar conductivities are significantly different from their parent populations at the 99 per cent level of confidence.

The measurement of the polar conductivities at ground level in light winds (Fig. 8.9) gives a statistically significant increase in positive conductivity with a corresponding decrease in negative conductivity; this is a manifestation of the influence of the 'electrode effect'.

This effect has been defined by BENT and HUTCHINSON (1966) as follows: in atmospheric electricity the electrode effect is the modification of

Fig. 8.9. The effect of light winds on the diurnal variations. November 1968 — April 1969.

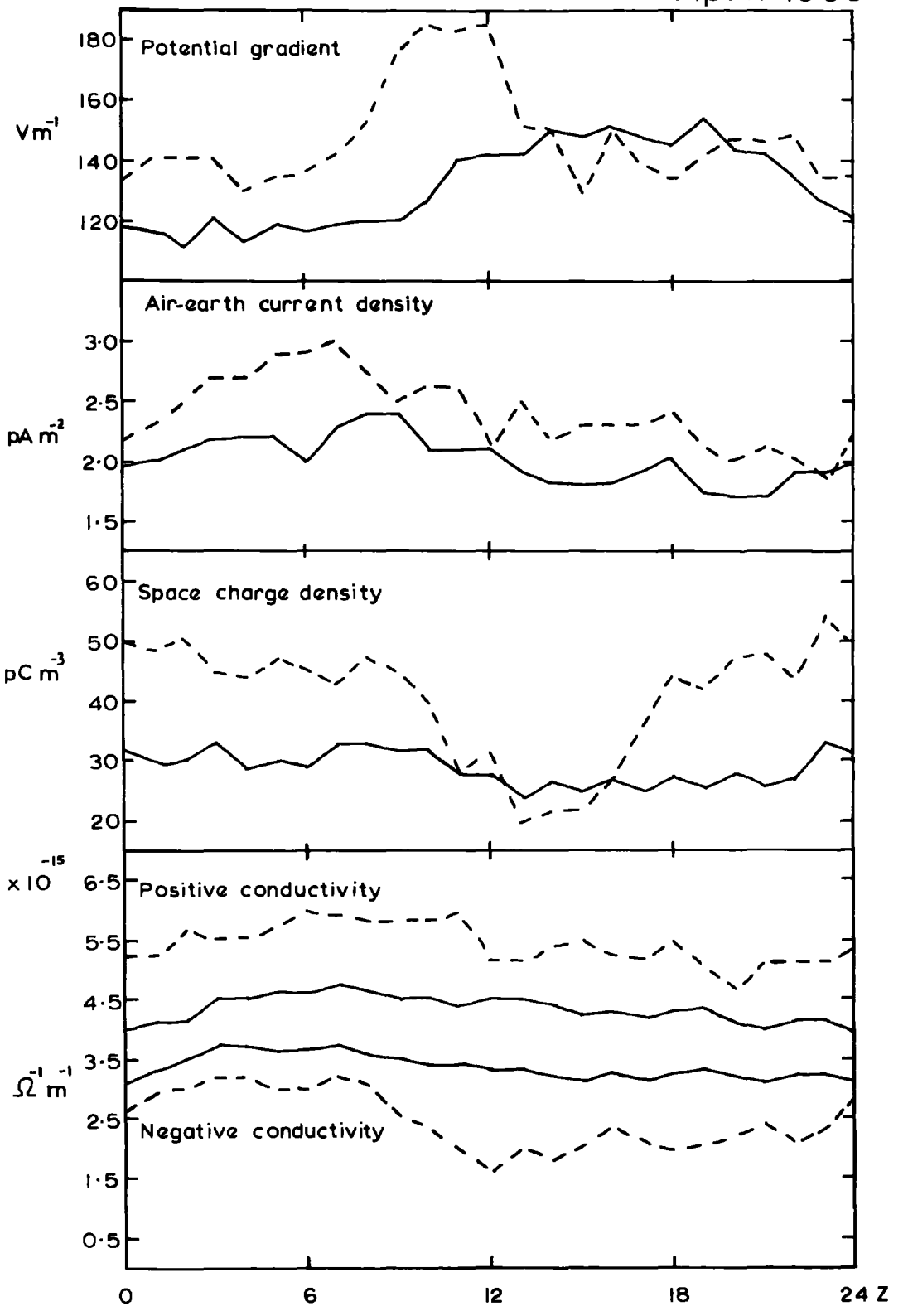

elements such as space charge distribution, conductivity and potential gradient near an earthed electrode, which may be a raised object or the surface of the earth itself, because in the prevailing field ions of one sign are attracted towards the electrode, whilst those of the opposite sign are repelled from it.

The electrode effect has been detected by PLUVINAGE and STAHL (1953), and by RUHNKE (1962) over the polar ice cap, and by MUHLEISEN (1961) above Lake Constance. COBB (1968) reports the influence of the electrode effect on measurements made at Mauna Loa Observatory, well above the austausch region, but the only evidence of this effect within the austausch is given by CROZIER (1963). His measurements with a filtration instrument, indicated an enhancement of space charge density in periods of low wind speed but during night time only. This result should be compared with the diurnal variation of the same parameter, for light winds, given in Fig. 8.9, where it will be seen that there is no indication of the electrode effect during the limited hours of winter daylight. No explanation of this puzzling state of affairs can be offered but it is important in view of the fact that most atmospheric electric instruments are operated at ground level, that further study of such effects should be carried out.

8.6 Diurnal variations of air-earth currents and total conductivity in light winds

In line with the work of Sect. 8.4, the conduction current component of the total air-earth current in light winds can be separated from the mechanical-transfer component and the result is shown in Fig. 8.10. In this case, the conduction current density is less constant than before, being a consequence of greater variation in both total conductivity and

potential gradient. It will be recalled (Sect. 8.4) that the correlation of mechanical-transfer current with space charge density was + 0.82 for all fair weather and that this constituted the major cause of variation in the total air-earth current density. In light winds, however, the total air-earth current is correlated, not with space charge density, but with total conductivity, the coefficient being + 0.78, significant at the 99.5 per cent level of confidence. The two component currents, mechanical and conduction, of the total current show small correlations (+ 0.53 and + 0.54) with the total conductivity and this suggests that variations in the driving forces, small-scale air movements in one case and electrical potential in the other, are the two major governing factors here. More extensive measurements would resolve the exact relationships of these various atmospheric electric and mechanical processes which transfer charge to the surface of the earth in fair weather.

Fig. 8.10. Diurnal variations of air-earth currents and total conductivity in light winds. November 1968–April 1969.

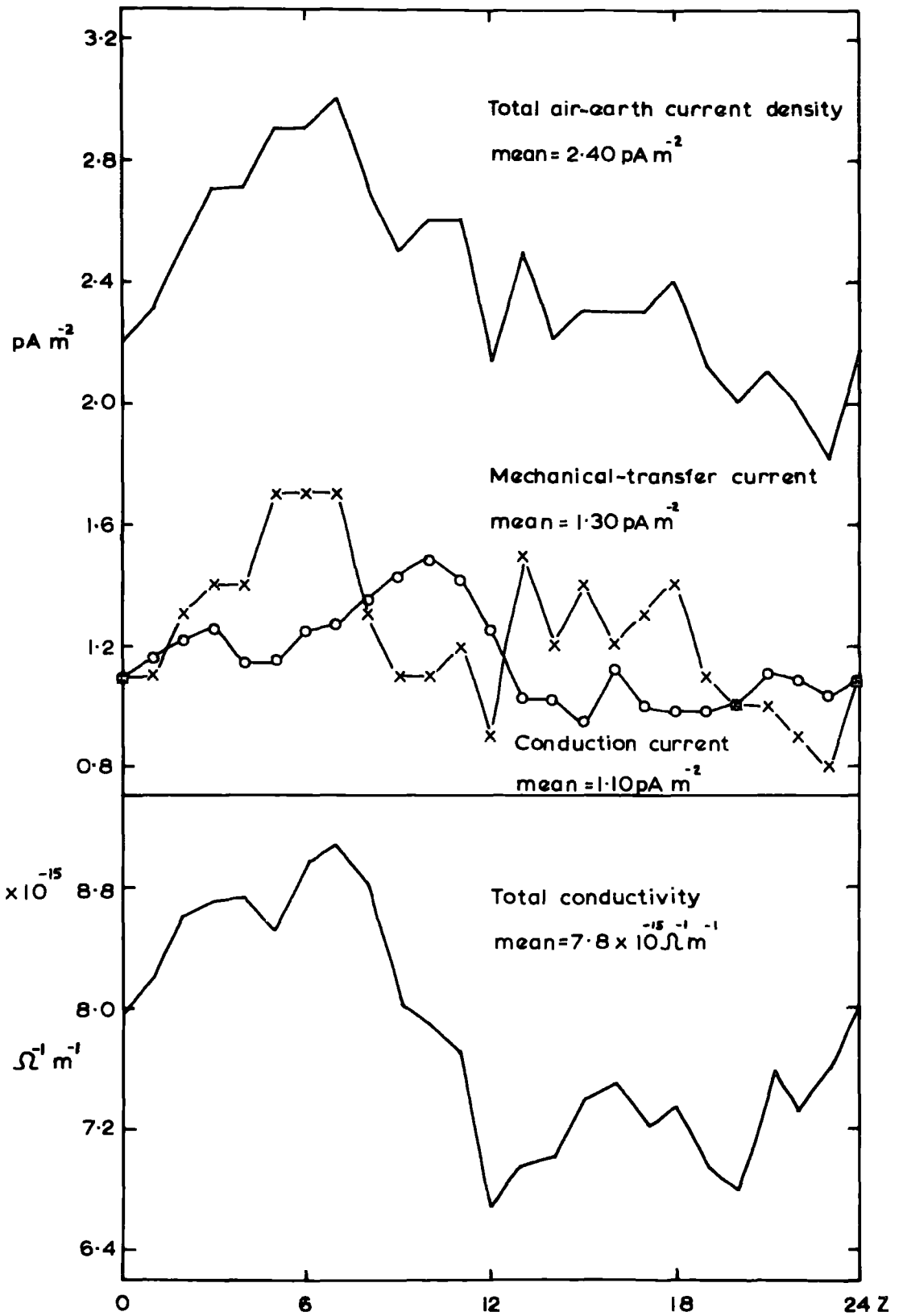

CHAPTER 9

GENERAL CONCLUSIONS AND SUGGESTIONS FOR FURTHER STUDY

This chapter deals with the broad conclusions to be drawn from the work and endeavours to highlight some problems of interest and the methods which could be adopted to investigate them.

9.1 The digitization of data

The development of the digital computer has given research a powerful tool for processing vast quantities of data and the recording of data in digital form, suitable for computer input, has become an established technique in the Atmospheric Physics Research Group at Durham. The automatic recording system, described in Chapter 3, was built for this purpose and proved satisfactory both in its remote tape-recording facilities and in its applications as a single station device. The physical action of making a permanent but manageable record of atmospheric electric conditions becomes embodied in the paper-tape punch and this relieves the researcher of the necessity to read meters or inspect charts for long periods of time. This advantage of the system was equally valuable both for the precipitation measurements, when some records were of more than 6 hours duration, and for the continuous fair weather observations which would have been impossible to collect and analyse without the time saving allowed by a digital data system.

Whilst extolling the virtues of the system, a cautionary note should be sounded about some aspects of digital data processing. The problems of discretely sampled time series are discussed in Chapter 5 and the reader is referred to BLACKMAN and TUKEY (1958) as the definitive work on this important topic. The automatic nature of the system also means that, from the time of recording to the moment of processing in the computer,

the operator is unlikely to be fully acquainted with all the data collected and thereby loses some of the personal 'contact' which develops when taking down data by hand. This is an important point in a discipline like Atmospheric Physics where subjective inspection can often give birth to ideas for more rigorous analysis and, for this reason, the author believes it desirable to be equipped either with a simultaneous chart record of conditions or with a computer-drawn record of the type illustrated in Fig. 6.1.

A real advantage of the system, on the other hand, is that the data-processing capability of digital computers allows the adoption of the analysis techniques which would otherwise have been impossible to complete. The functions of cross-correlation and autocorrelation involve prohibitive quantities of repetitive arithmetic for a desk calculator and other techniques, for example, the spectral analysis used in this work, probably owe their existence and development to the computer. An assessment of spectral analysis techniques is given in the next section.

The digitization of the potential gradient observations in precipitation was an essential step in the compensation for displacement currents in the precipitation current measurements (Sect. 5.1.2) and, in this way, digitization became an integral part of the measuring technique. This method was considered very satisfactory in view of the difficulties encountered by other workers with electronic compensation circuitry (for example, GROOM, 1966), and its use is recommended for future investigations in precipitation electricity.

The investment of digital data in an information bank might prove to be a very useful enterprise. This would require a standardised procedure for data collection and a standardised format of the data on computer cards; for instance, records every 5s of potential gradient, in Vm^{-1}, and

precipitation current, in pA m^{-2}, for conditions of nimbostratus, would accrue and enable researchers, testing a new theory or trying a new analysis technique, to have sufficient data to make a meaningful assessment of their ideas. A lack of data is often the stumbling block for a promising idea which may not be pursued again. The scheme of data collection could be reviewed, if necessary, every few years.

Meanwhile, it is hoped that the automatic recording system will continue to give useful and efficient service.

9.2 Variance spectrum analysis

In this work, the preference for variance spectrum analysis introduced a fundamental difference in approach from other investigations of nimbostratus electrification in that the time series records were split up into different frequency components to present a new view of the information contained in the records. This analysis technique produced several noteworthy results, outlined in Sect. 9.3, which, together with successes in the kindred subject of boundary layer dynamics, suggest that there is promising scope for its application to many of the problems of atmospheric electricity, both in fair weather and disturbed. For precipitation electricity, the present investigation has scratched the surface and there is more information to be derived from the spectra obtained. This may be achieved by refining the records with digital filters; a single exercise of this technique (Sect. 6.3) detected the presence of a current to the receiver due to a mechanical transfer of space charges, similar in nature with the effect found in fair weather (Sect. 8.4). The scope in fair weather is also wide; there are many outstanding problems which might succumb to suitable spectral analysis, for example, the mechanical movement of space charges in the lowest layers of the atmosphere,

and the puzzling space charge pulses of fine convective weather (OGDEN, 1967). The physical mechanisms of the point discharge could also be studied in this way.

Spectral analysis is a growing subject, becoming stronger as the gap closes between theoretical concepts and practical techniques for measuring and interpreting data, and it is likely that in future it will be a major aid to progress in experimental Atmospheric Electricity.

9.3 Precipitation electricity

9.3.1 Meteorological and electrical structure in nimbostratus

The results of the variance spectrum analysis of measurements of potential gradient and precipitation current in conditions of electrically quiet rain have been presented in detail in Sect. 6.2.

Significant peaks in the coherency spectra of these two parameters (Sect. 6.2.2.) were taken to indicate a fundamental periodicity in the process, assumed to be located in the cloud, which gives opposite charges to the precipitation and to the charging region. This suggests that the process is not uniform for the whole cloud but that it has regions of greater and lesser activity. In a similar manner, the physical appearance of any stratiform cloud is never uniform; the cloud has structure which is dependent on small-scale meterorological fluctuations. Studies of the nature of this structure were mentioned in Sect. 6.2.2 where it was argued that links might exist between the electrical and the physical structures of nimbostratus with the important consequence that cross-identification of characteristics in both sorts of processes could lead to more refined weather forecasting on the sub-synoptic scale. The intensive meteorological studies to be undertaken in Project Scillonia (MASON, 1969) should give a good opportunity for joint research along these

lines and it would be a great pity if the electrical aspects of one of our more common weather patterns were ignored.

9.3.2 A model for nimbostratus electrification

A brief outline of a theory to explain the effects of nimbostratus electrification, which has been developed by a colleague, Mr. M.F.Stringfellow was given in Sect. 6.2.4, and details of results which support its predictions were given in Sect. 6.2.5. These comprised estimations of the height of electrical activity which corresponded well with the observed melting level for the record in question. As a consequence, it can be seen that there are electrical effects associated with the melting and freezing of water in nimbostratus just as in cumulonimbus, although the magnitude of the charge separation is very much smaller. It seems that the increased separation in the thunder cloud must, in some way, be dependent on the more violent turbulent and convective activity normally associated with these conditions.

The periodic behaviour of Stringfellow's model as a function of the electrical relaxation time of the charging region was discussed in Sect. 6.2.8. This allowed an estimate of the conductivity of the region to be made which was found to be in accord with the values of conductivity for non-precipitating clouds. This augurs well for the validity of the theory and it is hoped that Mr. Stringfellow will very shortly publish details of his model so that more exhaustive tests may be made on its design.

9.3.3 Electrical processes near the ground

Most students of the problem of the electrification of nimbostratus, following CHALMERS (1956), preferred to assume a single charge separation in the snow cloud with a second process at melting for the rain cloud.

Recent measurements, mentioned in Sect. 2.2.3, have indicated a charge separation occurring well below the melting band and this will obviously interfere with those measurements made at the ground which are intended to study the activity in the cloud. The relationship of negative small-ion conductivity excess with potential gradient, discovered in Sect. 6.2.9, poses several questions. Two effects, drop splashing and drop shattering, were put forward as possible causes of the charge production but no clue was available to choose between them. Some relationship of negative conductivity excess with wind speed at the ground was hinted at but the evidence was not sufficiently strong to be presented here. It is possible that both effects were working in tandem, and a further series of conductivity and wind speed measurements, possibly at different heights close to the ground, should be conducted to investigate these effects.

A question mark also rests over the performance of the inverted field mill in precipitation. SHARPLESS (1968) established that the exposure factor of the mill was not influenced by space charges close to the ground in fair weather, but it would be a worthwhile exercise to test this conclusion when the space charge density is much greater than its normal fair weather value. This could be achieved, using an artificial ion generator, by comparing the performance of the inverted mill with an upright one in the plane of the earth's surface where high densities of space charge are present close to the ground.

9.3.4 Mechanical-transfer currents to an exposed collector

The existence of currents of space charges being transferred to an exposed air-earth current collector by mechanical means has been detected in fair weather (Sect. 8.4) and during precipitation (Sect. 6.3).

The magnitude of this current in the latter conditions is uncertain

but it was shown (Sect. 6.3.1) that it could conceivably be of the same order as the precipitation current. Therefore, the totally exposed receiver, often held to be the most reliable device to measure precipitation currents, displacement effects notwithstanding, is prone to spurious currents which probably do not affect a shielded collector. This is another aspect of the instrumentation for precipitation electricity measurements which should be fully investigated, possibly by using simultaneously rain receivers of both types. The design of the shielded collector is discussed theoretically by OWOLABI and OLAOFE (1969).

9.4 Fair weather Atmospheric Electricity

9.4.1 The 1-hour recording system

The design and performance of this system, which smooths measurements of atmospheric electric parameters and samples them once an hour, were described in Sect. 7.3. The device was installed at Lanehead, resulting in a major saving of time and effort in the collection, and later in the computer analysis, of the data; this type of recording unit can form the backbone of any field station where long-term continuous measurements are required for subsequent statistical analysis. The problems inherent in measurements out-of-doors, however, remain; for example, insulation breakdown caused by moisture or insects can only be checked by regular inspection.

The 1-hour recording unit was based on the general purpose analogue-to-digital recording system developed for the precipitation measurements and this had a capacity for sampling and recording the ten different parameters. Five fair weather electric parameters, time and an indication of the occurrence of rainfall comprised the seven channels occupied in this work, and suggestions may be entertained for utilising the remaining channels.

It should not be a difficult task to devise a means for recording that wind speed was less than a given value during an hour-long record. This suggestion is prompted by the interesting results of Sects. 8.5 and 8.6 on measurements in light winds, which involved some time being spent on paper chart inspection. A device similar to the rain 'switch' (Sect. 7.3.3.) would be ideal.

As it stands at present, the 1-hour system is only effectively being used for fair weather conditions. It is possible, using metal-oxide field effect transistors (Sect. 7.3) to design an electronic circuit which will integrate and hold the charge arriving at, say, a shielded rain collector during the period of an hour. The measured value of charge could be sampled and recorded by the digital system, and the integrator reset for the next hour. A record of this nature, for a year's measurements, would produce a more reliable figure for the charge brought to earth by precipitation currents than can be derived with estimates from individual records.

A third suggestion is that duplication of some of the instruments might prove to be a worthwhile experiment. For example, the measurement of potential gradient or space charge density at two heights near the ground, while still providing the information required before, would also give a valuable insight into the way these elements vary with height. Alternatively, the recording system could be used as a test-bed for atmospheric electric instruments: the behaviour of the inverted field mill could be compared with an upright mill either in the long-term, using the 1-hour system, or in finer detail by using the recording system in its fast sampling mode.

9.4.2 Seasonal differences in the diurnal variations of the main atmospheric electric elements

Sect. 8.3 was devoted to a discussion of the seasonal differences in

form of the diurnal variations of potential gradient, total air-earth current density and space charge density. The similarities of the air-earth current variations and the space charge variations were explained in terms of the 'mechanical-transfer' current of space charges to an exposed receiver (Sect. 8.4).

An explanation was also offered for the reason why the more marked diurnal variation of potential gradient occurred in the winter months whilst the distinctive diurnal variation of space charge density was more apparent in summer. The existence of enhanced convective activity in the lower atmosphere in summer was introduced as the basic influence controlling these electric parameters; the lifting of small ion-capturing nuclei away from the ground produces an increased total conductivity, and hence a smaller potential gradient, at the surface of the earth. This predicts that we should find a seasonal increase of total conductivity in the afternoon hours for summer months, but, in the present work, measurements were made only for the period October 1968 to June 1969 and these cannot produce the necessary details of seasonal differences. Here, then, is the basis of a test for the explanation offered: measurements at the ground are needed, almost certainly of more than 2 years duration, to determine the existence, if any, of seasonal differences in the diurnal variation of total conductivity.

9.4.3 The mechanical-transfer current

Four separate pieces of evidence can be produced to support the existence of a mechanically controlled current of space charges to an exposed plate of the sort first used by WILSON (1906). In this work, the current has been identified twice: firstly, in fair weather results (Sect. 8.4) and secondly in conditions of precipitation (Sect. 6.3), when there is generally a greater density of space charges close to the ground.

The other two effects were observed concurrently by a colleague, Dr. L. H. Dayaratna. In his work DAYARATNA (1969) found that an exposed plate collected more current than did a horizontal wire of much greater conduction cross-section. To test his suggestion that this difference was due to space charge advection to the plate, Dayaratna conducted some wind tunnel experiments with artificially produced space charges passing over a model plate. The effects of the air speed and of the potential applied to a parallel plate were assessed with the conclusion that, for potential gradients of less than 1000 Vm^{-1}, the movements of large ions were entirely controlled by air motion.

This evidence and these assertions must cause us to examine critically the purpose and the properties of the exposed plate current receiver. It is generally assumed, under the concept of the quasi-static state, that the charge distribution in the atmosphere in fair weather is unchanging and that, allowing currents continuity across boundaries, the only resultant current to a plate in the surface of the earth will be the conduction current determined by the potential of the electrosphere and the conductivity of air. Small, localised perturbations of this state, it is thought, will be random and will cancel out over a period of time. This, however, does not appear to be the case in view of the results given in Sect. 8.4 which show that the mechanical-transfer current is of the same order of magnitude as the conduction current. An exposed plate measures the total current to that particular plate and not just a representative fraction of the conduction current.

It is important to determine how the total current to a plate depends upon the size and nature of the exposed surface and how it depends upon wind speed and other meteorological factors. Thought must be then given to the value of such a device as an instrument of Atmospheric Electricity.

APPENDIX 1

THE MONTHLY DIURNAL VARIATIONS - AUGUST 1968 TO JULY 1969

The following 12 diagrams depict the average diurnal variations for 5 atmospheric electric elements measured in fair weather at Lanehead for the period August 1968 to July 1969.

The parameters are:

F - potential gradient in Vm^{-1},

I - total air-earth current density in $pA\ m^{-2}$,

ρ - space charge density in $pC\ m^{-3}$,

λ_+ - positive small-ion conductivity in $\Omega^{-1}m^{-1}$,

and λ_- - negative small-ion conductivity in $\Omega^{-1}m^{-1}$.

Diurnal variations — August 1968.

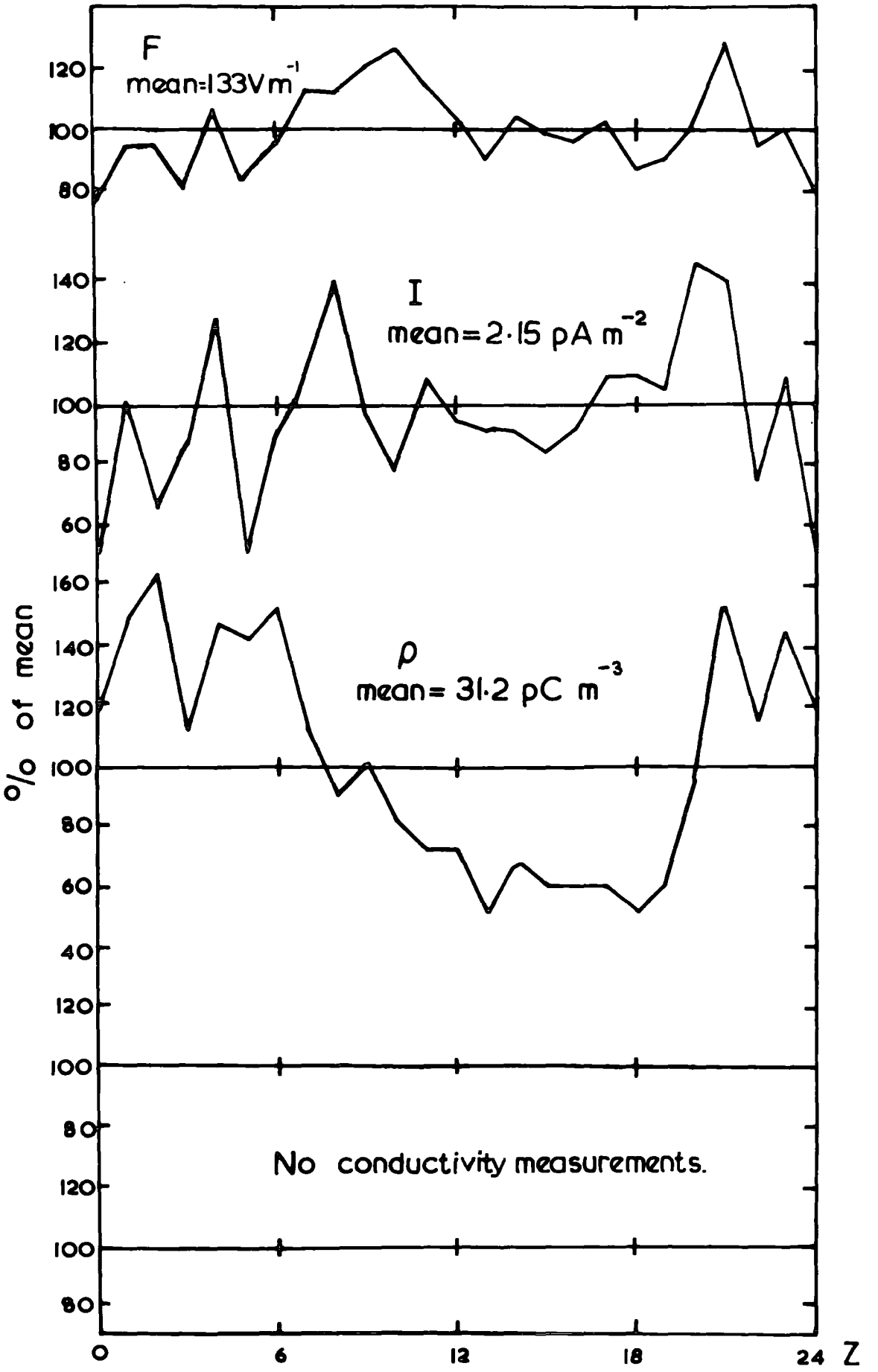

Diurnal variation — September 1968.

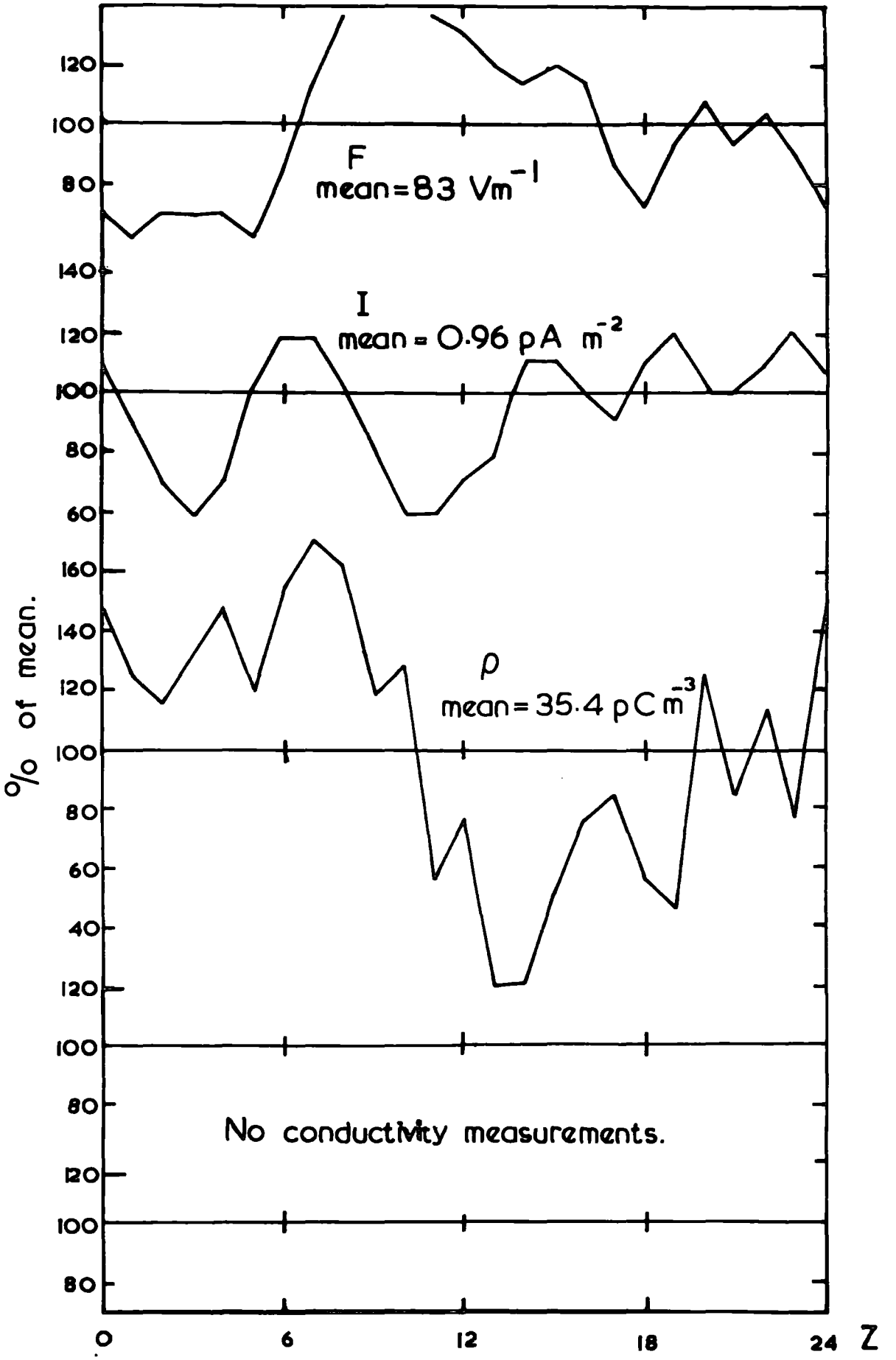

Diurnal variations — October 1968

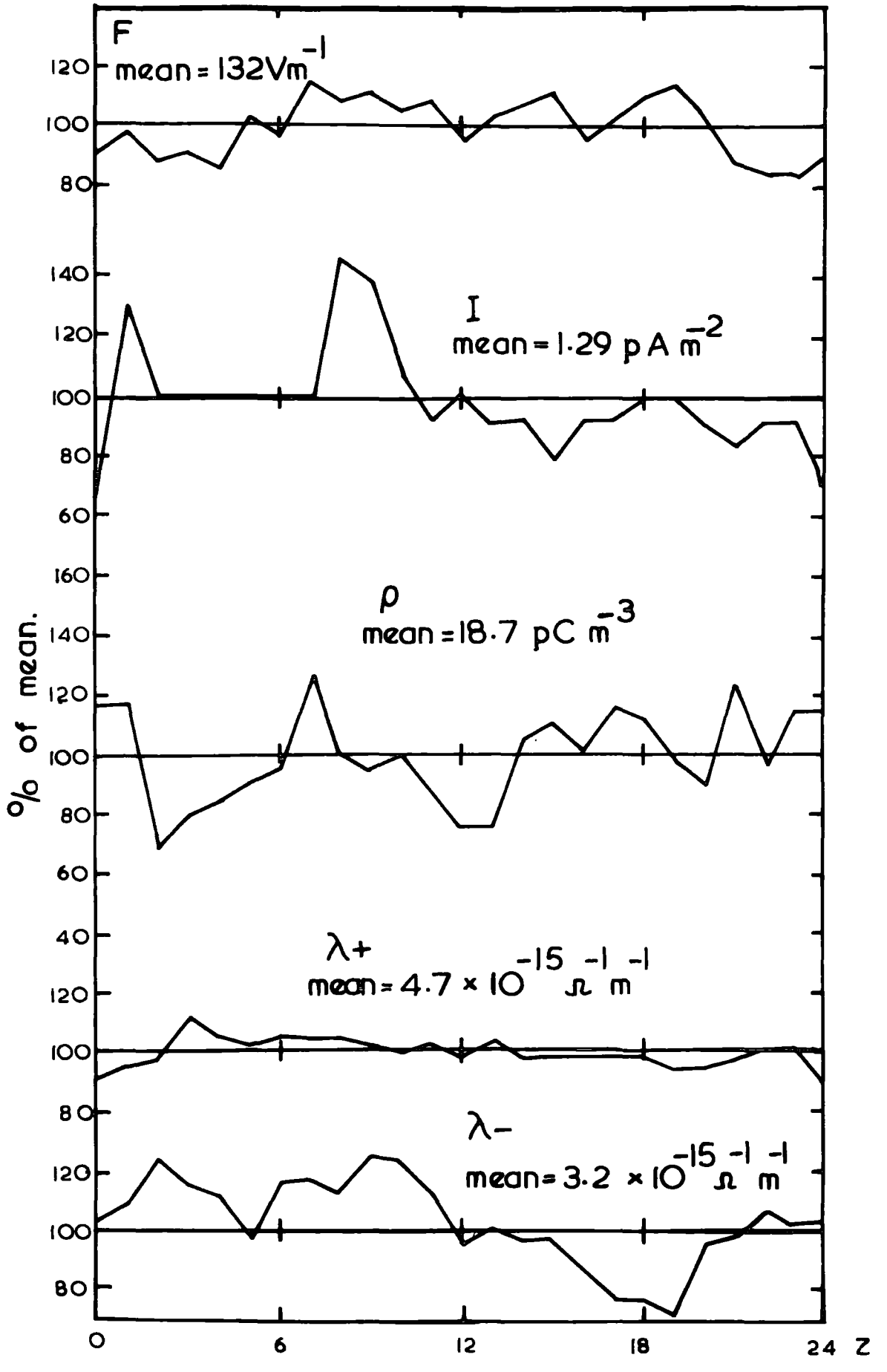

Diurnal variations — November 1968

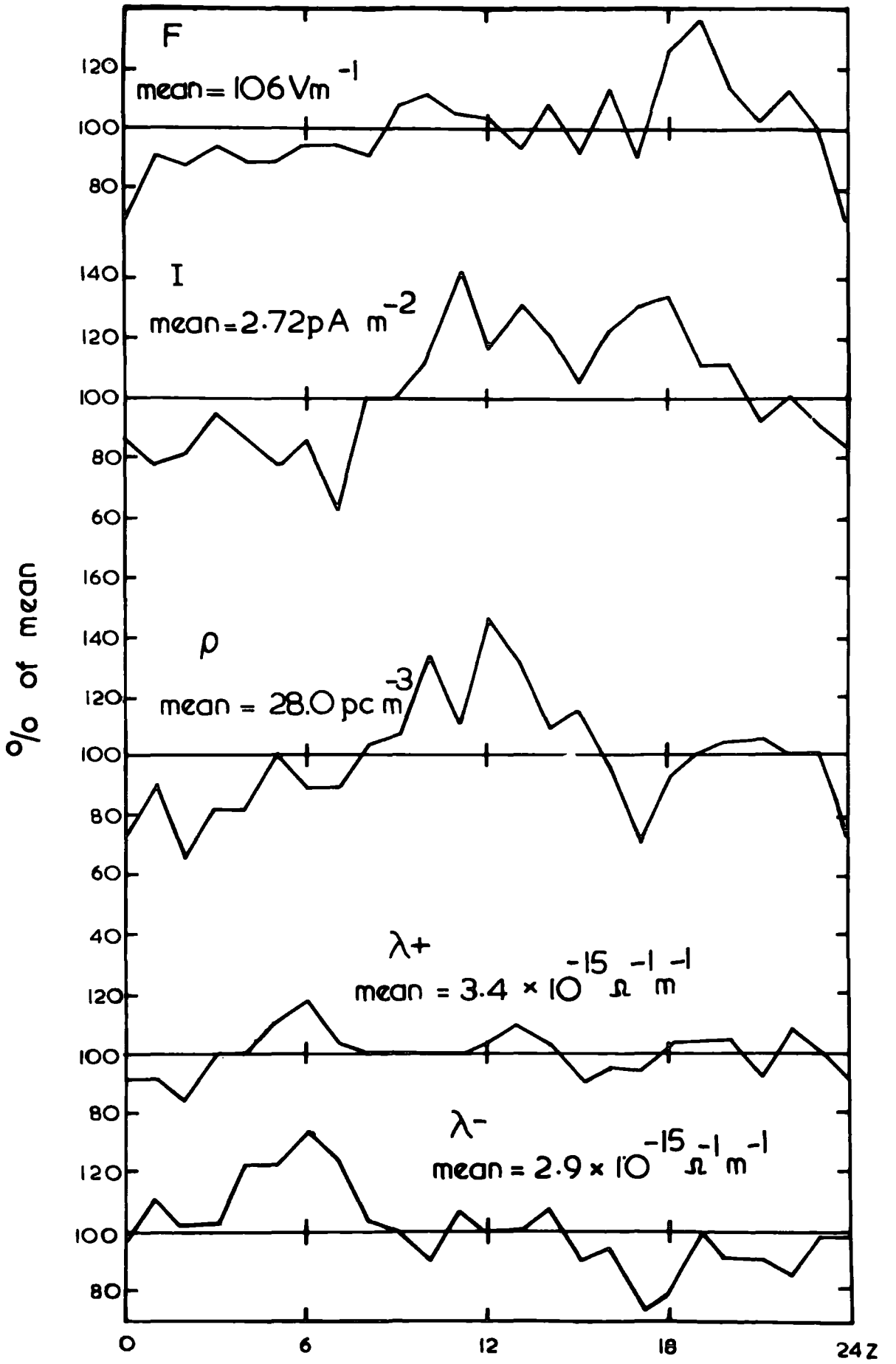

Diurnal variations – December 1968

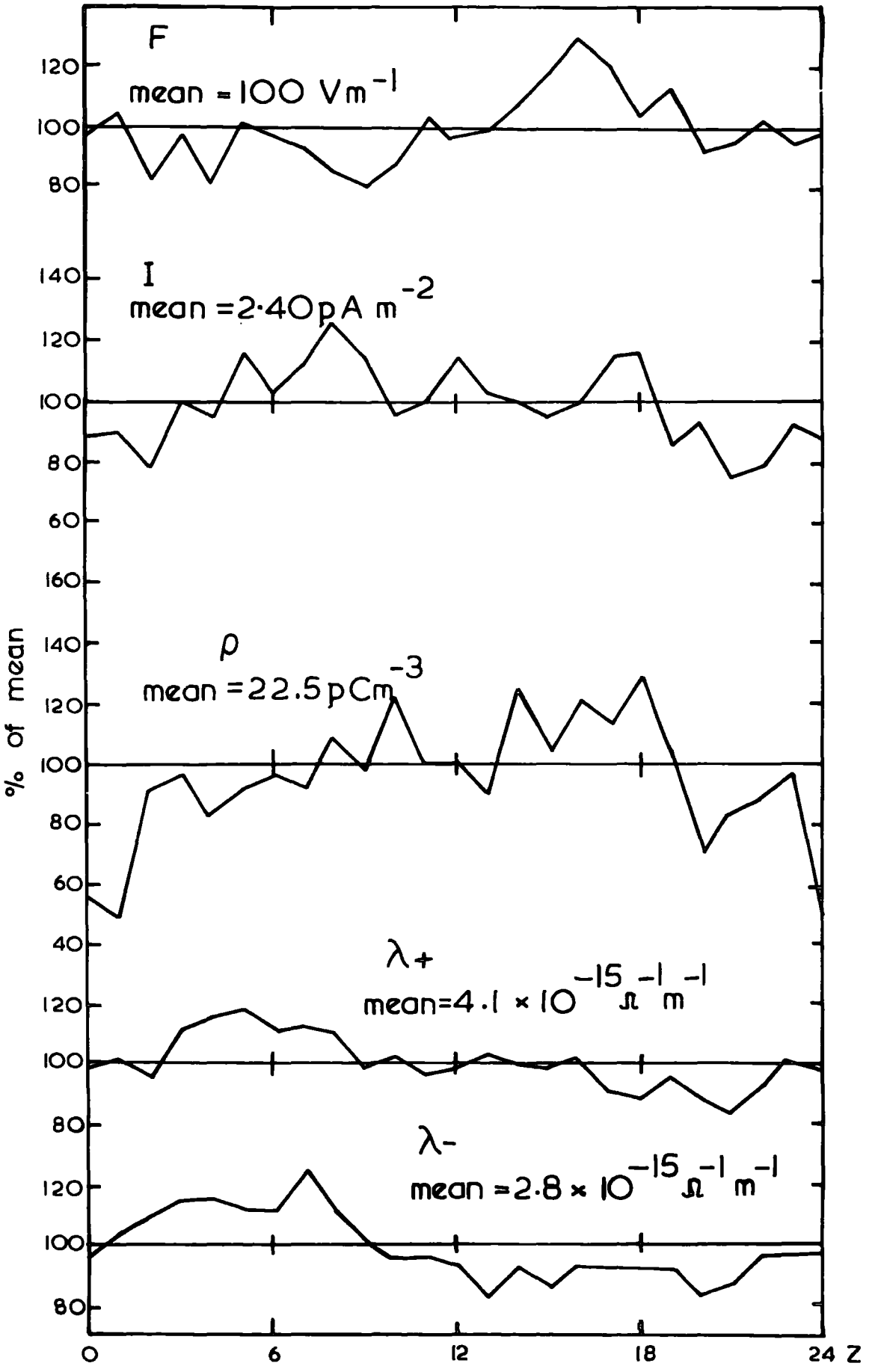

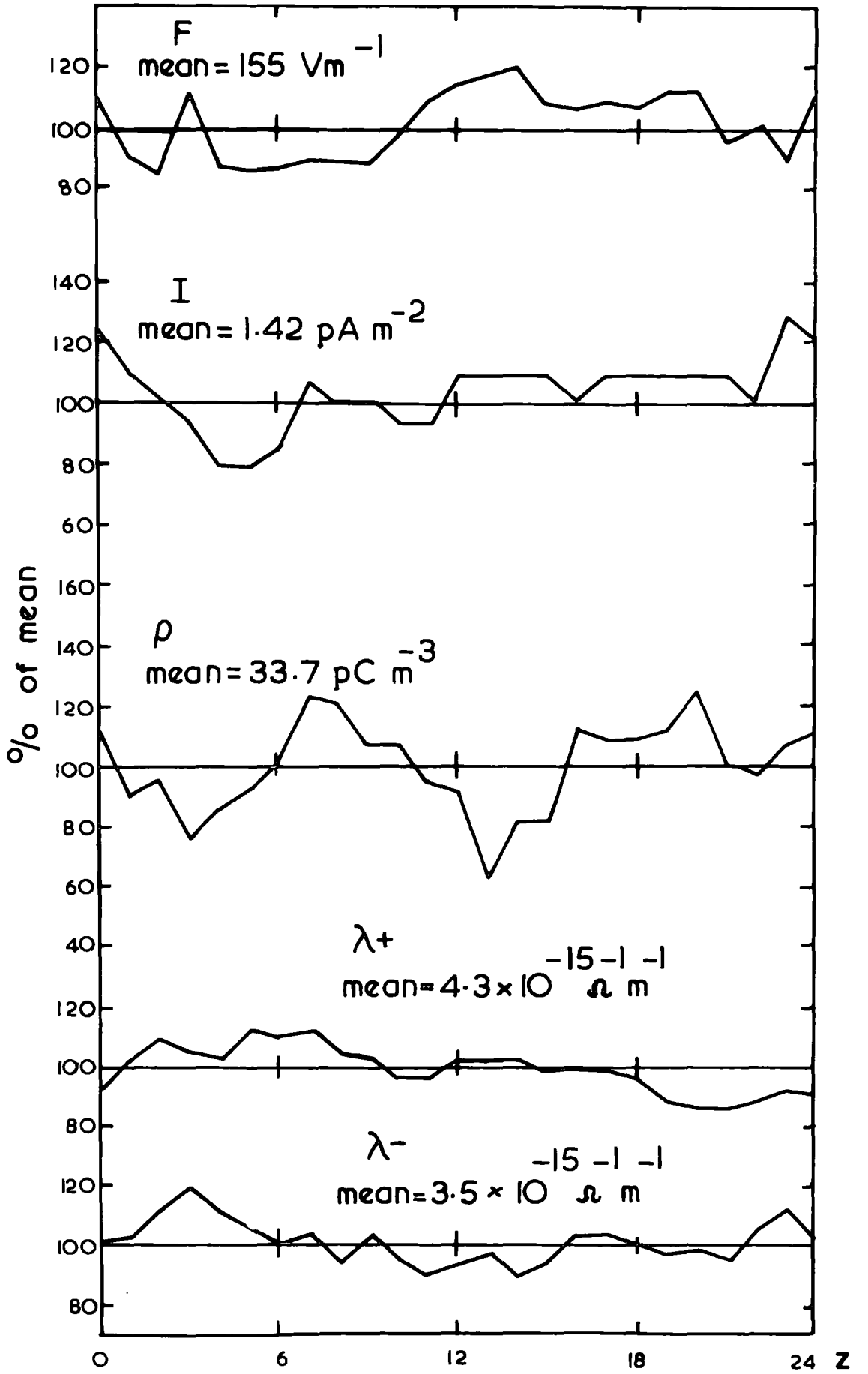
Diurnal variations — January 1969
F
mean = 155 Vm⁻¹
I
mean = 1·42 pA m⁻²
ρ
mean = 33·7 pC m⁻³
λ+
mean = 4·3 × 10⁻¹⁵ Ω⁻¹ m⁻¹
λ−
mean = 3·5 × 10⁻¹⁵ Ω⁻¹ m⁻¹
% of mean
120
100
80
140
120
100
80
60
160
140
120
100
80
60
40
120
100
80
120
100
80
0
6
12
18
24
Z

Diurnal variations — February 1969

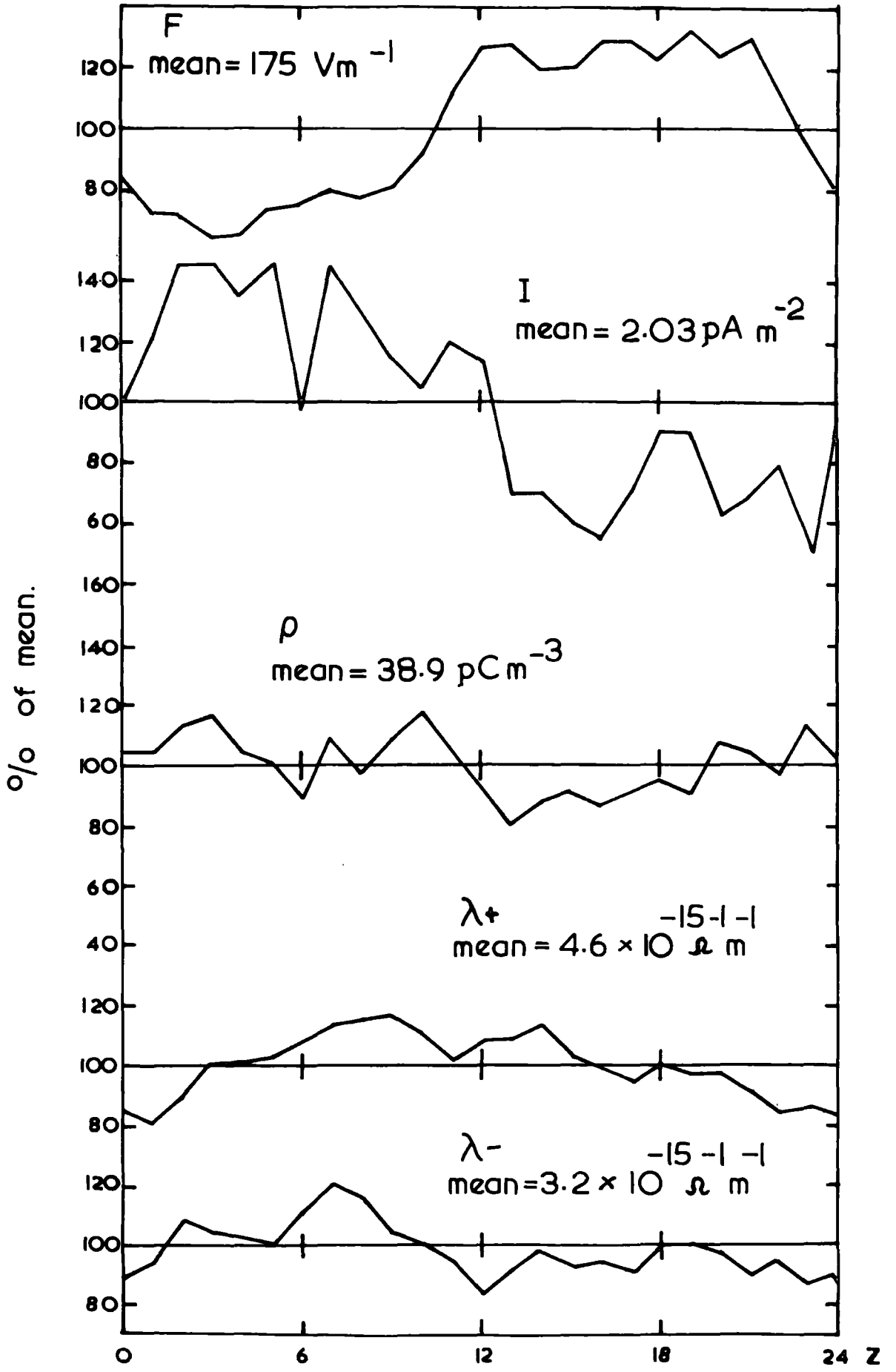

Diurnal variations - March 1969

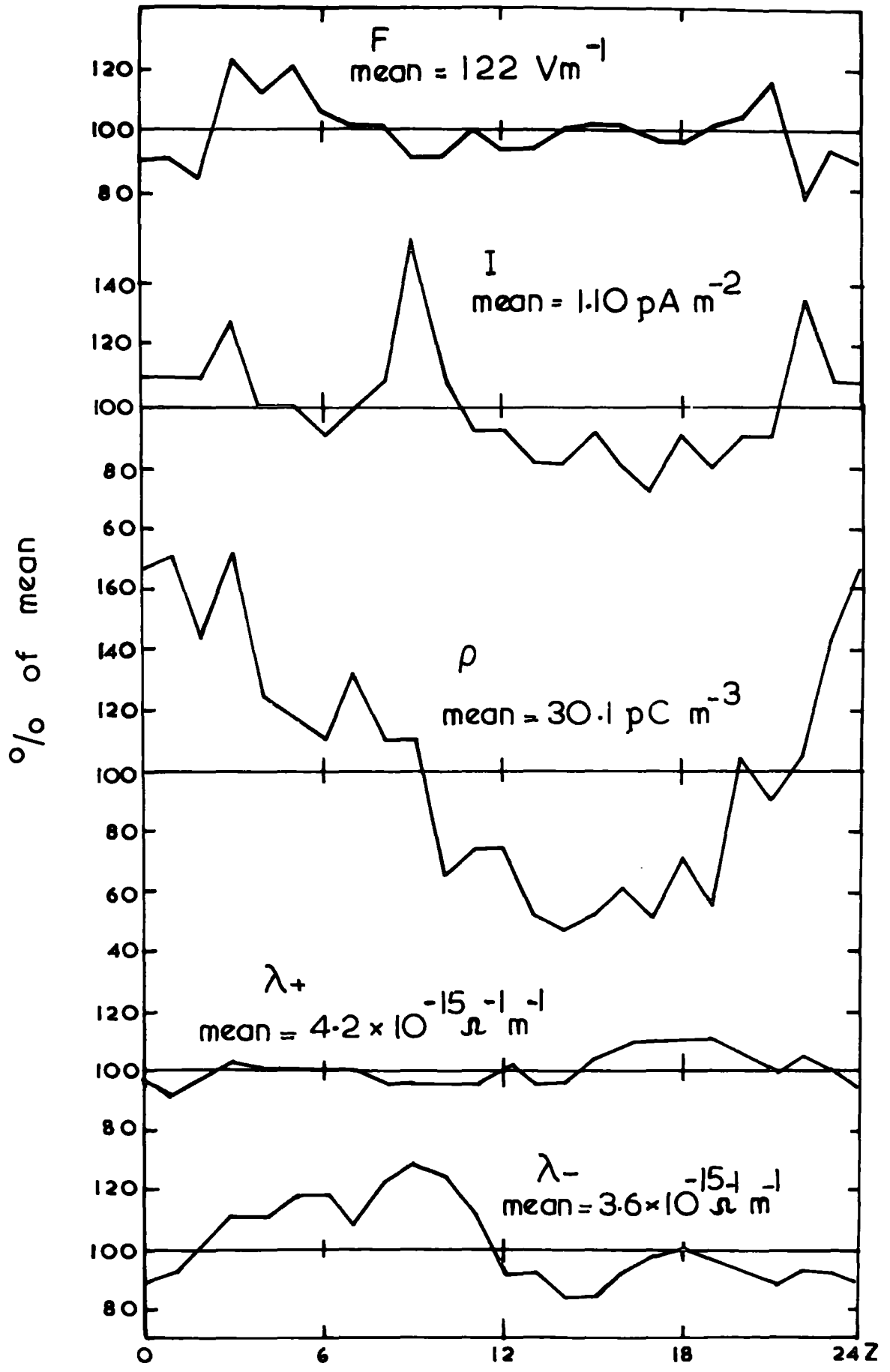

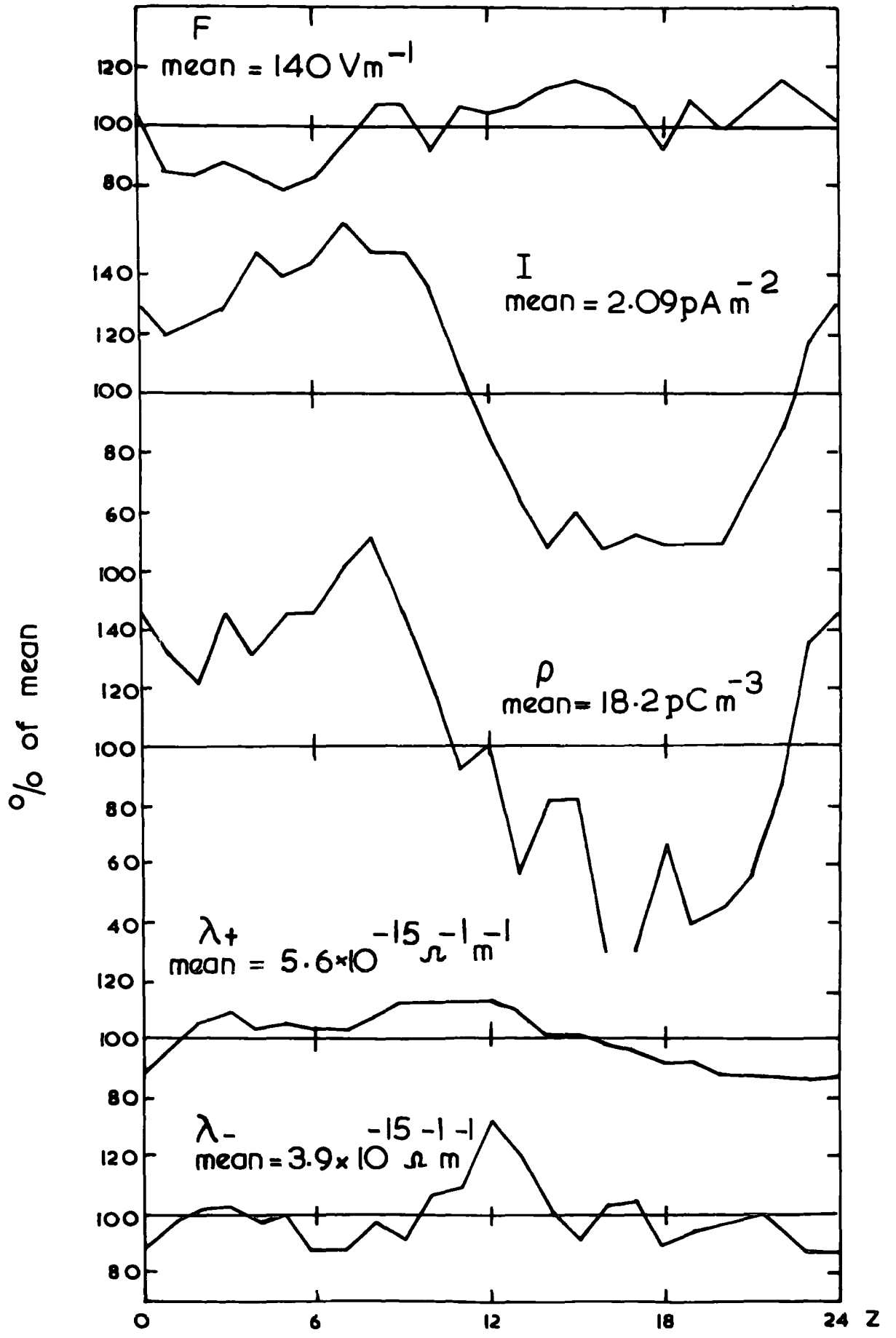
Diurnal variations – April 1969
F
mean = 140 Vm⁻¹
I
mean = 2.09pA m⁻²
ρ
mean= 18·2pC m⁻³
λ+
mean = 5·6×10⁻¹⁵ Ω⁻¹ m⁻¹
λ-
mean = 3.9× 10⁻¹⁵ Ω⁻¹ m⁻¹
% of mean
120
100
80
140
120
100
80
60
100
140
120
100
80
60
40
120
100
80
120
100
80
0
6
12
18
24 Z

Diurnal variations – May 1969.

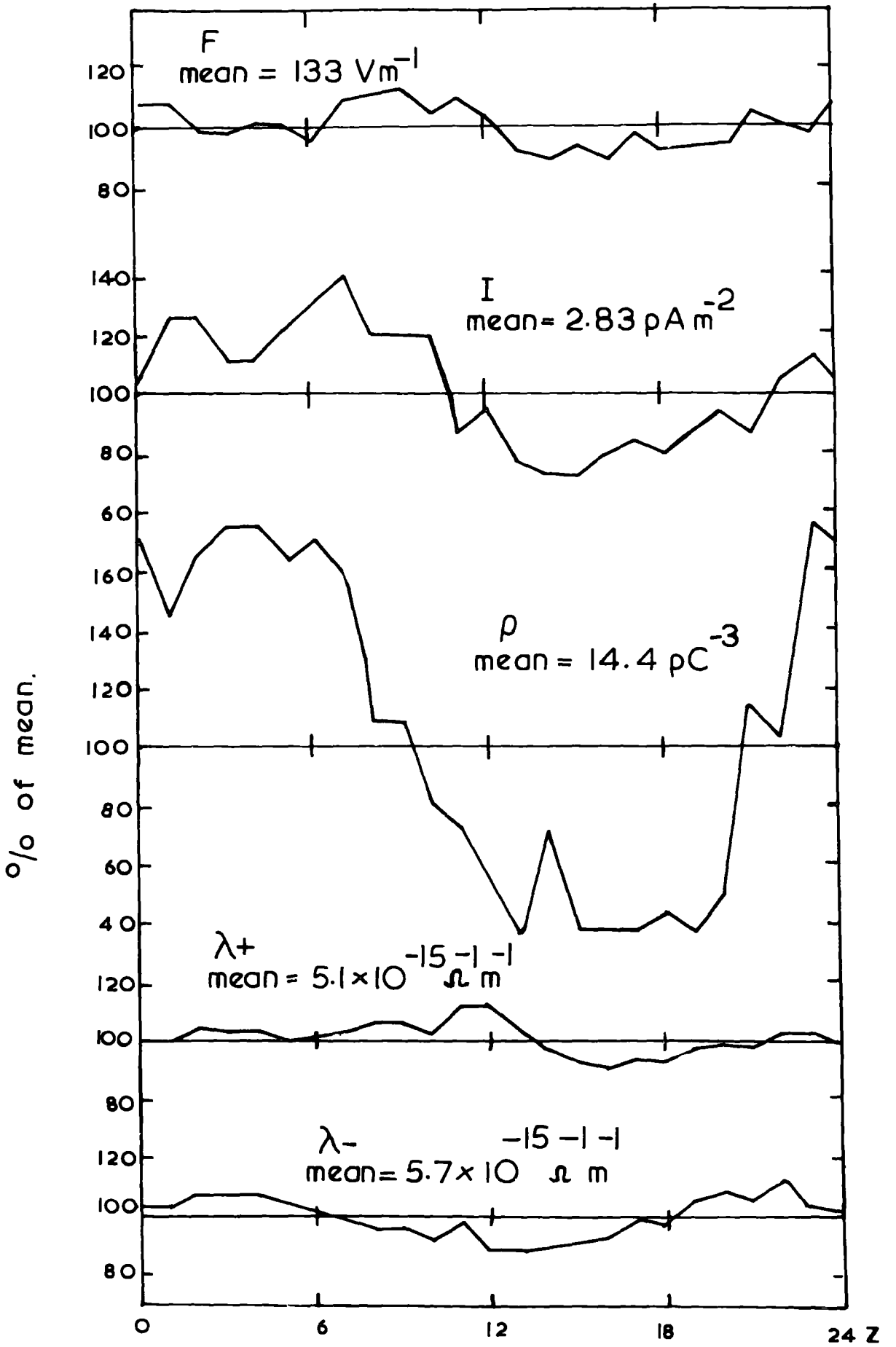

Diurnal variations — June 1969

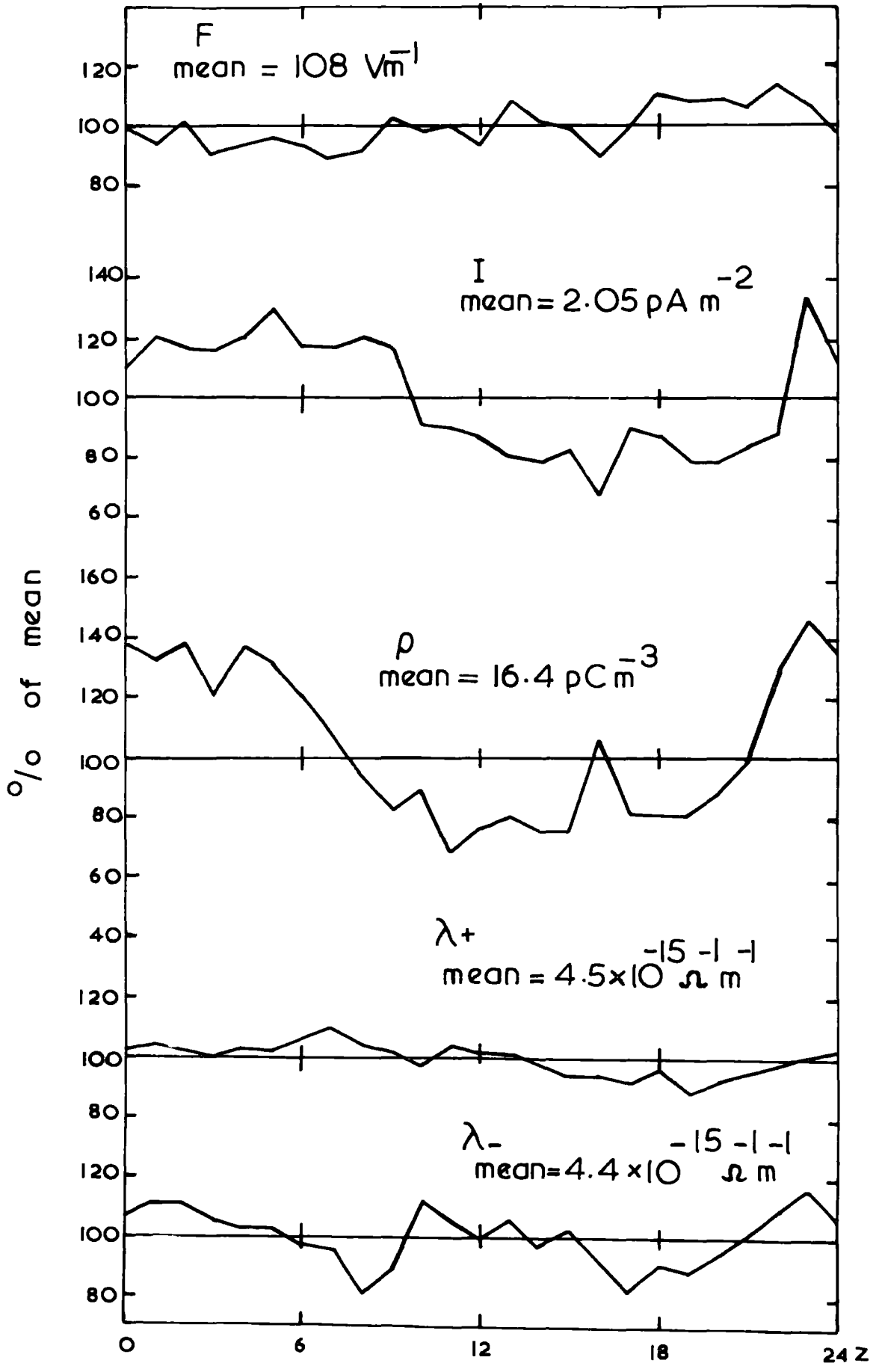

Diumal variations — July 1969

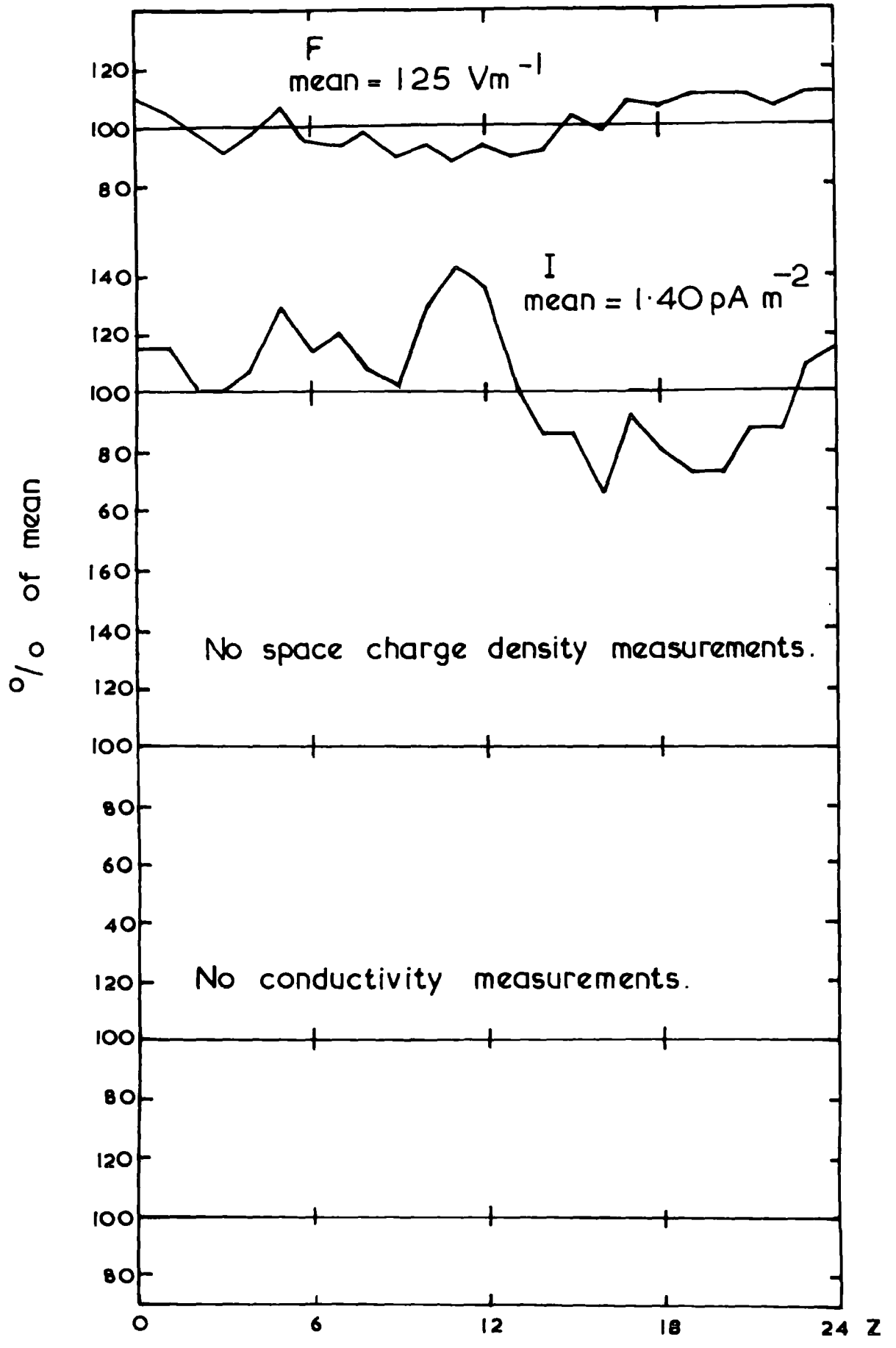

APPENDIX 2

HORIZONTAL WIND FORCES ON A FALLING PRECIPITATION PARTICLE

A differential equation is set up, in Sect. 6.2.6, which describes the horizontal behaviour of a falling drop when it is acted upon by a vertical wind shear. The equation is:

$$\frac{dw}{dt} = \beta \left\{ (V - \epsilon t) - w \right\}^2$$

This is a differential equation of the form:

$$\frac{dy}{dx} = (y + x)^2$$

which may be altered by the identity:

$$1 + \frac{dy}{dx} = \frac{d}{dx}(y + x)$$

Thus:

$$\frac{d}{dx}(y+x) = 1^2 + (y + x)^2$$

This has a standard form of solution.

We may rewrite the equation for the force on the drop as:

$$\epsilon + \frac{dw}{dt} = \beta \left\{ \frac{\epsilon}{\beta} + \left((V - \epsilon t) - w \right)^2 \right\}$$

The solution is:

$$\frac{\beta^{\frac{1}{2}}}{\epsilon^{\frac{1}{2}}} \tan^{-1} \left\{ \frac{\beta^{\frac{1}{2}}}{\epsilon^{\frac{1}{2}}} \left((V - \epsilon t) - w \right) \right\} = - \beta t + c$$

where c is a constant of integration.

When $t = 0$, $w = V$ and $c = 0$.

We may substitute $\frac{dx}{dt}$ for w, thus:

$$V - \epsilon t - \frac{dx}{dt} = - \frac{\epsilon^{\frac{1}{2}}}{\beta^{\frac{1}{2}}} \tan \left(\epsilon^{\frac{1}{2}} \beta^{\frac{1}{2}} t \right)$$

This equation describes the horizontal displacement, x, of the drop with time t:

$$\frac{dx}{dt} = -\epsilon t + V + \frac{\epsilon^{\frac{1}{2}}}{\beta^{\frac{1}{2}}} \tan\left(\epsilon^{\frac{1}{2}}\beta^{\frac{1}{2}}t \right)$$

In its turn, this equation is solved to give the horizontal range of the drop, X_D, in terms of the total fall time from the point of interest, H' (Sect. 6.2.6). The solution is:

$$X_D = \frac{(V+v)}{2\mu} H - \frac{(V-v)H'^2}{2H\mu} - \frac{vH'}{\mu}$$

The range of the cloud, X_c, is given by theproduct of cloud speed and elapsed time from the origin (see Fig. 6.6):

$$X_c = \frac{V(H - H')}{\mu}$$

where μ is the vertical terminal velocity of the particle. Therefore:

$$X_c - X_D = \frac{V(H - H')}{\mu} - \frac{(V+v)H}{2\mu} + \frac{(V-v)H'^2}{2H\mu} + \frac{vH'}{\mu}$$

The time lag between the charge centre being overhead and the arrival of the precipitation at the ground is:

$$\Delta T = \frac{(X_c - X_D)}{\text{charge speed}}$$

That is:

$$\Delta T = \left(\frac{V(H-H')}{\mu} - \frac{(V+v)H}{2\mu} + \frac{(V-v)H'^2}{2\mu H} + \frac{vH'}{\mu} \right) \Big/ \left(V - \frac{(V-v)H'}{H} \right)$$

This reduces to the quadratic equation:

$$(V-v)H'^2 + \left\{ 2(V+v)H + 2\mu\,(V-v)\,\Delta T \right\} H' + \left\{ (V-v)H^2 - 2\mu HV\Delta T \right\} = 0.$$

ACKNOWLEDGEMENTS

This work was carried out with the support of research grants from the United States Office of Naval Research and from the Natural Environment Research Council.

It is a pleasure to thank Dr. W. C. A. Hutchinson for supervising the research and for his counsel on the presentation of this thesis.

I am indebted to two Heads of Department in the University: Professor G. D. Rochester, F.R.S., of Physics, for his interest in my progress and for the provision of research and workshop facilities, and to Professor W. B. Fisher, of Geography, for granting use of the Lanehead Field Centre.

I gratefully acknowledge the advice and assistance rendered to me both by the Technical Staff of the Physics Department, especially Mr. Jack Moralee, and also by the Staff of the Durham University Computer Unit. The preparation of the typescript is the work of Mrs. J. Moore, to whom I am very obliged for her speed and efficiency.

I must thank my fellow research students in the Atmospheric Physics Group for their collective erudition and for their individual precepts, frequently promulgated for my sole benefit.

I am particularly indebted to Dr. and Mrs. J. G. Holland, of Hatfield College, for ensuring my physical well-being during the period of this work.

Finally, I wish to record my gratitude to my parents.

W.P.A.

Durham, 1969

REFERENCES

ACKERMAN, B (1966) The application of variance spectrum analysis to cloud measurements.
Tech. Note 34, Cloud Physics Lab., University of Chicago.

ANDERSON, R.V. (1969) Universal diurnal variations in air-earth current density.
J. Geophys. Res. 74, 6, 1697-1700.

APPLETON, E.V. (1925) Discussion on ionization in the atmosphere.
Proc. Phys. Soc., Lond., 37, 48D-50D.

AWE, O. (1964) Errors in the correlation between time-series.
J. Atmosph.Terr.Phys., 26, 1239-1255.

BAKER, W.G., and D. F. MARTYN (1953) Electric currents in the ionosphere, 1, The conductivity.
Phil. Trans.Roy.Soc.Lond., 246,281-294.

BARBER, N.F. (1966) Fourier methods in Geophysics. Methods and techniques of Geophysics.
(Ed. RUNCORN). Wiley, London.

BENDAT, J.S. and A. G. PIERSOL (1966) Measurement and analysis of random data.
Wiley, N.Y.

BENT, R.B. (1964) The electrical space charge in the lower atmosphere.
Ph.D. Thesis, Univ. of Durham.

BENT, R.B., and W. C. A. HUTCHINSON (1966) Electric space charge measurements and the electrode effect within the height of a 21 m mast.
J.Atmosph.Terr.Phys., 28, 53-73.

BEYERS, N.J., and B. T. MIERS (1965) Diurnal temperature in the atmosphere between 30 km and 60 km over White Sands Missile Range.
J. Atmos.Sci., 22, 262 - 266.

BLACKMAN, R.B., and T. W. TUKEY (1958) The measurement of power spectra.
Dover Publications, N.Y.

BROOKS, C.E.P. (1925) The distribution of thunderstorms over the globe.
Geophys. Mem., Lond., 24.

BROOKS, C.E.P., and N. CARRUTHERS (1953) Handbook of statistical methods in meteorology. H.M.S.O., London.

BROWNING, K.A., and T. W. HARROLD (1969) Air motion and precipitation growth in a wave depression. Quart.J.R.Met.Soc., 95, 288-309.

BUSHBY, F. H., and M. S. TIMPSON (1967) A 10-level atmospheric model for frontal rain. Quart.J.R.Met.Soc., 93, 1-17.

CHALMERS, J.A. (1949) Atmospheric Electricity. 1st Ed., Clarendon Press, Oxford.

CHALMERS, J.A. (1953) The charge on the ionosphere. J. Atmosph.Terr.Phys., 3, 345-346.

CHALMERS, J.A. (1956) The vertical electric current during continuous rain and snow. J.Atmosph.Terr.Phys., 9, 311-321.

CHALMERS, J.A. (1957) Point-discharge current, potential gradient and wind speed. J. Atmosph.Terr.Phys., 11, 301-302.

CHALMERS, J.A. (1966) The theory of the electrode effect. J.Atmosph.Terr.Phys., 28, 565-572.

CHALMERS, J.A. (1967) Atmospheric Electricity. 2nd Ed., Pergamon Press, Oxford.

CHALMERS, J.A. and E. W. R. LITTLE (1947) Currents of atmospheric electricity. Terr. Magn.Atmos.Elect.,52, 239-260.

CHAPMAN, S., and J. BARTELS (1940) Geomagnetism, Vol. I - II. pps. 417 - 448. Clarendon Press, Oxford.

COBB, W.E. (1968) The Atmospheric Electric Climate at Mauna Loa Observatory, Hawaii. J. Atmos.Sci., 25, 470-480.

COBB, W.E., and B. B. PHILLIPS (1962) Atmospheric electric measurement results at Mauna Loa Observatory. Tech. Paper 64, Weather Bureau, U.S. Dept. of Commerce.

COLLIN, H.L. (1969) An investigation of atmospheric electrical phenomena within 22 m of the ground during disturbed weather. Ph.D. Thesis, Univ. of Durham.

COLLIN, H.L., K. N. GROOM and K. A. HIGAZI (1966) The 'memory' of the atmosphere. J. Atmosph. Terr. Phys., 28, 695-697.

CROZIER, W.D. (1963) Electrode effect during nighttime Low wind periods. J. Geophys.Res., 68, 3451-3458.

CURTIS, H.O. and M. C. HYLAND (1958) Aircraft measurements of the small-ion density and electrical conductivity of the stratosphere. J. Geophys. Res., 70, 2751-2761.

DAYARATNA, L.H. (1969) Atmospheric electric conduction and convection currents near the earth's surface. Ph.D. Thesis, Univ. of Durham.

DE'SA, O., and L. MOLYNEUX (1962) A transistor voltage-to-frequency converter. Electronic Engineering 34, 468-469.

ELSTER, J., and H. GEITEL (1888) Über eine Methode die Elektrische Natur der atmosphärischen Niederschläge zu bestimmen. Met. Z., 5, 95-100.

GERDIEN, H. (1905) Demonstration eines Apparates zur absoluten Messung der elektrischen Leitfahigkeit der Luft. Phys. Z., 6, 647-666.

GISH, O.H., and K. L. SHERMAN (1936) Electrical conductivity of air to an altitude of 23 km. Nat. Geog.Soc. Stratosphere 2, 94-116.

GISH, O.H., and G. R. WAIT (1950) Thunderstorms and the earth's general electrification. J. Geophys.Res., 55, 473-484.

GROOM, K.N. (1966) Disturbed weather measurements in atmospheric electricity using an instrumented van. Ph.D. Thesis, Univ. of Durham.

HATAKEYAMA, H., and M. KAWANO (1953) On the diurnal variation of atmospheric potential gradient in the Japan Archipelago. Pap. Met. Geophys., 4, 55.

HIGAZI, K.A. (1966) Measurements of conductivity near the ground. Ph.D. Thesis, Univ. of Durham.

IMYANITOV, I.M., and E. V. CHUBARINA (1967) Electricity of the free atmosphere. Jerusalem: Israel Program for Scientific Translations - 1967.

ISRAËL, H. (1953) Bemerkung zum Energieumsatz im Gewitter. Geofis. Pur. Appl., 24, 3-11.

ISRAËL, H. and P. DE BRUIJN (1967) The present status of atmospheric electric research. Arch. Met. Geoph. Bickl. 16, 281-299.

ISRAËL, H., and H. W. KASEMIR (1952) Beispiele für das Verhalten Luftelektrischer Elemente bei Nebel. Arch.Met., Wien A, 5, 71-85.

JENKINS, G.M. (1961) General considerations in the analysis of spectra. Technometrics 3, 133-165.

JENKINS, G.M. and D. G. WATTS (1968) Spectral analysis and its applications. Holden-Day, San Francisco.

KASEMIR, H.W. (1955) Measurement of the air-earth current density. Proceedings of the Conference on Atmospheric Electricity held at Wentworth-by-the-Sea, Portsmouth, N.H. (Eds. HOLZER and SMITH).

KORN, G.A. (1966) Random-process simulation and measurements. McGraw-Hill, N.Y.

LAW, J. (1963) The ionization of the atmosphere near the ground in fair weather. Quart.J. R. Met. Soc., 89, 107-121.

LECOLAZET, R. and P. PLUVINAGE (1948) États de regimes permanents électrodynamiques dans l'atmosphère. Am. Géophys. 4, 96-108.

M'CLELLAND, J.A., and J. J. NOLAN (1912) The electric charge on rain. Proc. R. Irish Acad., 30, 72-91.

MAGONO, C., and S. KOENUMA (1958) On the electrification of water drops by breaking due to the electrostatic induction under a moderate electric field. J. Met. Soc. Japan, 36, 108-111.

MAGONO, C., and K. ORIKASA (1961) On the surface electric field caused by the space charge of charged raindrops. J. Met. Soc. Japan, 39, 1-11.

MANLEY, G., (1945) The Helm Wind of Crossfell, 1937-1939. Quart.J.R.Met. Soc., 71, 197-219.

MAPLESON, W.W., and W. S. WHITLOCK (1955) Apparatus for accurate and continuous measurement of the earth's electric field. J. Atmosph.Terr.Phys., 7, 61-72.

MASON, B.J. (1957) The physics of clouds. Oxford University Press.

MASON, B.J. (1969) Outstanding problems in cloud physics. Quart.J.R.Met.Soc., 95, 445-485.

MATTHEWS, J.B., and B. J. MASON (1964) Electrification produced by the rupture of large water drops in an electric field. Quart.J.R.Met.Soc., 90, 275-286.

MAUCHLY, S.J. (1923) Diurnal variation of the potential gradient of atmospheric electricity. Terr. Magn. Atmos. Elect. 28, 61-81.

MIERS, B.T. (1965) Wind oscillations between 30 km and 80 km over White Sands Missile Range, New Mexico. J. Atmos. Sci. 22, 4, 382-387.

MORGAN, W.A. (1960) Determination of the straight line of best fit to observational data of two related variables when both sets of values are subject to error. Quart. J. R. Met.Soc., 86, 107-113.

MUHLEISEN, R. (1961) Electrode effect measurements above the sea. J. Atmosph. Terr. Phys., 20, 79-81.

NOLAN, J.J., and P. J. NOLAN (1937) Atmospheric electrical conductivity and the current from air to earth. Proc. R. Irish Acad. 43, 79-93.

OGDEN, T. L. (1967) Electric space charge measurements in convective and other weather conditions. Ph.D. Thesis, Univ. of Durham.

OWOLABI, I.E. and J. A. CHALMERS (1965) Correlations of precipitation currents. J. Atmosph. Terr. Phys., 27, 303-308.

OWOLABI, I.E., and G. O. OLAOFE (1969) The exposure factor of a cylindrical shield in the measurement of precipitation currents. J. Atmosph.Terr.Phys., 31, 481-490.

PALTRIDGE, G.W. (1965) Experimental measurements of the small-ion density and electrical conductivity of the stratosphere. J. Geophys. Res., 70, 2751-2761.

PASQUILL, F. (1962) Atmospheric Diffusion. Van Norstrand, London.

PLUVINAGE, P., and P. STAHL (1953) Le conductibilité Électrique dans l'air de l'islandsis groenlandais. Ann Géophys. 9, 76-85.

QUENOUILLE, M.H. (1950) Introductory statistics. Pergammon Press, London.

RAMSAY, M. W. (1959) The relation between precipitation current, potential gradient, and rate of precipitation. Ph.D. Thesis, Univ. of Durham.

RAMSAY, M.W., and J. A. CHAIMERS (1960) Measurements on the electricity of precipitation. Quart. J.R.Met.Soc., 86, 530-539.

RANDHAWA, J.S. (1967) Ozonesonde for rocket flight. Nature, 213, 5071, 53-54.

REITER, R. (1956) Results of 2-year synoptic atmospheric-electric recordings at 7 mountain stations, between 700 and 3000 m a.s.l. Tech. Rep., Munich, Contract AF(514) 732-C.

REITER, R. (1958) Behaviour of atmospheric electricity magnitudes recorded simultaneously at 7 stations between 700 and 3000 m a.s.l. : results ofanalysis of fine and disturbed weather data, with special attention being given to precipitation and its nitrate and nitrite content. Tech. Rep., Contract AF61 (052)-55.

REITER, R. (1960) Relationships between atmospheric electric phenomena and simultaneous meteorological conditions. Tech. Rep., Contract AF61 (052)-55.

REITER, R. (1965) Precipitation and cloud electricity. Quart. J. R. Met. Soc., 91, 60-72.

REITER, R. (1968) A contribution to the atmospheric-electric phenomenology of non-thunderstorm clouds and precipitation. Paper to the 4th International Conference on the Universal Aspects of Atmospheric Electricity, at Tokyo.

RODÉS, R.P.L. (1933) Barcelona, Mem. Acad. Cienc.Art. 23,11.

RUHNKE, L.H. (1962) Electrical conductivity of air on the Greenland ice-cap. J. Geophys. Res. 67, 2767-2772.

SAGALYN, R.G. (1958) The production and removal of small ions and charged nuclei over the Atlantic Ocean. Wentworth Conference, 101-108.

SCHILLING. G.F., and J. CARSON (1953) On the electrical conductivity of air inside buildings. Arch.Met., Wien, B, 5, 52-57.

SCHILLING, G.F., and R. W. HOLZER (1954) Über mogliche Zusammenhange Zwischen Bioklimatologie und Luftelektrizität. Wett. u. Leben, 6, 13-16.

SCHINDELHAUER, F. (1913) Über die Elektrizität der Niederschlage Phys. Z. 14, 1292.

SCHONLAND, B.F.J. (1964) The Flight of Thunderbolts, 2nd Edt., Clarendon Press, Oxford.

SCRASE, F.J. (1933) The air-earth current at Kew Observatory. Geophys. Mem. Lond., 58.

SCRASE, F.J. (1934) Observations of Atmospheric Electricity at Kew Observatory. Geophys. Mem. Lond., 60, 1-27.

SCRASE, F.J. (1938) Electricity on rain. Geophys. Mem. Lond., 75.

SHARPLESS, G.T. (1968) An experimental study of the atmospheric electric elements at a rural site in conditions of low air pollution. Ph.D. Thesis, Univ. of Durham.

SHERMAN, K.L. (1937) Atmospheric electricity at College Fairbanks, Polar Year Station. Ferr. Magn. Atmos. Elect., 42,371-390.

SIMPSON, G.C. (1909) On the electricity of rain and its origin in thunderstorms. Phil. Trans. A, 209, 379-413.

SIMPSON, G.C. (1919) British Antarctic Expedition, 1910-1913.
Meteorology (Calcutta) 1, 302-312.

SIMPSON, G.C. (1927) The mechanism of a thunderstorm.
Proc. Roy. Soc. A, 114, 376-401.

SIMPSON, G.C. (1949) Atmospheric Electricity during disturbed weather.
Geophys. Mem. Lond., 84, 1-51.

SIMPSON, G.C., and G. D. ROBINSON (1946) The distribution of electricity in thunderclouds II.
Proc. Roy. Soc. A, 177, 281-329.

SIMPSON, G.C., and F. J. SCRASE (1937) The distribution of electricity in thunderclouds I.
Proc. Roy. Soc. A, 161, 309-352.

SIVARAMAKRISHNAN, M.V. (1952) Changes of atmospheric electric potential gradient at Poona during disturbed weather.
Indian J. Met. Geophys. 4, 62-75.

SIVARAMAKRISHNAN, M.V. (1960) The relation between raindrop size distribution, rate of rainfall, and the electric charge carried down by rain in the tropics.
Indian J. Met. Geophys. 12, 447-464.

SMITH, L.G. (1955) The electric charge of raindrops.
Quart. J.R. Met. Soc., 81, 23-47.

STERGIS, C.G., G. C. REIN, and T. KANGAS (1957) Electric field measurements above thunderstorms.
J. Atmosph, Terr.Phys., 11, 77-82.

STRINGFELLOW, M.F. Private communication

STROMBERG, I.M. (1968) Point discharge pulse measurements in Atmospheric Electricity.
Ph.D. Thesis, Univ. of Durham.

TORRESON, O.W., O.H. GISH, W. C. PARKINSON, and G. R. WAIT (1946) Scientific Results of Cruise VII of the Carnegie during 1928-1929.
Pub. Carnegie Instn. Washington D.C., 568.

WAIT, G.R. (1950) Measurements by airplane of the electric charge passing vertically through thunderstorms to ground.
Arch. Met. Wien A, 3, 70-76.

WEBB, W.L. (1968) The source of atmospheric electricity.
J. Geophys. Res. 73, 5061-5071.

WEBB, W.L., et al. (1966) Meteorological rocket network probing of the stratosphere and lower mesosphere. Bull. Amer. Meteor.Soc.47, 10, 788-799.

WHIPPLE, F.J.W. (1929) On the association of the diurnal variation of electric potential gradient in fine weather with the distribution of thunderstorms over the globe. Quart. J.R.Met.Soc., 55, 351-361.

WHIPPLE, F.J.W., and F. J. SCRASE (1936) Point discharge in the electric field of the earth. Geophys. Mem. Lond., 68, 1-20.

WHITLOCK, W.S. (1955) Variations in the earth's electric field. Ph.D. Thesis, Univ. of Durham.

WHITLOCK, W.S., and J. A. CHALMERS (1956) Short period variations in the atmospheric electric potential gradient. Quart. J.R.Met.Soc., 82, 325-336.

WILSON, C.T.R. (1906) On the measurement of the air-earth current and on the origin of atmospheric electricity. Proc. Camb. Phil. Soc., 13, 363-382.

WILSON, C.T.R. (1925) The electric field of a thundercloud and some of its effects. Proc. Phys. Soc. Lond., 37, 32-37.

WORMELL, T.W. (1930) Vertical electric currents below thunderstorms and showers. Proc. Roy. Soc. A, 115, 443-455.

WORMELL, T.W. (1953) Atmospheric electricity; some recent trends and problems. Quart. J.R.Met.Soc., 79, 3-50.